

22628

NATIONAL LIBRARY  
OTTAWA



BIBLIOTHÈQUE NATIONALE  
OTTAWA

NAME OF AUTHOR....Mr. J. H. Klepper.....

TITLE OF THESIS: "Aspects of Airship Design"

UNIVERSITY.....McMaster University.....

DEGREE FOR WHICH THESIS WAS PRESENTED....M. Eng.....

YEAR THIS DEGREE GRANTED....1974.....

Permission is hereby granted to THE NATIONAL LIBRARY  
OF CANADA to microfilm this thesis and to lend or sell copies  
of the film.

The author reserves other publication rights, and  
neither the thesis nor extensive extracts from it may be  
printed or otherwise reproduced without the author's  
written permission.

(Signed)....*J. Klepper*.....

PERMANENT ADDRESS:

APT. 808  
50 GOVERNOR'S RD.  
DUNDAS, ONT.

DATED.. September 5.....19 74

NL-91 (10-68)

ASPECTS OF AIRSHIP DESIGN

**ASPECTS OF AIRSHIP DESIGN**

**By:**

**Hans J. Kleiner**

**A Thesis  
Submitted to the School of Graduate  
Studies in Partial Fulfillment of the  
Requirements for the Degree  
Master of Engineering**

**McMaster University**

**June 1974**

**TITLE:** Aspects of Airship Design

**AUTHOR:** Hans J. Kleiner

**SUPERVISOR:** Dr. J. L. Duncan

**NUMBER OF PAGES:** 334

**SCOPE AND CONTENTS:**

The objective of this study is to present both an update of airship design, by introducing the element of the digital computer, and the structural design of the cabin of airship CAS-1.

Various aspects of the preliminary design of an airship were subjected to refinement by use of the digital computer. These included the envelope shape, the airship static bending moment, performance characteristics such as drag, and also the pressure distribution over the envelope in both level flight and flight at angles of attack.

Another area in which extensive use was made of the digital computer involved the development of a dynamic model of the airship flying characteristics. This model, in the form of a user oriented computer programme, allows the evaluation of the flight characteristics of various design alternatives. The maneuvers specified are those required to comply with government airworthiness requirements. The initial output is intended to form part of the compliance report for CAS-1.

The final section of this thesis involves the design and analysis of the structure of the cabin of airship CAS-1. This portion of the thesis was of immediate practical value as the construction of this cabin has been completed.



## Acknowledgements

The author is grateful to Dr. J. L. Duncan for his help in the selection of the material for this study and also for his patient guidance and advice. In addition the author would like to acknowledge the financial support received from the National Research Council and Hoverjet, Inc. of Thornhill.

The author also wishes to acknowledge the valuable assistance received from Dr. J. H. T. Wade and Professor W. R. Newcombe, both of McMaster University and also the contribution of Mr. R. Schneider of Hoverjet.

Thanks are also due to Mr. D. Bonham for his assistance in the use of the computer software, to Miss D. Tudin for her work in typing this thesis, and to Mr. T. Pal for his help in the preparation of the thesis.

# CONTENTS

		<u>Page</u>
Chapter 1	Introduction	1
Chapter 2	Preliminary Design Analysis	7
2.1	Introduction	7
2.2	The Envelope Shape	8
2.3	Body Configuration Dependant Parameters	13
2.3.1	Drag	13
2.3.2	Surface Area	65
2.3.3	Center of Bouyancy	65
2.3.4	Center of Gravity of the Envelope	67
2.3.5	Control Surfaces: Location and Size	67
2.3.6	Static Bending Moment	72
2.3.7	Aerodynamic Bending Moment	73
2.3.8	Internal Pressure	73
2.3.9	Programme and Results	74
2.4	Pressure Distribution Analysis	74
2.4.1	Introduction	74
2.4.2	Theodor Von Karman's Pressure Distribution on Airship Hulls	77
2.5	Static Shear Force and Bending Moment	92
2.5.1	Introduction	92
2.5.2	Programme Inputs and Sample Results	93
Chapter 3	Computer Aided Trajectory and Load Calculations	98
3.1	Introduction	98
3.2	Static Force and Moment Analysis	100
3.2.1	Description of Airship Axis	100
3.2.2	Center of Bouyancy	103
3.2.3	Definitions and Assumptions	104
3.2.4	Forces and Moments Acting on an Airship	105
3.2.5	Longitudinal Steady Motion	115
3.2.6	Stability in Roll	117
3.2.7	Steady Motion at a Fixed Yaw Angle	117
3.3	Dynamic Force and Moment Analysis	123
3.3.1	Altitude Control	123
3.3.2	Directional Control	124
3.3.3	Mechanics Equations	127
3.3.4	Forces and Moments Acting on the Airship	132
3.3.5	Determination of the Accelerations	132
3.4	User Oriented Computer Programme Description	136
3.5	Programme Results	141

## CONTENTS Continued

		<u>Page</u>
Chapter 4	CAS-1 Cabin Structure Design	187
4.1	Introduction	187
4.2	Upper Transverse Section Loading Analysis	192
4.3	Upper Side Members Loading Analysis	205
4.3.1	Basic Case 1	215
4.3.2	Basic Case 2	221
4.4	Underfloor Structure Loading Analysis	221
4.4.1	Longitudinal Truss Structure Static Condition	224
4.4.2	Longitudinal Truss Structure Static Castored Condition	232
4.4.3	Longitudinal Truss Structure Dynamic Condition	236
4.4.4	Underfloor Structure Transverse Sections	240
4.5	Summary	244
Chapter 5	Conclusions	247
Appendix A	Programme for Envelope shapes	248
Appendix B	Programme for body dependent parameters	260
Appendix C	Programme for pressure distribution	266
Appendix D	Programme for static shear force and bending moment	276
Appendix E	Programme for airship trajectories	295
References		332

## LIST OF ILLUSTRATIONS

	DESCRIPTION	PAGE
Figure 1.1	The transportation cost spectrum	3
Figure 2.1	Approximate comparison of equation $y = \frac{(n+m)^{n+m}}{2fn^nm} \frac{x^n}{n+m-1} (L-x)^m$ to Goodyear Model XZP5K Airship	11
Figure 2.2	Approximate comparison of equation $y = \frac{(n+m)^{n+m}}{2fn^nm} \frac{x^n}{n+m-1} (L-x)^m$ to Class "C" Airship	12
Figure 2.3	Shape of envelope for $n=0.2$ , $m=0.5$ , $f=2.25$	15
Figure 2.4	Shape of envelope for $n=0.2$ , $m=0.6$ , $f=2.25$	16
Figure 2.5	Shape of envelope for $n=0.3$ , $m=0.5$ , $f=2.25$	17
Figure 2.6	Shape of envelope for $n=0.3$ , $m=0.6$ , $f=2.25$	18
Figure 2.7	Shape of envelope for $n=0.4$ , $m=0.5$ , $f=2.25$	19
Figure 2.8	Shape of envelope for $n=0.4$ , $m=0.6$ , $f=2.25$	20
Figure 2.9	Shape of envelope for $n=0.2$ , $m=0.5$ , $f=2.50$	21
Figure 2.10	Shape of envelope for $n=0.2$ , $m=0.6$ , $f=2.50$	22
Figure 2.11	Shape of envelope for $n=0.3$ , $m=0.5$ , $f=2.50$	23
Figure 2.12	Shape of envelope for $n=0.3$ , $m=0.6$ , $f=2.50$	24
Figure 2.13	Shape of envelope for $n=0.4$ , $m=0.5$ , $f=2.50$	25
Figure 2.14	Shape of envelope for $n=0.4$ , $m=0.6$ , $f=2.50$	26

LIST OF ILLUSTRATIONS continued

	Description	Page
Figure 2.15	Shape of envelope for $n=0.2$ , $m=0.5$ , $f=2.75$	27
Figure 2.16	Shape of envelope for $n=0.2$ , $m=0.6$ , $f=2.75$	28
Figure 2.17	Shape of envelope for $n=0.3$ , $m=0.5$ , $f=2.75$	29
Figure 2.18	Shape of envelope for $n=0.30$ , $m=0.6$ , $f=2.75$	30
Figure 2.19	Shape of envelope for $n=0.400$ , $m=0.50$ , $f=2.75$	31
Figure 2.20	Shape of envelope for $n=0.4$ , $m=0.6$ , $f=2.75$	32
Figure 2.21	Shape of envelope for $n=0.2$ , $m=0.5$ , $f=3.00$	33
Figure 2.22	Shape of envelope for $n=0.2$ , $m=0.6$ , $f=3.00$	34
Figure 2.23	Shape of envelope for $n=0.3$ , $m=0.5$ , $f=3.00$	35
Figure 2.24	Shape of envelope for $n=0.3$ , $m=0.6$ , $f=3.00$	36
Figure 2.25	Shape of envelope for $n=0.400$ , $m=0.500$ , $f=3.0$	37
Figure 2.26	Shape of envelope for $n=0.4$ , $m=0.6$ , $f=3.00$	38
Figure 2.27	Shape of envelope for $n=0.185$ , $m=0.400$ , $f=4.00$	39
Figure 2.28	Shape of envelope for $n=0.200$ , $m=0.400$ , $f=4.00$	40
Figure 2.29	Shape of envelope for $n=0.250$ , $m=0.400$ , $f=4.00$	41
Figure 2.30	Shape of envelope for $n=0.275$ , $m=0.400$ , $f=4.00$	42
Figure 2.31	Shape of envelope for $n=0.300$ , $m=0.400$ , $f=4.00$	43
Figure 2.32	Shape of envelope for $n=0.350$ , $m=0.400$ , $f=4.00$	44

LIST OF ILLUSTRATIONS Continued

	Description	Page
Figure 2.33	Shape of envelope for $n=0.375$ , $m=0.4$ , $f=4.00$	45
Figure 2.34	Shape of envelope for $n=0.400$ , $m=0.40$ , $f=4.00$	46
Figure 2.35	Shape of envelope for $n=0.185$ , $m=0.5$ , $f=4.00$	47
Figure 2.36	Shape of envelope for $n=0.200$ , $m=0.5$ , $f=4.00$	48
Figure 2.37	Shape of envelope for $n=0.25$ , $m=0.5$ , $f=4.00$	49
Figure 2.38	Shape of envelope for $n=0.275$ , $m=0.5$ , $f=4.00$	50
Figure 2.39	Shape of envelope for $n=0.300$ , $m=0.5$ , $f=4.00$	51
Figure 2.40	Shape of envelope for $n=0.350$ , $m=0.5$ , $f=4.00$	52
Figure 2.41	Shape of envelope for $n=0.375$ , $m=0.5$ , $f=4.00$	53
Figure 2.42	Shape of envelope for $n=0.400$ , $m=0.5$ , $f=4.00$	54
Figure 2.43	Shape of envelope for $n=0.185$ , $m=0.6$ , $f=4.00$	55
Figure 2.44	Shape of envelope for $n=0.200$ , $m=0.6$ , $f=4.00$	56
Figure 2.45	Shape of envelope for $n=0.275$ , $m=0.6$ , $f=4.00$	57
Figure 2.46	Shape of envelope for $n=0.250$ , $m=0.6$ , $f=4.00$	58
Figure 2.47	Shape of envelope for $n=0.300$ , $m=0.6$ , $f=4.00$	59
Figure 2.48	Shape of envelope for $n=0.350$ , $m=0.60$ , $f=4.00$	60
Figure 2.49	Shape of envelope for $n=0.375$ , $m=0.6$ , $f=4.00$	61
Figure 2.50	Shape of envelope for $n=0.4$ , $m=0.6$ , $f=4.00$	62

LIST OF ILLUSTRATIONS Continued

	Description	Page
Figure 2.51	A comparison of three drag equations	66
Figure 2.52	Control Surface Chart $\sqrt{A_H L}$ and $\sqrt{A_V L}$ vs. $\sqrt{V}$	69
Figure 2.53	Control Surface Chart $\sqrt{A_E L}$ and $\sqrt{A_R L}$ vs. $\sqrt{V}$	70
Figure 2.54	Control Surface Chart A.C vs. $V$	71
Figure 2.55	Pressure distribution for an Airship in level flight $m=0.6$ , $n=0.4$ , $f=3.00$ , $V=110$ ft/sec	75
Figure 2.56	Pressure distribution for an Airship in non-level flight $m=0.6$ , $n=0.4$ , $f=3.00$ , $V=110$ ft/sec, $\alpha=5.00$	76
Figure 2.57	Co-ordinate systems used in the analysis	80
Figure 2.58	Trigonometric relationships for a general point along the hull shape	82
Figure 2.59	Static shear force diagram	96
Figure 2.60	Static bending moment diagram	97
Figure 3.1	Airship axis	101
Figure 3.2	Forces Acting on an Airship (idealized case)	106
Figure 3.3	Airship trajectories for various loading conditions and angles of attack	108
Figure 3.4	Forces acting on an airship for the loading condition of Case #3	111
Figure 3.5	Forces acting on an airship at a fixed yaw angle	118
Figure 3.6	Angle of yaw variation over the airship length	121

## LIST OF ILLUSTRATIONS Continued

	Description	Page
Figure 3.7	Action of an airship during a turn	125
Figure 3.8	Action of an airship during obstacle avoidance	126
Figure 3.9	Modified set of axis	131
Figure 3.10	Trajectory programme input deck setup	137
Figure 3.11	Graphical illustration of the programme output-take-off trajectory	143
Figure 3.12	Graphical illustration of the programme output - full rudder until a 75° turn achieved	144
Figure 3.13	Graphical illustration of the programme output - full opposite rudder until the original heading regained	145
Figure 3.14	Graphical illustration of the programme output - full up elevators and a steady state turn from 0 to 180 degrees	146
Figure 4.1	Cabin structure illustration front and side view	189
Figure 4.2	Lower cabin structure	190
Figure 4.3	Upper cabin structure	191
Figure 4.4	Engine attachment idealization	193
Figure 4.5	Engine static weight input arrangement	194
Figure 4.6	Engine static weight input	195
Figure 4.7	System free body diagram	197
Figure 4.8	Transverse structure load components	199
Figure 4.9	Transverse structure left loading diagram	201



LIST OF ILLUSTRATIONS Continued

	Description	Page
Figure 4.10	Transverse structure right loading diagram	202
Figure 4.11	Graphical analysis left transverse structure	203
Figure 4.12	Graphical analysis right transverse structure	204
Figure 4.13	Wind gust situation	208
Figure 4.14	Load analysis gust situation	209
Figure 4.15	Gust loading left transverse structure	210
Figure 4.16	Gust loading right transverse structure	211
Figure 4.17	Graphical analysis gust condition left transverse structure	212
Figure 4.18	Graphical analysis gust condition right transverse structure	213
Figure 4.19	Upper side structure	216
Figure 4.20	Upper side structure loading situation	217
Figure 4.21	Upper side structure actual loading Basic case 1	218
Figure 4.22	Upper side structure idealized loading, Basic case 1	218
Figure 4.23	Upper side structure actual loading Basic case 2	220
Figure 4.24	Upper side structure idealized loading, Basic case 2	220
Figure 4.25	Transverse truss configuration	222
Figure 4.26	Longitudinal truss configuration	223
Figure 4.27	Longitudinal truss loading	225
Figure 4.28	Landing gear arrangement	228
Figure 4.29	Shear force diagram (normal)	230

### LIST OF ILLUSTRATIONS Continued

	Description	Page
Figure 4.30	Bending moment diagram (normal)	231
Figure 4.31	Shear force diagram (Castored)	234
Figure 4.32	Bending moment diagram (Castored)	235
Figure 4.33	Transverse section loading	241
Figure 4.34	Graphical analysis of transverse section	242
Figure 4.35	Cabin structure as completed	245
Figure 4.36	Cabin structure during construction	246

## LIST OF TABLES

	Description	Page
Table 2.1	Design parameters for various airship shapes with the velocity in feet per second = 110.000000; volume in cubic feet = 91798.60 and with all areas in square feet and all distances in feet and pressure in lbs/sq. ft.	63
Table 3.1	Nomenclature	102
Table 3.2	Coefficients of additional mass of ellipsoids of various length/diameter ratios [13]	116
Table 3.3	Computer trajectory test input variables	142
Table 3.4	Selected trajectories, accelerations and velocities	148
Table 3.5	Selected trajectories and forces	169
Table 4.1	Section loading	206
Table 4.2	Member loads level condition	207
Table 4.2(a)	Combined side force and level condition loads (ultimate loads)	214
Table 4.3	Upper side structure loading	219
Table 4.4	Airship Load Distribution	226
Table 4.5	Load distribution on underfloor structure	227
Table 4.6	Longitudinal underfloor structure static loading	233
Table 4.7	Longitudinal underfloor structure static loading (on castors)	237
Table 4.8	Longitudinal underfloor structure dynamic loading	239
Table 4.9	Transverse Section Loads	243

## CHAPTER I INTRODUCTION

At the present time airships are experiencing a renewal of public interest. Technical and financial interest has also been evident for some time, as shown by the proposals and feasibility studies by Gordon<sup>[5]</sup>, Sonstegaard<sup>[6]</sup>, Howe<sup>[7]</sup>, Kleiner<sup>[4]</sup>, Stinton<sup>[8]</sup>, Morse<sup>[10]</sup>, Jurich<sup>[9]</sup>, Hecks<sup>[11]</sup>, Mowforth<sup>[14]</sup>, Rynish<sup>[16]</sup>, Vaeth<sup>[31]</sup>, and Seemann<sup>[32]</sup>. Goodyear Aerospace [17-22,30] has also carried out various studies.

What is responsible for the revived interest of engineers and transportation planners? The rebirth of the airship can be attributed to the following reasons:

- 1) Airships were ahead of their time in their demands upon technology. Use of computer technology might be expected to produce airships that would far exceed the performance and safety of pre World War II commercial airships.
- 2) Airships have better ton-mile/unit energy ratios than other airborne transportation systems. This has become of prime consideration in view of the present energy situation.
- 3) New materials have been developed which affect every aspect of airship construction. Plastic films, foams, and carbon fibres are among the materials

2  
that might make significant contributions to any new airships.

4) Helium, the "safe" airship gas, is no longer a scarce gas controlled politically by only one nation.

5) Airships have several inherent attributes which airborne transportation designers strive for in other systems. These include:

- (a) low levels of noise and air pollution
- (b) low risk potential for fatal accidents
- (c) STOL and VTOL capability
- (d) long range and endurance
- (e) all weather capability (when aloft)

The airship has been suggested as a possible solution for:

- i) maritime patrol
- ii) search and rescue
- iii) airborne police work
- iv) survey and exploration work
- v) bulk and gaseous freight transportation

Figure 1:1 shows the sort of costs that might be achieved by airships as compared to other modes of transportation.

The development of the airship actually dates from the construction of the first elongated balloon designed by A. J. and M. N. Roberts in 1784. The envelope had an internal air cell to maintain a constant internal pressure and the airship

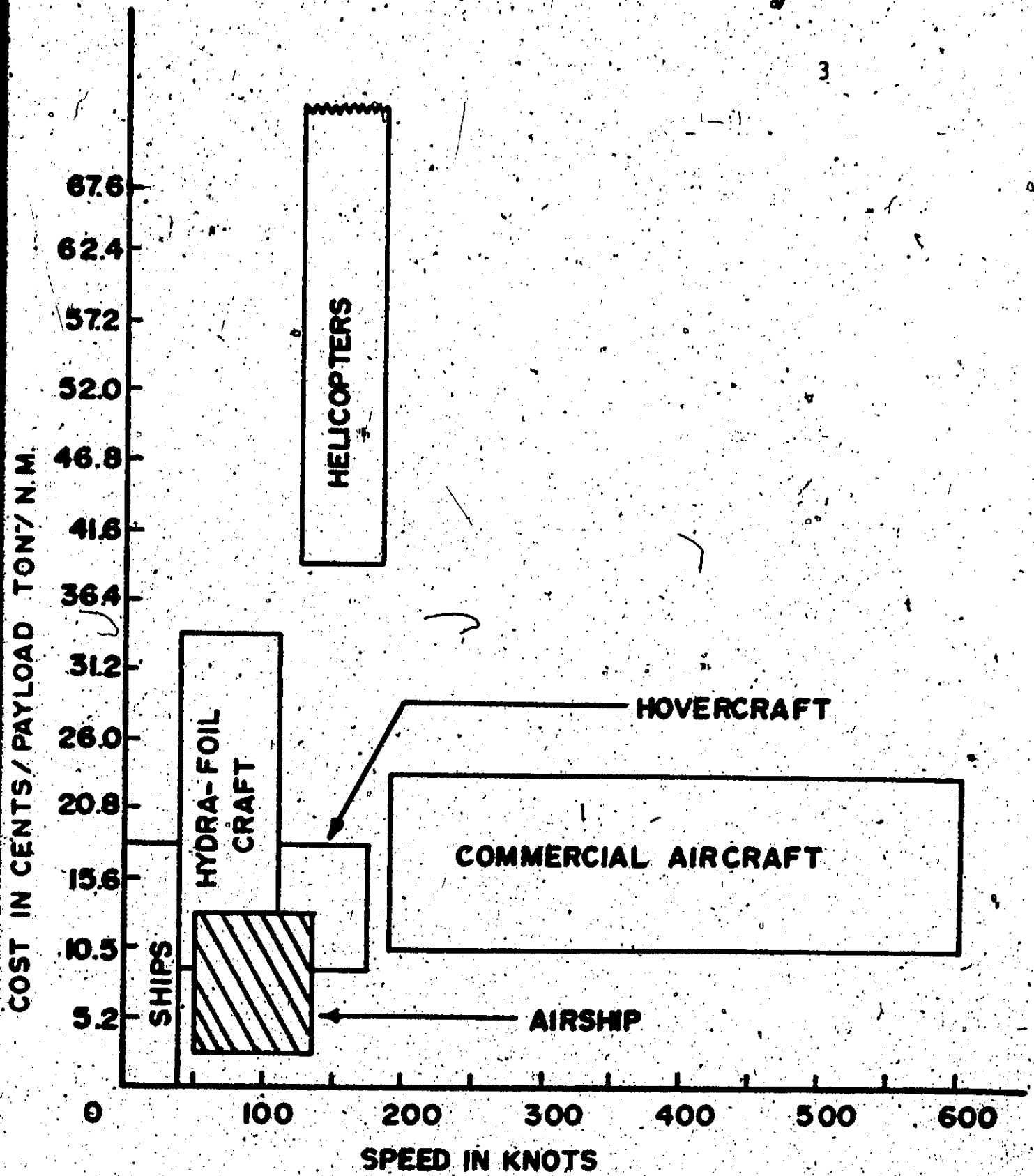


FIGURE 1.1 THE TRANSPORTATION COST SPECTRUM

was propelled and steered by means of oars. Although the vehicle was claimed to be successful, further development had to await the development of a suitable power source. Monck Mason, in 1843, tried a clockwork driven propellor and Henri Giffard, in 1852, used a steam engine on a hydrogen filled envelope and attained a speed of six miles per hour. It was not until the 1890's, with the development of the gasoline engine, that a power source, of a power to weight ratio which allowed sustained flight, was available. Santos Dumont, in France, and Count von Zeppelin, in Germany, around 1900 built and flew successful airships. The development of the airship progressed rapidly in the interval until the start of World War I. The extent of the progress can be measured by the fact that before the outbreak of the war a successful and safe commercial airship operation was already well established. It operated, in Germany, under the name of DELAG and flew three large, ~~for~~ their time, rigid airships.

During World War I, the airship underwent rapid development. This development had as its main aim the production of an efficient weapon system. However, this development lead to the airship becoming the first long range air transport after the termination of hostilities. The first transatlantic flight was made in 1919, and in 1928 the famous Graf Zeppelin started regularly scheduled transatlantic flights. Even larger commercial airships followed in the form of the British R100,

R101, and the German Hindenburg. The potential of the airship at this stage of development can be seen by examining the commercial payload of the 7,060,000 cubic foot airship Hindenburg. The commercial payload was 74,000 lbs. over transatlantic ranges. At the same time, the DC-3 represented the most efficient aircraft system. However, despite the promise shown, the lack of really suitable materials, design techniques, research and development funds, and the international politics of the pre-World War II era saw the demise of the large commercial rigid airships culminating in a series of accidents. Despite this, the airship, in non-rigid form, continued to give valuable service. During World War II extensive convoy escort work was done by airships. No ship was lost to submarines while under airship escort. After the war, even larger non-rigid airships were developed by the U. S. Navy to perform anti-submarine and early airborne warning duties. Interest waned, however, as airships came to be regarded as relics of an era past and in 1962 the U. S. Navy disbanded its airship service. Thus arose the present situation in which the only airships left flying in the world are those used by the Goodyear Aerospace Corporation as symbols of its corporate image.

Despite the many proposals mentioned earlier, it has been many years since a new airship has emerged from the design-proposal stage to an actual piece of hardware. For one reason or another all of these proposals died a quiet death without



initiating any new design procedures or producing any advances in the multitude of areas where the incorporation of modern techniques could help provide a safe, efficient, optimum design.

This thesis, which was sponsored in part by the builders of airship CAS-1, is aimed at providing a start in the application of modern computer techniques to airship design. Two separate areas have been examined. First the computer has been used to examine the preliminary design stage. It is an ideal tool with which to cover the many alternatives available to the designer. Secondly the computer has been put to use to determine the loads on an airship by simulating the airship maneuvers which are specified in the government airworthiness regulations [3].

The final part of this thesis covers the design of the cabin structure of the airship CAS-1. The fabrication of this structure was completed during February of 1974.

It is hoped that this work will be the first of many on the subject of airships and that the interest displayed by the various individuals and agencies will produce new hardware and a new airship era.

## Chapter Two Notation

$x$	the co-ordinate along the longitudinal axis of the airship envelope
$y$	the co-ordinate along the vertical axis of the envelope
$L$	the length of the airship
$m$	airship envelope shape parameter
$n$	airship envelope shape parameter
$f$	fineness ratio
$C_f$	friction drag coefficient
$\rho$	density of air (slugs/ft <sup>3</sup> )
$V$	velocity (ft/sec)
$V$	volume of airship (ft <sup>3</sup> )
$V_K$	airship velocity in knots
$\nu$	kinematic viscosity of air (ft <sup>2</sup> /sec)
$\delta_{SL}$	unit lift of gas at sea level (lbs/ft <sup>3</sup> )
$CB_x$	position of the center of buoyancy along the longitudinal axis
$COE_x$	position of the center of gravity of the envelope along the longitudinal axis
$A_{CS}$	the control surface area
$A_H$	the fixed horizontal control surface area
$A_V$	the fixed vertical control surface area
$A_E$	the elevator area
$A_R$	the rudder area
$C$	the distance between the center of buoyancy and the center of area of the total control surfaces

$BM_H$	the hogging bending moment
$BM_A$	the aerodynamic bending moment
$P_{INT}$	the internal pressure of the gas containing envelope (psi) -
$r$	the perpendicular distance from the x axis
$U_x$	the velocity component in the x direction
$U_r$	the velocity component in the r direction
$U_\phi$	the velocity component in the $\phi$ direction
$\theta$	the angle between the radius vector and the axis of symmetry
$U_\theta$	the velocity component in the $\theta$ direction
$\phi$	the potential function
$\psi$	the stream function
$q$	the source strength per unit length
$a$	the source length
$\rho'$	the distance to a point from the left end of a line source
$\rho''$	the distance to a point from the right end of a line source
$U$	the free stream velocity
$S$	the transverse force coefficient
$W_x$	the parallel velocity component in the x direction
$W_r$	the parallel velocity component in the r direction

## CHAPTER 2

### PRELIMINARY DESIGN ANALYSIS

#### 2.1 Introduction

The general consensus, in the modern day literature dealing with airships, is that any new airship appearing in the future will be of the pressure airship type (ie. non-rigid or semi-rigid). A pressure airship is an airship whose envelope shape and strength is provided by a slight internal pressure. Thus the preliminary design information presented in this chapter will apply directly to this type of airship. Some parts of the information may also apply to rigid airships, however, no special differentiation will be made.

The data presented can be segregated into four distinct areas. These are:

- (i) selection of the envelope shape,
- (ii) analysis of various parameters that are dependent on the envelope shape,
- (iii) static shear force and bending moment analysis,
- and (iv) an analysis of the pressure distribution of an envelope shape at various speeds and angles of attack.

With the aid of this data, the design of the airship shape can be made in a much more rational manner than has been the case previously.

## 2.2 The Envelope Shape

Most airship forms have been developed by a trial and error method, resorting to wind tunnel tests to obtain data upon which to base a decision as to the best form. Stream-line shapes have sometimes been developed mathematically from the theoretical flow resulting from arbitrarily assumed systems of sinks and sources. Wind tunnel tests have not indicated any outstanding virtues in forms developed by this method. Shapes drawn by designers with a natural aptitude for these matters have been as successful as any [13]. In early years shapes were often formed by simply combining various solids of revolution into a "smooth" body. Later attempts were made to fulfill various conditions with these solids, e.g., achieving a particular rate of change of curvature. The position has now been attained where mathematical expressions, capable of generating various types of bodies of revolution, are available. The value of an expression of this type is quite apparent especially if the generating function is integrable. One such mathematical form has been developed by General Mills [28], in the following manner:

A generalized shape generation equation of the form

$$y = K_1 x^n (K_2 - x) \quad (2.1)$$

where  $x$  = the co-ordinate along the central axis, and  $y$  = the radius at a value of  $x$ , was obtained from a commonly used shape generation expression.

$$y = 1/3x^{1/2}(1-x) \quad (2.2)$$

The constants  $K_1$  and  $K_2$  of equation (2.1) were then determined from the boundary conditions  $y_0 = 0$ ,  $v_2 = 0$  and  $y_{\max.} = L/2f$ , such that

$$y = \frac{(n+1)(n+1)x^n(L-x)}{2fn^nL^n} \quad (2.3)$$

where  $x$  = the co-ordinate along the central axis,

$y$  = the radius of the body of revolution about the central axis at each value of  $x$ ,

$L$  = the length of the body,

$f$  = the fineness ratio =  $L/2y_{\max.}$ ,

and  $n$  = a dimensionless parameter.

The endpoint conditions of the generated shape are given by

$$\left. \begin{aligned} \left(\frac{dy}{dx}\right)_{x=0} &= \begin{cases} 0 & 0 < n < 1 \\ 2/f & n = 1 \\ 0 & n > 1 \end{cases} \\ \left(\frac{dy}{dx}\right)_{x=L} &= -\frac{(n+1)(n+1)}{2fn^n} \end{aligned} \right\}$$

However, the generating power of (2.3) is limited in the variety of shapes that it is possible to generate.

The introduction of another dimensionless parameter,  $m$ , into equation (2.1) results in a more general expression.

$$y = K_3 x^n (K_4 - x)^m \quad (2.4)$$

which, assuming the boundary conditions previously stated, gives upon solving for  $K_3$  and  $K_4$ ,

$$y = \frac{(n+m)(n+m)x^n(L-x)^m}{2fn^nm^nL(n+m-1)} \quad (2.5)$$

with the boundary conditions:

$$\left. \begin{aligned} \left(\frac{dy}{dx}\right)_{x=0} &= \begin{cases} a & 0 < n < 1, \text{ all } m \\ \frac{(m+1)(n+1)}{2fn^m} & n = 1, \text{ all } m \\ 0 & n > 1, \text{ all } m \end{cases} \\ \left(\frac{dy}{dx}\right)_{x=L} &= \begin{cases} -a & 0 < m < 1, \text{ all } n \\ \frac{-(n+1)(m+1)}{2fn^n} & m = 1, \text{ all } n \\ 0 & m > 1, \text{ all } n \end{cases} \end{aligned} \right\}$$

Equation (2.5) if employed with the following conditions will generate an infinite variety of airship hull shapes.

$$\begin{aligned} m &> n \\ 0 &< n < 1 \\ 0 &< m < 1 \end{aligned}$$

Figure 2.1 illustrates a comparison of equation (2.5) to the Goodyear Model XZP5K Airship. Figure 2.2 illustrates a comparison of equation (2.5) to the class "C" airship shape that was much in favour during the airship era. These comparisons indicate the accuracy available when using (2.5). The three parameters which directly affect the airship shape,  $m$ ,  $n$ , and  $f$ , can be varied to suit the designer.

The adaptation of (2.5) to the digital computer and modern computer plotting software permits examination of many shapes. A programme to accomplish this has been developed. The variety of shapes possible is illustrated by Figures 2.3

APPROXIMATE COMPARISON OF EQUATION  $y = \frac{(n+m)^{n+m}}{2 f n^m m^m} \frac{x^n}{L^{n+m-1}} (L-x)^m$   
 TO GOODYEAR MODEL XZP5K AIRSHIP

$f = 4.17$

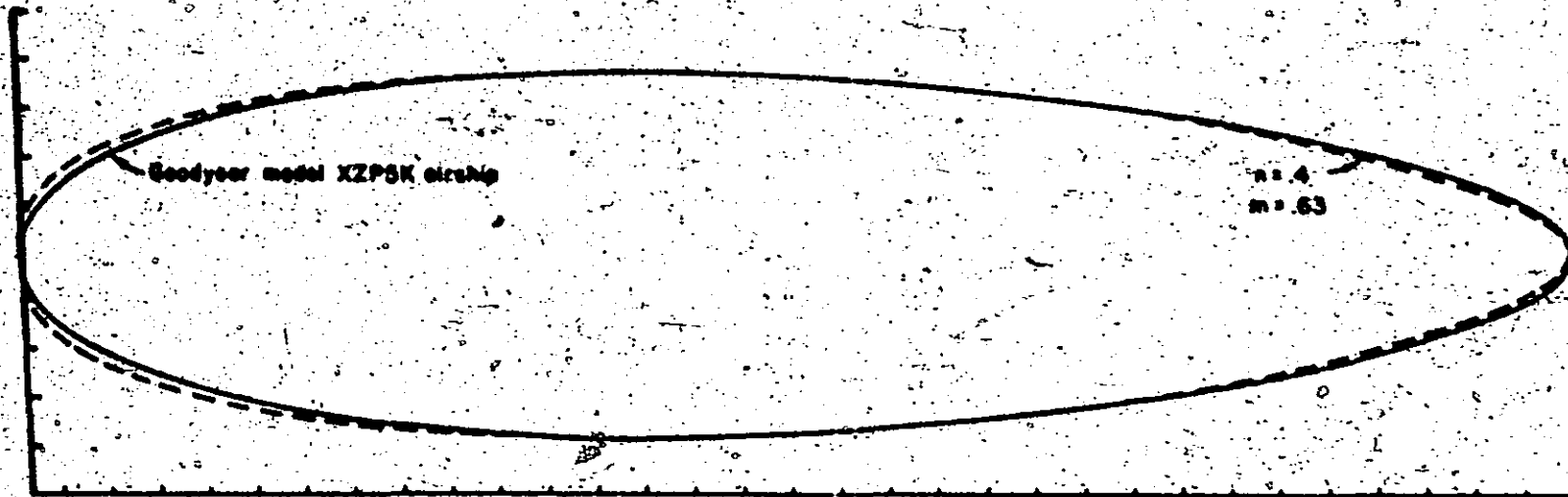


Figure 2.1: Approximate Comparison of Equation

$$y = \frac{(n+m)^{n+m}}{2 f n^m m^m} \frac{x^n}{L^{n+m-1}} (L-x)^m$$

to Goodyear Model XZP5K Airship



$$\text{APPROXIMATE COMPARISON OF EQUATION } y = \frac{(n+m)^{n+m}}{2^n n^m m^n} \frac{x^n}{L^{n+m-1}} (L-x)^m$$

TO CLASS "C" AIRSHIP

$f = 4.19$



Figure 2.2: Approximate Comparison of Equation

$$y = \frac{(n+m)^{n+m}}{2^n n^m m^n} \frac{x^n}{L^{n+m-1}} (L-x)^m$$

to Class "C" Airship

to 2.50 which are an output of the programme. A printout of the actual programme is given in Appendix A and should prove amenable to modification for other values of  $f$ ,  $m$ , and  $n$ .

### 2.3 Body Configuration Dependent Parameters

The choice of envelope shape has an effect on many parameters and in turn influences which shape will finally be used. In general, it is desirable to have maximum volume for minimum weight and minimum aerodynamic drag. In actual fact the selection of a particular shape also depends on such factors as the propulsive technique, stability and control requirements, boundary layer effects, the degree of resistance to aerodynamic bending moments, and the flight profile. Although no shape can be optimum for all of the above conditions, a shape that is a satisfactory compromise must be ultimately decided upon. With the aid of (2.5) various pleasing shapes can be examined to determine which best meets the design specifications. A programme has been written which will calculate the following parameters for each shape required. An example of the type of output obtainable is given by Table 2.1.

#### 2.3.1 Drag

One of the most important of the parameters in determining the suitability of the envelope shape is the drag.

Figures 2.3 to 2.50 to follow. They represent various envelope shapes developed by use of equation

$$y = \frac{(n + m)^{n+m}}{2f n^n m^m} \frac{x^n}{[n+n-1]} (L - x)^m$$

Various values of f, m, and n are used.



Figure 2.3: Shape of Envelope for

$n = 0.2, m = 0.5, f = 2.25$

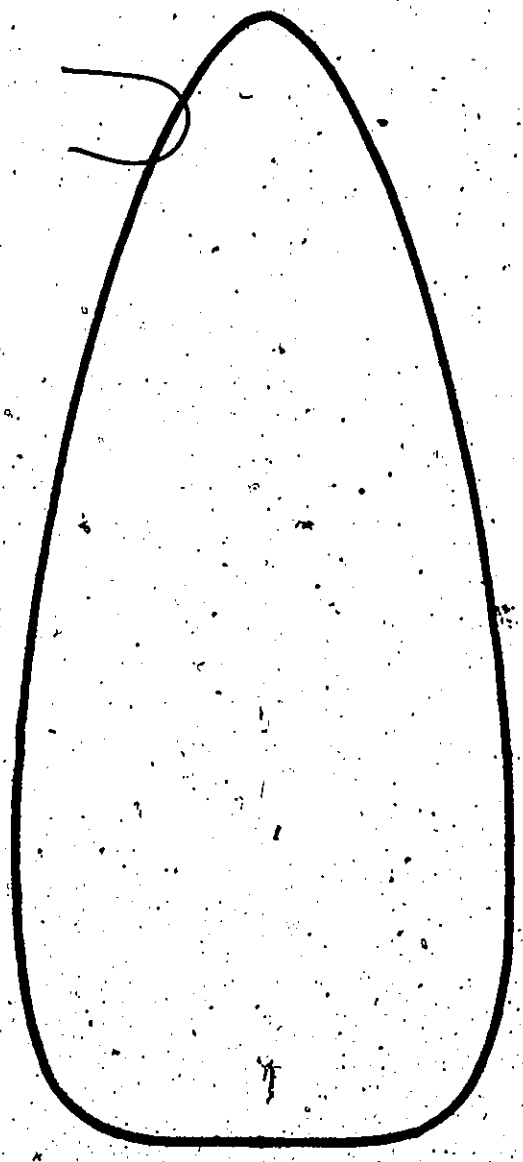


Figure 2.4: Shape of Envelope for

$n = 0.2, m = 0.6, r = 2.25$



Figure 2.5: Shape of Envelope for

$$n = 0.3, m = 0.5, \zeta = 2.25$$

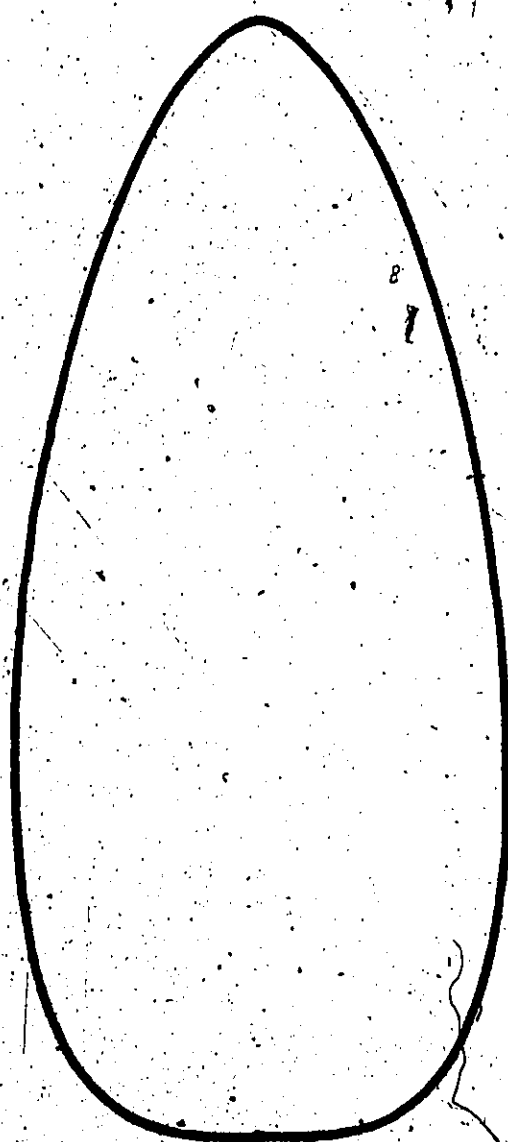


Figure 2.6: Shape of Envelope for

$n = 0.3, m = 0.6, r = 2.25$

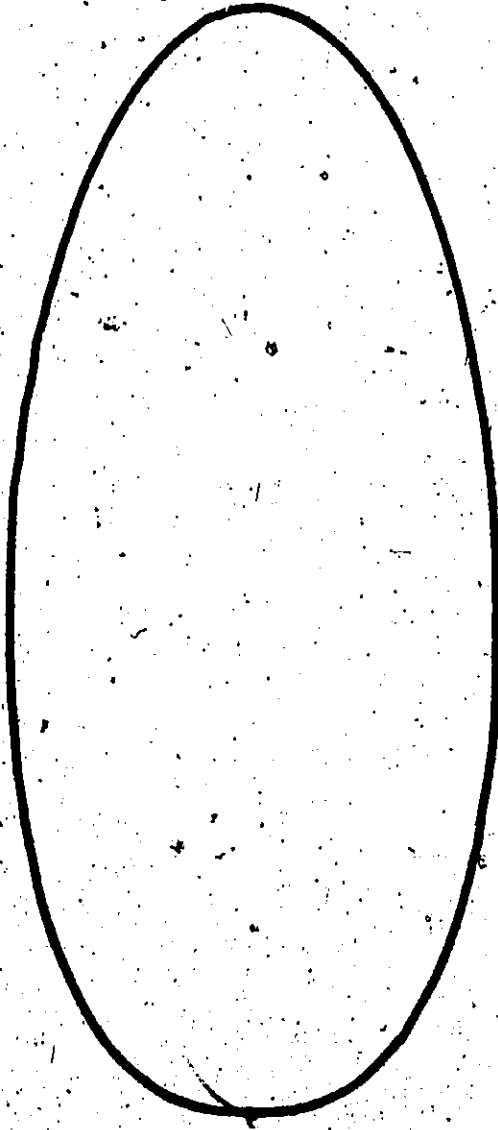


Figure 2.7: Shape of Envelope for

$n = 0.4, m = 0.5, \ell = 2.25$



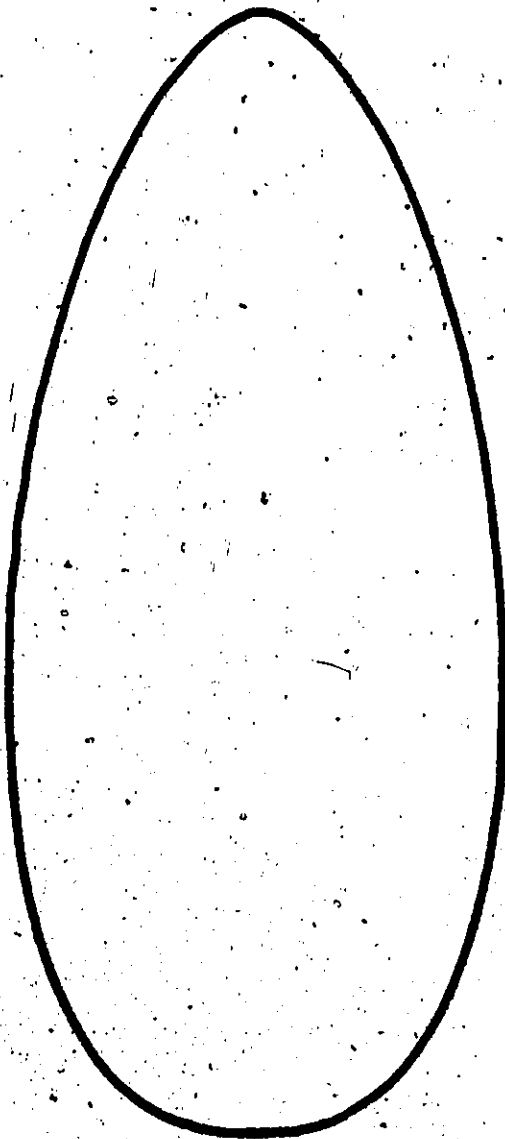


Figure 2.8: Shape of Envelope for

$n = 0.4$ ,  $m = 0.6$ ,  $r = 2.25$



Figure 2.9: Shape of Envelope for

$n = 0.2, m = 0.5, f = 2.50$

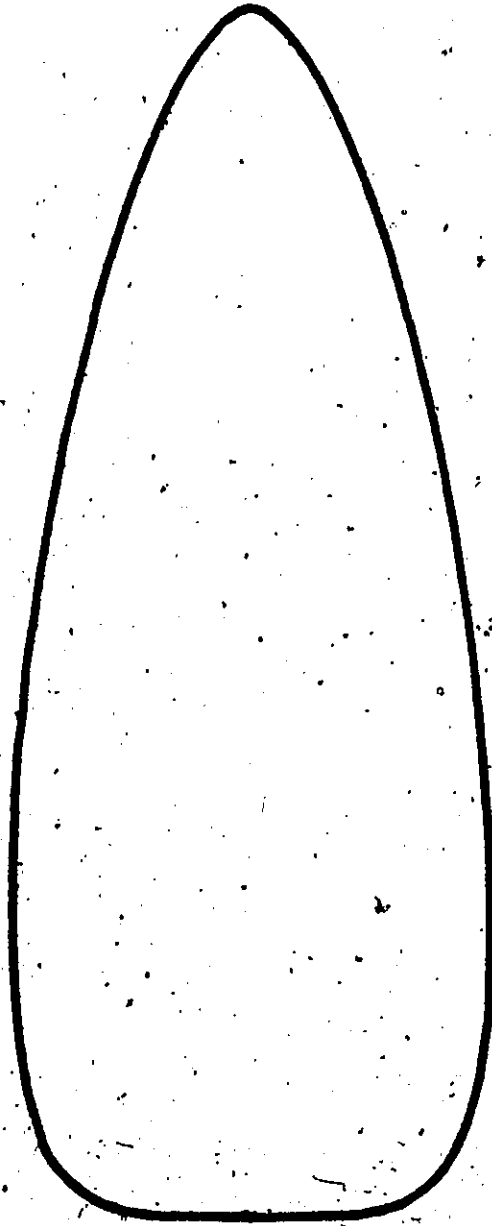


Figure 2.10: Shape of Envelope for  
 $n = 0.2, m = 0.6, r = 2.50$

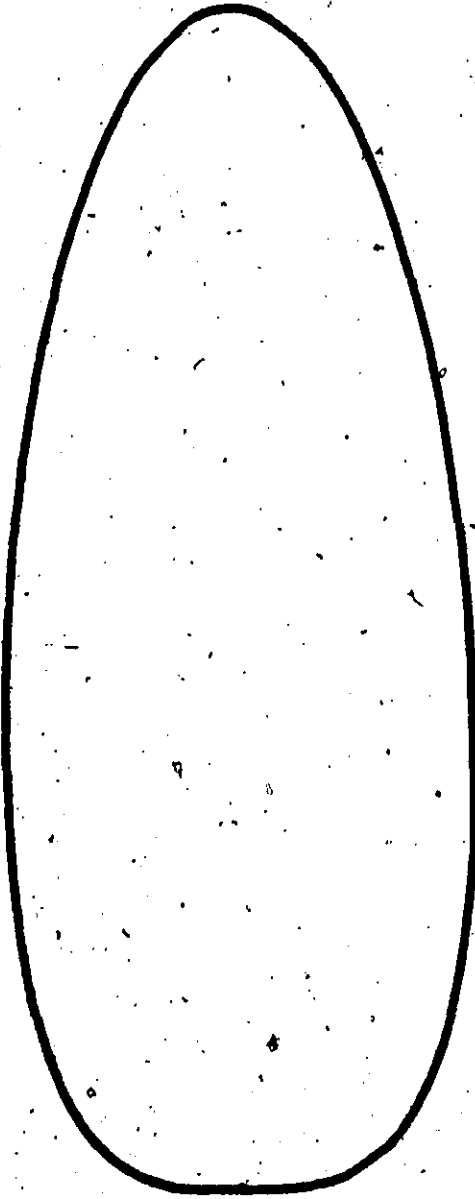


Figure 2.11: Shape of Envelope for

$n = 0.3, m = 0.5, r = 2.50$

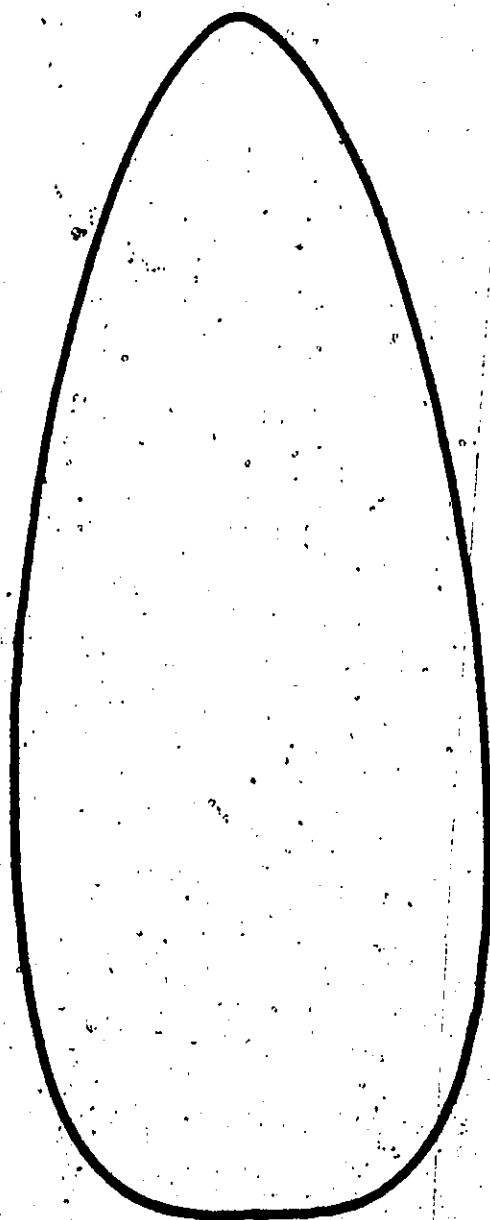


Figure 2.12: Shape of Envelope for

$n = 0.3, m = 0.6, f = 2.50$

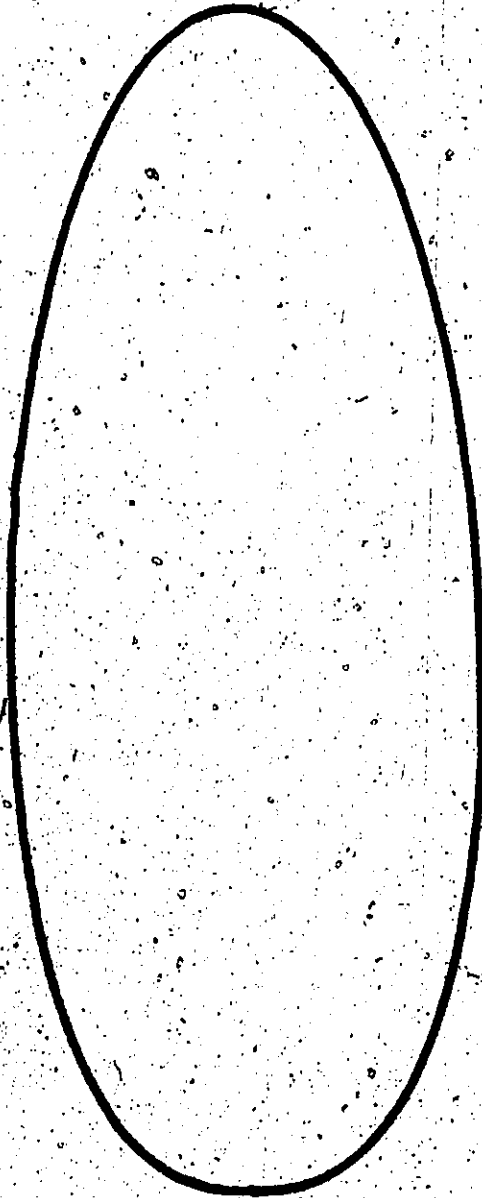


Figure 2.13: Shape of Envelope for

$$n = 0.4, m = 0.5, f = 2.50$$

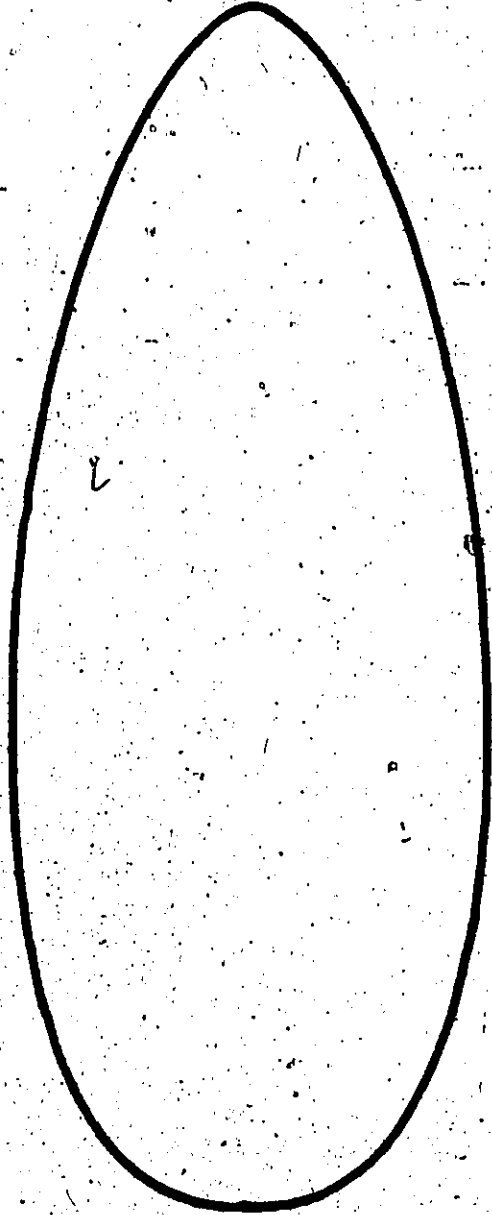


Figure 2.14: Shape of Envelope for

$n = 40.4, m = 0.6, r = 2.50$

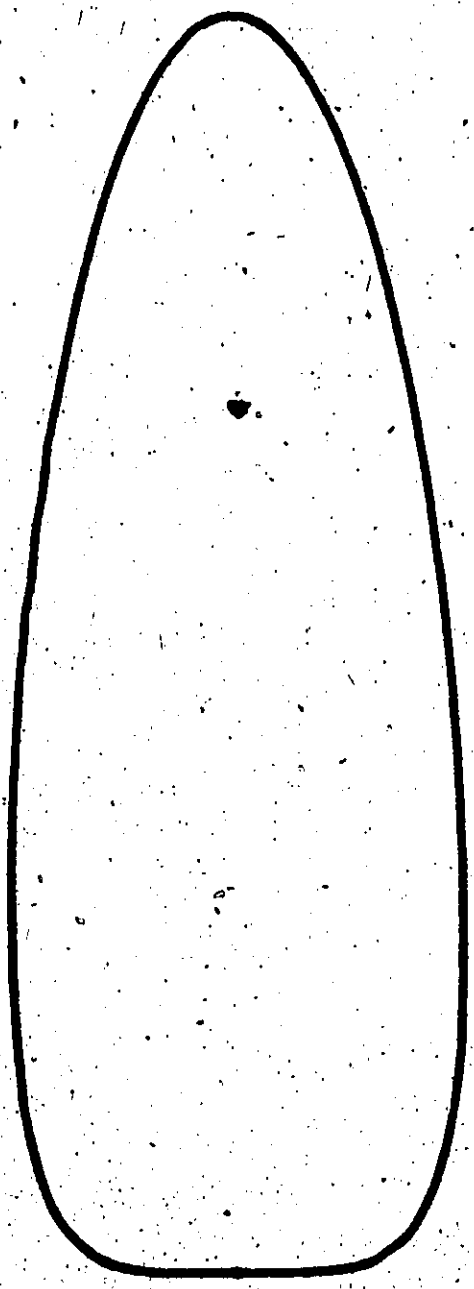


Figure 2.15: Shape of Envelope for

$n = 0.2, m = 0.5, r = 2.75$





Figure 2.16: Shape of Envelope for

$n = 0.2, m = 0.6, r = 2.75$

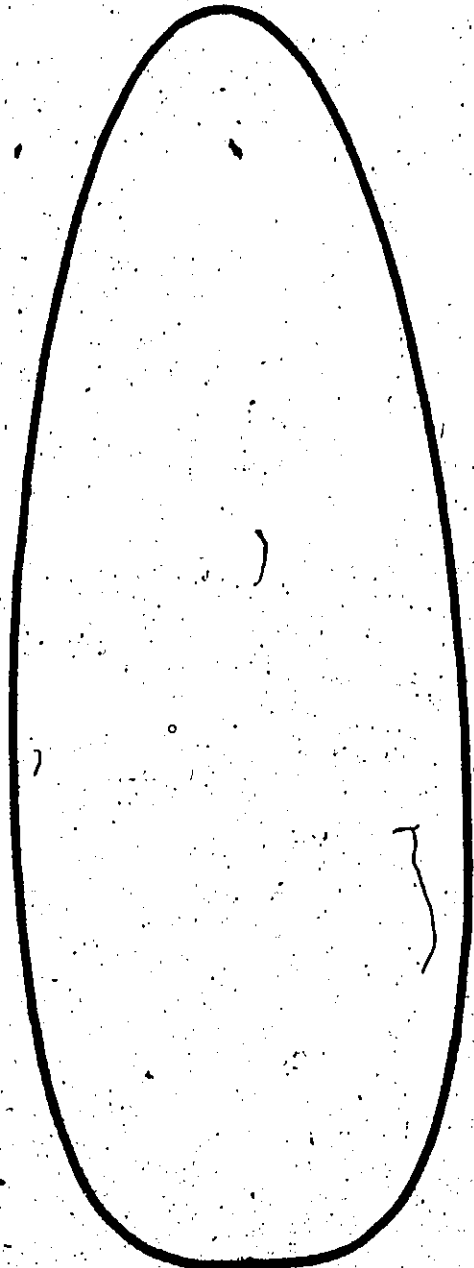


Figure 2.17: Shape of Envelope for  
 $n = 0.3, m = 0.5, f = 2.75$



Figure 2.18: Shape of Envelope for

$n = 0.30, m = 0.6, r = 2.75$



Figure 2.19: Shape of Envelope for

$n = 0.400, m = 0.50, f = 2.75$

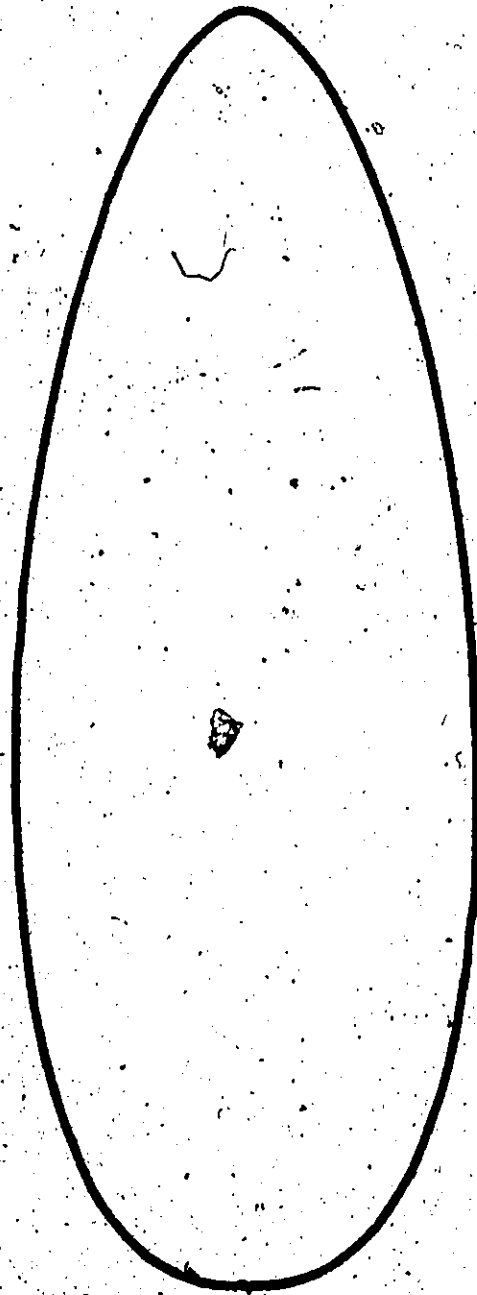


FIGURE 2.20: Shape of Envelope for

$n = 0.4, m = 0.6, f = 2.75$

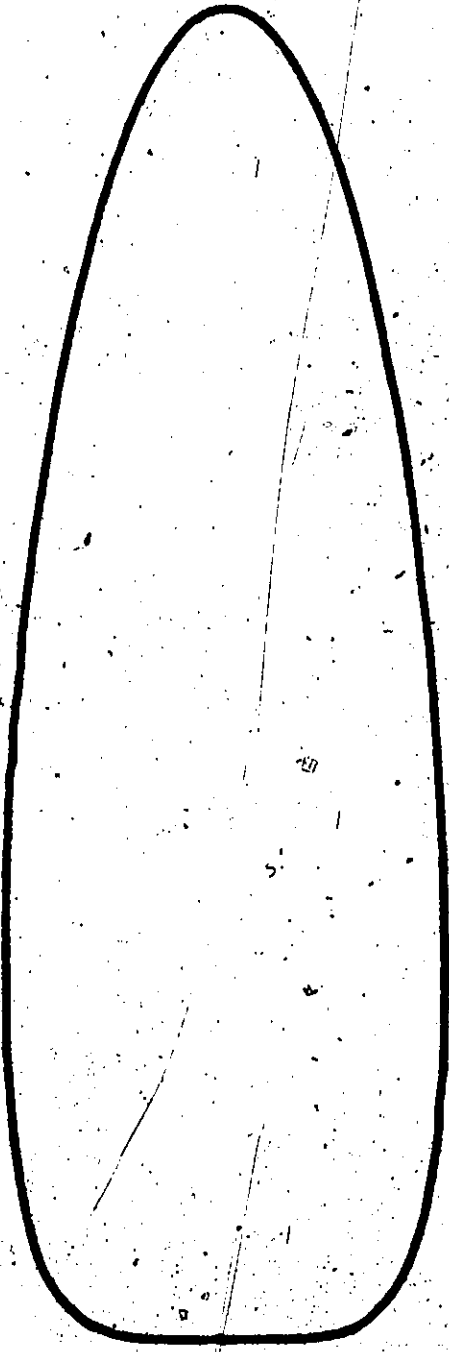


FIGURE 2.21: Shane of Envelope for

$n = 0.2, m = 0.5, f = 3.00$

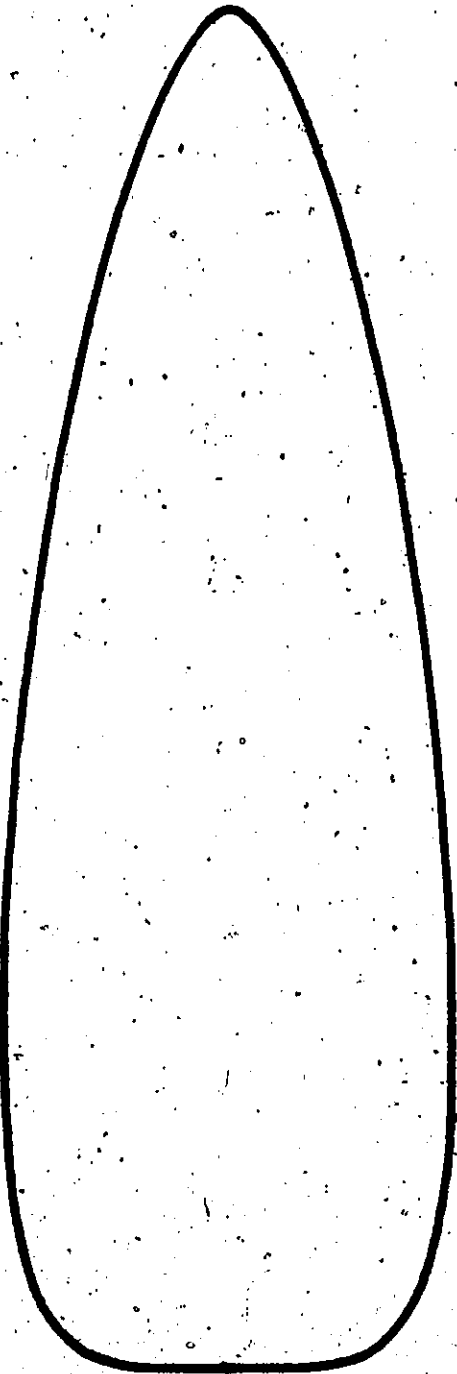


Figure 2.22: Shape of Envelope for  $n = 0.2, m = 0.6, f = 3.0$

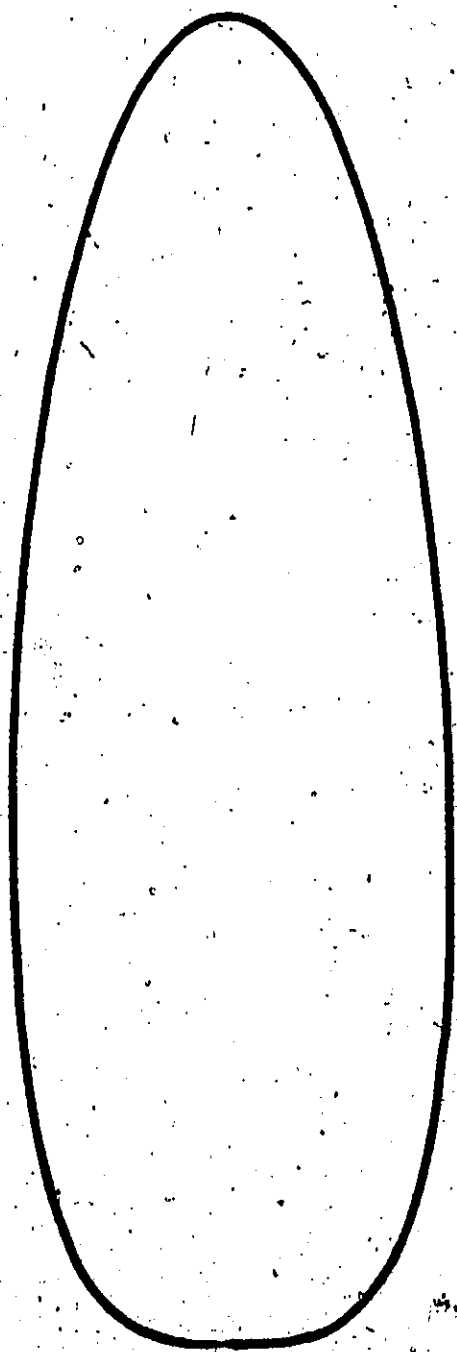


Figure 2.23: Shape of Envelope for

$n = 0.3, m = 0.5, r = 3.00$



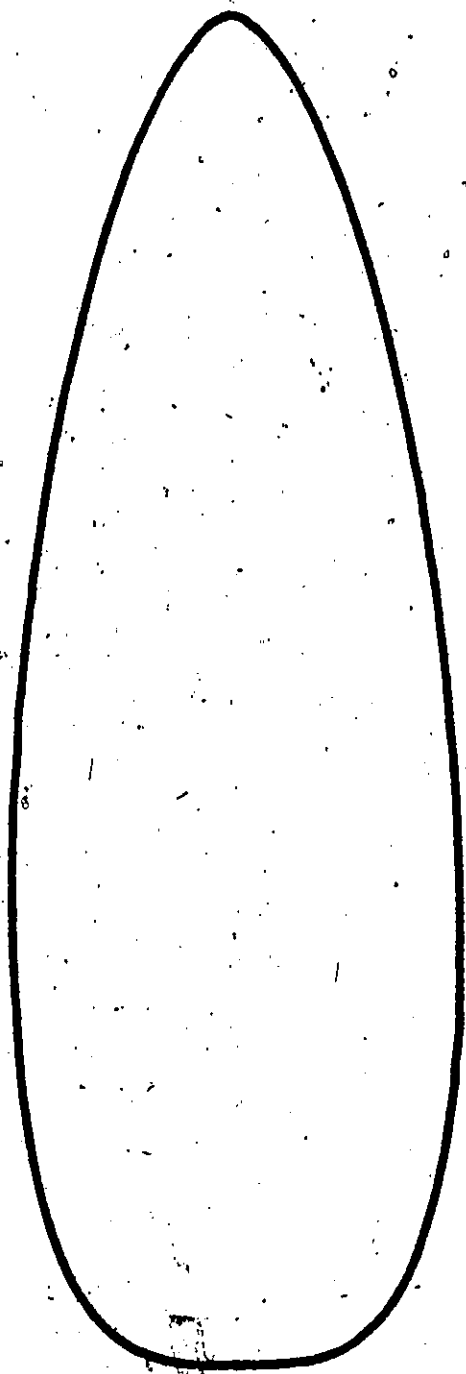


Figure 2.24: Shape of Envelope for

$n = 0.3, m = 0.6, r = 3.00$

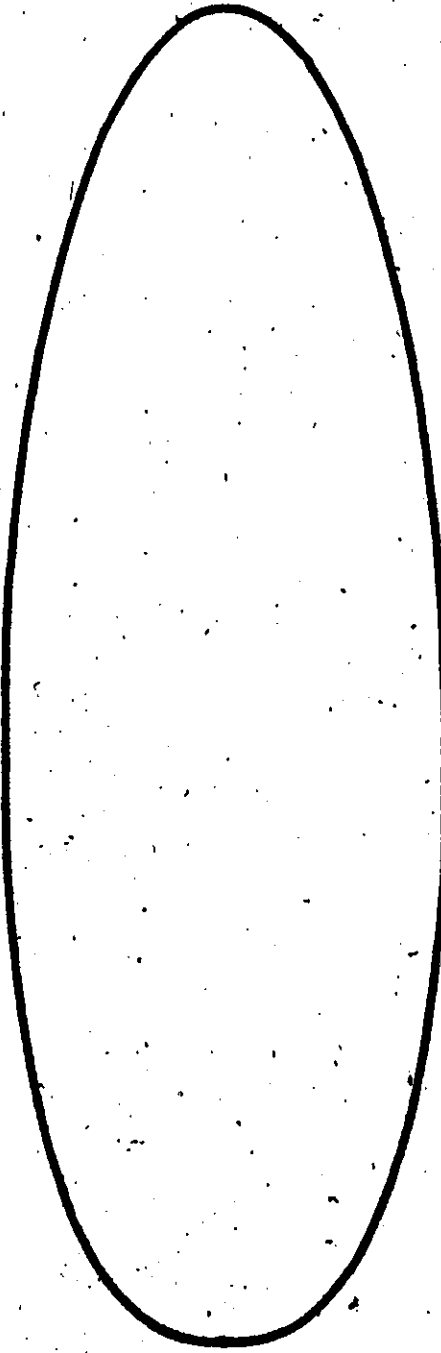


Figure 2.25: Shape of Envelope for

$n = 0.400, m = 0.500, r = 3.0$

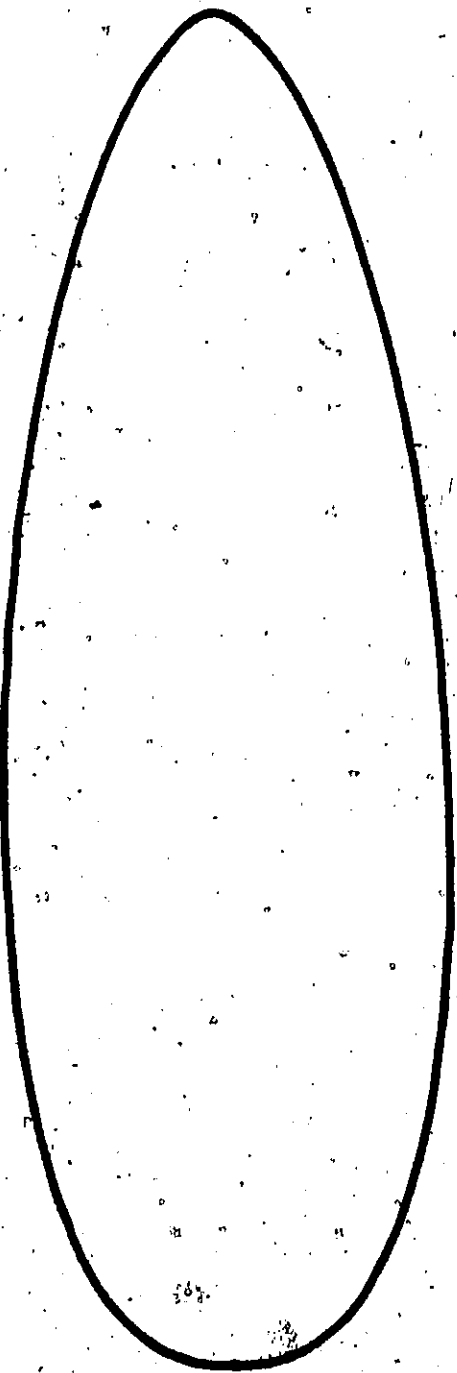


Figure 2.26: Shape of Envelope for

$n = 0.4, m = 0.6, r = 3.00$

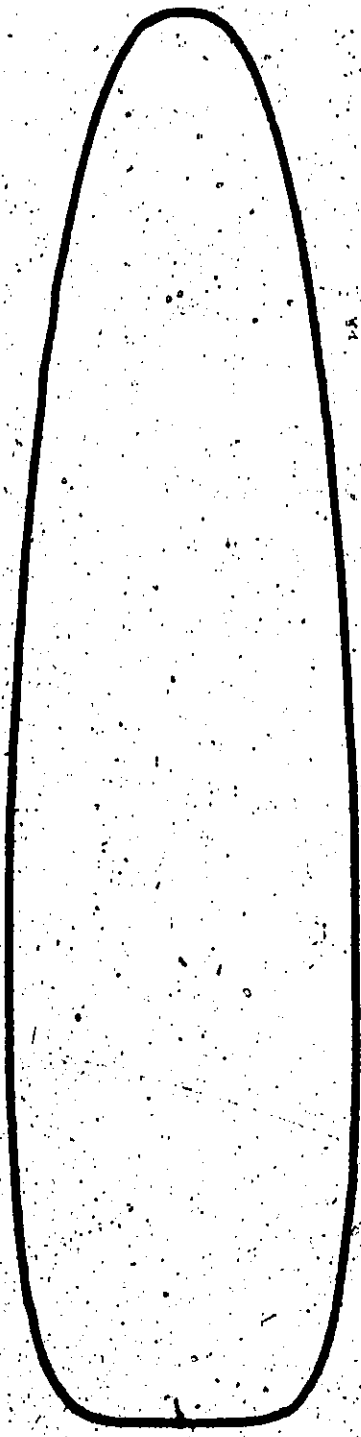


Figure 2.27: Shape of Envelope for

$$n = 0.185, m = 0.400, f = 4.00$$

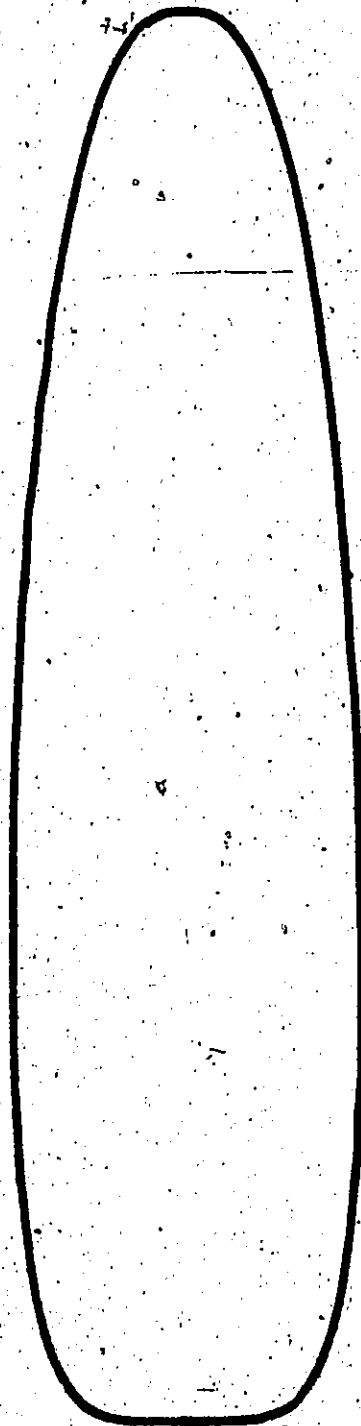


Figure 2.28: Shape of Envelope for

$$n = 0.200, m = 0.400, f = 4.00$$

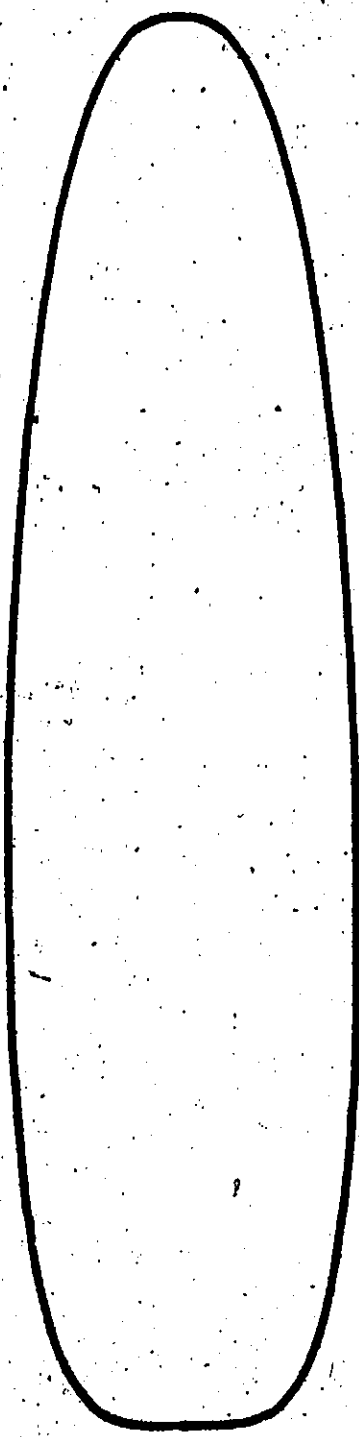


Figure 2.29: Shape of Envelope for  $n = 0.250, m = 0.400, r = 4.00$

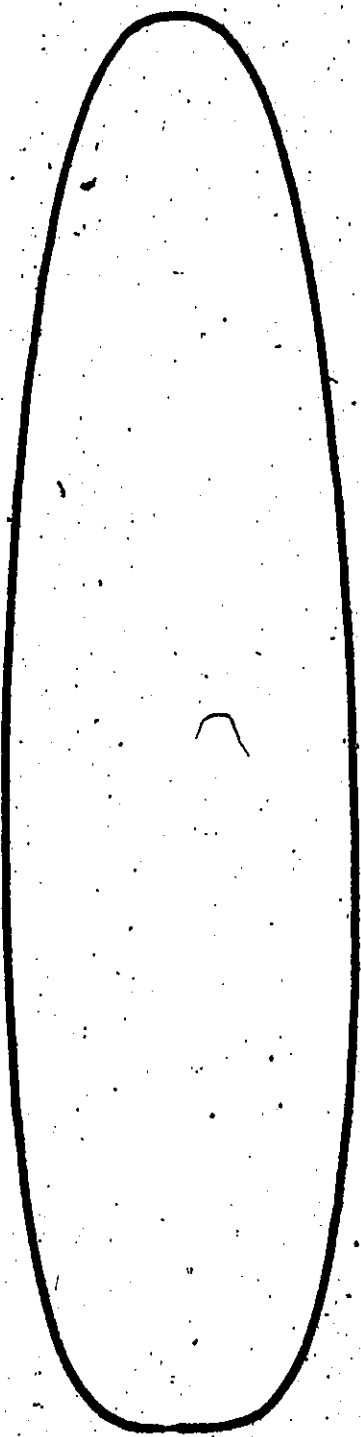


Figure 2.30: Shape of Envelope for

$n = 0.275, m = 0.400, r = 4.00$

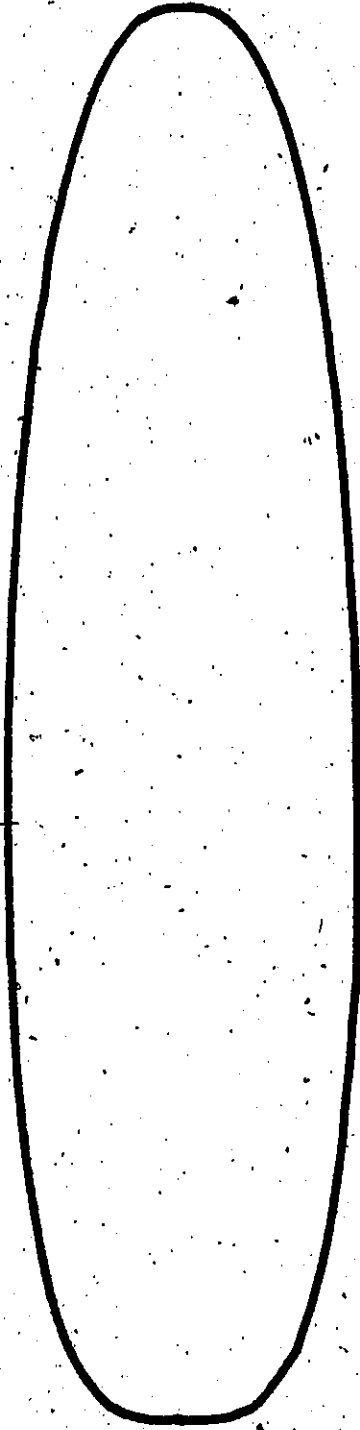


Figure 2.31: Shape of Envelope for

$$n = 0.300, m = 0.400, f = 4.00$$



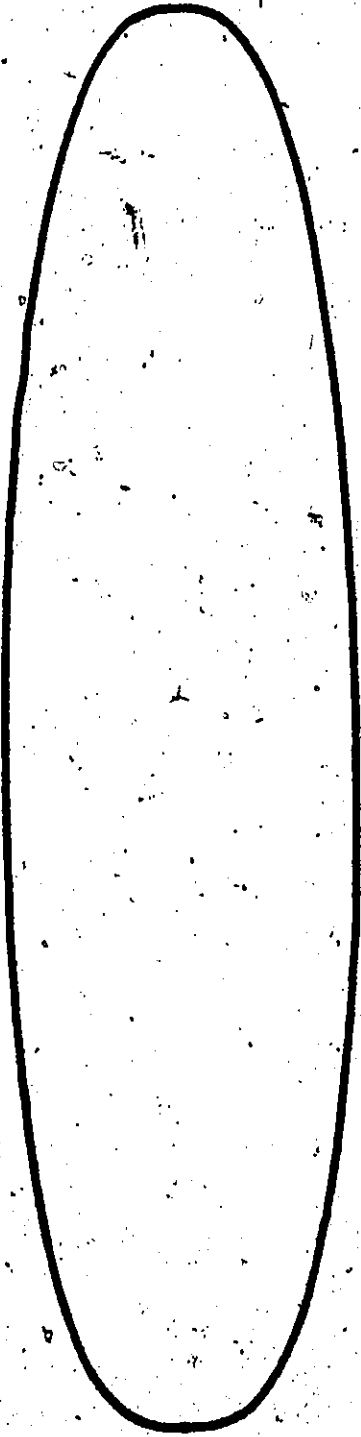


Figure 2.32: Shape of Envelope for

$n = 0.350, m = 0.400, r = 4.00$



Figure 2.33: Shape of Envelope for

$n = 0.375, m = 0.4, f = 4.00$

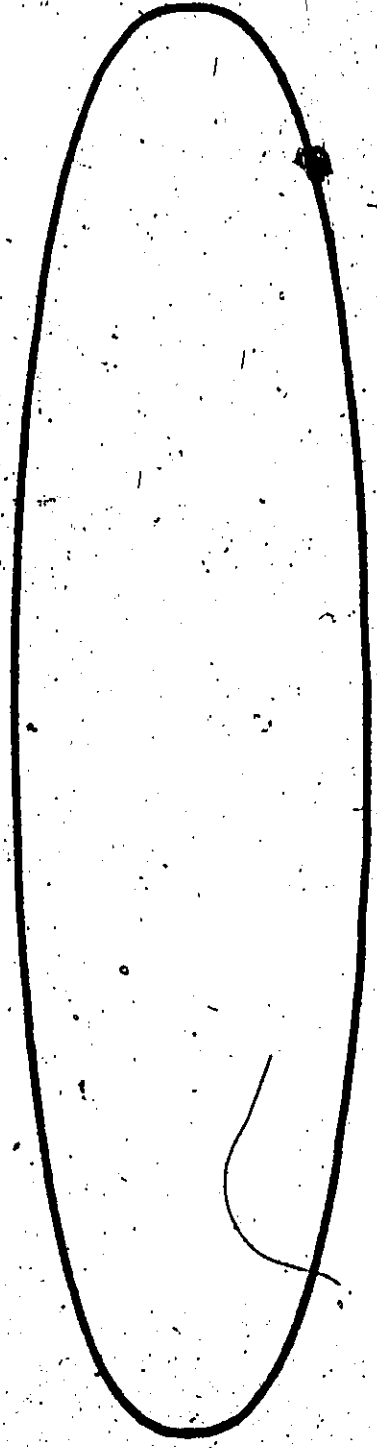


Figure 2.34: Shape of Envelope for

$n = 0.400, m = 0.40, f = 4.00$

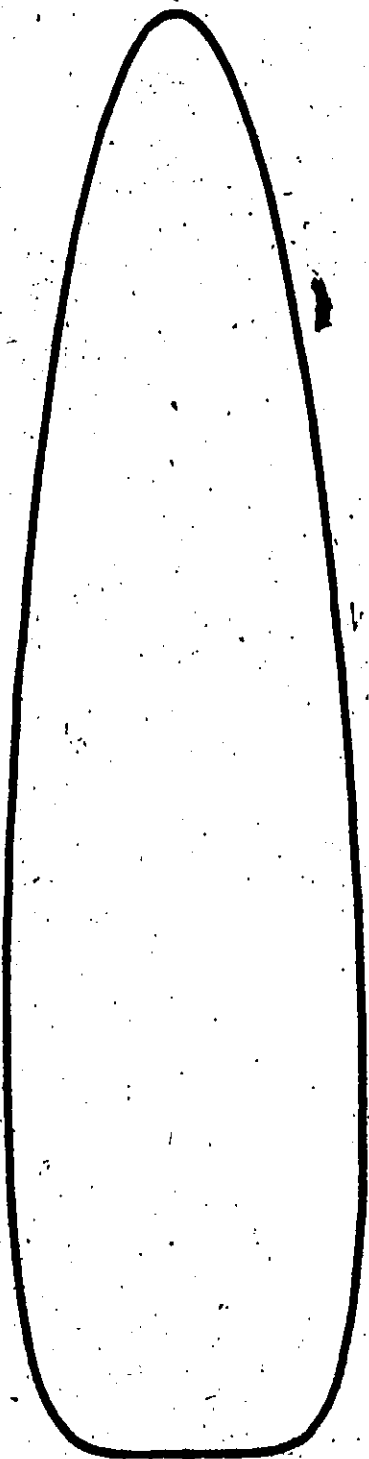


Figure 2.35: Shape of Envelope for

$n = 0.185, m = 0.5, f = 4.00$

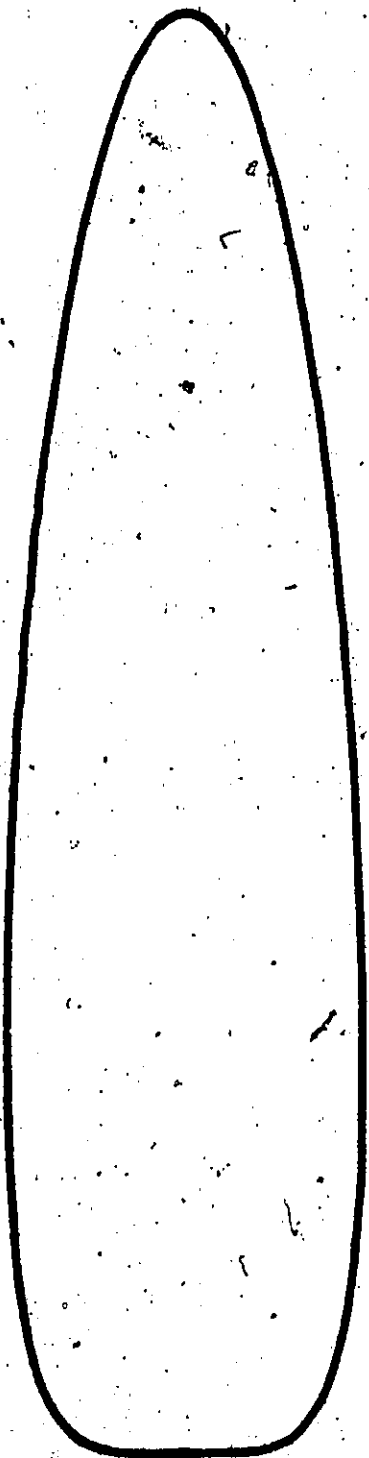


Figure 2.16: Shape of Envelope for  $n = 0.200, m = 0.5, f = 4.00$

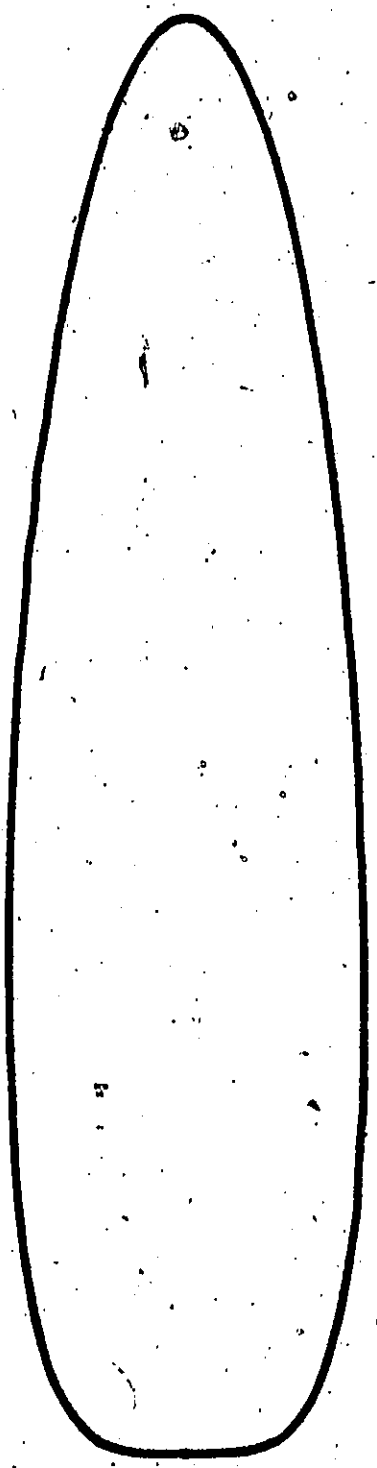


Figure 2.37: Shape of Envelope for

$n = 0.25, m = 0.5, r = 4.00$

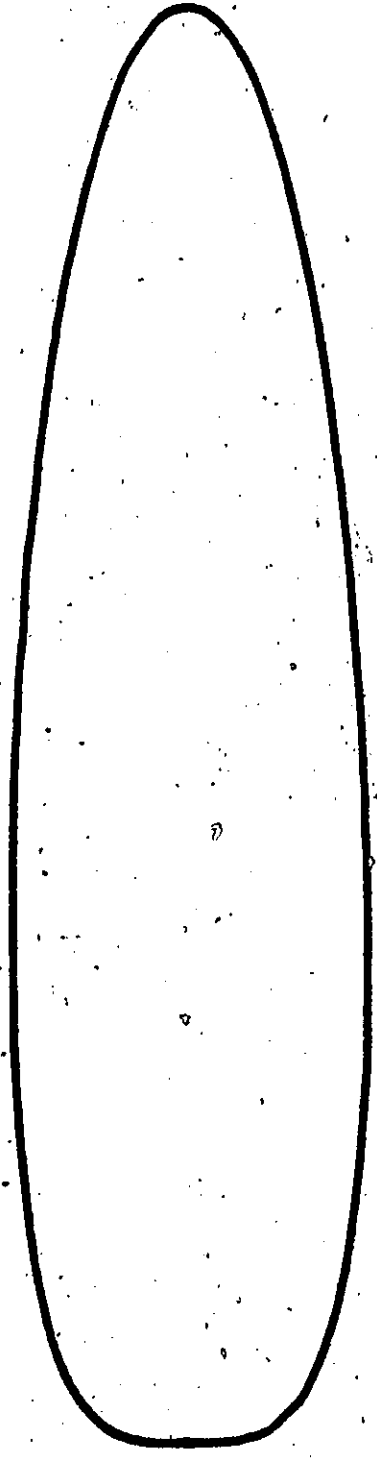


Figure 2.38: Shape of Envelope for

$n = 0.275, m = 0.5, f = 4.00$

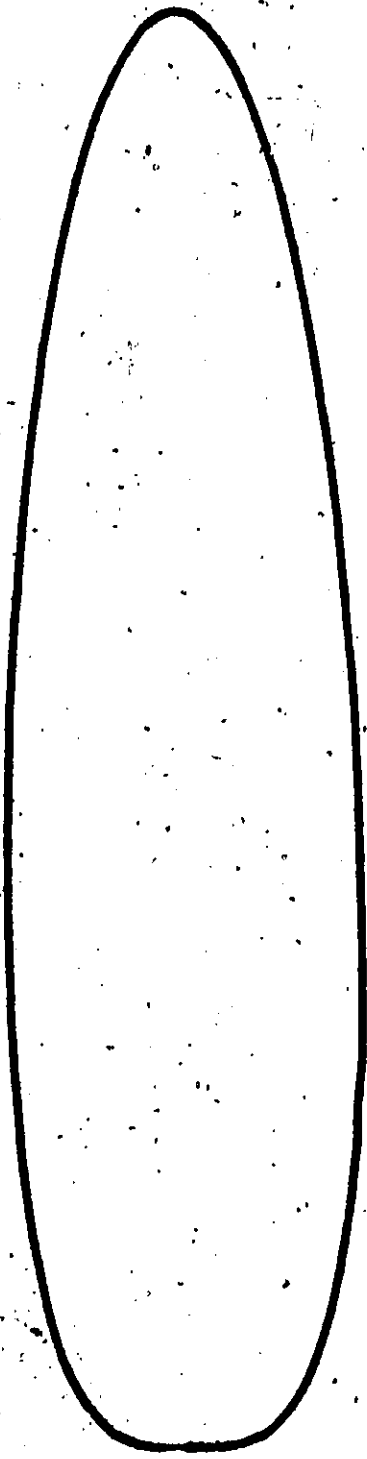


Figure 2.39: Shape of Envelope for

$n = 0.300, m = 0.5, f = 4.00$





Figure 2.40: Shape of Envelope for

$n = 0.350, m = 0.5, f = 4.00$



Figure 2.41: Shape of Envelope for

$n = 0.375, m = 0.5, r = 4.00$

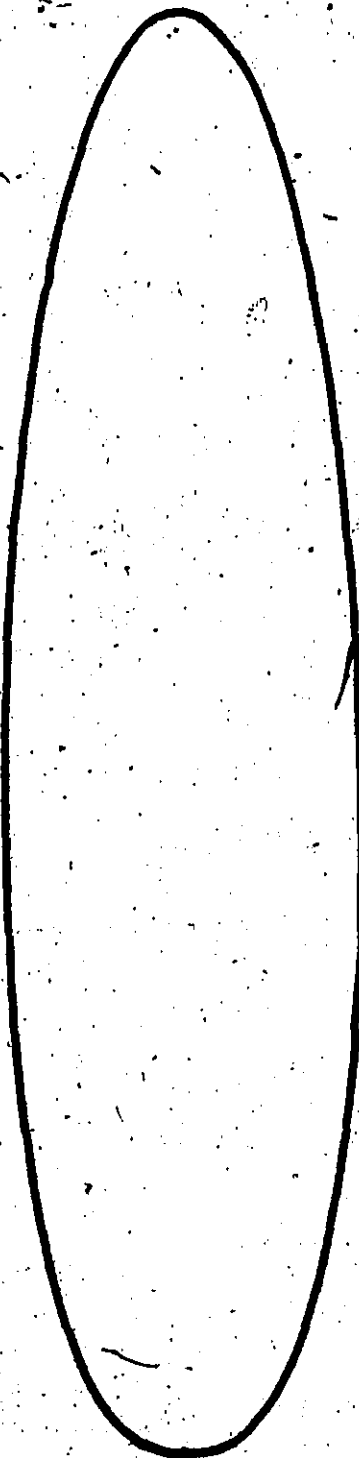


FIGURE 2.42: Shape of Envelope for

$n = 0.400, m = 0.5, r = 4.00$

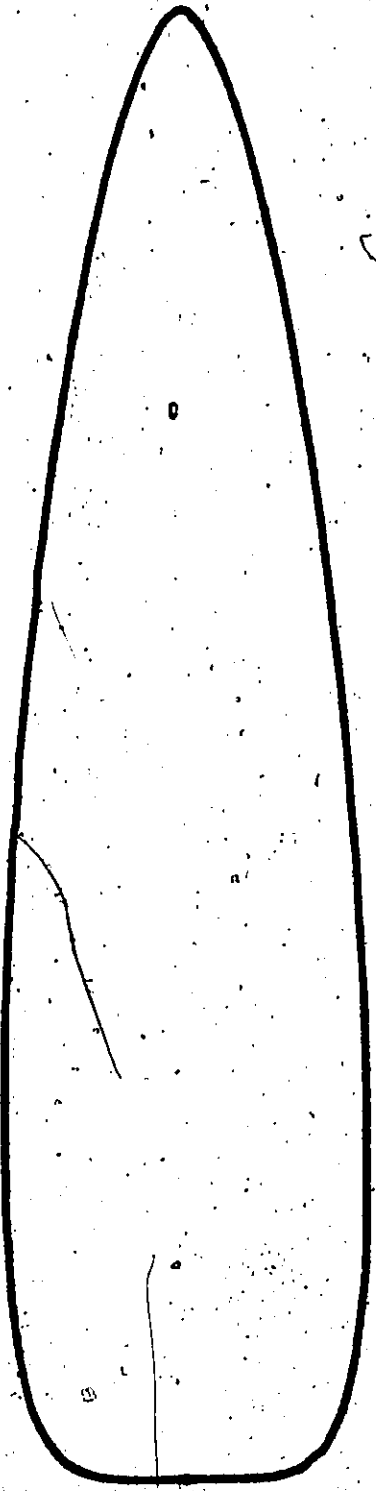


Figure 2.43: Shape of Envelope for

$n = 0.185, m = 0.6, f = 4.00$

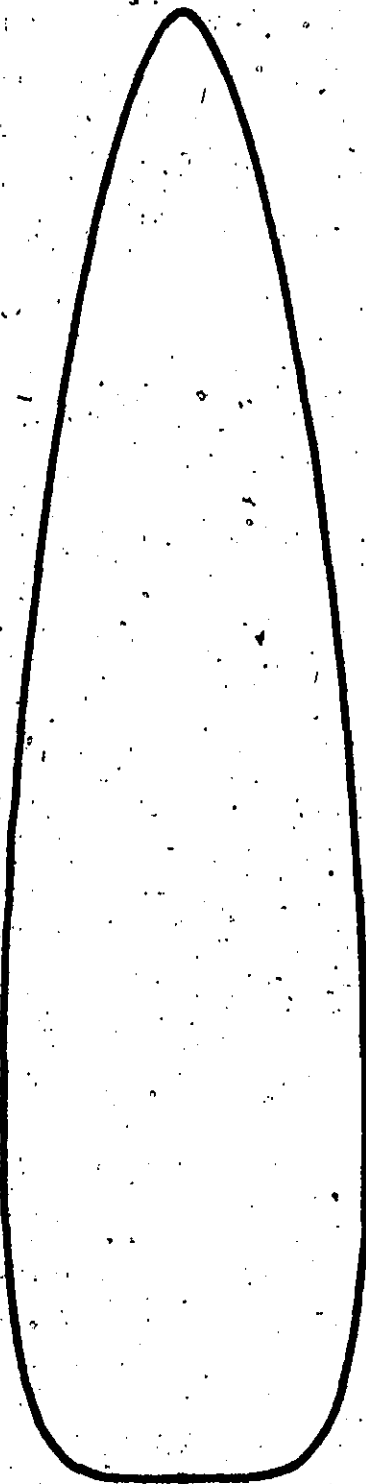


Figure 2.44: Shape of Envelope for

$n = 0.200$ ,  $m = 0.6$ ,  $r = 4.00$



Figure 2.45: Shape of Envelope for

$n = 0.275, m = 0.6, r = 4.00$

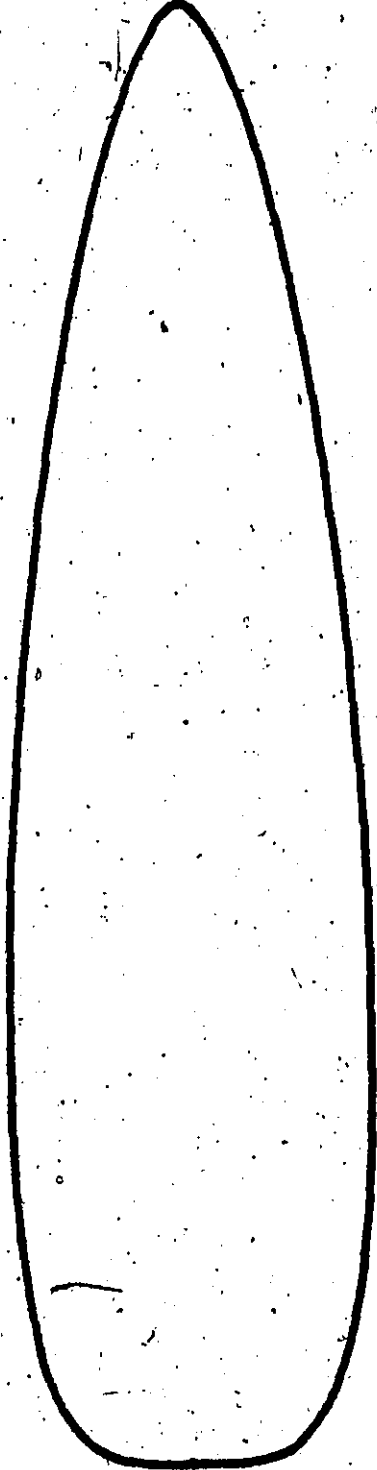


Figure 2.46: Shape of Envelope for  
 $n = 0.250, m = 0.6, r = 4.00$

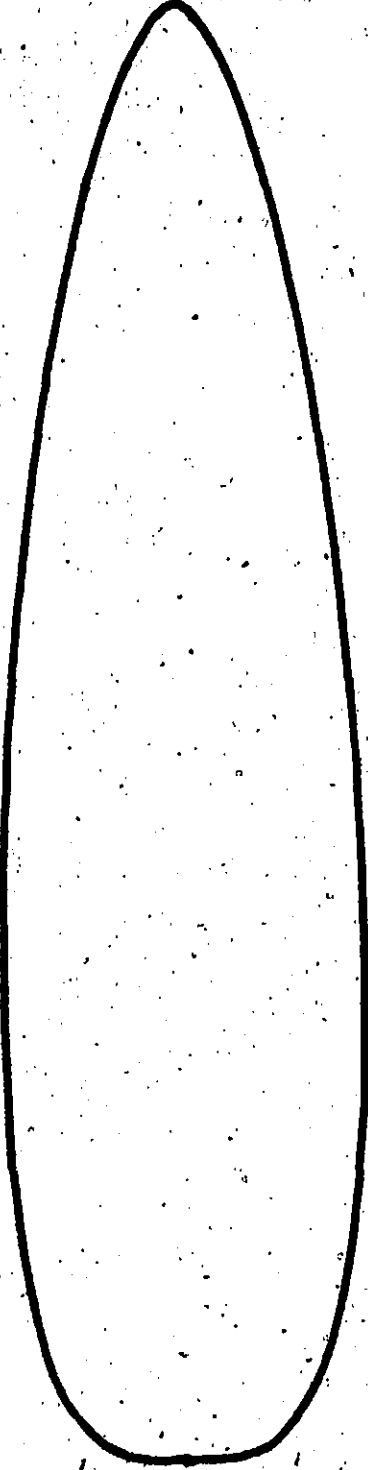


Figure 2.47: Shape of Envelope for

$n = 300, m = 0.6, f = 4.00$



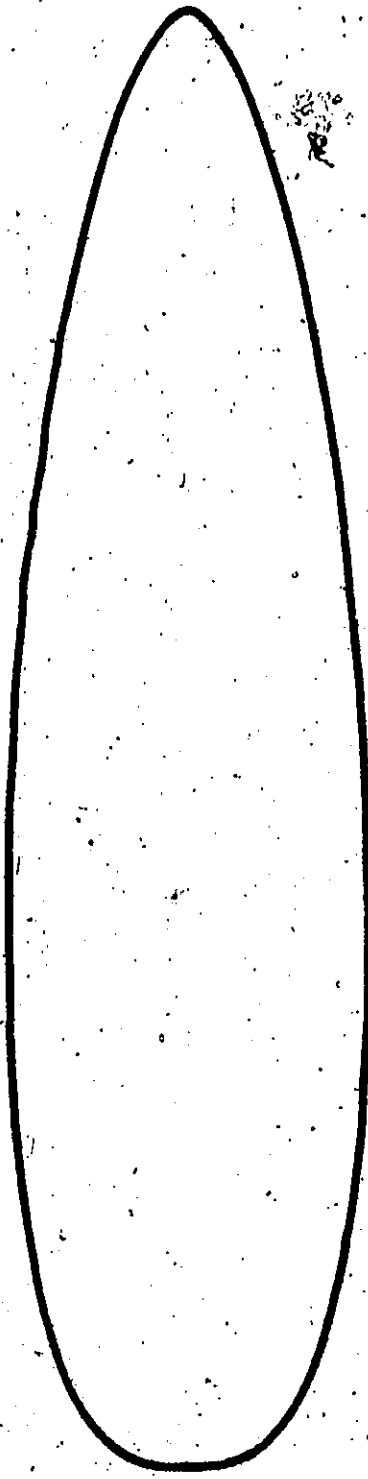


Figure 2.48: Shape of Envelope for

$n = 0.350, m = 0.60, r = 4.00$

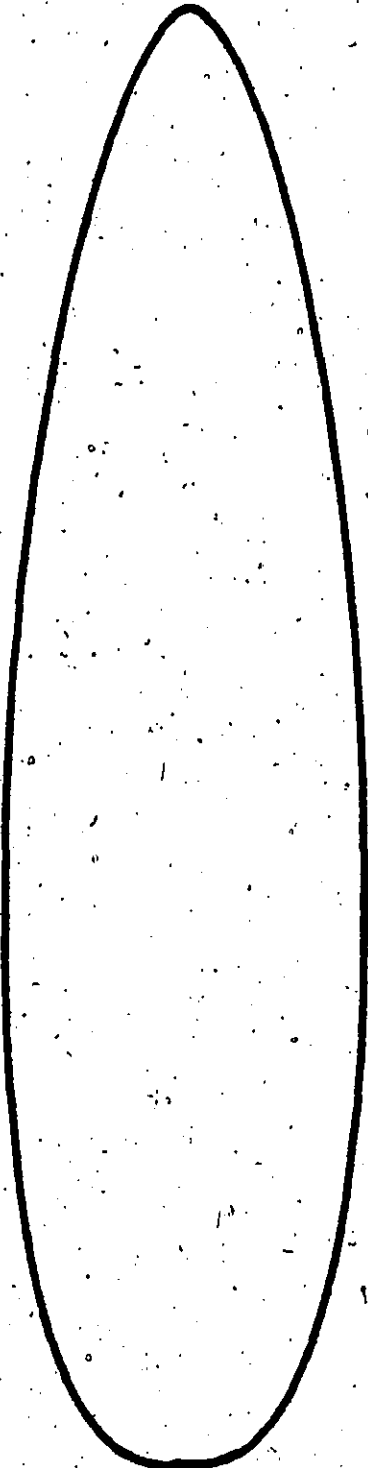


Figure 2.49: Shape of Envelope for  $n = 0.375$ ,  $m = 0.6$ ,  $f = 4.00$

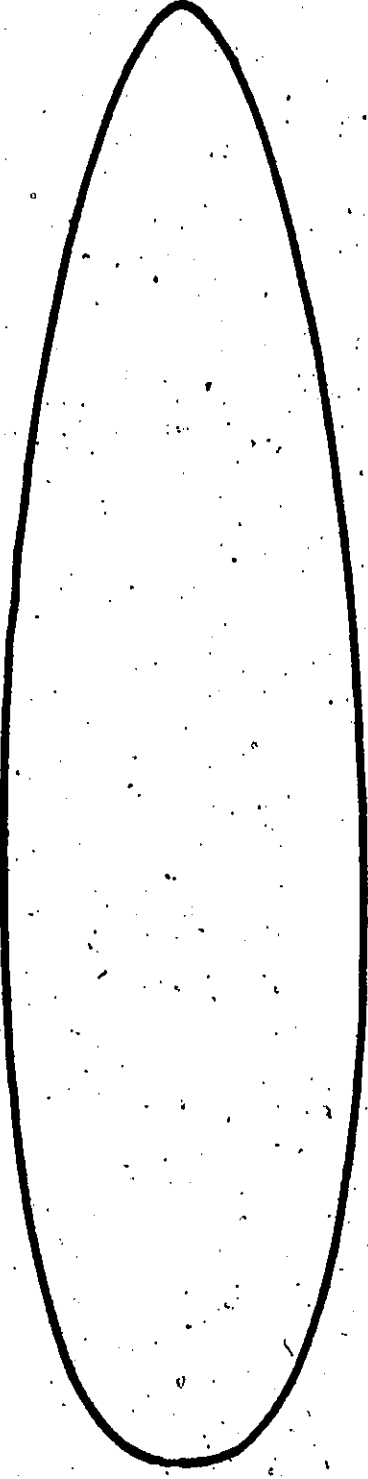


FIGURE 2.50: Shane of Envelope for

$n = 0.4, m = 0.6, r = 4.00$

TABLE 2.1: DESIGN PARAMETERS FOR VARIOUS AIRSHIP SHAPES WITH THE VELOCITY IN FEET PER SECOND = 110.00000, VOLUME IN CUBIC FEET = 91798.60 AND WITH ALL AREAS IN SQUARE FEET AND ALL DISTANCES IN FEET AND PRESSURE IS IN LBS/SQ. FT.

N	M	P	LENGTH	DRAO	ENVELOPE AREA	ENVELOPE CO.	ENVELOPE CU	HOOING BENDING MOMENT	AERO-DYNAMIC BENDING MOMENT	MINIMUM INTERNAL PRESSURE	FIXED VERTI-CAL FIN AREA	FIXED HORI-ZONTALE CONTROL AREA	ELEVA-TOR AREA	RUD-DER AREA	CENTRE OF TAIL SUR-FACE AREA LOCATION
.3	.4	2.5	100.2	1012.7	10488.0	48.3	47.2	15961.8	60957.6	4.8	493.7	383.3	144.4	72.5	77.3
.3	.5	2.5	101.8	1009.5	10483.3	47.3	45.2	16995.9	61921.8	4.7	486.1	377.3	142.2	71.4	75.8
.3	.6	2.5	103.5	1006.2	10467.1	46.4	43.6	18148.9	62946.2	4.5	478.1	371.2	139.9	70.2	74.7
.3	.7	2.5	105.2	1002.9	10441.2	45.6	42.1	19387.7	63994.0	4.4	470.3	365.1	137.6	69.1	73.7
.4	.4	2.5	101.1	1011.0	10494.0	50.5	50.5	16527.6	61490.8	4.7	489.5	379.9	143.2	71.9	80.9
.4	.5	2.5	102.3	1008.6	10490.1	49.4	48.4	17313.0	62208.6	4.6	483.8	375.6	141.5	71.1	79.2
.4	.6	2.5	103.6	1006.0	10476.0	48.4	46.6	18237.0	63022.5	4.5	477.6	370.7	139.7	70.1	77.8
.4	.7	2.5	105.0	1003.3	10453.1	47.4	45.0	19257.8	63886.5	4.4	471.1	365.7	137.8	69.2	76.6
.3	.4	3.0	113.2	875.7	11145.1	54.5	53.3	12517.2	68835.9	6.5	437.2	339.4	127.9	64.2	87.3
.3	.5	3.0	115.0	872.9	11140.1	53.4	51.1	13328.2	69924.8	6.3	430.4	334.1	125.9	63.2	85.6
.3	.6	3.0	116.9	870.1	11122.9	52.4	49.2	14232.3	71081.6	6.1	423.4	328.4	123.9	62.2	84.3
.3	.7	3.0	118.8	867.2	11095.4	51.5	47.5	15209.8	72264.7	5.9	416.5	323.3	121.8	61.2	83.2
.4	.4	3.0	114.2	874.1	11151.6	57.1	57.1	12960.9	69438.0	6.4	433.4	336.5	126.8	63.7	91.4
.4	.5	3.0	115.5	872.1	11147.4	55.8	54.7	13576.8	70248.6	6.3	428.4	332.6	125.3	62.9	89.4
.4	.6	3.0	117.0	869.8	11132.4	54.6	52.6	14301.4	71167.8	6.1	422.9	328.3	123.7	62.1	87.8
.4	.7	3.0	118.6	867.5	11108.1	53.6	50.8	15101.9	72143.4	5.9	417.2	323.8	122.0	61.3	86.5
.3	.4	4.0	137.1	760.2	12266.8	66.0	64.5	8529.5	83388.8	10.6	360.9	280.2	105.6	53.0	105.7
.3	.5	4.0	139.3	757.8	12261.3	64.7	61.9	9082.1	84707.8	10.2	355.3	275.8	103.9	52.2	103.7
.3	.6	4.0	141.6	755.3	12242.4	63.5	59.6	9698.2	86109.2	9.9	349.5	271.3	102.2	51.3	102.1
.3	.7	4.0	143.9	752.8	12212.1	62.4	57.6	10360.2	87542.5	9.6	343.8	266.9	100.6	50.5	100.8
.4	.4	4.0	138.3	758.9	12273.9	69.1	69.1	8831.8	84118.2	10.4	357.8	277.7	104.7	52.6	110.7
.4	.5	4.0	139.9	757.1	12269.3	67.5	66.3	9251.5	85100.1	10.1	353.7	274.5	103.4	51.9	108.3
.4	.6	4.0	141.7	755.1	12252.8	66.1	63.8	9745.3	86213.6	9.9	349.1	271.0	102.1	51.3	106.4
.4	.7	4.0	143.7	753.1	12226.0	64.9	61.6	10290.8	87395.5	9.6	344.4	267.3	100.7	50.6	104.7

Various empirical equations have been developed over the years. Goodyear<sup>[23]</sup> for non-rigid airships suggests

$$\text{DRAG} = \frac{1}{2} \rho V \left[ (.289) \left[ \frac{V_K V^{1/3}}{\gamma} \right]^{-.154} V^{2/3} + 19.7 + 0.0000003 V - \frac{50}{(0.00001 V^2)} \right] \quad (2.6)$$

where  $\rho$  = density of air in slugs/ft<sup>3</sup>

$V$  = velocity in ft/sec.

$V$  = volume of the airship in ft<sup>3</sup>

$V_K$  = airship velocity in KNOTS

$\gamma$  = kinematic viscosity of air in ft<sup>2</sup>/sec

General Mills<sup>[28]</sup> has developed

$$\text{DRAG} = \frac{20.0 \cdot 233}{10^6 (\delta_{SL})^{.617}} V^{1.85} L^{.617} (3.6 + \delta_{SL} \sigma) + .0025 \rho V^2 \quad (2.7)$$

where  $\sigma = \rho / 0.002377$

$\delta_{SL}$  = unit lift of the gas at sea level  $\left( \frac{\text{lbs.}}{\text{ft.}} \right)$

$L$  = net static lift (lbs.)

Kleiner<sup>[4]</sup> has developed, based on developments by Hoerner<sup>[29]</sup>,

$$\text{DRAG} = 0.5 \rho V^{1.86} C_f \left( 1 + \frac{1}{2f} \right) \left( 4 f^{1/3} + 6 \left( \frac{1}{f} \right)^{1.2} + 24 \left( \frac{1}{f} \right)^{2.7} \right) \frac{V^{2/3}}{0.40} \quad (2.8)$$

where  $C_f = \frac{0.074}{(V L \rho / \gamma)^{1/5}}$

A comparison of these equations, which only predict the drag due to level flight, is shown in Figure 2.51. It can be seen that (2.8) provides the most conservative estimate of the drag. In view of the fact that many previous airships have been underpowered (2.8) would seem to be the expression to be used. It must also be remembered that flight at any angle of attack also produces an extra drag. This need not be of concern at this stage of the design and an appropriate expression will be developed in Chapter 3.

### 2.3.2 Surface Area

The provision of a value for the surface area of the envelope is difficult. No exact expressions are available. General Mills<sup>[28]</sup> gives

$$A \approx \frac{\pi(n+\eta)(n+\pi)}{\pi^n \pi^m} \frac{\pi(n+1)\pi(m+1)}{\pi(n+\eta+2)} L^2 \quad (2.9)$$

The area as given by (2.9) is only an approximate value and is suitable only for use over a particular range of  $f$  values. If  $f = 1$  and (2.9) is used to find the area of a sphere, the value that results is about 20% lower than the actual value. This error decreases rapidly as the value of  $f$  increases.

### 2.3.3 Center of Bouyancy

The location of the center of bouyancy is of major importance to the airship designer. It is about this point

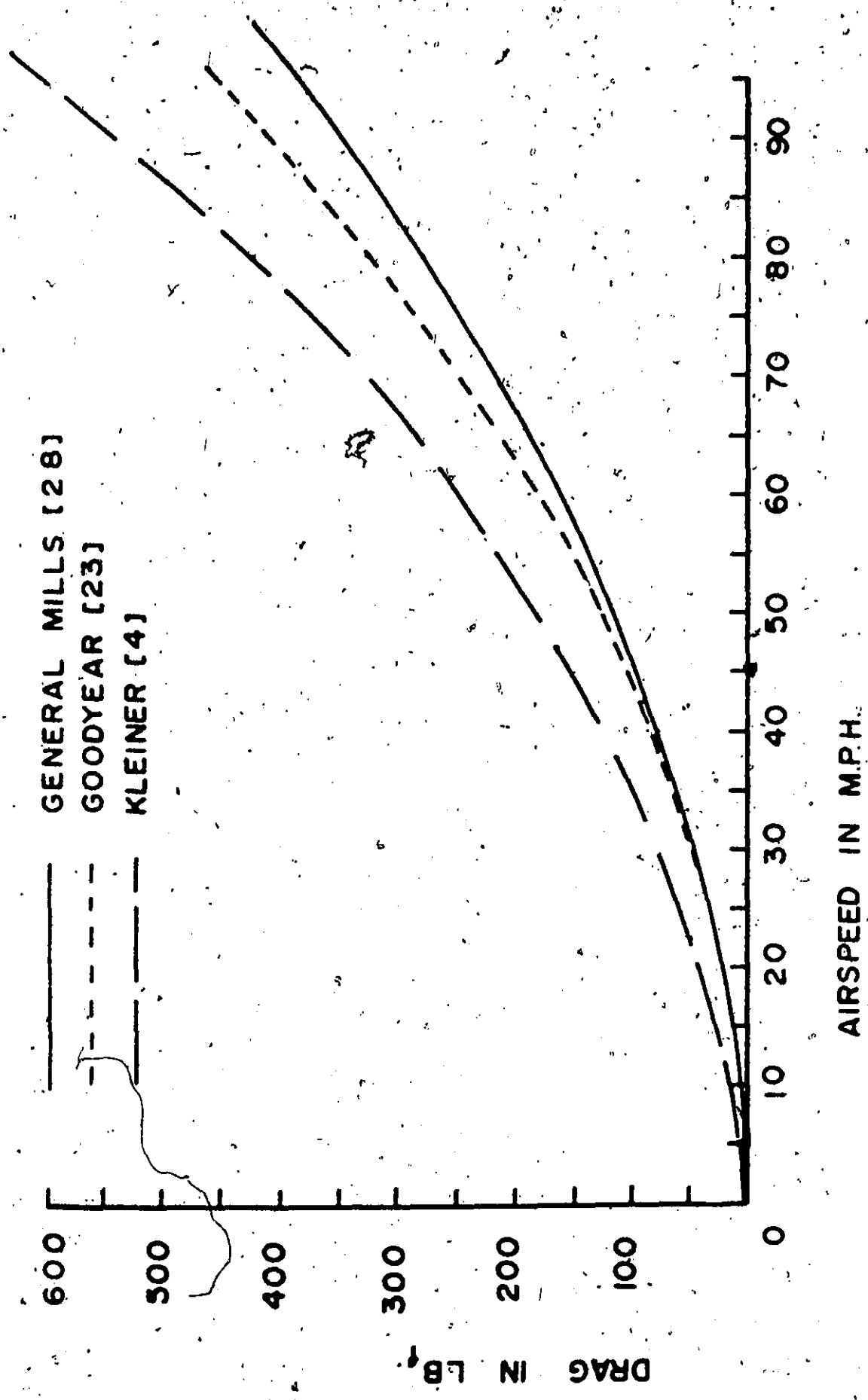


Figure 2.51: A Comparison of three Drag Equations

DRAG IN LB.

AIRSPEED IN M.P.H.

that the designer must balance all the other elements of the airship. An exact definition of this position is presented in Chapter 3. A convenient expression given for the position of the center of Bouvance,  $CB_x$ , along the longitudinal axis by General Mills<sup>[28]</sup> is:

$$CB_x = \frac{2n + 1}{2n + 2m + 2} L \quad (2.10)$$

#### 2.3.4 Center of Gravity of the Envelope

This position again is of great importance to the designer in trying to balance all the elements of the airship about the center of bouyancy. General Mills<sup>[28]</sup> gives the location of the center of gravity of the envelope,  $CGE_x$ , along the longitudinal axis as:

$$CGE_x = \frac{n + 1}{n + m + 2} L \quad (2.10)$$

#### 2.3.5 Control Surfaces; Location and Size

The correct prediction of the control surface area and location is also of importance. Airships designed to date all have control surface designs based on empirical expressions. This may seem rather a crude method of design. However, as long as an airship uses no modern aerodynamic refinements such as boundary layer control or blown surfaces, there seems to be, fortunately, a large margin of control surface size within which the stability is satisfactory, for nearly all



airships built have been found to possess satisfactory stability [33]. In this case the major function of the designer is to use all possible data to design surfaces of minimum size and hence minimum weight. Several expressions have been suggested. Munk [33] suggests that  $A_{cs}$ , the control surface area, can be found from

$$A_{cs} = C_1 C_2 C_3 S_{max} \quad (2.12)$$

where  $C_1$ ,  $C_2$ , and  $C_3$  are factors determined by secondary dimensions and  $S_{max}$  is the maximum cross-sectional area of the airship.

Burgess [13] gives

$$A_{cs} = 0.13 V^{2/3} \quad (2.12)$$

and Blakemore [12] has developed an empirical method based on data from previously satisfactory designs. Figures 2.52, 2.53, and 2.54 are used to determine the correct location and size. Figure 2.52 is a plot of  $\sqrt[3]{A_H L}$  and  $\sqrt[3]{A_V L}$  versus  $\sqrt[3]{V}$ . Figure 2.53 is a plot of  $\sqrt[3]{A_E L}$  and  $\sqrt[3]{A_R L}$  versus  $\sqrt[3]{V}$ . Figure 2.54 is a plot of  $\sqrt[3]{A \cdot C^3}$  versus  $\sqrt[3]{V}$ . The factors involved are:

$A_H$  = fixed horizontal surface area

$A_V$  = fixed vertical surface area

$A_E$  = elevator area

$A_R$  = rudder area

$V$  = total airship volume

$L$  = airship length

$C$  = distance between the center of buoyancy and the

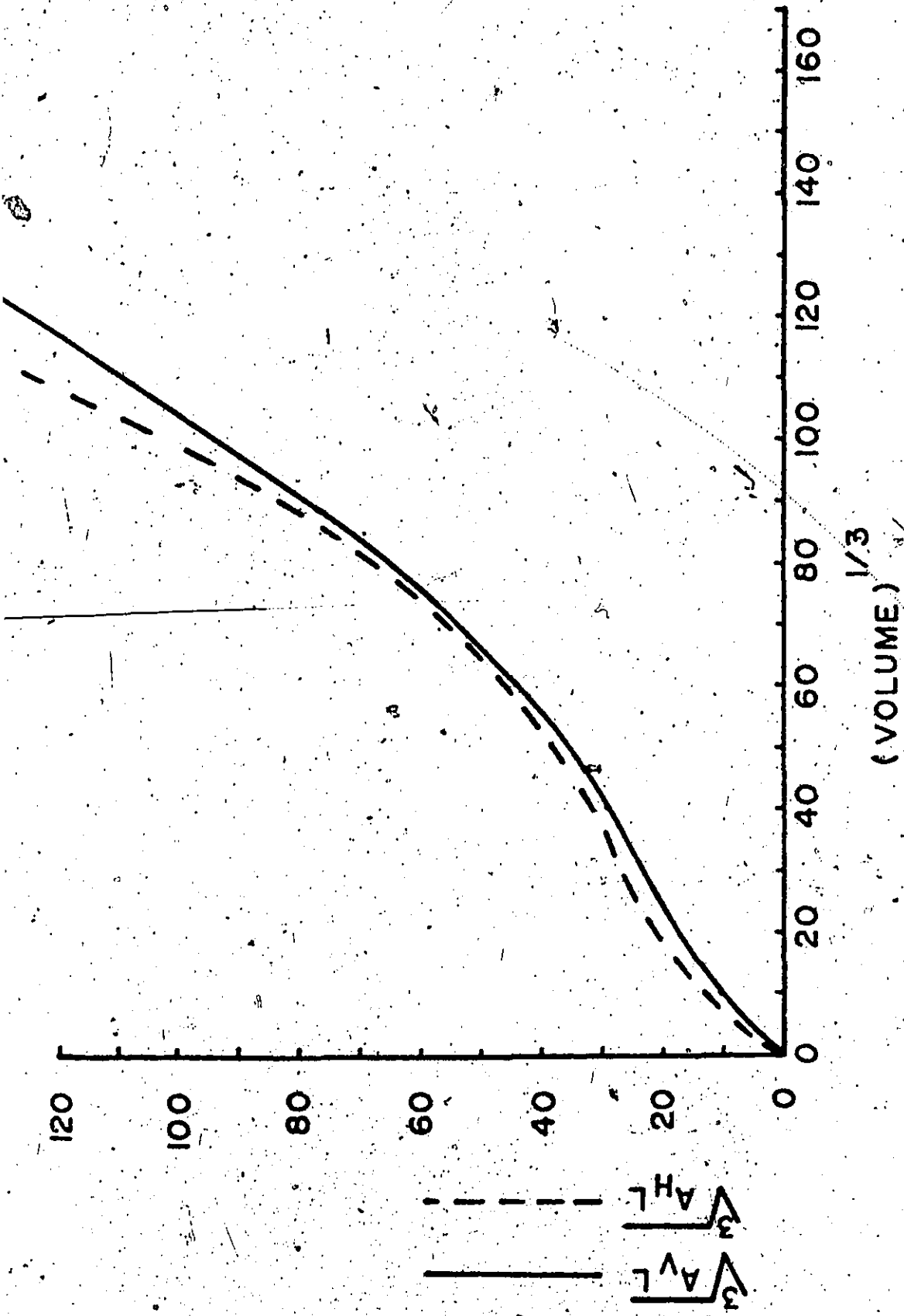


Figure 2.52: Control Surface Chart  $\sqrt[3]{A_{H L}}$  and  $\sqrt[3]{A_{V L}}$  vs.  $\sqrt[3]{V}$

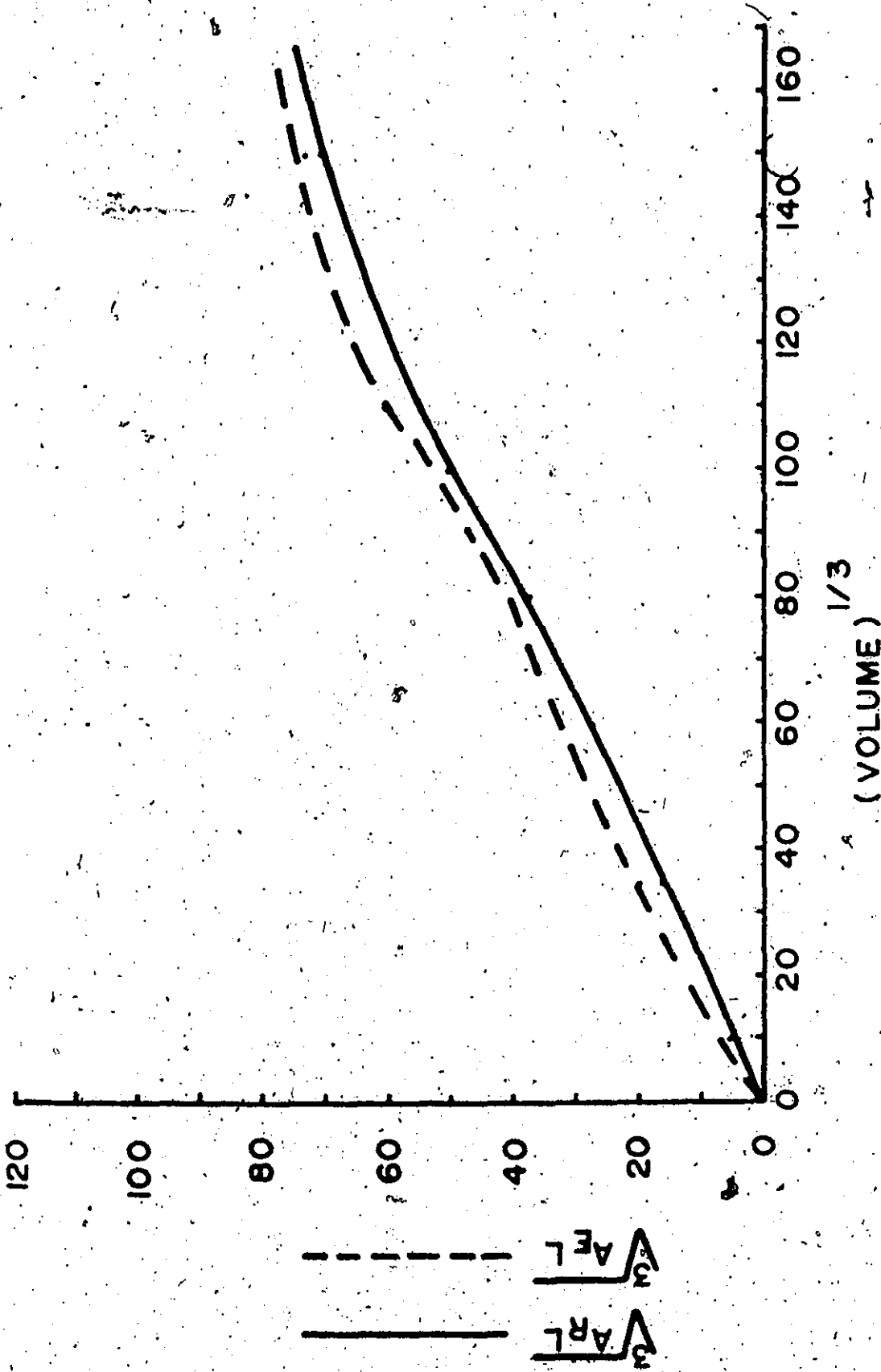


FIGURE 2.53: Control Surface Chart  $\sqrt[3]{A_{EL}}$  and  $\sqrt[3]{A_{RL}}$  vs.  $\sqrt[3]{V}$

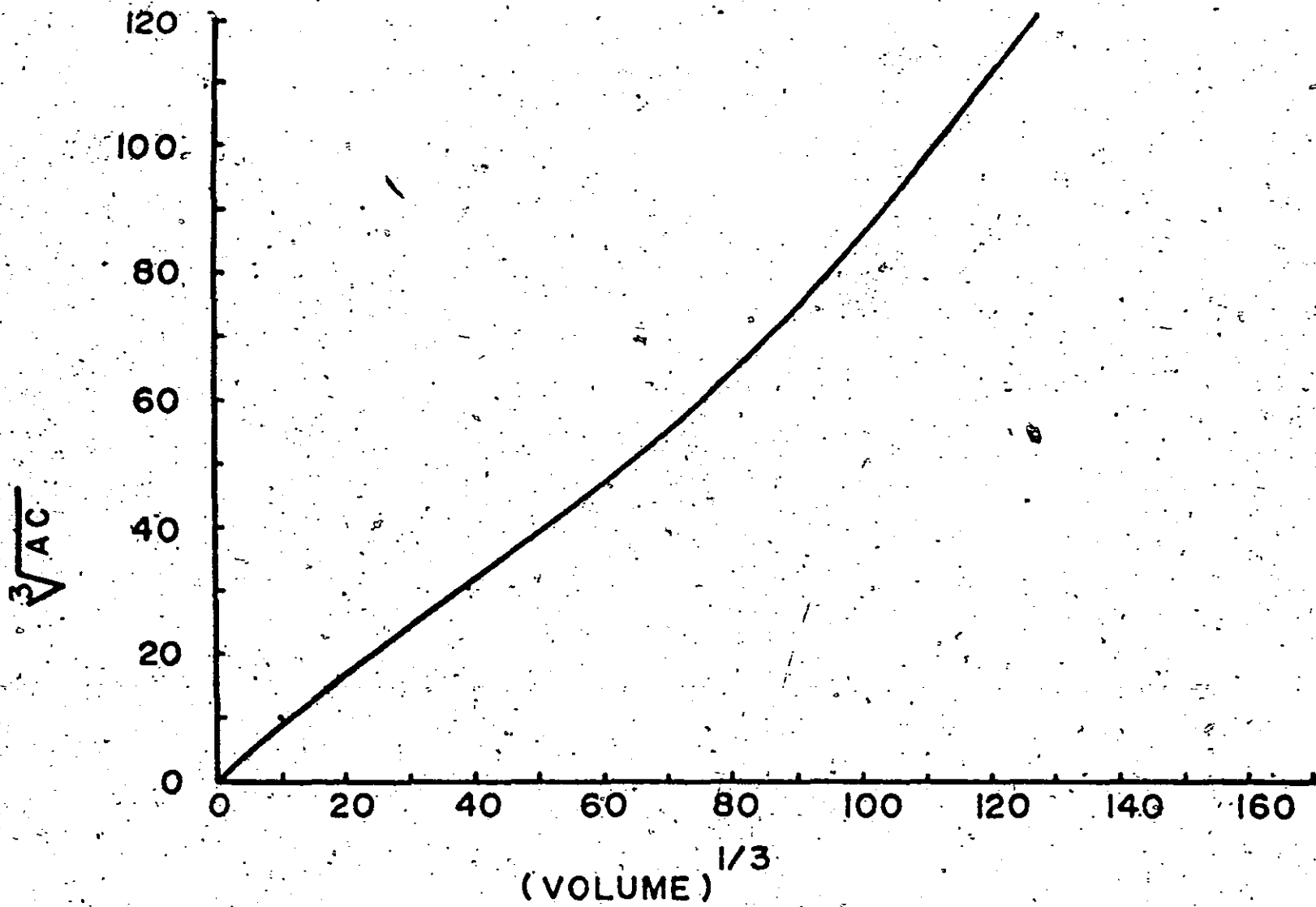


Figure 2.54: Control Surface Chart  $\sqrt[3]{A.C}$  vs.  $\sqrt[3]{V}$

center of area of the total surfaces  
and  $A$  = total control surface area

The procedure is as follows:

- 1) calculate  $\sqrt[3]{V}$
- 2) from the figures determine values for

$$\sqrt[3]{A_H L} = e$$

$$\sqrt[3]{A_V L} = f$$

$$\sqrt[3]{A_E L} = g$$

$$\sqrt[3]{A_R L} = h$$

$$\sqrt[3]{A_C} = j$$

- 3) then

$$A_H = e^3/L \quad (2.13)$$

$$A_V = f^3/L \quad (2.14)$$

$$A_E = g^3/L \quad (2.15)$$

$$A_R = h^3/L \quad (2.16)$$

$$C = j^3/A \quad (2.17)$$

Satisfactory results have been achieved by this method.

### 2.3.6 Static Bending Moment

In airships the disposable load should be distributed such that the static bending moment is minimized. However, the airship still has a static bending moment. This bending moment is called the "Hopping Moment". This moment is due to the gas head. If  $h$  is the gas head measured upward, then a pressure due to gas head is produced. This is given by

kh where k is the unit lift of the contained gas. This pressure produces a constant longitudinal force. The pressure, due to gas head, increases toward the top of the airship and therefore the resultant of the longitudinal force acts above the airship envelope neutral axis.

Consequently, a hogging bending moment is produced, the maximum value of which is given, by Klikoff<sup>[2]</sup>, for a fully inflated airship as

$$BM_H = k r^3 h/4 \quad (2.18)$$

where  $k$  = unit lift of the contained gas

$r$  = the maximum radius of the airship

$h$  = the head of the gas

### 2.3.7 Aerodynamic Bending Moment

Naatz<sup>[25]</sup> has developed an empirical expression for the maximum aerodynamic bending moment.

$$BM_A = 0.01 \rho V^2 V^{2/3} L \quad (2.19)$$

### 2.3.8 Internal Pressure

Assuming that the hogging moment as given by (2.18) resists all static bending moments, the internal pressure of the airship may then be used to resist the aerodynamic bending moment. Klikoff<sup>[2]</sup> gives:

$$P_{INT} = \frac{0.02 \rho V^2 V^{2/3}}{r^3} \quad (2.20)$$

74

where all the parameters are as previously defined. The assumption that the hogging bending moment resists the static bending moments is reasonable for design purposes. Keeping in mind the need to achieve an airship center of gravity location, in the static condition, directly below the center of bouvancy the designer can arrange the loading to achieve a minimum total static bending moment. A programme that calculates the static loading bending moment is presented in a later section of this chapter.

### 2.3.9 Programme and Results

A programme to calculate the foregoing factors has been developed. Eight shapes have been examined for three different fineness ratios. The results of this investigation are presented in Table 2.1. The programme itself is to be found in APPENDIX B and can easily be modified to give the output for any shapes desired. The output can be utilized, in combination with further criteria presented in later sections of this chapter, to determine the final design.

## 2.4 Pressure Distribution Analysis

### 2.4.1 Introduction

The pressure distribution over the airship envelope is one of the major considerations in determining the

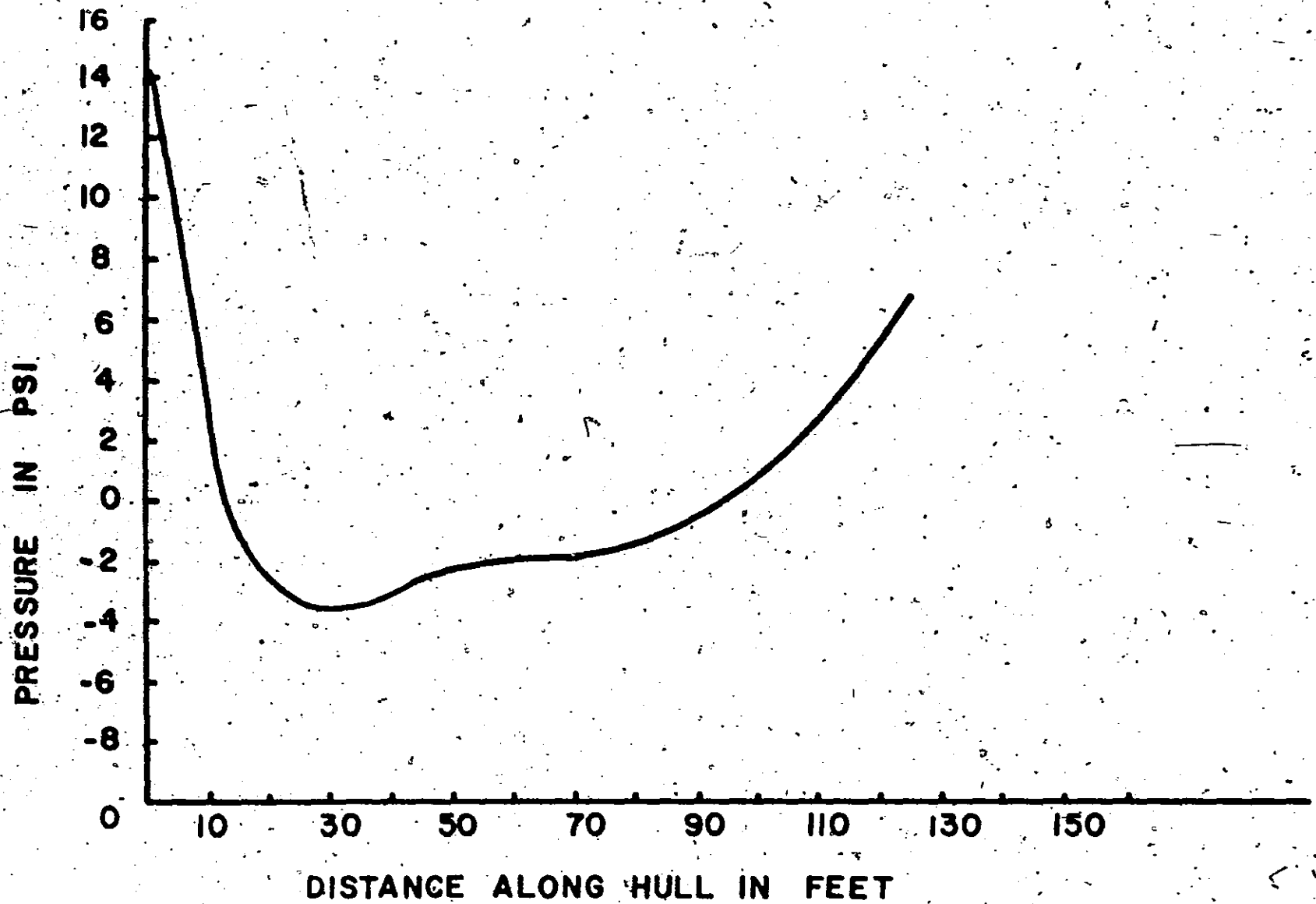


Figure 2.55: Pressure Distribution for an Airship in Level Flight

$m = 0.6$ ,  $n = 0.4$ ,  $f = 3.00$ ,  $V = 110$  ft/sec.



TRANSVERSE FORCE COEFF.

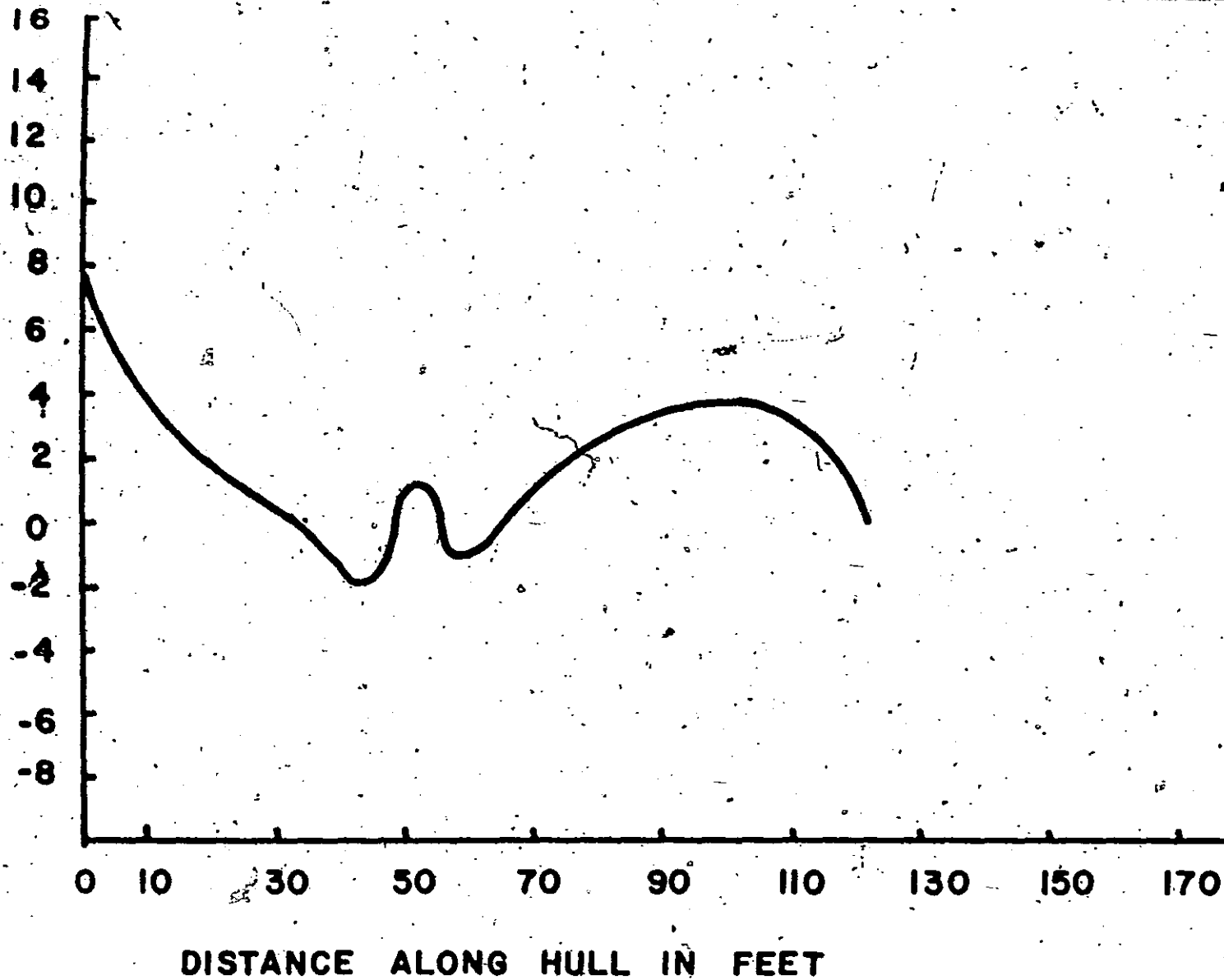


Figure 2.56: Pressure Distribution for an Airship in Non-Level Flight

$m = 0.6$ ,  $n = 0.4$ ,  $f = 3.00$ ,  $V = 110$  ft/sec,  $\alpha = 5.00$

suitability of the shape of the hull. The information supplied by the pressure distribution is of the subjective type. It does not provide any hard data beyond the actual shape of the pressure distribution. However, from the shape of the distribution, an approximate separation point may be determined. Thus, the suitability of any shape may be determined by the comparative distance aft of the bow of the separation point. The further aft the separation point is, the more stable the airship is likely to be. The pressure distribution as calculated by Von Karman<sup>[1]</sup> is used as the basis of a computer programme which calculates the pressure distribution of any airship hull shape at any velocity and at angles of attack up to  $\pm 10.0$  degrees. The programme is listed in Appendix C and examples of the results to be obtained are illustrated by Figure 2.55 and 2.56.

#### 2.4.2 Theodor Von Karman's Pressure Distribution on Airship Hulls

In order to understand the workings of the programme developed, a condensed version of the theory of Von Karman will be presented. Any modifications made will also be shown:

The following simplifications were made by Von Karman:

- 1) cabins, fins, and rudders were not considered
- 2) all cross-sections were represented by circular cross-sections

Two cases were calculated:

- 1) flow parallel to the longitudinal axis
- 2) flow at an angle to the longitudinal axis

Case #2 follows directly from Case #1

(a) Case #1

The flow was assumed to be produced by superposing a flow arising from a system of line sources and sinks, of differing productiveness, positioned along the longitudinal axis. The flow over the front part of the hull must be separated from that over the rear of the hull. Von Karman developed his theory for airships with long constant radius center sections and used a constant distance between the sources, or sinks, on both the bow and the stern sections. As modern airships are unlikely to have the former feature it is necessary to divide the airship hull into bow and stern sections at the point of maximum diameter and due to the difference in length between the bow and stern sections, different separation values must be used in each half.

Introducing the cylindrical co-ordinate system to be used:

$x$  = the longitudinal axis of symmetry

$r$  = the perpendicular distance from the  $x$  axis

$\phi$  = the angle of orientation of the meridian plane, as calculated from the vertical section of the body of revolution

The velocity components in these directions are:

$$U_x = \frac{\partial \phi}{\partial x}$$

$$U_r = \frac{\partial \phi}{\partial r}$$

$$U_\theta = 0$$

where  $\phi$  is the potential function.

Using the stream function,  $\psi$ , the velocity components now read

$$U_x = \frac{1}{r} \frac{\partial \psi}{\partial r}$$

$$U_r = - \frac{1}{r} \frac{\partial \psi}{\partial \theta}$$

$$U_\theta = 0$$

Replacing the cylindrical co-ordinate system by a spatial polar co-ordinate system (Figure 2.57) where

$\rho$  = the length of the radius vector

$\theta$  = the angle between the radius vector and the axis of symmetry

$\phi$  = the potential function

The velocity components, in the direction of the radius vector and perpendicular to it, are

$$U_\rho = \frac{\partial \phi}{\partial \rho} = \frac{1}{\rho^2 \sin \theta} \frac{\partial \phi}{\partial \theta}$$

$$U_\theta = \frac{1}{\rho} \frac{\partial \phi}{\partial \theta} = - \frac{1}{\rho \sin \theta} \frac{\partial \phi}{\partial \rho}$$

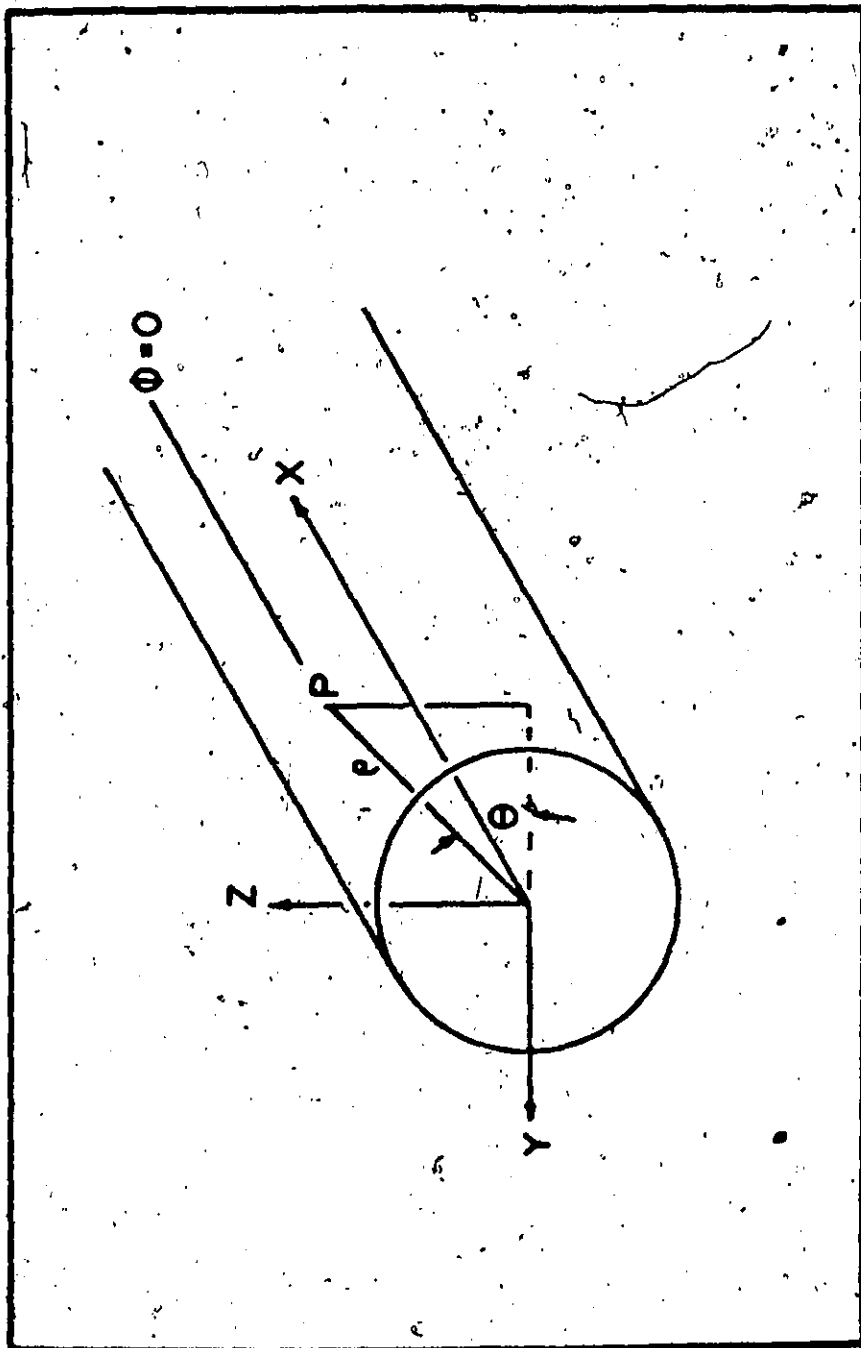


Figure 2.57: Coordinate Systems Used in the Analysis

The potential and stream functions, for a simple source of strength  $Q$ , read

$$\phi = -\frac{Q}{4\pi r}$$

$$\psi = -\frac{Q}{4\pi} (1 + \cos\theta)$$

For the remainder of the derivation:

$$Q = \sigma a$$

where  $\sigma$  = source strength per unit length

$a$  = length of the source

The contribution of any element  $d\ell$  to the stream function at a point  $P$  is

$$d\psi = -\frac{\sigma}{4\pi} (1 + \cos\theta) d\ell$$

giving

$$\psi = -\frac{\sigma}{4\pi} \int_0^a (1 + \cos\theta) d\ell$$

Referring to Figure 2.58

$$d\ell \cos\theta = -d\rho$$

then

$$\psi = -\frac{\sigma}{4\pi} \int_0^a (d\ell - d\rho)$$

Defining  $\rho'$  and  $\rho''$  as the distance of point  $P$  from the left and right end of the line source,

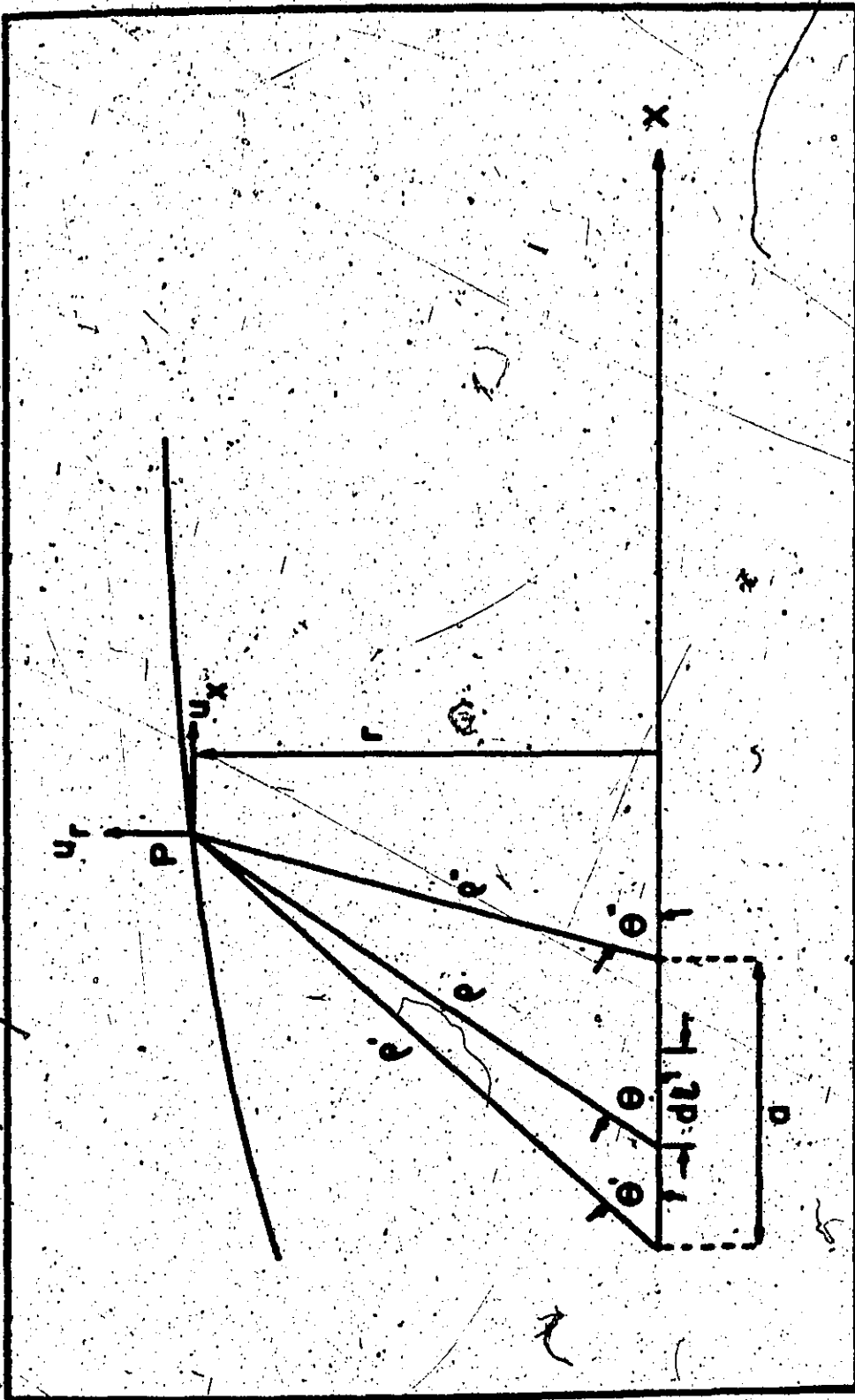


Figure 2:58: Trigonometric Relationships for a General

Point Along the Hull Shape

$$\psi = -\frac{Q}{4\pi} (a + \rho' - \rho'')$$

$$= -\frac{Q}{4} \left(1 + \frac{\rho' - \rho''}{a}\right)$$

The velocity components  $U_x$  and  $U_r$  become

$$U_x = \frac{Q}{4\pi ar} \left(\frac{\partial \rho''}{\partial r} - \frac{\partial \rho'}{\partial r}\right)$$

$$U_r = -\frac{Q}{4\pi ar} \left(\frac{\partial \rho''}{\partial x} - \frac{\partial \rho'}{\partial x}\right)$$

In general  $\rho = \sqrt{r^2 + x^2}$  and

$$\frac{\partial \rho}{\partial r} = \sin \theta$$

$$\frac{\partial \rho}{\partial x} = \cos \theta$$

yielding

$$U_x = \frac{Q}{4\pi ar} (\sin \theta'' - \sin \theta')$$

$$U_r = -\frac{Q}{4\pi ar} (\cos \theta'' - \cos \theta')$$

Designating the distances of a given streamline point from the end points of the  $i^{\text{th}}$  line source by  $\rho'_i$  and  $\rho''_i$

$$\psi = -\frac{Q_i}{4} \sum_{i=1}^n \left(1 + \frac{\rho'_i - \rho''_i}{a}\right)$$

where  $n$  is the number of sources.

The lines  $\psi = \text{constant}$  represent streamlines and the line  $\psi = 0$  yields the envelope curve. Therefore, putting  $\psi = 0$  for as many points of the envelope as there are unknown line sources, a system of linear equations is obtained for the determination of  $Q_i$ .



$$Z_1 = \frac{Q_1}{2U \cdot a^2}$$

where U is the free stream velocity.

Denoting the length of the radius vectors from the end points of the i<sup>th</sup> source to any point k on the envelope, a coefficient, C<sub>ik</sub> can be defined.

$$C_{ik} = 1 + \frac{a'_{ik} - a''_{ik}}{a}$$

The system of linear equations is

$$C_{11}Z_1 + C_{21}Z_2 + \dots + C_{n1}Z_n = \left(\frac{r_1}{a}\right)^2$$

$$C_{12}Z_1 + C_{22}Z_2 + \dots + C_{n2}Z_n = \left(\frac{r_2}{a}\right)^2$$

" " " "

$$C_{1n}Z_1 + C_{2n}Z_2 + \dots + C_{nn}Z_n = \left(\frac{r_n}{a}\right)^2$$

According to Bernoulli's equation, the pressure increase, at any point where the flow velocity is kU, is

$$\Delta P = \frac{\gamma}{2g} (1 - k^2)U^2$$

Introducing the quantity Z<sub>i</sub> into the expressions for U<sub>x</sub> and U<sub>r</sub>, a value for k<sup>2</sup> can be obtained

$$k^2 = \left[1 - \frac{a}{2r_k} \sum_{i=1}^n Z_i (\sin \theta''_i - \sin \theta'_i)\right]^2 + \frac{a^2}{4r_k^2}$$

$$\left[\sum_{i=1}^n Z_i (\cos \theta''_i - \cos \theta'_i)\right]^2$$

$\Delta P$  = the change in the dynamic pressure

$$= P - P_0$$

The boundary condition is  $P_0 = 0$  as  $P_0$  is the dynamic pressure at a distance from the ship. Hence

$$P = \frac{\rho}{2g} (1 - k^2) U^2$$

and for the stagnation point  $k^2 = 0$

The introduction of  $Z_1$  into the expressions for  $U_x$  and  $U_y$  results in

$$U_x = U - U \frac{a}{2r_k} \sum_{i=1}^n Z_1 (\sin''_i - \sin'_i)$$

$$U_y = U \frac{a}{2r_k} \sum_{i=1}^n Z_1 (\cos''_i - \cos'_i)$$

These quantities are not required in this case but are necessary in the following case and for that reason are defined at this point.

(b) Case #2

The situation of oblique flow can be obtained by superposing the cases of flow at zero incidence angle and an incidence angle of ninety degrees. Flow at zero incidence angle has been investigated in the preceding section. To solve for the case of a ninety degree incidence angle, a perpendicular flow of velocity  $W$  must be assumed and the flow potential calculated using the following theorem.

"If the x axis of an x, y, z system of co-ordinates is covered with double sources whose axes are oriented in the z direction, then the flow resulting from these double sources, superposed on a parallel flow in the z direction, produces a streamline form about a body of revolution exposed to a flow at right angles to the axis of symmetry."

The principle formulae for a double source are derived as follows:

Consider a source and a sink of equal yield  $Q$  separated by a distance  $2c$ . This gives  $x = y = 0$  and  $z = \pm c$ . The potential functions of the source and sink are:

$$\phi(+c) = -\frac{Q}{4\pi} (x^2 + y^2 + (z - c)^2)^{-1/2}$$

$$\phi(-c) = \frac{Q}{4\pi} (x^2 + y^2 + (z + c)^2)^{-1/2}$$

Addition of the potential functions yields

$$\phi = -\frac{Q}{4\pi} \frac{2cz}{(x^2 + y^2 + z^2)^{3/2}} + \text{higher order terms}$$

The angle of inclination of any radius vector to the z axis can be designated by  $\gamma$  giving

$$\cos \gamma = \frac{z}{\sqrt{x^2 + y^2 + z^2}}$$

and

$$P = \frac{z}{\sqrt{x^2 + y^2 + z^2}}$$

giving

$$\phi = -\frac{2Qc}{4\pi P^2} \cos \gamma + \text{higher order terms}$$

Letting  $c$  approach zero and  $Q$  approach infinity so that the product of  $2Qc$  approaches a finite value  $M$ , we get

$$\phi = -\frac{M}{4\pi\rho^2} \cos \gamma,$$

the potential function for a doublet.

Superposing the parallel flow in the  $z$  direction produces flow about a sphere. The velocity component in the direction of the radius vector,  $\rho$ , is

$$W_\rho = \frac{M}{2\pi\rho^3} \cos \gamma.$$

If the parallel flow has a velocity of  $-W$  then,

$$W_\rho = -W \cos \gamma$$

Putting

$$W_\rho + W_\rho = 0$$

for the surface of a sphere of radius

$$\rho = \frac{M}{2\pi W}$$

the velocity component perpendicular to the surface of the sphere disappears. Hence, flow about a sphere is produced.

If the entire  $x$  axis is covered with these doublets of constant intensity, then the flow crosswise to an infinitely long cylinder is obtained. Introducing the polar co-ordinates  $\rho, \theta, \phi$ , where  $\theta$  is the angle between the radius vector and the  $x$  axis and  $\phi$  determines the position of the meridian plane passing through the  $x$  axis then

$$\cos \gamma = \sin \theta \cos \phi$$

and

$$\phi = -\frac{M}{4\pi} \frac{\sin \theta \cos \phi}{\rho^2}$$

$$= -\frac{u}{4\pi} \frac{d}{r^2} \frac{\sin\theta \cos\theta}{\sin^2\theta}$$

Returning to Figure 2.58

$$x - z = r \cos\theta$$

$$\text{and } dz = \frac{r}{\sin^2\theta} d\theta$$

$$r = a \sin\theta$$

so that

$$dz = -\frac{u}{4\pi r} \sin\theta d\theta \cos\theta$$

Integrating for a constant line doublet length "a"

$$\phi = \frac{u}{4\pi a} [\cos\theta]_0^a \cos\theta$$

or indicating the angles to the left and right ends of the doublet line by  $\theta'$  and  $\theta''$

$$\phi = \frac{u}{4\pi a} (\cos\theta'' - \cos\theta') \cos\theta$$

Integrating from  $\theta = 0$  to  $\theta = \pi$  yields

$$\phi = -\frac{u}{2\pi r} \cos\theta$$

The velocity in the r direction is

$$W_r = \frac{u}{2\pi r^2} \cos\theta$$

Therefore the flow around a cylinder of radius

$$r = \sqrt{\frac{u}{2\pi W}}$$

can be obtained by covering the cylinder axis with a doublet of moment.

$$u = 2\pi r^2 W$$

The potential function of a system of doublets can be expressed by

$$\phi = \cos\theta \phi_0(\rho, \theta)$$

in which  $\phi_0$  represents the potential function for the vertical section,  $\theta=0$ , and depends only on  $\rho$  and  $\theta$  or  $x$  and  $r$ .

The streamline pattern in the vertical section immediately furnishes the streamline pattern and the corresponding velocity components in any meridian plane by multiplying by  $\cos\theta$ . The task of determining the perpendicular flow about the airship hull is, therefore, reduced to the solution of the problem in the plane  $\theta=0$  ( $x, z$  plane). Following a similar method, as in Case #1, the potential function of the 1<sup>th</sup> source is

$$\phi_1 = -\frac{u_1}{4\pi r} (\cos\theta'_1 - \cos\theta''_1)$$

and

$$W_{x1} = \frac{\partial \phi_1}{\partial x} = \frac{u_1}{4\pi r} (\sin\theta'_1 - \sin\theta''_1 \frac{\partial \theta''_1}{\partial x})$$

$$W_{r1} = \frac{\partial \phi_1}{\partial r} = \frac{u_1}{4\pi r} (\sin\theta'_1 \frac{\partial \theta'_1}{\partial r} - \sin\theta''_1 \frac{\partial \theta''_1}{\partial r}) + \frac{u_1}{4\pi r^2} (\cos\theta'_1 - \cos\theta''_1)$$

where  $\theta = \arctan \frac{r}{x}$

Hence

$$\frac{\partial \theta}{\partial x} = \frac{-\frac{r}{x^2}}{1 + \left(\frac{r}{x}\right)^2}$$

$$\frac{\partial \theta}{\partial r} = \frac{\frac{1}{x}}{1 + \left(\frac{r}{x}\right)^2}$$

and

$$\sin \theta = \frac{\frac{r}{x}}{1 + \left(\frac{r}{x}\right)^2}$$

$$\cos \theta = \frac{1}{1 + \left(\frac{r}{x}\right)^2}$$

Introducing

$$f\left(\frac{r}{x}\right) = \sin \theta$$

$$g\left(\frac{r}{x}\right) = 2 \cos \theta - \cos^3 \theta$$

and again designating them by  $f'_1$  or  $f''_1$  and  $g'_1$  or  $g''_1$

gives

$$W_x = \frac{1}{4\pi r^2} \sum_{l=1}^n \mu_l (f''_1 - f'_1)$$

$$W_r = \frac{1}{4\pi r^2} \sum_{l=1}^n \mu_l (g'_1 - g''_1)$$

The parallel flow has components

$$W_x = 0$$

$$W_r = -W$$

Let  $\alpha$  denote the angle of inclination to the meridian plane.

Then

$$\tan \alpha = \frac{W_r + W_x}{W_x} = \frac{W_r - W}{W_x}$$

or

$$W_r - W_x \tan \alpha = W$$

giving

$$\frac{1}{4\pi r^2} \sum_{i=1}^n v_i [(r'_i - r''_i) + \tan \alpha (r'_i - r''_i)] = W$$

Defining  $Z_i$  as

$$Z_i = \frac{v_i}{4\pi a^2 W}$$

where  $a$  is the separation distance gives

$$\sum_{i=1}^n Z_i [(r'_i - r''_i) + \tan \alpha (r'_i - r''_i)] = \frac{r_1^2}{a^2}$$

If the  $i^{\text{th}}$  station of the hull were to be replaced by a portion of an infinite cylinder of radius  $r_1$ , the strength of the doublet is given by

$$v_i = 2\pi r_1^2 W$$



or

$$z_1 = \frac{1}{2} \left( \frac{r_1}{a} \right)^2$$

The velocity components at any point  $k$  can now be expressed by

$$W_x = \frac{W}{2} \left( \frac{r_1}{r_k} \right)^2 (r_{1k}'' - r_{1k}')^2$$

$$W_r = \frac{W}{2} \left( \frac{r_1}{r_k} \right)^2 (r_{1k}' - r_{1k}'')$$

Instead of calculating the pressure distribution, Von Karman calculated a quantity,  $B$ , the "transverse force coefficient". For the purposes that we require the data, this has no effect as the shape of the pressure distribution curve and the transverse force coefficient curve are the same.

$$B = 2\pi r \frac{UW}{U^2 + W^2} \left( \frac{U_x W_x}{UW} + \frac{U_r W_r}{UW} \right)$$

Assuming

$$U = W = 1$$

then

$$B = \pi r (W_x U_x + W_r U_r)$$

where  $W_x$ ,  $W_r$ ,  $U_x$  and  $U_r$  are quantities that have already been defined.

## 2.5 Static Shear Force and Bending Moment

### 2.5.1 Introduction

The static shear force and static bending moment are of considerable importance in determining the suitability of

any airship design. The static shear force can be used to determine the optimum locations of the major structural components from a loading point of view. In addition, a knowledge of the static shear force can considerably aid the design of the internal suspension system of the airship. The static bending moment has its value as an indicator of the degree of optimization achieved in the location of the major structural components. The minimum bending moment indicates the optimum location.

A computer programme has been developed which enables the user to compare various designs by computing the static shear force and bending moment given the necessary inputs. This programme is listed in APPENDIX D.

### 2.5.2 Programme Inputs and Sample Results

The programme as developed is user oriented and by substituting various values for the following parameters alternative designs can be evaluated.

- XH - airship shape factor
- XM - airship shape factor
- P - airship fineness ratio
- XL - airship length
- N - number of 1 foot interval stations into which the airship is divided starting with 1 at the bow

- CABXS - starting position of the cabin
- CABXST - stopping position of the cabin
- TAILXS - starting position of the tail assembly
- TAILXST - stopping position of the tail assembly
- SUSPXS - starting position of the internal suspension system
- SUSPXST - stopping position of the internal suspension system
- NOSEXST - stopping position of the bow cap
- WNOSE - the bow cap weight
- WCAB - the cabin weight
- WTAIL - the tail weight
- WEIGHT - the weight of the envelope material (oz./sq.yd)
- XCCO - the position of the center of gravity of the cabin
- XNCO - the position of the center of gravity of the bow cap
- XTCO - the position of the center of gravity of the tail assembly

The programme assumes that all weights are distributed evenly over the distances concerned and also assumes one integral straight line ballonnet. The programme has been tested for the following design parameters and the results are shown in Figure 2.59 and Figure 2.60.

- XN - 0.4
- XM - 0.6
- R - 3.00
- XL - -117.0
- N - -118.0

SUSPXS	- 20.0
SUSPXST	- 90.0
HOSEXST	- 20.0
CABXS	- 38.6
CABXST	- 61.6
TAILXS	- 85.0
TAILXST	-100.0
WNOSE	-200.0
WCAB	-3200.0
WTAIL	-500.0
WEIGHT	- 11.40
XCCG	- 52.6
XNCR	- 10.0
XTCG	- 90.0

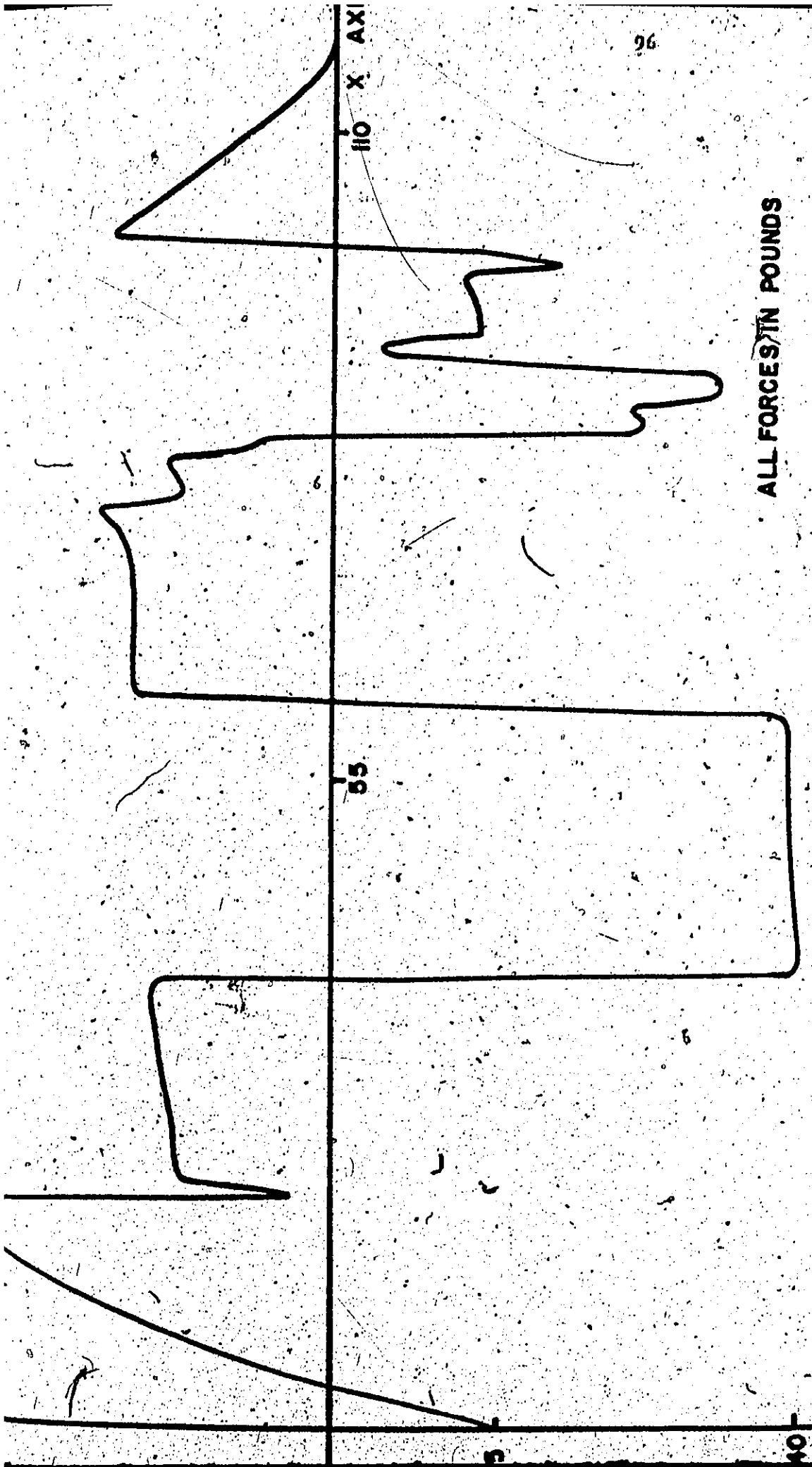
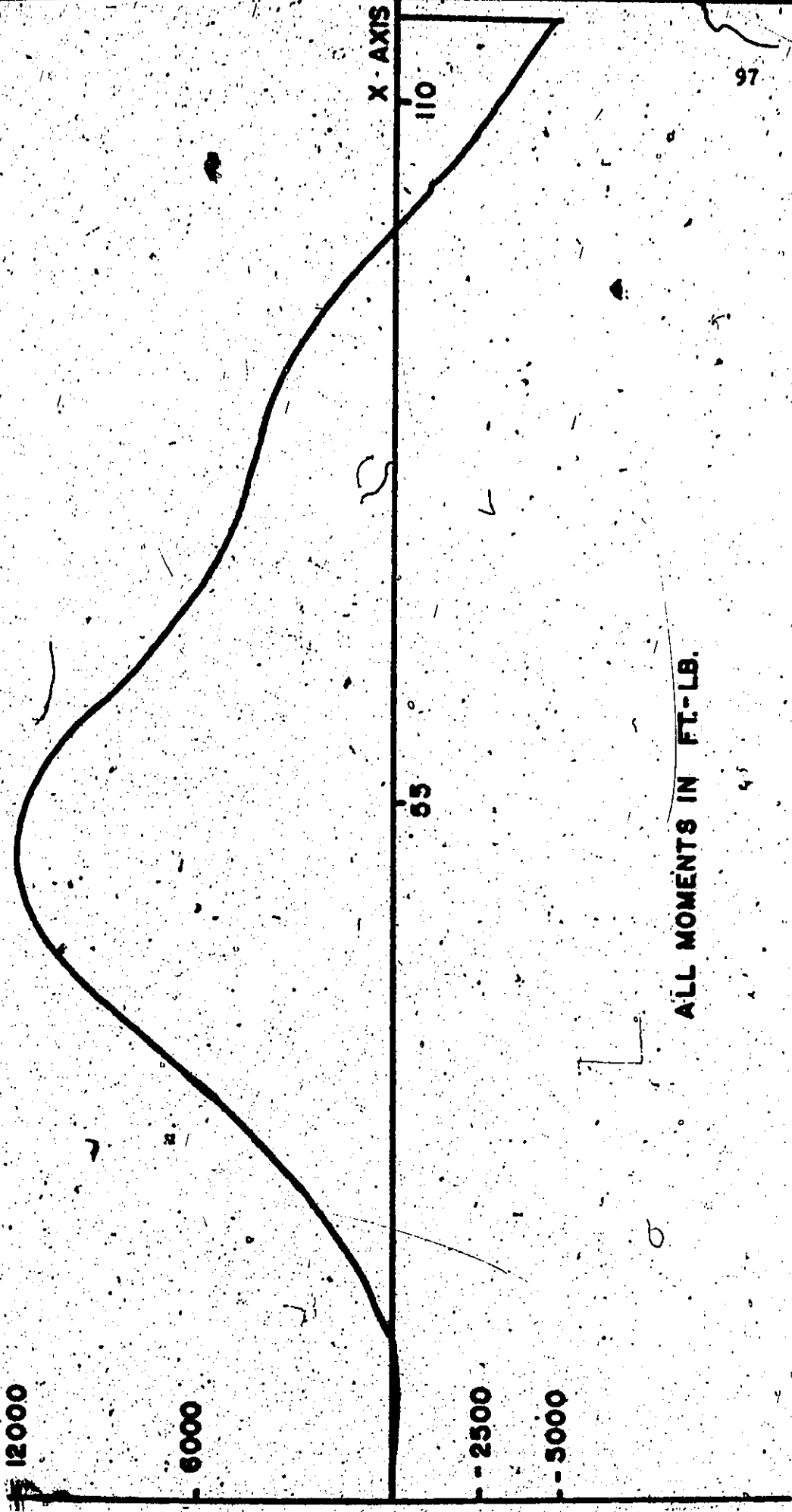


Figure 2.59: Static Shear Force Diagram



ALL MOMENTS IN FT.-LB.

Figure 2.60: Static Bending Moment Diagram

## Chapter Three Notation

$\gamma$	the angle of inclination
$\alpha$	the angle of attack
$\phi$	the roll angle
$\psi$	the yaw angle
$\theta$	the angle of rotation
$V_{TOT}$	the total volume of the envelope
$V_{BAL}$	the volume of the ballonets
$\rho_{AIR}$	the density of air
$\rho_{HE}$	the density of Helium
$F_G$	the lifting gas force
$F_W$	the weight of the airship
$F_D$	the drag force
$F_T$	the engine thrust force
$F_L$	the dynamic lift force
$F_{S_f}$	the lift force of the fixed tail surfaces
$F_{D_s}$	the drag force of the fixed tail surfaces
$F_e$	the elevator force
$F_R$	the rudder force
$C_L$	the lift coefficient

$C_D$  the drag coefficient  
 $V$  the volume of the airship  
 $v$  the velocity of the airship  
 $A$  the area coefficient  
 $\rho$  the density of air  
 $W$  the weight of the airship  
 $L$  the length of the airship  
 $S$  the cross sectional area  
 $R$  the radius of the turning circle  
 $CB$  the position of the center of bouyancy  
 $CPT$  the center of pressure of the tail  
 $CP$  the center of pressure of the airship  
 $I$  the mass moment of inertia  
 $a$  the linear acceleration  
 $\dot{\omega}$  the angular acceleration  
 $m$  the mass of the system  
 $x_c$  the position of the center of mass of the system in the x direction  
 $y_c$  the position of the center of mass of the system in the y direction  
 $z_c$  the position of the center of mass of the system in the z direction  
 $m$  airship envelope shape parameter  
 $n$  airship envelope shape parameter  
 $f$  airship fineness ratio



## CHAPTER 3

### COMPUTER AIDED TRAJECTORY AND LOAD CALCULATIONS

#### 3.1 Introduction

The question of how an airship will behave when required to perform certain maneuvers has always been one of the uncertainties of airship design. Wind tunnel experiments and model studies have been inconclusive<sup>[11]</sup>. During the period of quantity construction of airships, designers based their decisions upon empirical data that had been gathered from previous designs. However, recent airworthiness regulations require that the forces acting during various maneuvers be calculated and taken into account at the structural design stage. The calculations involved in this task would be very tedious and time consuming if done by hand; the problem is tractable, however, using the high speed digital computer.

The requirements that must be met are given in the "Ministry of Transport, Civil Aeronautics, Provisional Airworthiness Requirements, Airships" subpart C, Structure, sections SC. 4(a) through SC. 4(e)<sup>[3]</sup>.

Maneuvering Load Conditions. The airship structure shall be designed to withstand the limit loads resulting from the following maneuvering conditions, conducted at airspeed of  $V_D$ , critical statically-heavy weight, and at the centre-of-gravity location critical for each maneuver:

(a) In level flight, application of full rudder, applied at the maximum control rate attainable, until a heading of 75 degrees off the original heading is attained, followed by immediate application of full opposite rudder, applied at the maximum control rate attainable to original heading. The effects of overcontrol shall be taken into account.

(b) In level flight, maintain a steady-state turn with rudder fully deflected in the direction of turn.

(c) The maneuvers of SC.1(a) through SC.1(b), combined with full-up elevator, applied at the maximum control rate attainable, and alternatively, with full-down elevator, similarly applied.

(d) In level flight, apply full-down elevator at maximum control rate attainable until the specified maximum rate of descent is obtained followed immediately by full-up elevator at maximum control rate until rate of descent equals zero. The effects of overcontrol shall be taken into account.

(e) The maneuvers of SC.4(d) combined with alternatively a left and right steady-state turn."

The theory needed to provide the trajectories dictated by these maneuvers and the resulting loads will be examined and a user-oriented computer package which has been developed will be described.

### 3.2 Static Force and Moment Analysis

A static force and moment analysis is performed in order to reveal the forces and moments involved when an airship travels at a constant velocity. A simple unrealistic situation will be analysed first, and then extended to the real situation. The initial situation is unrealistic due to the fact that it assumes an airship in neutral buoyancy, that is with the static lift force exactly equal to the weight of the system, in level flight. This an airship cannot accomplish without use of the control system.

The analysis shown here will later be developed further in order to include acceleration effects. A full understanding of the static situation is necessary before dealing with the dynamic situation.

#### 3.2.1 Description of Airship Axis.

An airship hull is a solid of revolution. Labelling its axis of rotation as the x axis produces the co-ordinate system illustrated in Figure 3.1. Any angular deviation of the airship, will be either pitch, yaw, or roll, or a combination of these motions.

The nomenclature related to the previously described axis system is shown in Table 3.1.

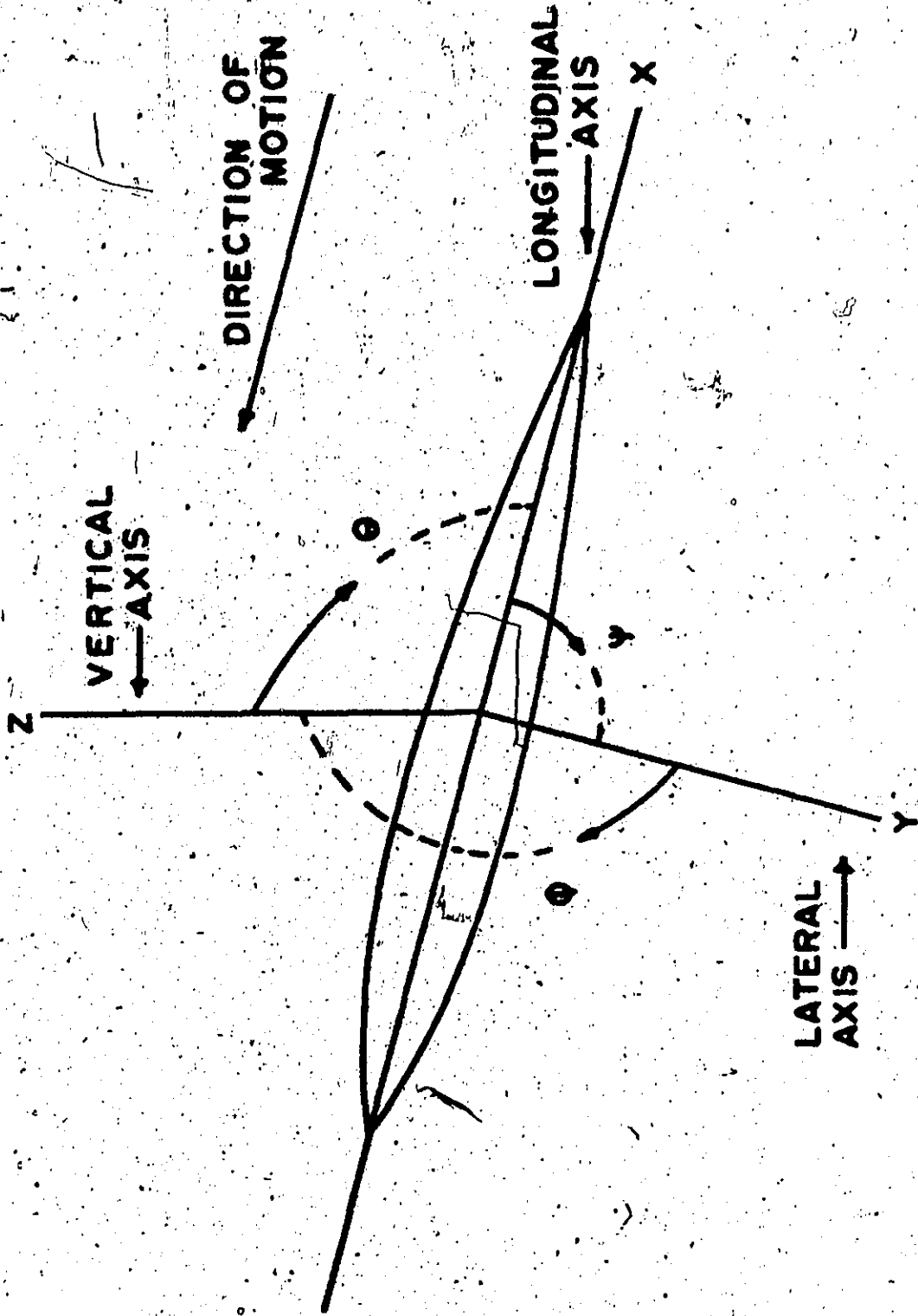


Figure 3.1: Airship Axes

TABLE 3.1  
Nomenclature

Axis		Moment about axis		Angle	Velocities		Acc.	
Designation	Symbol	Designation	Symbol	Symbol	Linear	Ang.	Linear	Ang.
Longitudinal	X	Roll	L	•	VX	WX	AX	WX
Lateral	Z	Pitch	M	•	VZ	WZ	AZ	WZ
Vertical	Y	Yaw	N	•	VY	WY	AY	WY

Various angles in both the pitch and yaw directions must be defined. Referenced to the moving axes of the airship three angles are required. The angle of attack in the vertical plane, with respect to the center of bouyancy, is  $\theta$  and the angle of attack in the horizontal plane, once again with respect to the center of bouyancy is  $\phi$ . The roll angle,  $\psi$ , is also referenced to the center of bouyancy. The motion of the airship axes produces angles which are referenced to the fixed ground level axis. Motion in the X-Y plane is referenced to the X axis and produces an angle of inclination,  $\gamma$ . Motion in the X-Z plane produces an angle of rotation,  $\beta$ , with respect to the longitudinal direction. Thus the total angle of pitch is given by  $\gamma + \theta$  and the total angle of yaw by  $\phi + \beta$ .

### 3.2.2 Center of Bouyancy

The center of bouyancy of an airship may be defined as the center of mass of the fluid displaced by the external shape of the envelope. This definition implies that the airship is at its ceiling altitude and the ballonets are completely deflated. If the ballonets are inflated equally, assuming fore and aft ballonets, then properly placed ballonets produce no center of mass shifts. If, however, unequally inflated ballonets are used to trim the airship, center of mass shifts will occur. The degree of inflation will have no effect on the lifting force produced by the enclosed Helium as

$$(V_{TOT} - V_{BAL}) \times (\gamma_{AIR} - \gamma_{He}) = C$$

at any altitude. The degree of inflation of the ballonets possible is a function of the altitude.

$$\begin{aligned} V_{BAL} &= f(h) \\ &= (1-x)V_{TOT} \end{aligned}$$

where  $x$  is the ratio of the density of air at sea level to the density of air at the requisite altitude.

For an airship which is in static equilibrium the center of bouyancy should be located directly above the center of gravity of the airship and on the longitudinal axis.

### 3.2.3 Definitions and Assumptions

Motion of an airship in flight may be defined in terms of roll, pitch, and yaw about the longitudinal axis. An airship differs from an aircraft in that the three types of motion are independent of one another.

The following analysis will be based on the assumption that -

- 1) the static lift force remains constant,
- 2) the total weight remains constant,
- 3) the air speed of the airship remains constant,
- 4) the airship form remains unchanged,
- 5) the center of gravity and the center of bouyancy remain fixed with respect to the airship axes,

- 6) the controls remain neutral,
- 7) the airship moves in an ideal, incompressible, frictionless fluid.

### 3.2.4 Forces and Moments Acting on an Airship

An unrealistic situation will be examined first in order to establish a simple image of some of the forces and moments. Suppose an airship is travelling in neutral buoyancy, at a constant speed, with the horizontal axis co-incident with the direction of motion (angle of attack is zero), as illustrated by Figure 3.2. The forces and moments acting are as follows:

#### 1) Forces:

- (a)  $F_L$  = the force due to the lifting gas acting through the center of buoyancy, CB.
- (b)  $F_W$  = the total weight of the airship acting through the center of gravity, CG.
- (c)  $F_D$  = the drag force acting on the center of pressure, CP.
- (d)  $F_T$  = the thrust force of the engines acting along the thrust line of the engines, CT.

#### 2) Moments about the center of buoyancy:

- (a)  $M_W$  = moment due to the weight.  
= 0
- (b)  $M_L$  = moment due to the lifting gas  
= 0
- (c)  $M_{Td}$  = moment due to the thrust and drag  
=  $T(a)$

(3.1)



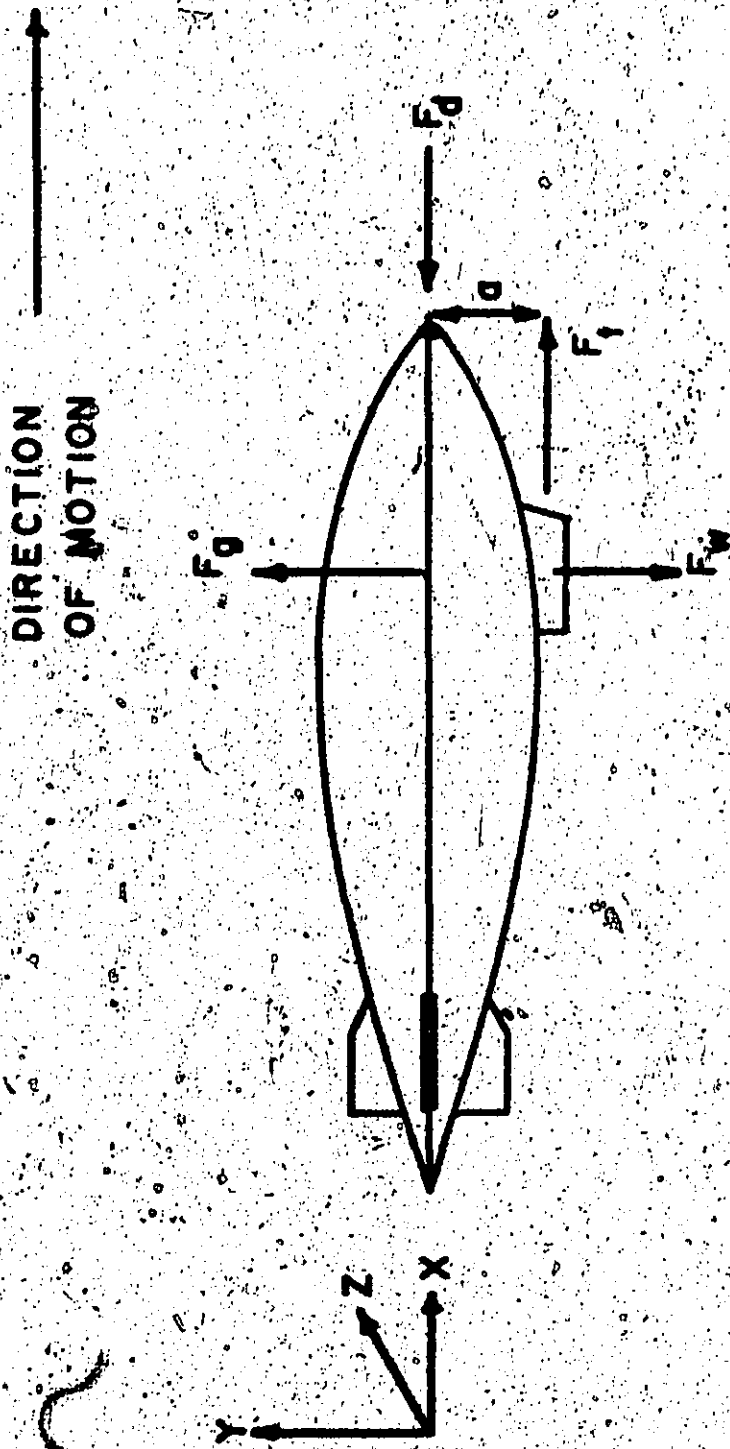


Figure 3.2: Forces Acting on an Airship (idealized case)

where "a" is the vertical distance between the engine thrust line and the center of buoyancy.

Hence, for static equilibrium and constant velocity

$$F_g = F_b$$

$$F_d = F_t$$

However, the thrust-drag moment,  $M_{td}$ , is unbalanced and would tend to force the nose of the airship in an upward direction.

In order to overcome this problem airships are trimmed nose down until a balancing moment is produced ( $\theta \neq 0$ ). The force and moment analysis thus becomes much more complex than in the situation just described.

Six different situations can be identified depending on the static condition of the airship and its direction of inclination. These six situations are illustrated in Figure 3.3.

Case No. 1 - The airship is in neutral buoyancy flying with the nose trimmed up an angle of  $\alpha$ . Thus, since  $\theta = 0^\circ$ , the airship will climb at an angle of  $\gamma = \alpha$ .

Case No. 2 - The airship is in neutral buoyancy flying with the nose trimmed down an angle of  $\alpha$ . Once again  $\theta = 0^\circ$  and the airship will dive at an angle of  $\gamma = \alpha$ .

Case No. 3 - The airship is flying statically heavy (the static lifting force is less than the total system weight) with the nose trimmed up an angle of  $\alpha$ . Here the airship will have an angle of attack of  $\theta$  and an angle of motion of  $\gamma$ . Thus the angle of trim  $\alpha$  must equal  $\gamma + \theta$ .

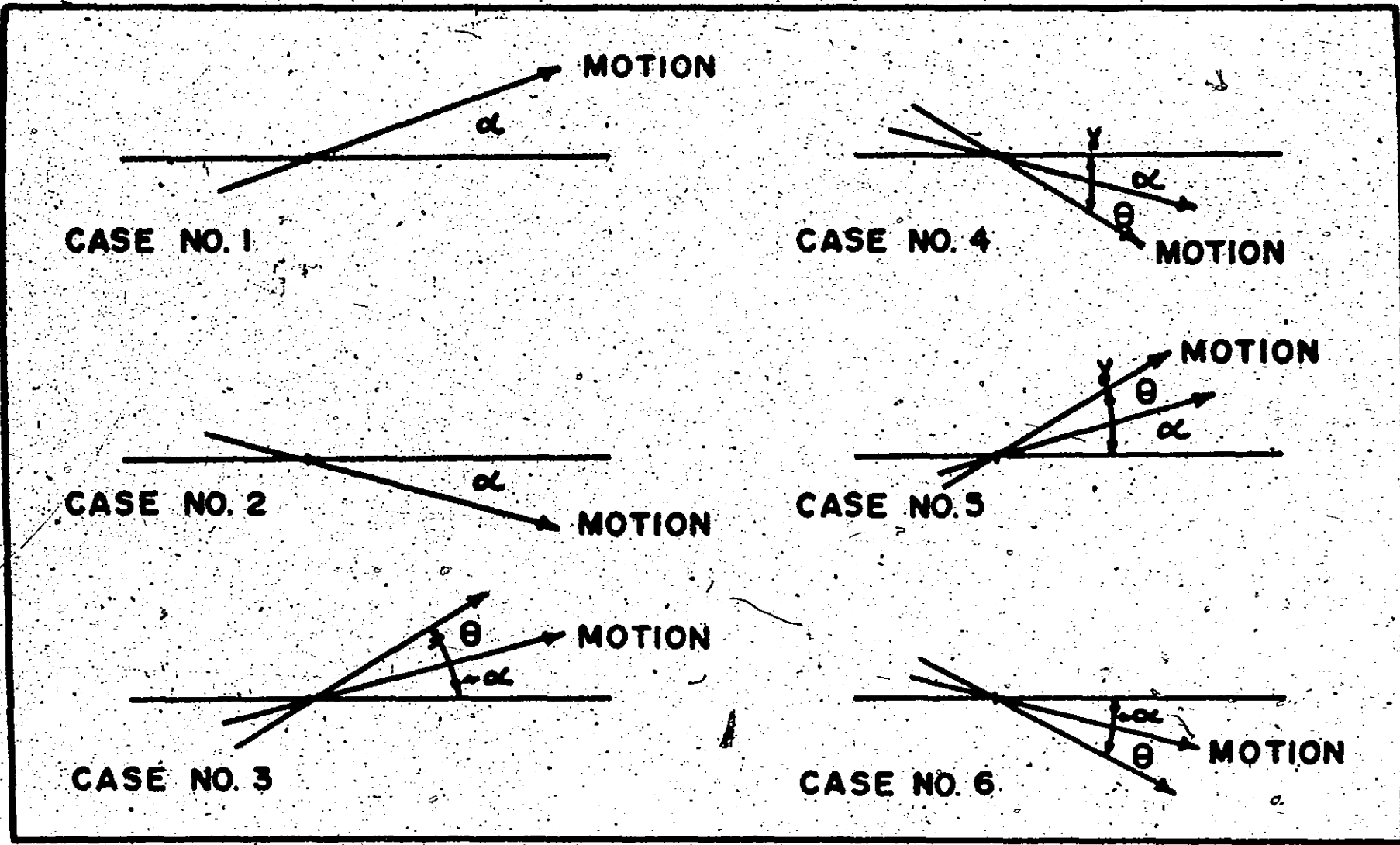


Figure 3.3: Airship Trajectories for Various Loading Conditions and Angles of Attack.

Case No. 4 - The airship is flying statically heavy with the nose trimmed down an angle of  $\alpha$ . Here the airship will have an angle of attack of  $-\theta$ , and an angle of motion of  $-\gamma$ . Thus the angle of trim  $\alpha$ , which can be defined as the angle between the airship longitudinal axis and the fixed horizontal axis, must equal  $\gamma - \theta$  as  $\gamma > \theta$  due to the heaviness of the airship.

Case No. 5 - The airship is flying statically light (the static lifting force is greater than the total system weight) with the nose trimmed up an angle of  $\alpha$ . This case is similar to Case No. 4. The angle of motion is  $\gamma$  and the angle of attack is  $\theta$ . Due to the lightness of the system  $\gamma > \theta$  and the trim angle  $\alpha$  must equal  $\gamma - \theta$ .

Case No. 6 - The airship is flying statically light, with the nose trimmed down an angle of  $\alpha$ . The angle of attack is  $-\theta$  and the angle of motion is  $-\gamma$ . Due to the lightness of the system  $\theta > \gamma$  and the trim angle  $\alpha$  must equal  $\gamma + \theta$ .

Cases 1 and 2 almost never occur and thus only four actual situations must be contemplated.

An examination of one of these cases in detail will reveal the forces and moments actually operating on an airship. Case number three is shown in Figure 3.4. Referring to this figure, a general situation can be identified. The forces and moments are:

1) Forces

- (a)  $P_g$  - the force due to the lifting gas acting through the center of buoyancy, CB.

- (b)  $F_w$  = the total weight of the airship acting through the center of gravity, CG
- (c)  $F_d$  = the drag force acting on the airship through the center of pressure, CP.
- (d)  $F_t$  = the thrust force of the engines acting along the thrust line of the engines, CT.
- (e)  $F_L$  = the dynamic lift force on the hull due to flying at an angle of pitch of  $\theta$ , acting through the center of pressure, CP.
- (f)  $F_g$  = the lift of the fixed tail surfaces due to flying at an angle of pitch  $\theta$ , acting through the center of pressure of these surfaces.
- (g)  $F_{ds}$  = the drag of the tail surfaces, acting through the center of pressure of these surfaces.
- (h)  $F_e$  = the force due to deployment of the elevators. This force acts through the center of pressure of the tail, CPT.

Several of these forces have been defined in the previous chapter. These include:

- $F_g$  - the lifting force due to the contained gas
- $F_w$  - the gross weight of the system
- $F_d$  - the drag force as given by <sup>[A]</sup>
- $F_t$  - the thrust force due to the engines

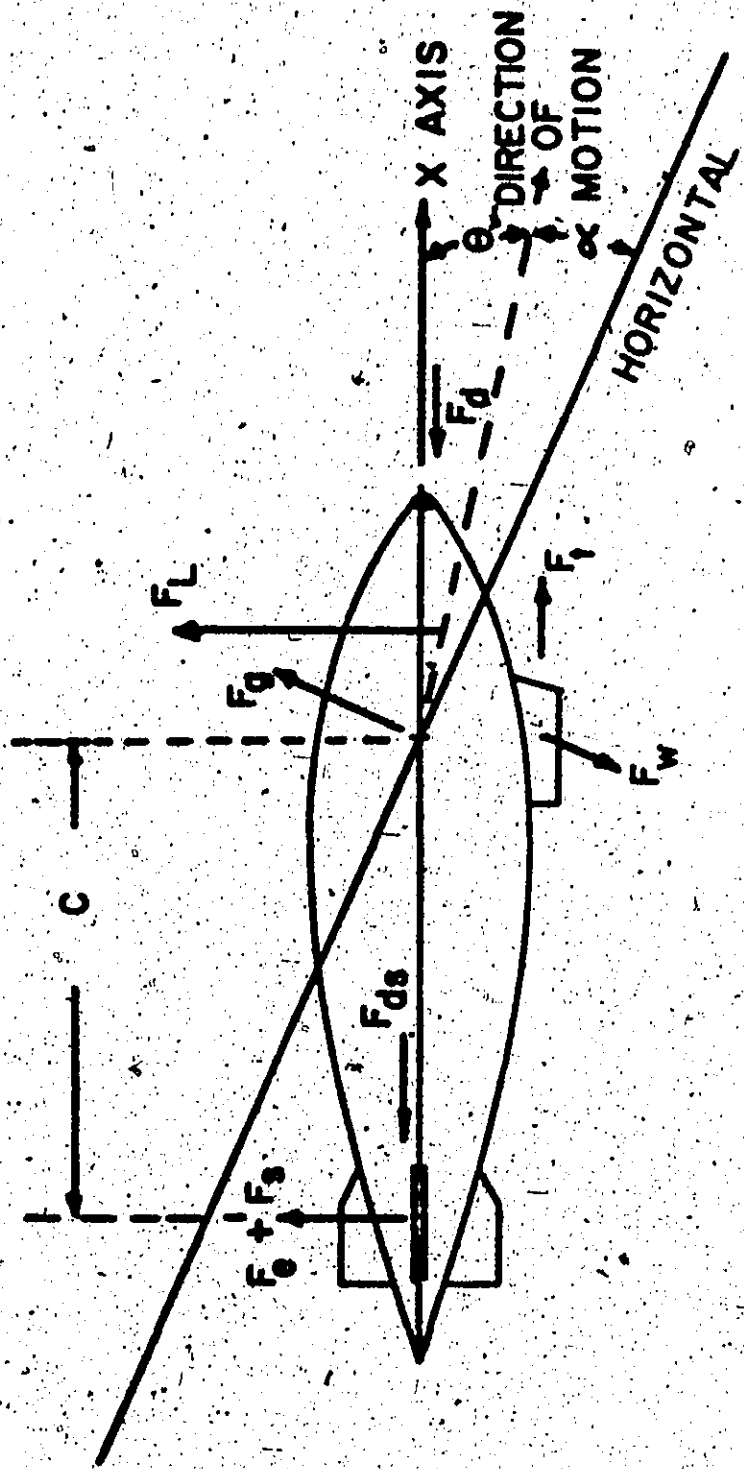


Figure 3.4: Forces Acting on an Airship for the Loading Condition of Case #3.

However, the remaining forces  $F_L$ ,  $F_s$ ,  $F_{ds}$ , and  $F_e$  must be defined.

(a) The dynamic lift force,  $F_L$ , occurs as a result of the symmetrical airfoil shape of the airship hull. The equation for the dynamic lift of an airship is [27]

$$F_L = \frac{1}{2} C_L \rho V^2 V^2 / 1 \quad (3.3)$$

where the lift coefficient may be approximated by [28]

$$C_L = 1.25\gamma \quad (3.4)$$

and  $\gamma$  is the angle of pitch of the airship expressed in radians. This approximation holds up to an angle of pitch of ten degrees.

(b) The force,  $F_s$ , on the fixed tail surfaces is given by

$$F_s = \frac{1}{2} C_L \rho V^2 A \quad (3.5)$$

The lift coefficient in this case is dependent on the airfoil shape adopted for these surfaces and  $A$  is the product of the mean chord and the mean span.

(c) The drag force of the tail surfaces is determined from

$$F_{ds} = \frac{1}{2} C_D \rho V^2 A \quad (3.6)$$

and  $C_D$  is the drag coefficient for the chosen airfoil shape and  $A$  is the drag area of the airfoil.

(d) The elevator force,  $F_e$ , once again depends on the airfoil shape and is given by

$$F_e = \frac{1}{2} \rho C_L V^2 A \quad (3.7)$$

In this case  $C_L$  is the lift coefficient of the airfoil as determined with moveable surfaces. The quantities  $\rho$ ,  $V$ , and

$V$  are as defined in Chapter 2.

2) Moments about the center of buoyancy:

(a) Static righting moment

$$M_{SR} = Wh \sin(\gamma \pm \theta) \quad (3.2)$$

where  $W$  = total weight of the airship

$h$  = the vertical distance between the center of gravity and the center of buoyancy

(b) Engine thrust moment

$$M_{td} = T(a)$$

(c) Dynamic upsetting moment

This moment is due to the pressure difference between the two sides of the hull. It is assisted by reduced pressure on one side of the tail. These forces act in opposite directions, but as the force due to the hull is greater, the resultant is called the dynamic lift of the hull. However, both these forces cause rotation in the same direction producing the upsetting moment. The upsetting moment due to these aerodynamic forces is so great that when flying with a positive pitch angle it is necessary to hold the elevators down instead of up as would be expected. The converse applies when flying with a negative pitch angle. Munk [13] provides the expression

$$M_u = \rho/2 V^2 (K_2 - K_1) \sin 2\theta \quad (3.8)$$



where  $V$  = the total volume of the airship in  $\text{ft}^3$ ,

$v$  = the velocity of the airship in  $\text{ft}/\text{sec}$ ,

$\rho$  = the density of the air in  $\text{slugs}/\text{ft}^3$ ,

$\theta$  = the angle of pitch,

and  $(K_2 - K_1)$  = constants to correct for the fact that masses of air are carried along with the hull in both longitudinal and transverse motion. Values of  $K_1$  and  $K_2$  can be found in Table 3.2.

(d) Tail surface moment

This moment opposes the dynamic upsetting moment and results from the tail force generated by the tail airfoil when flying at an angle of pitch.

$$M_s = F_s \cdot C + F_{ds} \cdot C \sin(\theta) \quad (3.10)$$

(e) Damping moment

An airship travelling along a specific path is considered as having two superimposed motions, one of translation as a whole, and one of rotation about a point. During the rotation about the point moments are produced. Suppose the nose is rising. Every part of the airship forward of the center of rotation is moving upward, while all parts to the rear of that center are moving downward. Thus an upward pressure of the air against the rear of the airship will be produced, as will a downward pressure of the air on the forward part. These forces cancel as far as longitudinal motion is concerned, but act together to give a moment to resist the existing

motion. As this moment acts only to damp out rotational moments once the forces that have caused these moments have been removed they will not enter into the analysis necessary to perform the maneuvers outlined in 3.1.

(f) Elevator Force Moment

$$M_e = P_e (CPT - CB) \quad (3.11)$$

The elevators are not normally considered when examining the static situation. However, it is possible to be flying at such an angle of pitch that their employment is required to counter the dynamic upsetting moment.

3:2.5 Longitudinal Steady Motion

For pitch stability the sum of the restoring moments must equal the sum of the upsetting moments. Assuming no elevator deployment ( $M_e = 0$ )

$$M_{SR} + M_S = M_U + M_{td} \quad (3.12)$$

Equation 4.6 holds only for the case illustrated by figure 3.4. Rearranged versions of this equation apply in the other cases. For example, during a dive, the static righting moment aids the dynamic upsetting moment and the thrust moment.

TABLE 3.2

116

Coefficients of Additional Mass  
of Ellipsoids of Various Length/  
Diameter Ratios [13]

<u>Length</u> <u>Diameter</u>	$K_1$	$K_2$	$K_2 - K_1$	$K_1$ Rotation
1.0	.500	.500	0	0
1.50	.305	.621	.316	.094
2.00	.309	.702	.493	.240
2.51	.156	.763	.607	.367
2.99	.122	.803	.681	.465
3.99	.082	.860	.778	.608
4.99	.059	.895	.836	.701
6.01	.045	.918	.873	.764
6.97	.036	.933	.897	.805
8.01	.029	.945	.916	.840
9.02	.024	.954	.930	.865
9.97	.021	.960	.939	.883
	0	1.000	1.000	1.000

NOTE: L/D is for an equivalent ellipsoid shape and is calculated from:

$$L/D = \sqrt{\frac{L^3}{6 \cdot VOL}}$$

### 3.2.6 Stability in Roll

Stability in roll, which is a very difficult problem in aircraft, is not a problem in airships. The static righting moment acts also with regard to roll and since there is no dynamic upsetting moment, rolling only occurs due to side gusts against the car and envelope and due to centrifugal force when turning. The moments of these forces are immediately overcome by the large restoring moment due to the low position of the center of gravity. Rolling may be uncomfortable but there is never any danger of it reaching an excessive value.

### 3.2.7 Steady Motion at a Fixed Yaw Angle

The forces and moments acting during steady motion at a fixed yaw angle present a rather more complex picture.

Figure 3.5 illustrates the forces acting during this type of motion. Burgess<sup>[13]</sup> gives the following expression, derived by Dr. M. M. Munk, for the transverse aerodynamic forces acting on an airship moving at a fixed angle of yaw.

$$\frac{dP}{dx} = \frac{dS}{dx} (K_2 - K_1) V^2 \sin 2\phi + k' V^2 \frac{\phi}{R} S \cos \phi + k' V^2 \frac{\phi}{R} \frac{dS}{dx} \cos \phi \quad (3.13)$$

In essence, one could call this motion a steady state turn. The first term in the above equation represents the force along the hull due to the angle of yaw and is inward toward the center of the turn on the fore-body and outward on the after-body.

It produces a turning moment balanced by an inward force assumed to be applied at the center of area of the fins. The second term gives a transverse force almost equal in magnitude to the

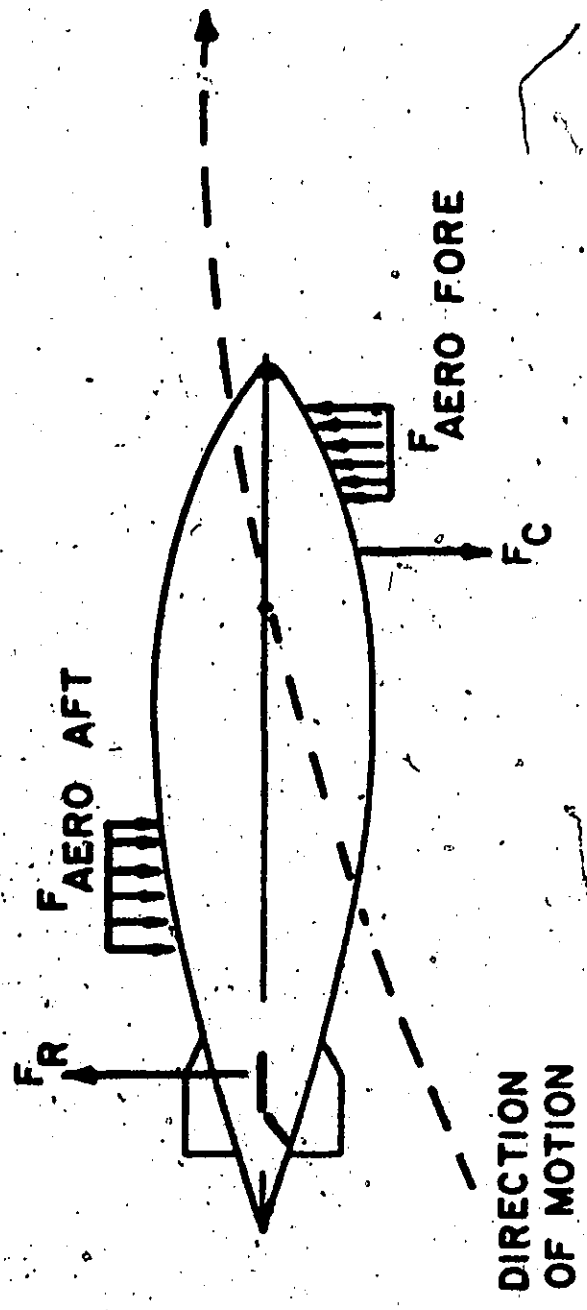


Figure 3.5: Forces Acting on an Airship at a Fixed Yaw Angle

centrifugal force of the displaced air and distributed in the same manner, but acting inward instead of outward. The third term represents outward forces on the tapered portions of the hull, having the same resultant as the forces represented by the second term, but of opposite sign, and acting through the center of buoyancy. The sum of the second and third terms gives no resultant force or moment.

The force  $F_{SV}$  on the tail surfaces acts inwardly toward the center of the turn, and since the theoretical forces on the bare hull have no resultant force, and only a resultant moment due to integration of the first term of (3.13),  $F_{SV}$  is equal in magnitude to the centrifugal force of the ship. Thus the forces acting include

(a) The tail surface force

$$F_{SV} = -F_C = - \sum_{i=1}^N k' V^2 (\rho/R) S x_i \cos \phi \quad (3.14)$$

where  $k'$  = coefficient of additional mass due to rotation

$x_i$  = the distance along the longitudinal axis

$S$  = the cross-sectional area at each value of  $x_i$

$\phi$  = the angle of yaw

$N$  = the number of stations along the  $x$  axis

and  $R = \frac{2b}{(K_2 - K_1) \sin 2\phi}$  the radius of the turning circle related to the angle of yaw at the center of buoyancy

$= \frac{2b}{(K_2 - K_1) \sin 2\phi}$

$(K_2 - K_1) \sin 2\phi$

All other quantities are as previously described. This force must offset the aerodynamic moment of the bare hull due to the angle of yaw.

(b) The rudder force

$$F_R = \frac{1}{2} \rho C_L V^2 A \quad (3.15)$$

where  $C_L$  = the rudder lift coefficient

$A$  = the lift area of the tail surfaces

= airfoil chord x airfoil span

(c) The aerodynamic forces on the bare hull

These forces cancel on the fore and after body. However, an expression is required to be able to calculate the moments produced.

$$\sum_{i=1}^N F_{HA} = \sum_{i=1}^N (K_2 - K_1) \Delta S V^2 \rho / 2 x_i \sin 2\phi = 0 \quad (3.16)$$

This force acts through the center of pressure of the tail, CPT, and from a purely static consideration  $C_L$  would be calculated using the angle of yaw at the center of buoyancy.

However, the radius of turn for an airship, unlike an airplane, is not much greater than the length of the airship.

Hecks<sup>[11]</sup> suggests that a factor of four is typical for the minimum radius. As a result the local flow direction relative to the axis of a turning airship changes considerably from the nose to the tail and hence the power of rudder is boosted. Figure (3.6) illustrates this effect. Hecks<sup>[11]</sup>, once again, suggests that the effective angle of yaw of the tail surfaces is doubled. Therefore,

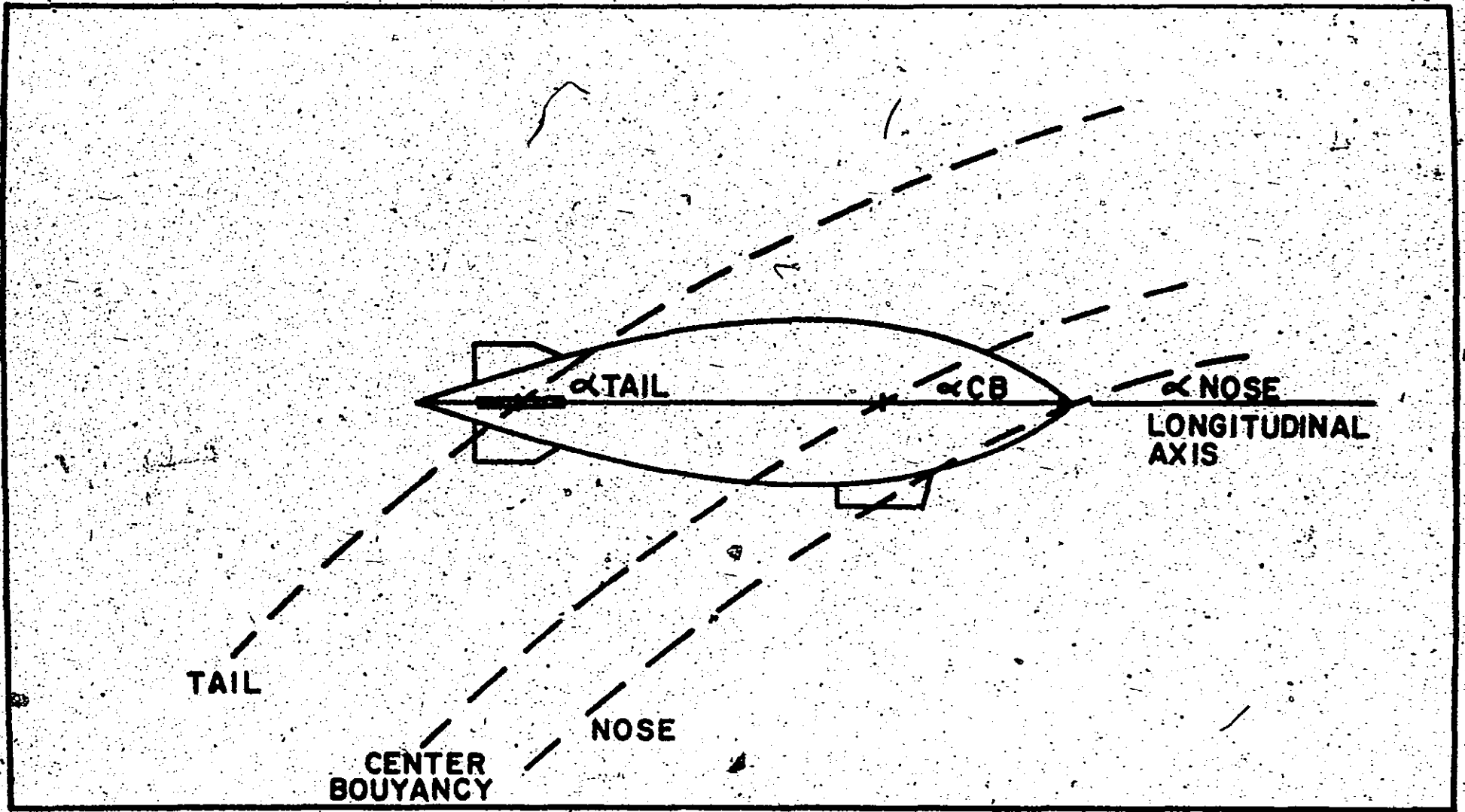


Figure 3.6: Angle of Yaw Variation Over the Airship Length



$$\dot{\theta}_s = 2 \dot{\theta}_{CB} \quad (3.17)$$

The moments produced by these forces are:

(a) Aerodynamic Moment

This is the moment due to the aerodynamic forces on the bare hull.

$$M_A = \sum_{i=1}^N F_{HA} (CB - x_i) \quad (3.18)$$

where  $x_i$  in this case is the longitudinal distance from the center of buoyancy.

(b) Rudder Moment

Moment due to the application of the rudder

$$M_R = F_R (CPT - CB) \quad (3.19)$$

(c) Pin Moment

The moment due to part of the tail surface force opposing the aerodynamic moment.

$$M_P = -M_A \quad (3.20)$$

(d) Yawing Moment

The damping moment due to the remaining aerodynamic force after the aerodynamic moment has been compensated for.

$$M_Y = \frac{(CB - CP)}{(CPT - CB)} F_{SV} \quad (3.21)$$

Thus for steady motion at a fixed yaw angle

$$M_A + M_R = M_P + M_Y \quad (3.22)$$

The static force analysis is now complete. The forces and moments described are all for no acceleration. However, the analysis must be extended to the accelerated or dynamic situation for this is the situation most commonly encountered by the airships and required to fulfill the specifications outlined in 3.1.

### 3.3 Dynamic Force and Moment Analysis

The analysis developed in the previous section will now be extended to include acceleration effects. The term "acceleration effects" includes both translational and rotational motion. Rotational acceleration of airships is normally derived from control effects. Control of airships may be subdivided into two classes, directional and altitude. Before developing the equations for these control classes, a brief description of each will be given so that the reader will be familiar with the control effects.

#### 3.3.1 Altitude Control

Altitude control is used to accomplish a change in altitude, either ascending or descending. Assume that the airship is flying in neutral trim and in static equilibrium. It is desired to climb. The elevators are raised. This action causes a rotation to occur and the airship acquires an angle of pitch  $\theta$ . The moments given by (3.6) act along with the moment due to the vertical deflection of the

elevators. The application of up elevators causes a downward force on the tail surfaces. Eventually the forces due to thrust acting at an angle of  $(\gamma + \theta)$ , due to the dynamic lift, and due to the fixed horizontal surfaces will overcome this force. However, it should be noted that the airship actually descends a short distance before climbing due to the reaction to the initial elevator force. For this reason extreme caution should be exercised in the use of elevators near the ground. If it is desired to descend the elevators are lowered. This causes an upward force on the tail surfaces and once again the situation previously described occurs, however with the direction of the forces and initial motion reversed. It should be noted, however, as mentioned when discussing the upsetting moment, that this moment becomes very large and thus once the desired altitude has been attained, it is necessary to climb with elevators down and to descend with the elevators up.

### 3.3.2 Directional Control

Directional control is attained by use of fins and rudders. It is essential to have a clear concept of the reaction of the airship to rudder control. Figure 3.7 illustrates the action of an airship during a turn and Figure 3.8 shows the action of an airship during obstacle avoidance.

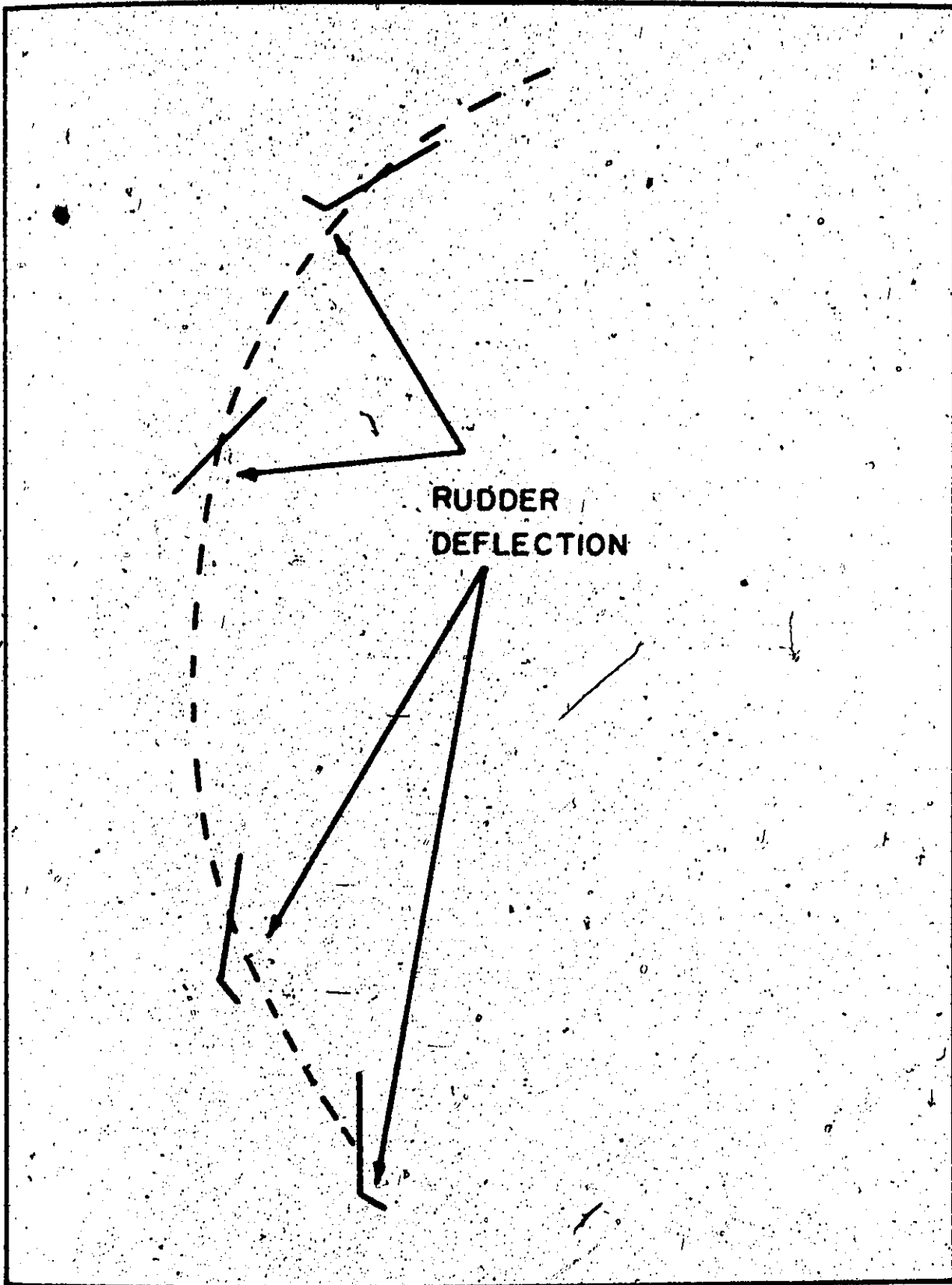


Figure 3.7: Action of an Airship During a Turn

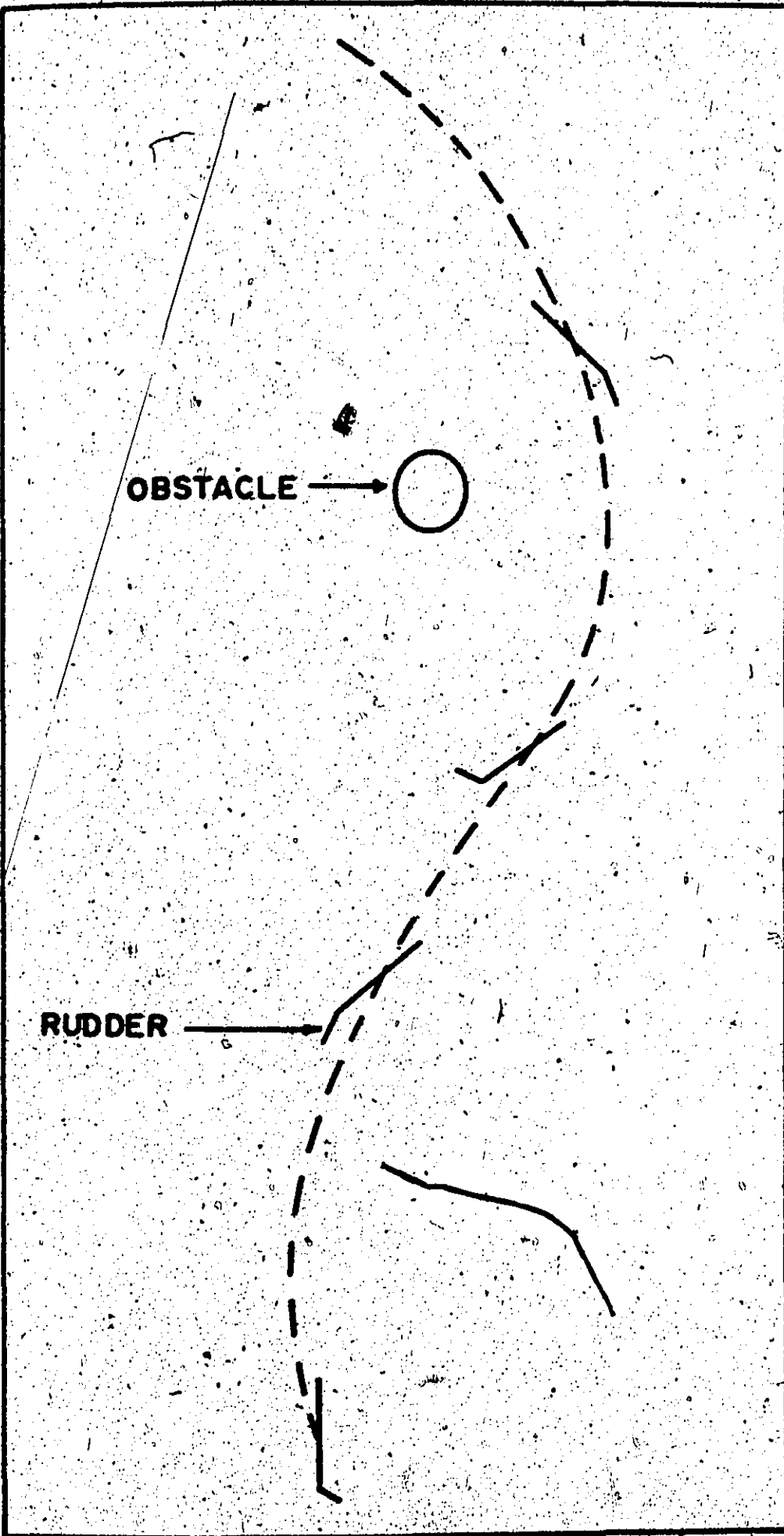


Figure 3.8: Action of an Airship During Obstacle Avoidance

When it is desired to turn to the right, the rudder is deflected to the right. This produces two effects. First an instantaneous force to the left acting on the right side of the rudder. Second, the airship rotates about its center of bouyancy such that the nose swings to the right. Thus initially the airship moves to the left and rotates to the right. The rotation of the nose to the right sets up a centrifugal force acting to the right. As the angle of yaw increases this centrifugal force increases until it is larger than the rudder force and the direction of lateral motion is to the right. However, the yaw moment is also increasing and thus the angular velocity of the airship will eventually decrease until the minimum turning radius is achieved. If the rudder is maintained in the hard right position, or even returned to the neutral position the turning will continue and in order to check this turn it is necessary to move the rudder to the hard left position. The turning radius is governed by the yaw moment and is greater for an airship of large fineness ratio than for one where this ratio is small.

### 3.3.3 Mechanics Equations

A rigid body having accelerated motion in space must obey the following equations;

$$\begin{aligned}
 IP_x &= m a_x \\
 IP_y &= m a_y \\
 IP_z &= m a_z \\
 IM_x &= I_x \dot{W}_x \\
 IM_y &= I_y \dot{W}_y \\
 IM_z &= I_z \dot{W}_z
 \end{aligned}
 \tag{3.23}$$

Where  $I_x$ ,  $I_y$ , and  $I_z$  are the sums of the mass moments of inertia of the various components of the body reference to a set of axes with their origin at the center of rotation by use of the parallel axis transformation.

$$\begin{aligned}
 I_x' &= I_x + m (y_c^2 + z_c^2) \\
 I_y' &= I_y + m (x_c^2 + z_c^2) \\
 I_z' &= I_z + m (x_c^2 + y_c^2)
 \end{aligned}
 \tag{3.24}$$

The response of an airship to an upsetting or a correcting moment is a function of the mass moment of inertia of the system. The mass moment of inertia of the system is composed of the inertial characteristics of the envelope, the enclosed gas, the payload, the propulsion devices, and any other independent major structural part. To simplify the problem the mass of several individual components of the airships have been taken as point loads acting through the center of mass of the particular component. Thus for these components:

$$I_x = 0$$

$$I_y = 0$$

$$I_z = 0$$

The parts of the airship treated in this manner include:

- 1) the nose cone,
  - 2) the cabin,
  - 3) the engines,
- and 4) the tail.

This is a reasonable simplification as the actual inertia of these components will only tend to make the airship more stable than the model would indicate.

The remaining moments of inertia, those related to the envelope and the enclosed gas, will be analysed about a set of axes perpendicular to the central axes and located at  $x = 0$ . General Mills<sup>[28]</sup> developed a set of equations, to determine these moments of inertia, which are quite convenient to use in conjunction with a digital computer.

The mass moment of inertia of the enclosed gas is given by:

$$I_x = \frac{vm (N+M)^4 (N+M)}{32 \pi^2 N^4 M^4} \frac{[(4N+1) (4M+1)]}{[4N+4M+2]} L^5 \quad (3.25)$$

$$I_y = I_z = I_x + \frac{vm (N+M)^2 (N+M)}{8 \pi^2 N^2 M^2} \frac{[(2N+3) (2M+1)]}{[2N+2M+4]} L^5 \quad (3.26)$$

All the factors used in these equations are as defined in Chapter 2.

The mass moment of inertia of the envelope is given by:



$$I_x = \frac{vm(N+M)3(N+M)}{4P^3N^3M^3} \frac{\sqrt{(3N+1)}\sqrt{(3M+1)}}{\sqrt{(3N+3M+2)}} L^4 \quad (3.27)$$

$$I_y = I_z = \frac{I_x}{2} + \frac{vm(N+M)(N+M)}{P^2N^2M^2} \frac{\sqrt{(N+3)}\sqrt{(M+1)}}{\sqrt{(N+M+4)}} L^4 \quad (3.28)$$

As these moments of inertia have been calculated with respect to a set of co-ordinate axes with their origin at the nose of the airship ( $x = 0$ ), a transformation must be performed to a set of axes whose origin is the point about which rotation occurs. This is done using the parallel axis transformation described previously. Those components whose moment of inertia about their own axis was taken as zero must also be referenced to the rotation center using the parallel axis transformation and these will thus acquire a moment of inertia by means of the quantities

$$m(x_c^2 + y_c^2)$$

$$m(x_c^2 + z_c^2)$$

$$m(y_c^2 + z_c^2)$$

The masses used in these equations are the individual masses of the components and the mass used in the mechanics equations is the system mass.

$$m = \frac{W_{\text{system}}}{G} \quad (3.28)$$

$G$  being the gravitational constant and  $W_{\text{system}}$  the total weight of the airship.

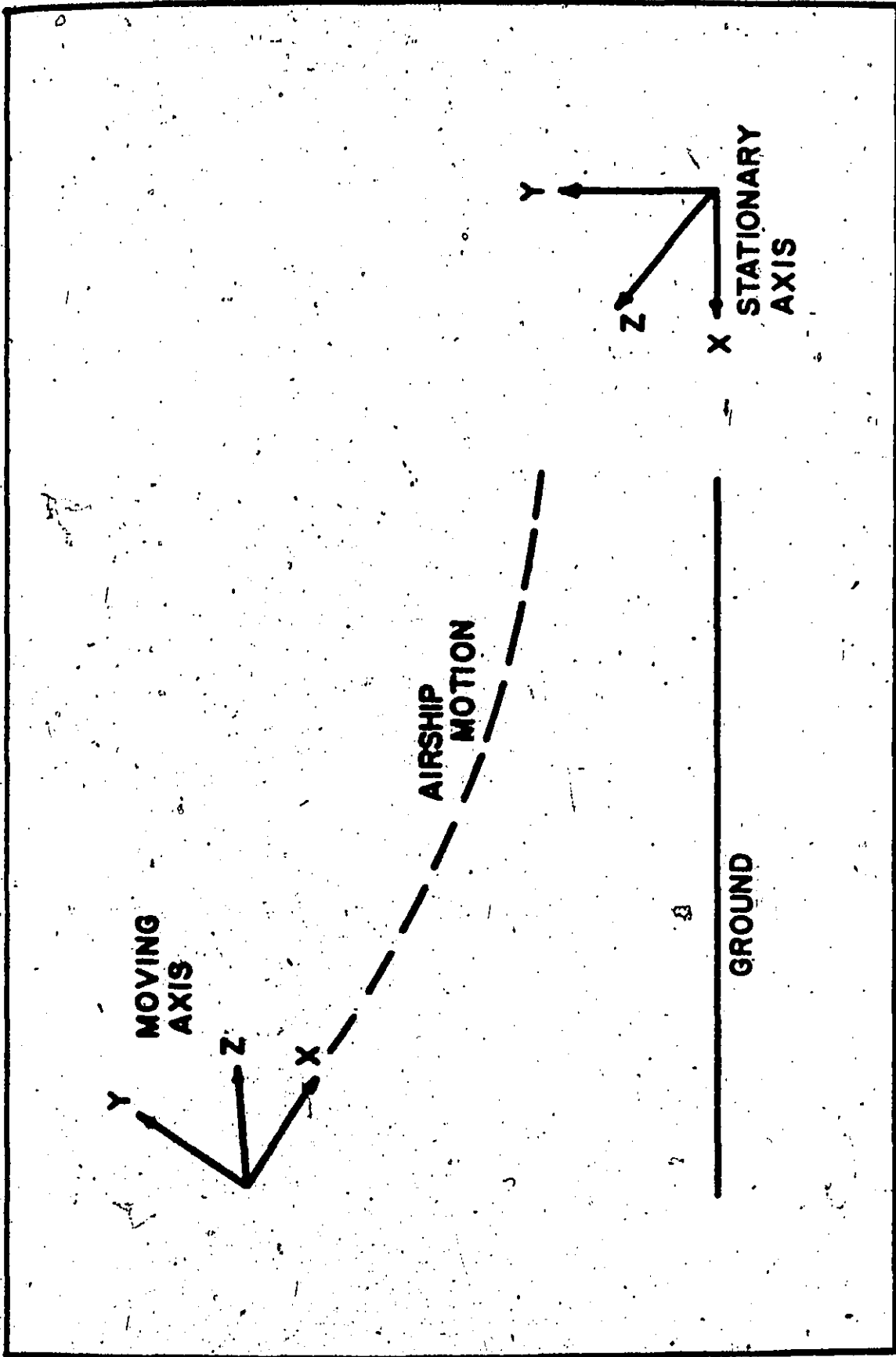


Figure 3.9: Modified Set of Axis

### 3.3.4 Forces and Moments Acting on the Airship

The forces and moments acting on the airship during accelerated motion are essentially similar to those discussed in the static case. However, both the linear acceleration and the angular acceleration which may occur cause the forces and angles to change continuously. Hence, when considering accelerated motion it is convenient to consider very small time increments and to consider the situations as being static within these time increments. The acceleration effects can be superposed when moving from one time interval to the next.

### 3.3.5 Determination of the Accelerations

Rotational and translational accelerations will be examined as the airship rotates about its center of gravity. Thus a modified set of axes is now introduced and illustrated in Figure 3.9. This new set of axes makes it possible to separate the effects on the airship and the motion with respect to the original horizontal axes.

#### (a) Translational Acceleration

##### (1) X direction

From the mechanics equations

$$a_x = \frac{F_x}{m}$$

(3.30)

where

$$IP_x = [(P_d + P_{ds}) \cos(\gamma) + (P_L - P_R + P_S) \sin(\gamma)] \cos(\phi + \theta) + [P_C + P_R] \sin(\phi + \theta) \quad (3.31)$$

(2) Y direction

Similarly in the y direction,

$$a_y = \frac{IP_y}{m} \quad (3.32)$$

where

$$IP_y = [P_G - P_W] + P_L \cos(\gamma) + P_S \cos(\gamma) + P_e \cos(\gamma) + P_t \sin(\epsilon) + (P_d + P_{ds}) \sin(\gamma) \quad (3.33)$$

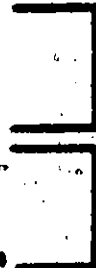
and  $\epsilon$  is defined by the cases discussed in section 3.2.4.

i.e.  $\epsilon = \gamma + \theta$  when climbing

$\epsilon = \gamma - \theta$  when diving

$\epsilon = \gamma - \theta$  when climbing

$\epsilon = \gamma + \theta$  when diving



in a heavy condition,

in a light condition,

and  $\epsilon = 0$  in a neutral condition.

(3) Z direction

Similarly in the z direction

$$a_z = \frac{IP_z}{m} \quad (3.34)$$

where

$$IP_z = [(P_d + P_{ds}) \cos(\gamma) + (P_L + P_e + P_S) \sin(\gamma)] \sin(\phi + \theta) + [P_C + P_R] \cos(\phi + \theta). \quad (3.35)$$

NOTE: the co-ordinates  $x, y, z$  used in these equations are referenced to the fixed ground axes. When determining the velocity of the airship, and all the quantities that it affects, it is necessary to reference this to the moving axis of the airship. Hence,

$$a_{\text{Airship Forward}} = \frac{(P_d + P_{ds}) + (P_w - P_L) \sin(\gamma) - P_t \cos(\gamma)}{m} \quad (3.36)$$

and

$$v_{\text{Airship Forward}} = \int_0^t a \, dt = at + v_0 \quad (3.37)$$

The sum of the forces acting on the airship with respect to its co-ordinate axes are:

$$\begin{aligned} \Sigma F_x &= P_d + P_{ds} - P_t \\ \Sigma F_y &= P_g - P_w + P_L + P_s + P_o \\ \Sigma F_z &= P_C + P_R \end{aligned} \quad (3.38)$$

## (b) Rotational Acceleration

### (1) Rotation about the $z$ axis

$$\dot{\omega}_z = \frac{M_z}{I_z} \quad (3.39)$$

where

$$IM_z = M_u + M_{td} + M_{SR} + M_e + M_g. \quad (3.40)$$

(ii) Rotation about the Y axis

$$\dot{W}_y = \frac{IM_y}{I_y} \quad (3.41)$$

where

$$IM_y = M_A + M_R + M_P + M_Y. \quad (3.42)$$

(iii) Rotation about the x axis

As explained previously, stability in roll in airships is taken care of almost automatically. Hence acceleration about this axis will be neglected.

### 3.3.6 Determination of Position

The trajectories can be determined if the position can be determined at all times. Once the accelerations have been determined the velocity can be determined from

$$V = \int_{t_1}^{t_2} a \, dt = at + V_{t_1} \quad (3.37)$$

and hence the position referenced to some initial co-ordinate

$$P = \int_0^t V \, dt = \frac{1}{2} at^2 + V_0 t + p_0 \quad (3.43)$$

where  $p_0$  = position at the previous time interval

$V_0$  = velocity at the previous time interval.

The velocities and positions must be determined for the x, y and z co-ordinates. Once these co-ordinates have been obtained and evaluated to ascertain that the correct maneuvers

have been carried out it is now possible to evaluate the flight forces acting on the airship, as expressed by (3.38), and thus satisfy the initial requirements.

### 3.4 User Oriented Computer Programme Description

The theory which has been presented in the previous sections lends itself to adaptation to computer usage. In order to both aid the designer and to submit as part of compliance report required by the Ministry of Transport, a user oriented computer programme has been developed. This programme computes the trajectories based on the presented theory and also calculates the forces acting on the airship. The designer may change any of the listed input variables in order to examine various design possibilities. Figure 3.10 illustrates the programme set up. A complete listing of the programme is included in Appendix E. The programme does not simulate the exact conditions that prevail in the airship at various times. To simplify matters the ballonets were considered to be fully deflated at all times. Thus center of gravity shifts, due to various degrees of inflation, were neglected as were axial shifts of the center of gravity due to fore-and-aft sloshing of the air in the ballonets. It is also assumed that the designer will provide two horizontal tail surfaces and two vertical tail surfaces. If this is not the case, then the quantities involving the tail forces must be suitably altered.

CONTROL CARDS

INPUT DATA (USER SUPPLIED)

MAIN PROGRAM (TST)

FUNCTION FTABLE

SUBROUTINE UMBZ

OUTPUT

Figure 9-10: Trajectory Programme Input Deck Setup



The user input variables are as follows:

- (1) XN Airship shape parameter N
- (2) XM Airship shape parameter M
- (3) XL Airship length in feet
- (4) F Airship fineness ratio
- (5) VOL Airship lifting gas volume in cubic feet
- (6) VOLT Airship total volume in cubic feet
- (7) XT Location of the center of gravity of the tail surfaces in the x direction
- (8) YT Location of the center of gravity of the tail surfaces in the y direction
- (9) ZT Location of the center of gravity of the tail surfaces in the z direction
- (10) XP Location of the nose cone center of gravity in the x direction
- (11) YN Location of the nose cone center of gravity in the y direction
- (12) ZN Location of the nose cone center of gravity in the z direction
- (13) XE Location of the engine center of gravity in the x direction
- (14) YE Location of the engine center of gravity in the y direction
- (15) ZE Location of the engine center of gravity in the z direction
- (16) XCAB Location of the cabin center of gravity in the x direction
- (17) YCAB Location of the cabin center of gravity in the y direction
- (18) ZCAB Location of the cabin center of gravity in the z direction

NOTE: All these locations measured in feet from the nose of the airship

- (19) WCAB The airship cabin weight in lbs.
- (20) WT The tail weight in lbs.
- (21) WN The nose weight in lbs.
- (22) EW The engine weight in lbs.
- (23) WE The airship envelope weight in lbs.
- (24) TOW The airship total weight in lbs.
- (25) CHH The average chord length of the horizontal tail surfaces in feet
- (26) CHV The average chord length of the vertical tail surfaces in feet.
- (27) TL The span of the horizontal surface (1) in feet
- (28) RL The span of the vertical surface (1) in feet
- (29) DH The maximum thickness of the airfoil in feet
- (30) CL Airfoil lift coefficient
- (31) AL The pitch angle corresponding to each lift coefficient
- (32) CD Airfoil drag coefficient
- (33) AD The pitch angle corresponding to each drag coefficient
- (34) CLD The airfoil lift coefficient when using a flap system
- (35) ALD The pitch angle corresponding to each lift coefficient
- (36) YMDR The maximum descent rate in ft/sec
- (37) YMC The maximum climb rate in ft/sec

(38) WX The airship envelope material weight in ozs/  
square yards.

Optionally the user may also introduce the following quantities:

(39) XXIN The mass moment of inertia of the airship  
nose - x direction

(40) YYIN The mass moment of inertia of the airship  
nose - y direction

(41) ZZIN The mass moment of inertia of the airship  
nose - z direction

(42) XXIC The mass moment of inertia of the cabin  
- x direction

(43) YYIC The mass moment of inertia of the cabin  
- y direction

(44) ZZIC The mass moment of inertia of the cabin  
- z direction

(45) XXITA The mass moment of inertia of the tail  
surfaces - x direction

(46) YYITA The mass moment of inertia of the tail  
surfaces - y direction

(47) ZZITA The mass moment of inertia of the tail  
surfaces - z direction

(48) XXIE The mass moment of inertia of the engines  
- x direction

(49) YYIE The mass moment of inertia of the engines  
- y direction

(50) ZZIE The mass moment of inertia of the engines  
- z direction

These quantities unless specifically otherwise defined  
are set to 0 by the programme. The input quantities should be  
entered into the programme via data cards placed after the  
appropriate comment cards.

For example variable (24) TOW should be entered after the cards;

#### WEIGHT DATA

DATA TOW/6000.0/

DATA .....

### 3.5 Programme Results

The programme has been used to evaluate the CANADIAN AIRSHIP DEVELOPMENT CORPORATION design CAS-1 in order to file a compliance report as required by the Ministry of Transport regulations. Table 3.3 presents the input quantities. Table 3.4 presents selected trajectories as well as the matching angles and velocities, both linear and angular. Finally Table 3.5 presents the same selected trajectories and the corresponding forces in the x, y, and z directions. Figures 3.11 through 3.15 illustrate several of the trajectories calculated by the programme.

TABLE 3.3: COMPUTER TRAJECTORY TEST INPUT VARIABLES

Quantity	Value
XN	0.4
XM	0.6
XL	117.0
F	3.0
VOL	80087
VOLT	91000
XT	93.0
YT	0.0
ZT	25.0
XF	5.0
XN	0.0
ZN	0.0
XE	52.6
YE	-25.0
ZE	20.0
XCAB	48.8
YCAB	-25.0
ZCAB	0.0
WCAB	3274.0
WT	500.0
WN	200.0
EW	400.0
WE	922.0
TOW	5400.0
CHH	17.2
CHV	12.0
TL	14.0
RL	15.0
DH	2.0
WX	11.40
YMDR	40.0
YMC	40.0
AL	1.0, 2.0, 3.0, 4.0, 5.0, 6.0, 7.0, 8.0, 9.0, 10.0
AD	1.0, 2.0, 3.0, 4.0, 5.0, 6.0, 7.0, 8.0, 9.0, 10.0
ALD	-14.0, -12.0, -10.0, -8.0, .....0.0, 2.0, .....10.0
CL	0.1, 0.2, 0.3, 0.4, .....1.0
CD	0.0092, 0.0095, 0.010, 0.0119, 0.0120, 0.0130, 0.0145, 0.0166, 0.0200
CLD	0.4, 0.0, 0.25, 0.48, 0.70, 0.95, 1.15, 1.35, 1.55, 1.75, 1.95, 2.10, 1.98



Figure 3.11: Graphical Illustration of the Programme Output-  
Take-off trajectory

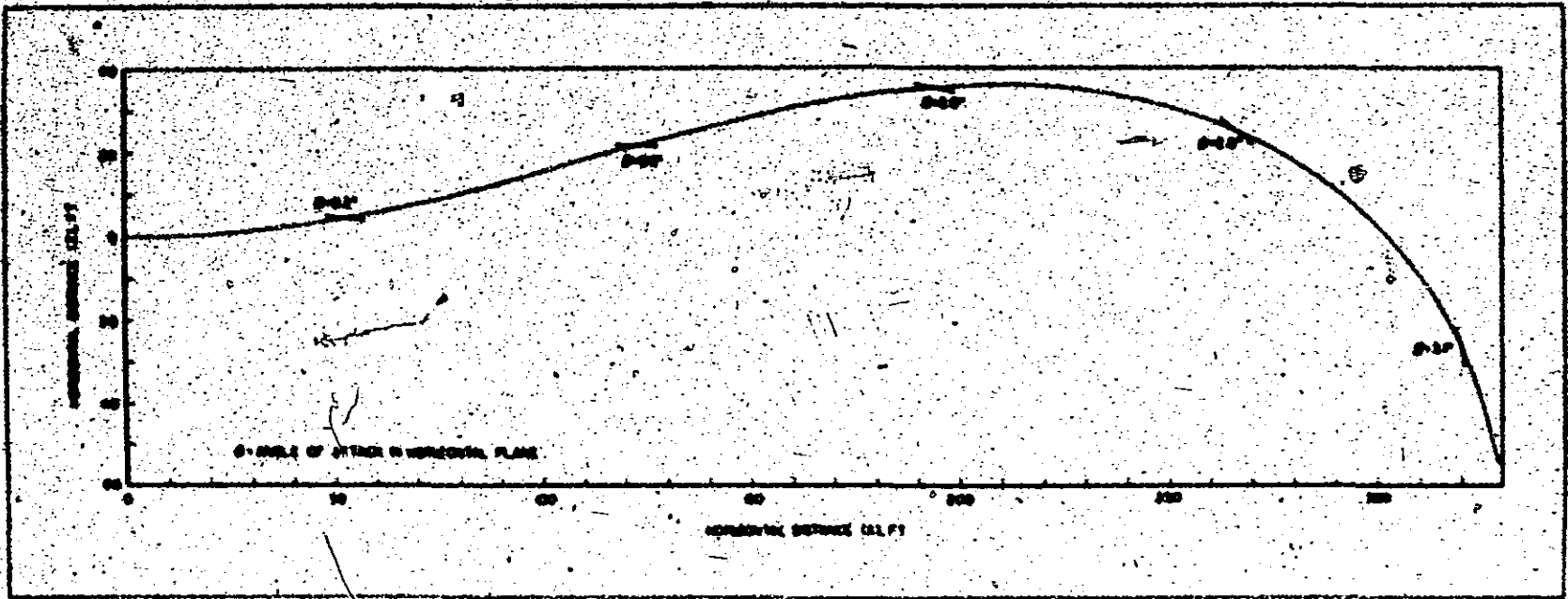


Figure 3.12: Graphical Illustration of the Programme Output- Full Rudder Until a 75° Turn Achieved

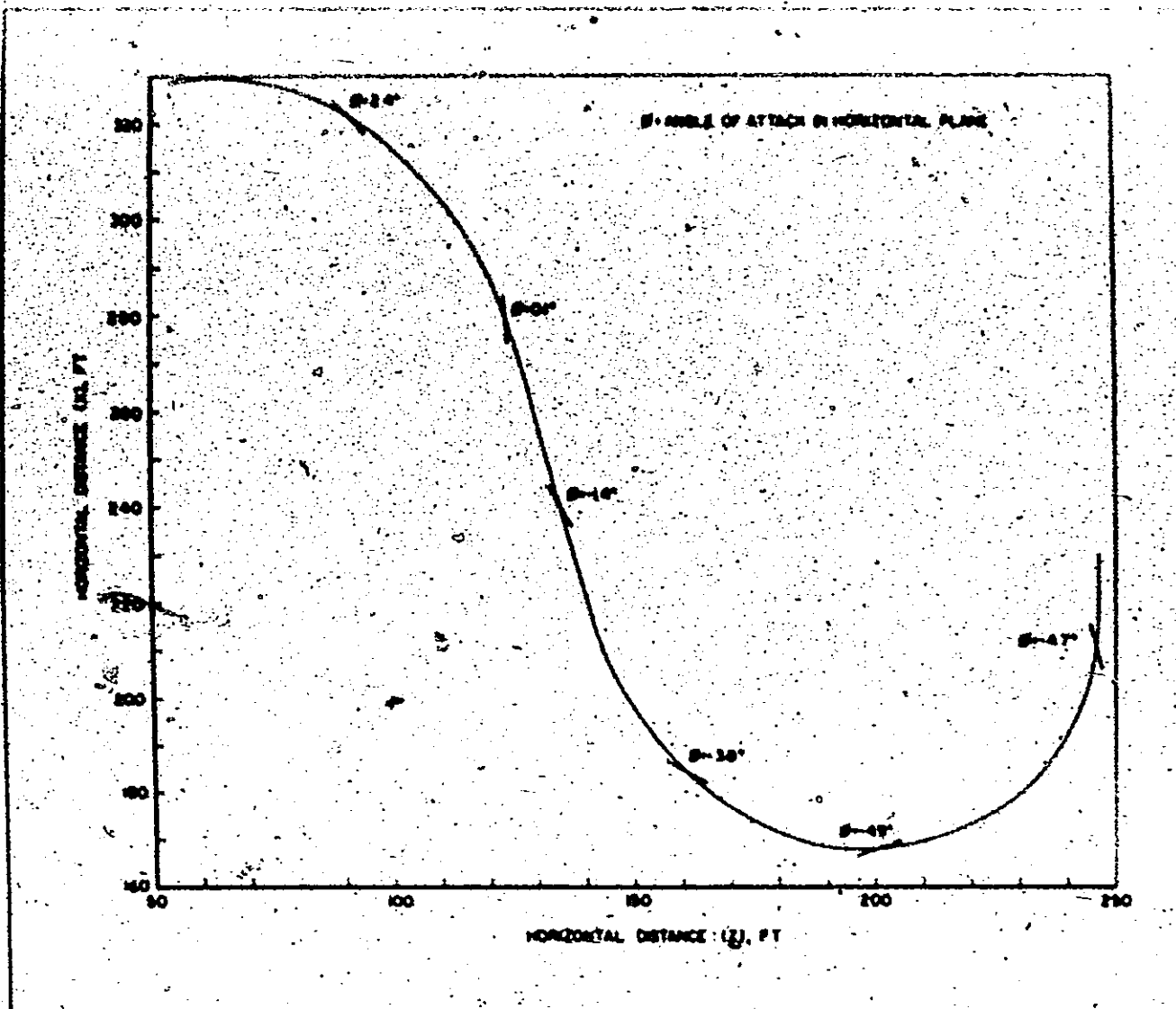


Figure 3.13: Graphical Illustration of the Programme Output- Full Opposite Rudder Until the Original Heading Regained



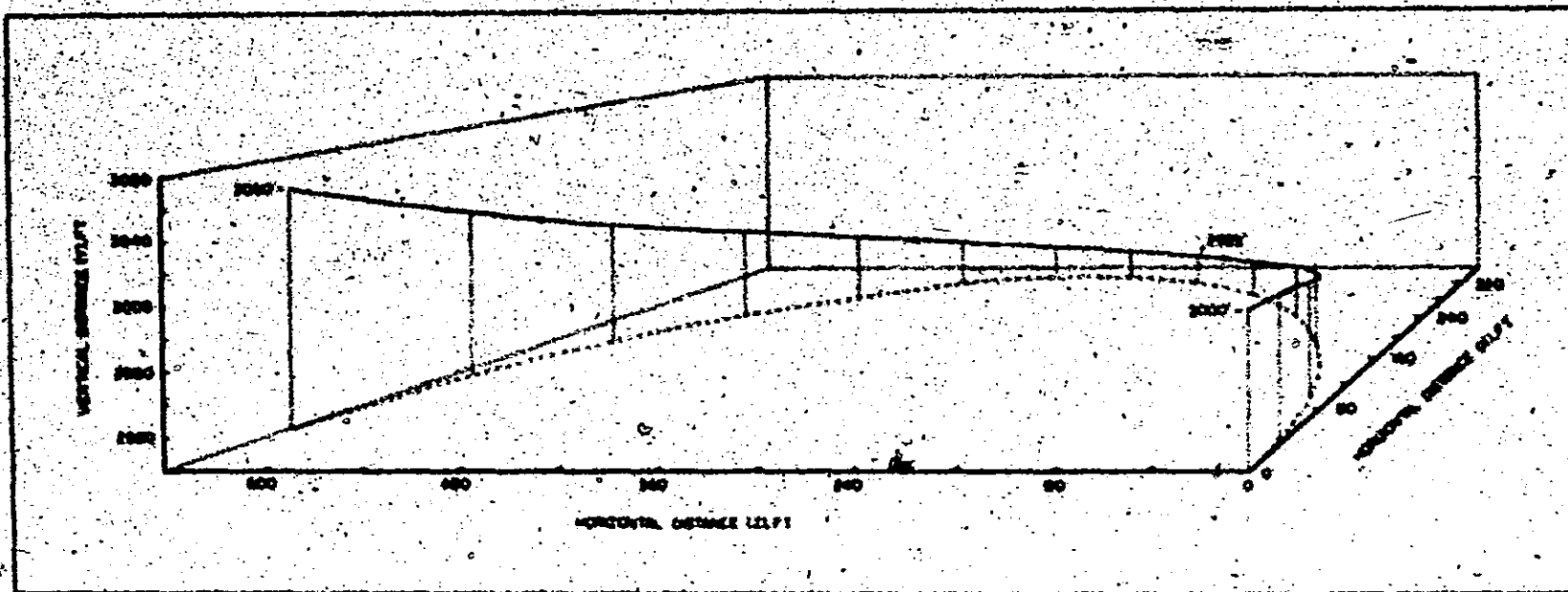


Figure 3.14: Graphical Illustration of the Programme Output-  
Full-up Elevators and a Steady State Turn From  
0 to 180 degrees

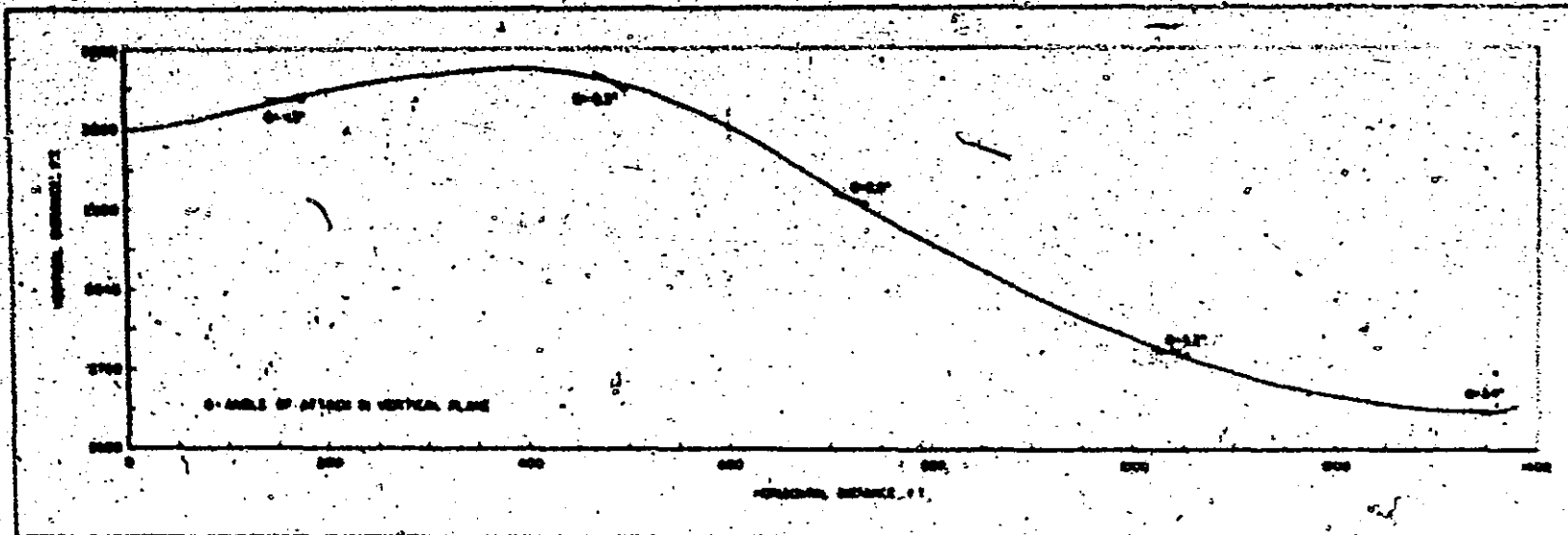


Figure 3.15: Graphical Illustration of the Programme Output-Full Down Elevator Until Maximum Descent Rate Achieved and Then Full Up Elevator Until Descent Rate Equals Zero

X ft.	Y ft.	Z ft.	Vx ft/sec	Vy ft/sec	Vz ft/sec	θ	γ	δ
TAKE OFF	AND CLIMB	OVER 100	OBSTACLE					
-0.025	0.000	0.000	-0.253	-1.812	0.000	0.000	0.000	0.000
-0.045	0.000	0.000	-0.53	0.000	0.000	0.000	0.000	0.000
-0.072	0.000	0.000	-0.63	0.000	0.000	0.000	0.000	0.000
-0.097	0.000	0.000	-0.115	0.000	0.000	0.001	0.000	0.000
-0.126	0.000	0.000	-0.149	0.000	0.000	0.001	0.000	0.000
-0.159	0.000	0.000	-0.185	0.000	0.000	0.001	0.000	0.000
-0.198	0.000	0.000	-0.224	0.000	0.000	0.002	0.000	0.000
-0.243	0.000	0.000	-0.266	0.000	0.000	0.002	0.000	0.000
-0.295	0.000	0.000	-0.312	0.000	0.000	0.003	0.000	0.000
-0.355	0.000	0.000	-0.363	0.000	0.000	0.004	0.000	0.000
-0.425	0.000	0.000	-0.419	0.000	0.000	0.005	0.000	0.000
-0.504	0.000	0.000	-0.482	0.000	0.000	0.006	0.000	0.000
-0.599	0.000	0.000	-0.554	0.000	0.000	0.007	0.000	0.000
-0.715	0.000	0.000	-0.639	0.000	0.000	0.009	0.000	0.000
-0.869	0.000	0.000	-0.740	0.000	0.000	0.010	0.000	0.000
-1.077	0.000	0.000	-0.866	0.000	0.000	0.012	0.000	0.000
-1.329	0.000	0.000	-1.035	0.000	0.000	0.014	0.000	0.000
-1.635	0.000	0.000	-1.268	0.000	0.000	0.017	0.000	0.000
-1.992	0.000	0.000	-1.794	0.000	0.000	0.021	0.000	0.000
-2.348	0.000	0.000	-2.300	0.000	0.000	0.028	0.000	0.000
			-2.806	0.000	0.000	0.032	0.000	0.000
			-3.311	0.000	0.000	0.039	0.000	0.000
			-3.816	0.000	0.000	0.048	0.000	0.000
			-4.320	0.000	0.000	0.058	0.000	0.000







Xc ft.	Y ft.	Z ft.	Vx ft/sec	Vy ft/sec	Vz ft/sec	θ	γ	φ	δ
-115.000	1.75	0.000	-37.871	1.200	0.000	3.709	6.711	0.000	0.000
-150.000	11.21	0.000	-38.816	5.302	0.000	3.709	7.266	0.000	0.000
-160.000	19.81	0.000	-39.329	8.802	0.000	3.709	8.028	0.000	0.000
-170.000	27.17	0.000	-40.002	11.206	0.000	3.709	7.458	0.000	0.000
-177.100	32.89	0.000	-40.698	12.766	0.000	3.709	6.805	0.000	0.000
-181.000	37.00	0.000	-41.179	14.271	0.000	3.709	6.760	0.000	0.000
-185.000	40.11	0.000	-41.636	15.711	0.000	3.709	6.152	0.000	0.000
-188.000	42.24	0.000	-42.067	17.076	0.000	3.709	5.852	0.000	0.000
-192.000	43.60	0.000	-42.483	17.977	0.000	3.709	10.172	0.000	0.000
-196.000	44.21	0.000	-42.889	18.542	0.000	3.709	10.020	0.000	0.000
-200.000	44.67	0.000	-43.278	19.024	0.000	3.709	11.605	0.000	0.000
-210.000	45.17	0.000	-44.027	19.224	0.000	3.709	17.008	0.000	0.000
-215.000	45.06	0.000	-44.669	19.428	0.000	3.709	11.327	0.000	0.000
-219.000	45.00	0.000	-45.200	19.570	0.000	3.709	14.134	0.000	0.000
-223.000	44.91	0.000	-45.717	19.692	0.000	3.709	15.060	0.000	0.000
-227.000	44.86	0.000	-46.219	19.800	0.000	3.709	15.060	0.000	0.000
-231.000	44.80	0.000	-46.706	19.896	0.000	3.709	15.060	0.000	0.000
-235.000	44.75	0.000	-47.179	19.970	0.000	3.709	14.607	0.000	0.000
-239.000	44.70	0.000	-47.638	20.026	0.000	3.709	14.607	0.000	0.000
-243.000	44.68	0.000	-48.083	20.069	0.000	3.709	14.607	0.000	0.000
-247.000	44.67	0.000	-48.514	20.100	0.000	3.709	14.607	0.000	0.000
-251.000	44.67	0.000	-48.931	20.119	0.000	3.709	14.607	0.000	0.000
-255.000	44.67	0.000	-49.335	20.126	0.000	3.709	14.607	0.000	0.000
-259.000	44.67	0.000	-49.726	20.126	0.000	3.709	14.607	0.000	0.000
-263.000	44.67	0.000	-50.104	20.119	0.000	3.709	14.607	0.000	0.000
-267.000	44.67	0.000	-50.469	20.100	0.000	3.709	14.607	0.000	0.000
-271.000	44.67	0.000	-50.821	20.069	0.000	3.709	14.607	0.000	0.000
-275.000	44.67	0.000	-51.159	20.026	0.000	3.709	14.607	0.000	0.000
-279.000	44.67	0.000	-51.484	19.970	0.000	3.709	14.607	0.000	0.000
-283.000	44.67	0.000	-51.796	19.900	0.000	3.709	14.607	0.000	0.000
-287.000	44.67	0.000	-52.095	19.819	0.000	3.709	14.607	0.000	0.000
-291.000	44.67	0.000	-52.381	19.726	0.000	3.709	14.607	0.000	0.000
-295.000	44.67	0.000	-52.654	19.619	0.000	3.709	14.607	0.000	0.000
-300.000	44.67	0.000	-52.914	19.500	0.000	3.709	14.607	0.000	0.000
-305.000	44.67	0.000	-53.161	19.369	0.000	3.709	14.607	0.000	0.000
-310.000	44.67	0.000	-53.395	19.226	0.000	3.709	14.607	0.000	0.000
-315.000	44.67	0.000	-53.616	19.070	0.000	3.709	14.607	0.000	0.000
-320.000	44.67	0.000	-53.824	18.900	0.000	3.709	14.607	0.000	0.000
-325.000	44.67	0.000	-54.019	18.719	0.000	3.709	14.607	0.000	0.000
-330.000	44.67	0.000	-54.201	18.526	0.000	3.709	14.607	0.000	0.000
-335.000	44.67	0.000	-54.370	18.319	0.000	3.709	14.607	0.000	0.000
-340.000	44.67	0.000	-54.526	18.100	0.000	3.709	14.607	0.000	0.000
-345.000	44.67	0.000	-54.669	17.869	0.000	3.709	14.607	0.000	0.000
-350.000	44.67	0.000	-54.799	17.626	0.000	3.709	14.607	0.000	0.000
-355.000	44.67	0.000	-54.916	17.370	0.000	3.709	14.607	0.000	0.000
-360.000	44.67	0.000	-55.020	17.100	0.000	3.709	14.607	0.000	0.000
-365.000	44.67	0.000	-55.111	16.819	0.000	3.709	14.607	0.000	0.000
-370.000	44.67	0.000	-55.189	16.526	0.000	3.709	14.607	0.000	0.000
-375.000	44.67	0.000	-55.254	16.219	0.000	3.709	14.607	0.000	0.000
-380.000	44.67	0.000	-55.306	15.900	0.000	3.709	14.607	0.000	0.000
-385.000	44.67	0.000	-55.345	15.569	0.000	3.709	14.607	0.000	0.000
-390.000	44.67	0.000	-55.371	15.226	0.000	3.709	14.607	0.000	0.000
-395.000	44.67	0.000	-55.384	14.870	0.000	3.709	14.607	0.000	0.000
-400.000	44.67	0.000	-55.384	14.500	0.000	3.709	14.607	0.000	0.000





X ft.	Y ft.	Z ft.	Vx ft/sec	Vy ft/sec	Vz ft/sec	θ	γ	φ	δ
FULL RUDDER UNTIL 75 DEGREE TURN MADE									
0.000	3000.00	0.000	-88.000	0.000	0.000	-0.022	0.000	0.000	0.000
-4.404	3000.00	-1.133	-88.155	.121	-7.665	-0.023	.039	.005	-0.868
-17.624	3000.00	-3.533	-88.272	.241	-5.324	-0.023	.117	.021	-2.595
-26.458	3000.00	-1.196	-88.309	.359	-7.937	-0.023	.194	.047	-4.297
-35.287	3000.00	-2.116	-88.272	.475	-10.468	-0.023	.269	.083	-5.954
-44.109	3000.00	-3.244	-88.173	.590	-12.879	-0.023	.343	.130	-7.541
-52.919	3000.00	-4.084	-88.025	.703	-15.133	-0.023	.415	.187	-9.038
-61.713	3000.00	-6.381	-87.846	.814	-17.197	-0.023	.486	.253	-10.422
-70.488	3000.00	-8.112	-87.655	.924	-19.035	-0.022	.556	.328	-11.671
-79.244	3000.00	-10.095	-87.473	1.032	-20.618	-0.022	.624	.412	-12.764
-87.984	3000.00	-12.222	-87.321	1.139	-21.915	-0.022	.692	.504	-13.643
-96.711	3000.00	-14.402	-87.214	1.244	-22.901	-0.022	.758	.604	-14.448
-105.430	3000.00	-16.745	-87.177	1.340	-23.549	-0.022	.823	.711	-14.922
-114.150	3000.00	-19.154	-87.224	1.450	-23.836	-0.022	.887	.824	-15.208
-122.880	3000.00	-21.533	-87.367	1.551	-23.741	-0.022	.951	.943	-15.251
-131.629	3000.00	-23.887	-87.411	1.651	-23.244	-0.022	1.013	1.066	-15.098
-140.407	3000.00	-26.161	-87.957	1.749	-22.327	-0.022	1.074	1.193	-14.558
-149.225	3000.00	-28.376	-88.395	1.846	-20.973	-0.022	1.135	1.323	-13.802
-158.090	3000.00	-30.533	-88.913	1.941	-19.167	-0.022	1.194	1.455	-12.763
-167.010	3000.00	-32.136	-89.445	2.035	-16.646	-0.022	1.252	1.588	-11.494
-175.988	3000.00	-33.688	-90.001	2.120	-14.149	-0.022	1.309	1.720	-9.814
-185.025	3000.00	-34.942	-90.659	2.220	-10.921	-0.021	1.366	1.852	-7.901
-194.117	3000.00	-35.848	-91.172	2.310	-7.208	-0.021	1.421	1.982	-5.696
-203.254	3000.00	-36.359	-91.564	2.399	-4.014	-0.021	1.475	2.109	-3.203
-212.421	3000.00	-36.427	-91.773	2.487	1.651	-0.021	1.528	2.232	-1.426
-221.595	3000.00	-36.007	-91.729	2.574	4.766	-0.021	1.579	2.350	2.628

15A

X ft.	Y ft.	Z ft.	Vx ft/sec	Vy ft/sec	Vz ft/sec	θ	γ	φ	δ
-230.750	3000.00	-35.051	-41.362	2.660	16.304	-.021	1.630	2.463	5.949
-239.648	3000.00	-33.527	-40.548	2.744	14.722	-.021	1.679	2.569	9.528
-248.846	3000.00	-31.392	-39.365	2.820	24.470	-.021	1.726	2.667	13.352
-257.694	3000.00	-29.020	-37.594	2.910	30.981	-.021	1.773	2.757	17.408
-266.335	3000.00	-25.147	-35.224	2.991	37.679	-.021	1.818	2.839	21.679
-274.707	3000.00	-21.074	-32.204	3.071	44.479	-.021	1.863	2.910	26.149
-282.742	3000.00	-16.292	-28.497	3.150	51.263	-.020	1.906	2.971	30.799
-290.371	3000.00	-10.632	-24.081	3.228	57.942	-.020	1.948	3.021	35.611
-297.522	3000.00	-4.715	-20.953	3.305	64.348	-.020	1.989	3.060	40.562
-304.126	3000.00	2.031	-17.130	3.381	70.590	-.020	2.029	3.086	45.631
-310.116	3000.00	9.367	-12.654	3.456	76.194	-.020	2.068	3.101	50.796
-315.428	3000.00	17.242	-7.586	3.529	81.318	-.020	2.107	3.103	56.029
-320.008	3000.00	25.298	-2.012	3.602	85.801	-.020	2.144	3.092	61.304
-323.810	3000.00	34.367	3.032	3.674	89.561	-.020	2.181	3.064	66.591
-326.799	3000.00	43.474	8.762	3.745	92.571	-.020	2.218	3.033	71.862
-328.954	3000.00	52.841	17.328	3.815	94.778	-.020	2.253	2.985	77.086
MANEUVER	COMPLETE								

x ft.	y ft.	z ft.	Vx ft/sec	Vy ft/sec	Vz ft/sec	θ	γ	φ	δ
FULL RUDDER UNTIL BACK ON ORIGINAL HEADING									
-328.444	3000.00	52.041	-17.320	3.014	94.770	-.020	2.253	2.985	77.086
-329.809	3000.00	62.469	-236	3.885	87.786	-.014	2.282	2.906	84.971
-328.866	3000.00	72.278	18.211	3.453	98.395	-.019	2.279	2.780	95.420
-326.165	3000.00	81.486	36.205	4.017	95.764	-.019	2.265	2.609	105.710
-321.687	3000.00	91.278	53.358	4.085	90.072	-.019	2.251	2.379	115.740
-315.576	3000.00	99.870	64.868	4.150	81.773	-.019	2.237	2.108	125.486
-308.028	3000.00	107.540	82.096	4.214	71.612	-.019	2.227	1.784	134.612
-299.290	3000.00	114.148	92.655	4.277	60.552	-.019	2.221	1.418	142.972
-289.634	3000.00	119.659	100.466	4.340	49.661	-.019	2.220	1.011	150.363
-279.324	3000.00	124.141	105.747	4.401	39.979	-.019	2.227	.567	156.585
-268.590	3000.00	127.759	108.923	4.462	32.396	-.019	2.242	.094	161.450
-257.618	3000.00	130.758	110.511	4.523	27.573	-.019	2.263	-.402	164.798
-246.546	3000.00	133.413	110.937	4.583	25.935	-.018	2.290	-.912	166.500
-235.417	3000.00	136.115	110.439	4.642	27.690	-.018	2.320	-1.430	166.467
-224.505	3000.00	139.142	109.004	4.701	32.868	-.018	2.351	-1.945	164.656
-213.740	3000.00	142.854	106.306	4.758	41.358	-.018	2.380	-2.450	161.061
-203.339	3000.00	147.570	101.700	4.815	52.966	-.018	2.402	-2.935	155.686
-193.540	3000.00	153.580	94.242	4.872	67.230	-.018	2.416	-3.392	148.556
-184.674	3000.00	161.169	83.018	4.927	83.345	-.018	2.413	-3.813	139.732
-177.187	3000.00	170.282	66.725	4.981	100.126	-.018	2.397	-4.188	129.286
-171.633	3000.00	181.081	44.351	5.034	115.856	-.018	2.362	-4.508	117.275
-168.657	3000.00	193.283	15.174	5.085	128.172	-.018	2.308	-4.765	103.761
-168.940	3000.00	206.392	-20.832	5.134	134.016	-.018	2.233	-4.946	88.809
-173.108	3000.00	219.580	-62.525	5.182	129.739	-.018	2.137	-5.040	72.498
-181.586	3000.00	231.640	-107.041	5.226	111.474	-.018	2.023	-5.034	54.922
-194.401	3000.00	241.012	-144.262	5.265	75.365	-.018	1.893	-5.012	35.121

150

X ft.	Y ft.	Z ft.	Vx ft/sec	Vy ft/sec	Vz ft/sec	θ	γ	φ	δ
-210.951	3000.00	245.911	-181.735	5.300	22.003	-.01R	1.754	-4.658	16.496
-229.421	3000.00	244.627	-145.663	5.327	-47.671	-.01R	1.610	-4.255	-3.893
MANOEUVER	COMPLETE								

X ft.	Y ft.	Z ft.	Vx ft/sec	Vy ft/sec	Vz ft/sec	θ	γ	ψ	δ
FULL DOWN ELEVATOR UNTIL MAX DESCENT RATE ACHIEVED									
0.000	3000.000	0.000	-43.000	0.000	0.000	-0.22	0.000	0.000	0.000
-8.800	3000.160	0.000	-48.150	3.956	0.000	-0.29	1.092	0.000	0.000
-17.631	3000.672	0.000	-44.311	6.722	0.000	-0.48	3.270	0.000	0.000
-26.470	3001.512	0.000	-40.465	10.089	0.000	-0.80	5.435	0.000	0.000
-35.324	3002.404	0.000	-40.610	13.452	0.000	-1.25	7.576	0.000	0.000
-44.194	3004.202	0.000	-48.764	16.800	0.000	-1.83	9.683	0.000	0.000
-53.076	3006.000	0.000	-80.919	20.176	0.000	-2.53	11.746	0.000	0.000
-61.977	3008.225	0.000	-69.067	23.517	0.000	-3.37	13.754	0.000	0.000
-70.890	3010.553	0.000	-69.193	23.142	0.000	-4.26	14.645	0.000	0.000
-79.816	3012.852	0.000	-64.318	22.042	0.000	-5.14	14.453	0.000	0.000
-88.754	3015.121	0.000	-62.436	22.518	0.000	-6.01	14.246	0.000	0.000
-97.703	3017.355	0.000	-69.554	22.170	0.000	-6.88	14.025	0.000	0.000
-106.664	3019.553	0.000	-69.670	21.797	0.000	-7.74	13.790	0.000	0.000
-115.627	3021.713	0.000	-64.786	21.400	0.000	-8.59	13.541	0.000	0.000
-124.601	3023.842	0.000	-62.401	20.980	0.000	-9.44	13.278	0.000	0.000
-133.617	3025.968	0.000	-60.015	20.535	0.000	-1.024	13.000	0.000	0.000
-142.624	3027.998	0.000	-60.127	20.067	0.000	-1.114	12.708	0.000	0.000
-151.643	3029.920	0.000	-60.234	19.575	0.000	-1.149	12.402	0.000	0.000
-160.672	3031.842	0.000	-60.349	19.060	0.000	-1.243	12.042	0.000	0.000
-169.712	3033.731	0.000	-60.458	18.521	0.000	-1.368	11.748	0.000	0.000
-178.764	3035.555	0.000	-60.566	17.958	0.000	-1.453	11.399	0.000	0.000
-187.826	3037.371	0.000	-60.673	17.372	0.000	-1.539	11.036	0.000	0.000
-196.898	3039.020	0.000	-60.774	16.762	0.000	-1.625	10.659	0.000	0.000
-205.981	3040.673	0.000	-60.881	16.128	0.000	-1.711	10.268	0.000	0.000
-215.074	3042.253	0.000	-60.983	15.471	0.000	-1.798	9.862	0.000	0.000

X ft.	Y ft.	Z ft.	Vx ft/sec	Vy ft/sec	Vz ft/sec	θ	γ	φ	δ
-224.177	3043.766	0.000	-91.063	14.709	0.000	-1.886	9.441	0.000	0.000
-233.291	3043.209	0.000	-91.161	14.083	0.000	-1.974	9.006	0.000	0.000
-242.414	3042.541	0.000	-91.278	13.353	0.000	-2.064	8.556	0.000	0.000
-251.544	3041.874	0.000	-91.372	12.597	0.000	-2.154	8.090	0.000	0.000
-260.668	3041.094	0.000	-91.464	11.817	0.000	-2.246	7.610	0.000	0.000
-269.839	3040.241	0.000	-91.555	11.012	0.000	-2.339	7.114	0.000	0.000
-279.001	3039.358	0.000	-91.640	10.333	0.000	-2.438	6.956	0.000	0.000
-288.170	3038.500	0.000	-91.617	11.494	0.000	-2.546	7.096	0.000	0.000
-297.364	3037.644	0.000	-91.437	11.494	0.000	-2.659	7.136	0.000	0.000
-306.563	3036.749	0.000	-92.047	11.309	0.000	-2.777	7.069	0.000	0.000
-315.773	3035.902	0.000	-92.147	10.935	0.000	-2.900	6.889	0.000	0.000
-324.992	3035.066	0.000	-92.235	10.363	0.000	-3.028	6.592	0.000	0.000
-334.219	3034.264	0.000	-92.311	9.590	0.000	-3.159	6.174	0.000	0.000
-343.454	3033.475	0.000	-92.374	8.614	0.000	-3.293	5.634	0.000	0.000
-352.694	3032.670	0.000	-92.424	7.444	0.000	-3.430	4.970	0.000	0.000
-361.938	3031.853	0.000	-92.458	6.065	0.000	-3.570	4.181	0.000	0.000
-371.184	3031.080	0.000	-92.476	4.476	0.000	-3.711	3.264	0.000	0.000
-380.432	3030.274	0.000	-92.477	2.674	0.000	-3.854	2.216	0.000	0.000
-389.679	3029.405	0.000	-92.459	0.667	0.000	-3.997	1.037	0.000	0.000
-398.923	3028.361	0.000	-92.421	-1.556	0.000	-4.141	-0.275	0.000	0.000
-408.178	3027.104	0.000	-92.617	-3.983	0.000	-4.284	-1.715	0.000	0.000
-417.456	3025.552	0.000	-92.889	-6.652	0.000	-4.427	-3.282	0.000	0.000
-426.753	3023.741	0.000	-93.040	-9.567	0.000	-4.570	-4.988	0.000	0.000
-436.060	3021.626	0.000	-93.111	-12.733	0.000	-4.711	-6.835	0.000	0.000
-445.370	3019.182	0.000	-93.079	-16.151	0.000	-4.850	-8.823	0.000	0.000
-454.670	3015.383	0.000	-92.921	-19.822	0.000	-4.987	-10.952	0.000	0.000



X ft.	Y ft.	Z ft.	Vx ft/sec	Vy ft/sec	Vz ft/sec	θ	γ	ψ	δ
PULL UP ELEVATOR UNTIL DESCENT RATE = 0									
-691.314	3011.673	0.000	-82.982	-41.165	0.000	-5.250	-24.250	0.000	0.000
-616.183	3011.155	0.000	-87.330	-44.194	0.000	2.473	-23.017	0.000	0.000
-618.737	2934.974	0.000	-83.716	-47.425	0.000	2.494	-31.953	0.000	0.000
-627.101	2917.054	0.000	-83.574	-47.894	0.000	5.188	-14.597	0.000	0.000
-635.493	2917.208	0.000	-84.249	-47.303	0.000	5.135	-34.484	0.000	0.000
-643.949	2977.545	0.000	-84.882	-46.756	0.000	4.734	-34.012	0.000	0.000
-652.559	2972.061	0.000	-87.319	-53.939	0.000	3.559	-32.751	0.000	0.000
-661.343	2966.725	0.000	-88.350	-52.768	0.000	2.198	-31.292	0.000	0.000
-670.154	2961.400	0.000	-87.879	-53.728	0.000	2.175	-31.160	0.000	0.000
-678.917	2955.978	0.000	-87.384	-54.727	0.000	2.982	-11.766	0.000	0.000
-687.670	2950.515	0.000	-87.642	-54.532	0.000	3.256	-11.985	0.000	0.000
-696.413	2945.094	0.000	-88.371	-53.784	0.000	3.039	-31.618	0.000	0.000
-705.333	2939.741	0.000	-88.816	-53.372	0.000	2.752	-31.180	0.000	0.000
-714.220	2934.401	0.000	-88.943	-53.415	0.000	2.749	-31.011	0.000	0.000
-723.121	2929.058	0.000	-89.065	-53.463	0.000	2.913	-30.997	0.000	0.000
-732.043	2923.723	0.000	-89.369	-53.237	0.000	2.999	-30.894	0.000	0.000
-741.000	2918.417	0.000	-89.710	-52.864	0.000	2.958	-30.653	0.000	0.000
-749.994	2913.140	0.000	-90.122	-52.556	0.000	2.902	-30.387	0.000	0.000
-759.021	2907.902	0.000	-90.409	-52.339	0.000	2.910	-30.174	0.000	0.000
-768.076	2902.674	0.000	-90.705	-52.106	0.000	2.956	-29.986	0.000	0.000
-777.164	2897.485	0.000	-91.048	-51.792	0.000	2.982	-29.769	0.000	0.000
-786.287	2892.323	0.000	-91.419	-51.430	0.000	2.978	-29.512	0.000	0.000
-795.448	2887.196	0.000	-91.783	-51.071	0.000	2.973	-29.242	0.000	0.000
-804.644	2882.109	0.000	-92.139	-50.717	0.000	2.982	-28.976	0.000	0.000
-813.876	2877.056	0.000	-92.503	-50.343	0.000	3.000	-28.708	0.000	0.000
-823.145	2872.022	0.000	-92.881	-49.915	0.000	3.017	-28.424	0.000	0.000



X ft.	Y ft.	Z ft.	Vx ft/sec	Vy ft/sec	Vz ft/sec	θ	γ	δ	ε
-832.453	2867.070	0.000	-93.273	-49.502	0.000	3.019	-28.123	0.000	0.000
-841.000	2867.142	0.000	-93.666	-49.054	0.000	3.025	-27.812	0.000	0.000
-851.186	2857.780	0.000	-94.063	-48.591	0.000	3.034	-27.494	0.000	0.000
-860.613	2852.425	0.000	-94.465	-48.107	0.000	3.046	-27.167	0.000	0.000
-870.060	2847.640	0.000	-94.875	-47.600	0.000	3.056	-26.829	0.000	0.000
-879.588	2842.907	0.000	-95.291	-47.071	0.000	3.064	-26.479	0.000	0.000
-889.138	2834.227	0.000	-95.711	-46.522	0.000	3.073	-26.119	0.000	0.000
-898.730	2833.603	0.000	-96.134	-45.954	0.000	3.082	-25.749	0.000	0.000
-908.365	2829.037	0.000	-96.562	-45.364	0.000	3.091	-25.369	0.000	0.000
-918.043	2824.531	0.000	-96.994	-44.754	0.000	3.100	-24.979	0.000	0.000
-927.764	2820.088	0.000	-97.429	-44.121	0.000	3.109	-24.579	0.000	0.000
-937.529	2815.708	0.000	-97.867	-43.468	0.000	3.117	-24.168	0.000	0.000
-947.337	2811.395	0.000	-98.307	-42.793	0.000	3.126	-23.748	0.000	0.000
-957.190	2807.150	0.000	-98.749	-42.098	0.000	3.135	-23.318	0.000	0.000
-967.087	2802.977	0.000	-99.192	-41.380	0.000	3.143	-22.878	0.000	0.000
-977.029	2798.876	0.000	-99.637	-40.641	0.000	3.152	-22.429	0.000	0.000
-987.015	2794.849	0.000	-100.081	-39.880	0.000	3.160	-21.964	0.000	0.000
-997.045	2790.891	0.000	-100.526	-39.098	0.000	3.168	-21.500	0.000	0.000
-1007.120	2787.031	0.000	-100.970	-38.294	0.000	3.177	-21.022	0.000	0.000
-1017.239	2783.243	0.000	-101.413	-37.468	0.000	3.185	-20.534	0.000	0.000
-1027.402	2779.538	0.000	-101.854	-36.620	0.000	3.193	-20.036	0.000	0.000
-1037.610	2775.920	0.000	-102.293	-35.751	0.000	3.201	-19.529	0.000	0.000
-1047.861	2772.389	0.000	-102.730	-34.854	0.000	3.209	-19.013	0.000	0.000
-1058.156	2768.949	0.000	-103.163	-33.946	0.000	3.217	-18.488	0.000	0.000
-1068.493	2765.601	0.000	-103.592	-33.011	0.000	3.225	-17.953	0.000	0.000
-1078.874	2762.348	0.000	-104.017	-32.054	0.000	3.232	-17.410	0.000	0.000
-1089.297	2759.192	0.000	-104.437	-31.075	0.000	3.240	-16.857	0.000	0.000

x ft.	y ft.	z ft.	Vx ft/sec	Vy ft/sec	Vz ft/sec	θ	γ	ψ	δ
-1099.761	2756.134	0.000	-104.852	-30.074	0.000	3.248	-16.295	0.000	0.000
-1110.267	2753.178	0.000	-105.260	-29.052	0.000	3.255	-15.775	0.000	0.000
-1120.813	2750.325	0.000	-105.661	-28.008	0.000	3.262	-15.145	0.000	0.000
-1131.390	2747.577	0.000	-106.055	-26.942	0.000	3.270	-14.557	0.000	0.000
-1142.023	2744.937	0.000	-106.441	-25.855	0.000	3.277	-13.961	0.000	0.000
-1152.680	2742.407	0.000	-106.818	-24.757	0.000	3.284	-13.355	0.000	0.000
-1163.346	2739.989	0.000	-107.186	-23.648	0.000	3.291	-12.741	0.000	0.000
-1174.123	2737.685	0.000	-107.544	-22.467	0.000	3.298	-12.119	0.000	0.000
-1184.895	2735.497	0.000	-107.892	-21.295	0.000	3.305	-11.488	0.000	0.000
-1195.701	2733.427	0.000	-108.228	-20.103	0.000	3.312	-10.849	0.000	0.000
-1206.540	2731.477	0.000	-108.553	-18.890	0.000	3.319	-10.202	0.000	0.000
-1217.411	2729.650	0.000	-108.865	-17.657	0.000	3.325	-9.547	0.000	0.000
-1228.312	2727.947	0.000	-109.164	-16.403	0.000	3.332	-8.883	0.000	0.000
-1239.243	2726.370	0.000	-109.449	-15.130	0.000	3.338	-8.212	0.000	0.000
-1250.201	2724.922	0.000	-109.714	-13.837	0.000	3.345	-7.533	0.000	0.000
-1261.186	2723.604	0.000	-109.975	-12.525	0.000	3.351	-6.846	0.000	0.000
-1272.195	2722.418	0.000	-110.215	-11.193	0.000	3.357	-6.151	0.000	0.000
-1283.228	2721.366	0.000	-110.439	-9.843	0.000	3.363	-5.449	0.000	0.000
-1294.282	2720.450	0.000	-110.645	-8.475	0.000	3.369	-4.739	0.000	0.000
-1305.356	2719.672	0.000	-110.834	-7.088	0.000	3.375	-4.021	0.000	0.000
-1316.440	2719.033	0.000	-111.005	-5.684	0.000	3.381	-3.297	0.000	0.000
-1327.556	2718.536	0.000	-111.157	-4.262	0.000	3.387	-2.565	0.000	0.000
-1338.678	2718.182	0.000	-111.289	-2.824	0.000	3.393	-1.826	0.000	0.000
-1349.813	2717.972	0.000	-111.401	-1.369	0.000	3.398	-1.079	0.000	0.000
-1360.950	2717.909	0.000	-111.493	.102	0.000	3.404	-.326	0.000	0.000
-1372.111	2717.993	0.000	-111.563	1.588	0.000	4.169	.434	0.000	0.000
MANOEUVRE	COMPLETE								

x ft.	y ft.	z ft.	Vx ft/sec	Vy ft/sec	Vz ft/sec	θ	γ	ψ	δ
STEADY STATE TURN FROM 0-180 DEGREES									
0.000	3000.00	0.000	-08.000	0.000	0.000	-.022	0.000	0.000	0.000
-8.797	3000.00	.110	-87.933	.121	2.317	-.023	.039	1.645	.755
-17.585	3000.00	.463	-87.836	.241	4.632	-.023	.118	1.645	2.265
-26.361	3000.00	1.042	-87.674	.359	6.944	-.023	.195	1.645	3.776
-35.118	3000.00	1.852	-87.460	.475	9.252	-.023	.272	1.645	5.286
-43.850	3000.00	2.892	-87.180	.590	11.552	-.023	.347	1.645	6.797
-52.551	3000.00	4.162	-86.840	.704	13.845	-.023	.422	1.645	8.307
-61.215	3000.00	5.661	-86.440	.815	16.127	-.023	.495	1.645	9.818
-69.836	3000.00	7.387	-85.979	.925	18.399	-.022	.567	1.645	11.329
-78.406	3000.00	9.340	-85.459	1.034	20.657	-.022	.639	1.645	12.840
-86.925	3000.00	11.518	-84.880	1.141	22.901	-.022	.709	1.645	14.351
-95.381	3000.00	13.919	-84.242	1.247	25.129	-.022	.778	1.645	15.863
-103.770	3000.00	16.543	-83.545	1.351	27.340	-.022	.847	1.645	17.374
-112.087	3000.00	19.386	-82.790	1.453	29.531	-.022	.914	1.645	18.885
-120.325	3000.00	22.448	-81.977	1.555	31.701	-.022	.981	1.645	20.397
-128.479	3000.00	25.725	-81.108	1.655	33.850	-.022	1.047	1.645	21.908
-136.544	3000.00	29.216	-80.182	1.753	35.974	-.022	1.111	1.645	23.420
-144.513	3000.00	32.914	-79.201	1.850	38.074	-.022	1.175	1.645	24.932
-152.381	3000.00	36.830	-78.165	1.946	40.147	-.022	1.238	1.645	26.444
-160.143	3000.00	40.947	-77.074	2.041	42.192	-.022	1.300	1.645	27.956
-167.793	3000.00	45.267	-75.930	2.134	44.207	-.021	1.362	1.645	29.468
-175.327	3000.00	49.787	-74.733	2.226	46.192	-.021	1.422	1.645	30.980
-182.737	3000.00	54.503	-73.484	2.317	48.144	-.021	1.482	1.645	32.492
-190.021	3000.00	59.414	-72.184	2.406	50.062	-.021	1.541	1.645	34.004
-197.172	3000.00	64.518	-70.834	2.495	51.946	-.021	1.599	1.645	35.517

X ft.	Y ft.	Z ft.	Vx ft/sec	Vy ft/sec	Vz ft/sec	θ	γ	ψ	φ
-204.125	3000.00	69.801	-67.907	2.582	53.794	-0.021	1.656	1.645	37.079
-211.056	3000.00	75.271	-67.907	2.668	55.603	-0.021	1.713	1.645	38.542
-217.780	3000.00	80.720	-66.492	2.753	57.374	-0.021	1.769	1.645	40.055
-224.752	3000.00	86.144	-64.971	2.836	59.105	-0.020	1.824	1.645	41.567
-230.768	3000.00	92.439	-63.304	2.919	60.795	-0.020	1.878	1.645	43.080
-237.023	3000.00	98.701	-61.734	3.000	62.442	-0.020	1.932	1.645	44.593
-243.112	3000.00	105.229	-60.061	3.081	64.046	-0.020	1.985	1.645	46.106
-249.033	3000.00	111.709	-58.346	3.160	65.605	-0.020	2.037	1.645	47.619
-254.780	3000.00	118.344	-56.541	3.239	67.118	-0.020	2.088	1.645	49.133
-260.349	3000.00	125.129	-54.796	3.316	68.584	-0.020	2.139	1.645	50.646
-265.737	3000.00	132.059	-52.963	3.392	70.003	-0.019	2.189	1.645	52.159
-270.940	3000.00	139.127	-51.093	3.467	71.372	-0.019	2.239	1.645	53.673
-275.954	3000.00	146.330	-49.198	3.541	72.692	-0.019	2.288	1.645	55.187
-280.776	3000.00	153.663	-47.249	3.615	73.961	-0.019	2.336	1.645	56.700
-285.402	3000.00	161.129	-45.277	3.687	75.178	-0.019	2.384	1.645	58.214
-289.824	3000.00	168.699	-43.273	3.758	76.343	-0.019	2.430	1.645	59.728
-294.055	3000.00	176.380	-41.239	3.829	77.454	-0.019	2.477	1.645	61.242
-298.076	3000.00	184.184	-39.177	3.898	78.512	-0.019	2.523	1.645	62.756
-301.884	3000.00	192.085	-37.088	3.967	79.514	-0.018	2.568	1.645	64.270
-305.492	3000.00	200.084	-34.972	4.034	80.461	-0.018	2.612	1.645	65.784
-308.882	3000.00	208.175	-32.813	4.101	81.352	-0.018	2.656	1.645	67.299
-312.058	3000.00	216.352	-30.670	4.167	82.186	-0.018	2.700	1.645	68.813
-315.014	3000.00	224.609	-28.487	4.232	82.963	-0.018	2.742	1.645	70.328
-317.754	3000.00	232.941	-26.288	4.296	83.681	-0.018	2.785	1.645	71.842
-320.271	3000.00	241.342	-24.062	4.359	84.341	-0.018	2.826	1.645	73.357
-322.566	3000.00	249.807	-21.824	4.422	84.943	-0.017	2.868	1.645	74.872

x ft.	y ft.	z ft.	Vx ft/sec	Vy ft/sec	Vz ft/sec	$\theta$	$\gamma$	$\psi$	$\delta$
-324.635	3000.00	254.328	-17.570	4.413	15.484	-.017	2.908	1.645	76.387
-326.479	3000.00	266.901	-17.334	4.544	15.967	-.017	2.948	1.645	77.902
-328.095	3000.00	275.518	-15.025	4.604	16.389	-.017	2.988	1.645	79.417
-329.483	3000.00	284.175	-12.736	4.664	16.750	-.017	3.027	1.645	80.932
-330.642	3000.00	292.865	-10.438	4.722	17.051	-.017	3.066	1.645	82.447
-331.570	3000.00	301.583	-8.133	4.780	17.292	-.017	3.104	1.645	83.963
-332.266	3000.00	310.321	-5.822	4.837	17.471	-.016	3.141	1.645	85.478
-332.735	3000.00	319.074	-3.507	4.893	17.589	-.016	3.178	1.645	86.994
-332.970	3000.00	327.835	-1.190	4.949	17.646	-.016	3.215	1.645	88.509
-332.973	3000.00	336.600	1.127	5.004	17.642	-.016	3.251	1.645	90.025
-332.744	3000.00	345.361	3.444	5.058	17.576	-.016	3.287	1.645	91.541
-332.284	3000.00	354.112	5.758	5.111	17.449	-.016	3.322	1.645	93.057
-331.543	3000.00	362.847	8.068	5.164	17.261	-.016	3.357	1.645	94.573
-330.671	3000.00	371.561	10.372	5.216	17.012	-.015	3.391	1.645	96.089
-329.514	3000.00	380.247	12.669	5.267	16.702	-.015	3.425	1.645	97.605
-328.130	3000.00	388.898	14.956	5.318	16.331	-.015	3.459	1.645	99.121
-326.528	3000.00	397.510	17.234	5.368	15.901	-.015	3.492	1.645	100.637
-324.691	3000.00	406.075	19.499	5.417	15.410	-.015	3.524	1.645	102.154
-322.624	3000.00	414.589	21.750	5.466	14.859	-.015	3.557	1.645	103.670
-320.342	3000.00	423.044	23.986	5.514	14.249	-.015	3.588	1.645	105.187
-317.833	3000.00	431.436	26.205	5.562	13.580	-.015	3.620	1.645	106.704
-315.102	3000.00	439.757	28.405	5.609	12.852	-.014	3.651	1.645	108.221
-312.153	3000.00	448.003	30.585	5.655	12.067	-.014	3.681	1.645	109.737
-308.986	3000.00	456.168	32.744	5.701	11.224	-.014	3.712	1.645	111.254
-305.605	3000.00	464.245	34.880	5.746	10.324	-.014	3.741	1.645	112.771
-302.011	3000.0	472.230	36.991	5.790	9.368	-.014	3.771	1.645	114.289

X ft.	y ft.	z ft.	Vx ft/sec	Vy ft/sec	Vz ft/sec	θ	γ	ψ	δ
-248.248	3000.00	480.116	39.077	5.835	78.357	-.014	3.800	1.645	115.806
-244.197	3000.00	487.899	41.134	5.878	77.291	-.014	3.829	1.645	117.323
-249.983	3000.00	495.572	43.163	5.921	76.170	-.013	3.857	1.645	118.841
-255.566	3000.00	503.130	45.162	5.963	74.997	-.013	3.885	1.645	120.358
-260.452	3000.00	510.568	47.128	6.005	73.771	-.013	3.913	1.645	121.876
-276.142	3000.00	517.842	49.062	6.046	72.493	-.013	3.940	1.645	123.393
-271.191	3000.00	525.064	50.961	6.087	71.164	-.013	3.967	1.645	124.911
-265.952	3000.00	532.112	52.824	6.128	69.786	-.013	3.994	1.645	126.429
-260.578	3000.00	539.014	54.650	6.167	68.359	-.013	4.020	1.645	127.947
-255.024	3000.00	545.781	56.438	6.207	66.884	-.012	4.046	1.645	129.465
-249.293	3000.00	552.394	58.186	6.246	65.362	-.012	4.072	1.645	130.983
-243.389	3000.00	558.851	59.893	6.284	63.795	-.012	4.097	1.645	132.501
-237.316	3000.00	565.150	61.558	6.322	62.182	-.012	4.122	1.645	134.020
-231.079	3000.00	571.286	63.179	6.359	60.527	-.012	4.147	1.645	135.538
-224.683	3000.00	577.254	64.756	6.396	58.829	-.012	4.172	1.645	137.057
-218.130	3000.00	583.049	66.288	6.432	57.089	-.012	4.196	1.645	138.575
-211.427	3000.00	588.689	67.773	6.468	55.310	-.012	4.220	1.645	140.094
-204.578	3000.00	594.110	69.211	6.504	53.492	-.011	4.243	1.645	141.613
-197.588	3000.00	599.366	70.599	6.539	51.637	-.011	4.267	1.645	143.132
-190.461	3000.00	604.435	71.938	6.574	49.745	-.011	4.290	1.645	144.650
-183.203	3000.00	609.313	73.227	6.608	47.819	-.011	4.312	1.645	146.169
-175.818	3000.00	613.997	74.464	6.642	45.859	-.011	4.335	1.645	147.689
-168.312	3000.00	618.484	75.649	6.676	43.867	-.011	4.357	1.645	149.208
-160.691	3000.00	622.769	76.780	6.709	41.845	-.011	4.379	1.645	150.727
-152.454	3000.00	626.851	77.858	6.741	39.793	-.010	4.401	1.645	152.246
-145.122	3000.00	630.726	78.880	6.773	37.713	-.010	4.422	1.645	153.766

X ft.	Y ft.	Z ft.	Vx ft/sec	Vy ft/sec	Vz ft/sec	θ	γ	ψ	δ
-137.146	3000.00	634.392	79.848	6.805	35.607	-.010	4.443	1.645	155.286
-129.155	3000.00	637.846	80.759	6.837	33.476	-.010	4.464	1.645	156.805
-121.037	3000.00	641.006	81.613	6.868	31.322	-.010	4.485	1.645	158.325
-112.836	3000.00	644.110	82.410	6.899	29.145	-.010	4.505	1.645	159.845
-104.550	3000.00	646.914	83.149	6.929	26.949	-.010	4.525	1.645	161.365
-96.209	3000.00	649.500	83.829	6.959	24.733	-.009	4.545	1.645	162.885
-87.795	3000.00	651.860	84.451	6.989	22.500	-.009	4.565	1.645	164.405
-79.322	3000.00	653.946	85.013	7.018	20.252	-.009	4.584	1.645	165.925
-70.795	3000.00	655.710	85.515	7.047	17.990	-.009	4.604	1.645	167.445
-62.222	3000.00	657.595	85.957	7.075	15.715	-.009	4.623	1.645	168.966
-53.607	3000.00	659.052	86.330	7.104	13.429	-.009	4.641	1.645	170.486
MANEUVER	COMPLETE								

TABLE 3.5: SELECTED TRAJECTORIES AND FORCES

x ft.	y ft.	z ft.	Fx	Fy	Fz
TAKE OFF AND CLIMB OVER 100 F. OBSTACLE					
-0.025	0.000	0.000	-0.001	0.000	0.000
-0.05	0.000	0.000	47.221	-304.119	0.000
-0.12	0.000	0.000	49.997	-304.119	0.000
-0.22	0.000	0.000	53.119	-304.119	0.000
-0.35	0.000	0.000	56.657	-304.119	0.000
-0.52	0.000	0.000	60.699	-304.119	0.000
-0.72	0.000	0.000	65.363	-304.119	0.000
-0.97	0.000	0.000	70.804	-304.119	0.000
-1.26	0.000	0.000	77.234	-304.119	0.000
-1.59	0.000	0.000	84.949	-304.119	0.000
-1.98	0.000	0.000	94.379	-304.119	0.000
-2.43	0.000	0.000	106.167	-304.119	0.000
-2.95	0.000	0.000	121.324	-304.119	0.000
-3.55	0.000	0.000	141.535	-304.119	0.000
-4.24	0.000	0.000	169.833	-304.118	0.000
-5.04	0.000	0.000	212.287	-304.118	0.000
-5.99	0.000	0.000	283.056	-304.117	0.000
-7.15	0.000	0.000	424.628	-304.116	0.000
-8.69	0.000	0.000	849.465	-304.114	0.000
-10.74	0.000	0.000	849.072	-304.108	0.000
-1.329	0.000	0.000	848.599	-304.096	0.000
-1.635	0.000	0.000	848.052	-304.076	0.000
-1.992	0.000	0.000	847.436	-304.046	0.000
-2.398	0.000	0.000	846.755	-304.001	0.000
-2.858	0.000	0.000	846.118	-303.944	0.000
-3.374	0.000	0.000	845.521	-303.878	0.000
-3.948	0.000	0.000	844.961	-303.801	0.000
-4.582	0.000	0.000	844.434	-303.716	0.000
-5.278	0.000	0.000	843.938	-303.624	0.000
-6.037	0.000	0.000	843.471	-303.521	0.000



TABLE 3.5: SELECTED TRAJECTORIES AND FORCES

x ft.	y ft.	z ft.	Fx	Fy	Fz
-6.555	0.000	0.000	-307.197	-302.025	0.000
-7.464	0.000	0.000	-307.207	-302.653	0.000
-8.323	0.000	0.000	-307.124	-302.004	0.000
-9.231	0.000	0.000	-307.025	-301.470	0.000
-10.195	0.000	0.000	-307.373	-300.440	0.000
-11.170	0.000	0.000	-307.347	-300.103	0.000
-12.250	0.000	0.000	-307.000	-299.260	0.000
-13.303	0.000	0.000	-307.000	-298.254	0.000
-14.420	0.000	0.000	-307.000	-297.137	0.000
-15.521	0.000	0.000	-307.000	-295.856	0.000
-16.643	0.000	0.000	-307.323	-294.400	0.000
-17.825	0.000	0.000	-307.794	-292.775	0.000
-19.042	0.000	0.000	-307.220	-290.067	0.000
-20.344	0.000	0.000	-307.000	-288.004	0.000
-22.497	0.000	0.000	-307.000	-286.645	0.000
-23.698	0.000	0.000	-307.000	-284.141	0.000
-25.540	0.000	0.000	-307.000	-281.379	0.000
-27.140	0.000	0.000	-307.000	-278.344	0.000
-28.795	0.000	0.000	-307.000	-275.020	0.000
-30.400	0.000	0.000	-307.000	-271.344	0.000
-32.037	0.000	0.000	-307.000	-267.473	0.000
-33.624	0.000	0.000	-307.000	-263.379	0.000
-35.203	0.000	0.000	-307.000	-259.087	0.000
-36.781	0.000	0.000	-307.000	-254.453	0.000
-38.447	0.000	0.000	-307.000	-249.420	0.000
-40.071	0.000	0.000	-307.000	-244.010	0.000
-41.663	0.000	0.000	-307.000	-238.213	0.000
-43.215	0.000	0.000	-307.000	-232.010	0.000
-44.704	0.000	0.000	-307.000	-225.440	0.000
-46.171	0.000	0.000	-307.000	-218.510	0.000

TABLE 3.5: SELECTED TRAJECTORIES AND FORCES

x ft.	y ft.	z ft.	Fx	Fy	Fz
-52.241	0.000	0.000	111.111	-206.123	0.000
-46.200	0.000	0.000	107.122	-197.600	0.000
-40.177	0.000	0.000	103.240	-188.143	0.000
-34.131	0.000	0.000	99.334	-178.314	0.000
-28.043	0.000	0.000	95.402	-167.902	0.000
-21.912	0.000	0.000	91.442	-157.000	0.000
-15.749	0.000	0.000	87.453	-145.249	0.000
-9.554	0.000	0.000	83.434	-132.472	0.000
-3.329	0.000	0.000	79.385	-118.036	0.000
2.925	0.000	0.000	75.306	-102.423	0.000
9.139	0.000	0.000	71.197	-85.117	0.000
15.271	0.000	0.000	67.058	-65.000	0.000
21.321	0.000	0.000	62.889	-42.747	0.000
27.289	0.000	0.000	58.690	-17.924	0.000
33.175	0.000	0.000	54.461	8.264	0.000
38.979	0.000	0.000	50.202	24.470	0.000
44.701	0.000	0.000	45.913	40.713	0.000
50.341	0.000	0.000	41.594	56.503	0.000
55.899	0.000	0.000	37.245	71.609	0.000
61.375	0.000	0.000	32.866	85.839	0.000
66.769	0.000	0.000	28.457	99.082	0.000
72.081	0.000	0.000	24.018	110.439	0.000
77.311	0.000	0.000	19.549	119.816	0.000
82.469	0.000	0.000	15.050	127.214	0.000
87.555	0.000	0.000	10.521	132.631	0.000
92.569	0.000	0.000	6.962	137.066	0.000
97.511	0.000	0.000	3.373	139.516	0.000
102.281	0.000	0.000	-0.246	140.981	0.000
106.889	0.000	0.000	-3.885	141.461	0.000
111.335	0.000	0.000	-7.544	140.956	0.000
115.619	0.000	0.000	-11.223	139.466	0.000
119.741	0.000	0.000	-14.922	136.991	0.000
123.701	0.000	0.000	-18.641	133.531	0.000
127.509	0.000	0.000	-22.380	129.086	0.000
131.165	0.000	0.000	-26.139	123.656	0.000
134.669	0.000	0.000	-29.918	117.241	0.000
138.021	0.000	0.000	-33.717	109.841	0.000
141.221	0.000	0.000	-37.536	101.456	0.000
144.269	0.000	0.000	-41.375	92.086	0.000
147.165	0.000	0.000	-45.234	80.731	0.000
149.909	0.000	0.000	-49.113	68.391	0.000
152.501	0.000	0.000	-53.012	55.066	0.000
154.941	0.000	0.000	-56.931	40.756	0.000
157.229	0.000	0.000	-60.870	25.461	0.000
159.365	0.000	0.000	-64.829	9.181	0.000
161.349	0.000	0.000	-68.808	-7.184	0.000
163.181	0.000	0.000	-72.807	-23.499	0.000
164.861	0.000	0.000	-76.826	-39.124	0.000
166.389	0.000	0.000	-80.865	-54.059	0.000
167.765	0.000	0.000	-84.924	-68.304	0.000
168.989	0.000	0.000	-88.993	-81.859	0.000
170.061	0.000	0.000	-93.072	-94.724	0.000
170.981	0.000	0.000	-97.161	-106.899	0.000
171.749	0.000	0.000	-101.260	-118.384	0.000
172.365	0.000	0.000	-105.369	-129.179	0.000
172.829	0.000	0.000	-109.488	-139.284	0.000
173.141	0.000	0.000	-113.617	-148.699	0.000
173.301	0.000	0.000	-117.756	-157.424	0.000
173.311	0.000	0.000	-121.905	-165.459	0.000
173.171	0.000	0.000	-126.064	-172.804	0.000
172.881	0.000	0.000	-130.233	-179.459	0.000
172.441	0.000	0.000	-134.412	-185.424	0.000
171.851	0.000	0.000	-138.601	-190.709	0.000
171.111	0.000	0.000	-142.800	-195.314	0.000
170.221	0.000	0.000	-147.019	-199.239	0.000
169.181	0.000	0.000	-151.258	-202.484	0.000
168.001	0.000	0.000	-155.517	-205.049	0.000
166.681	0.000	0.000	-159.796	-206.934	0.000
165.221	0.000	0.000	-164.095	-208.139	0.000
163.621	0.000	0.000	-168.414	-208.664	0.000
161.881	0.000	0.000	-172.753	-208.509	0.000
160.001	0.000	0.000	-177.112	-207.674	0.000
157.981	0.000	0.000	-181.491	-206.159	0.000
155.821	0.000	0.000	-185.890	-204.074	0.000
153.521	0.000	0.000	-190.309	-201.419	0.000
151.081	0.000	0.000	-194.748	-198.204	0.000
148.501	0.000	0.000	-199.207	-193.529	0.000
145.781	0.000	0.000	-203.686	-187.404	0.000
142.921	0.000	0.000	-208.185	-178.829	0.000
140.021	0.000	0.000	-212.704	-167.814	0.000
136.981	0.000	0.000	-217.243	-154.359	0.000
133.801	0.000	0.000	-221.802	-138.464	0.000
130.481	0.000	0.000	-226.381	-120.129	0.000
127.021	0.000	0.000	-231.000	-99.354	0.000
123.421	0.000	0.000	-235.659	-77.139	0.000
119.681	0.000	0.000	-240.358	-53.484	0.000
115.801	0.000	0.000	-245.097	-28.389	0.000
111.781	0.000	0.000	-249.876	7.146	0.000
107.621	0.000	0.000	-254.695	31.541	0.000
103.321	0.000	0.000	-259.554	55.476	0.000
98.881	0.000	0.000	-264.453	78.851	0.000
94.301	0.000	0.000	-269.392	101.566	0.000
89.581	0.000	0.000	-274.371	123.621	0.000
84.721	0.000	0.000	-279.390	145.026	0.000
79.721	0.000	0.000	-284.449	165.781	0.000
74.581	0.000	0.000	-289.548	185.886	0.000
69.301	0.000	0.000	-294.687	205.341	0.000
63.881	0.000	0.000	-299.866	224.146	0.000
58.321	0.000	0.000	-305.085	242.301	0.000
52.621	0.000	0.000	-310.344	259.816	0.000
46.781	0.000	0.000	-315.643	276.691	0.000
40.801	0.000	0.000	-320.982	292.926	0.000
34.681	0.000	0.000	-326.361	308.521	0.000
28.421	0.000	0.000	-331.780	323.476	0.000
22.021	0.000	0.000	-337.239	337.791	0.000
15.481	0.000	0.000	-342.738	351.466	0.000
8.801	0.000	0.000	-348.277	364.501	0.000
2.081	0.000	0.000	-353.856	376.896	0.000
-4.681	0.000	0.000	-359.475	388.651	0.000
-11.401	0.000	0.000	-365.134	399.766	0.000
-18.081	0.000	0.000	-370.833	410.241	0.000
-24.721	0.000	0.000	-376.572	420.076	0.000
-31.321	0.000	0.000	-382.351	429.271	0.000
-37.881	0.000	0.000	-388.170	437.826	0.000
-44.401	0.000	0.000	-394.029	445.741	0.000
-50.881	0.000	0.000	-399.928	453.016	0.000
-57.321	0.000	0.000	-405.867	459.651	0.000
-63.721	0.000	0.000	-411.846	465.646	0.000
-70.081	0.000	0.000	-417.865	471.001	0.000
-76.401	0.000	0.000	-423.924	475.716	0.000
-82.681	0.000	0.000	-429.993	479.791	0.000
-88.921	0.000	0.000	-436.092	483.226	0.000
-95.121	0.000	0.000	-442.231	486.021	0.000
-101.281	0.000	0.000	-448.410	488.176	0.000
-107.401	0.000	0.000	-454.629	489.691	0.000
-113.481	0.000	0.000	-460.878	490.566	0.000
-119.521	0.000	0.000	-467.157	490.801	0.000
-125.521	0.000	0.000	-473.466	490.396	0.000
-131.481	0.000	0.000	-479.805	489.351	0.000
-137.401	0.000	0.000	-486.174	487.666	0.000
-143.281	0.000	0.000	-492.573	485.341	0.000
-149.121	0.000	0.000	-499.002	482.376	0.000
-154.921	0.000	0.000	-505.461	478.781	0.000
-160.681	0.000	0.000	-511.950	474.556	0.000
-166.401	0.000	0.000	-518.469	469.701	0.000
-172.081	0.000	0.000	-525.018	464.216	0.000
-177.721	0.000	0.000	-531.597	458.101	0.000
-183.321	0.000	0.000	-538.206	451.356	0.000
-188.881	0.000	0.000	-544.845	444.081	0.000
-194.401	0.000	0.000	-551.514	436.276	0.000
-200.001	0.000	0.000	-558.213	427.941	0.000
-205.561	0.000	0.000	-564.942	419.076	0.000
-211.081	0.000	0.000	-571.701	409.691	0.000
-216.561	0.000	0.000	-578.490	399.786	0.000
-222.001	0.000	0.000	-585.309	389.361	0.000
-227.401	0.000	0.000	-592.148	378.426	0.000
-232.761	0.000	0.000	-599.017	366.981	0.000
-238.081	0.000	0.000	-605.916	355.026	0.000
-243.361	0.000	0.000	-612.845	342.561	0.000
-248.601	0.000	0.000	-619.804	329.586	0.000
-253.801	0.000	0.000	-626.793	316.111	0.000
-258.961	0.000	0.000	-633.812	302.236	0.000
-264.081	0.000	0.000	-640.861	287.961	0.000
-269.161	0.000	0.000	-647.940	273.286	0.000
-274.201	0.000	0.000	-655.049	258.211	0.000
-279.201	0.000	0.000	-662.188	242.736	0.000
-284.161	0.000	0.000	-669.357	226.861	0.000
-289.081	0.000	0.000	-676.556	210.586	0.000
-293.961	0.000	0.000	-683.785	193.911	0.000
-298.801	0.000	0.000	-691.044	176.836	0.000
-303.601	0.000	0.000	-698.333	159.361	0.000
-308.361	0.000	0.000	-705.652	141.486	0.000
-313.081	0.000	0.000	-713.001	123.211	0.000
-317.761	0.000	0.000	-720.380	104.536	0.000
-322.401	0.000	0.000	-727.789	85.461	0.000
-327.001	0.000	0.000	-735.228	65.986	0.000
-331.561	0.000	0.000	-742.697	46.111	0.000
-336.081	0.000	0.000	-750.196	25.836	0.000
-340.561	0.000	0.000	-757.725	5.161	0.000
-345.001	0.000	0.000	-765.284	-15.814	0.000
-349.401	0.000	0.000	-772.873	-36.139	0.000
-353.761	0.000	0.000	-780.492	-55.864	0.000
-358.081	0.000	0.000	-788.141	-75.089	0.000
-362.361	0.000	0.000	-795.820	-93.814	0.000
-366.6					

TABLE 3.5: SELECTED TRAJECTORIES AND FORCES

x ft.	y ft.	z ft.	Fx	Fy	Fz
-147.337	1.600	0.000	713.177	623.753	0.000
-150.645	1.710	0.000	709.115	656.611	0.000
-154.304	1.815	0.000	706.513	690.200	0.000
-158.367	1.915	0.000	704.512	724.442	0.000
-161.437	2.015	0.000	703.410	759.250	0.000
-165.520	2.115	0.000	702.720	794.640	0.000
-169.642	2.215	0.000	702.350	831.255	0.000
-173.707	2.315	0.000	702.300	868.011	0.000
-177.100	2.415	0.000	702.000	905.281	0.000
-181.010	2.515	0.000	701.500	943.013	0.000
-185.201	2.615	0.000	700.970	981.163	0.000
-189.756	2.715	0.000	700.250	1019.670	0.000
-192.436	2.815	0.000	700.000	1058.477	0.000
-196.734	2.915	0.000	699.600	1097.529	0.000
-200.552	3.015	0.000	699.130	1136.750	0.000
-204.880	3.115	0.000	698.610	1176.094	0.000
-209.711	3.215	0.000	698.050	1215.570	0.000
-213.100	3.315	0.000	697.450	1255.027	0.000
-217.377	3.415	0.000	696.820	1294.570	0.000
-221.620	3.515	0.000	696.170	1334.140	0.000
-225.840	3.615	0.000	695.500	1373.741	0.000
-229.930	3.715	0.000	694.810	1413.367	0.000
-233.820	3.815	0.000	694.100	1453.004	0.000
-237.637	3.915	0.000	693.370	1492.657	0.000
-241.380	4.015	0.000	692.620	1532.324	0.000
-245.050	4.115	0.000	691.850	1571.998	0.000
-248.650	4.215	0.000	691.060	1611.685	0.000
-252.180	4.315	0.000	690.250	1651.381	0.000
-255.740	4.415	0.000	689.420	1691.080	0.000
-259.230	4.515	0.000	688.570	1730.780	0.000
-262.650	4.615	0.000	687.700	1770.480	0.000
-266.000	4.715	0.000	686.810	1810.180	0.000
-269.280	4.815	0.000	685.900	1849.880	0.000
-272.500	4.915	0.000	684.970	1889.580	0.000
-275.650	5.015	0.000	684.020	1929.280	0.000
-278.740	5.115	0.000	683.050	1968.980	0.000
-281.770	5.215	0.000	682.060	2008.680	0.000
-284.740	5.315	0.000	681.050	2048.380	0.000
-287.650	5.415	0.000	680.020	2088.080	0.000
-290.500	5.515	0.000	678.970	2127.780	0.000
-293.290	5.615	0.000	677.900	2167.480	0.000
-296.020	5.715	0.000	676.810	2207.180	0.000
-298.690	5.815	0.000	675.700	2246.880	0.000
-301.300	5.915	0.000	674.570	2286.580	0.000
-303.850	6.015	0.000	673.420	2326.280	0.000
-306.340	6.115	0.000	672.250	2365.980	0.000
-308.770	6.215	0.000	671.060	2405.680	0.000
-311.140	6.315	0.000	669.850	2445.380	0.000
-313.450	6.415	0.000	668.620	2485.080	0.000
-315.700	6.515	0.000	667.370	2524.780	0.000
-317.890	6.615	0.000	666.100	2564.480	0.000
-320.020	6.715	0.000	664.810	2604.180	0.000
-322.090	6.815	0.000	663.500	2643.880	0.000
-324.100	6.915	0.000	662.170	2683.580	0.000
-326.050	7.015	0.000	660.820	2723.280	0.000
-327.940	7.115	0.000	659.450	2762.980	0.000
-329.770	7.215	0.000	658.060	2802.680	0.000
-331.540	7.315	0.000	656.650	2842.380	0.000
-333.250	7.415	0.000	655.220	2882.080	0.000
-334.900	7.515	0.000	653.770	2921.780	0.000
-336.490	7.615	0.000	652.300	2961.480	0.000
-338.020	7.715	0.000	650.810	3001.180	0.000
-339.490	7.815	0.000	649.300	3040.880	0.000
-340.900	7.915	0.000	647.770	3080.580	0.000
-342.250	8.015	0.000	646.220	3120.280	0.000
-343.540	8.115	0.000	644.650	3159.980	0.000
-344.770	8.215	0.000	643.060	3199.680	0.000
-345.940	8.315	0.000	641.450	3239.380	0.000
-347.050	8.415	0.000	639.820	3279.080	0.000
-348.100	8.515	0.000	638.170	3318.780	0.000
-349.090	8.615	0.000	636.500	3358.480	0.000
-350.020	8.715	0.000	634.810	3398.180	0.000
-350.890	8.815	0.000	633.100	3437.880	0.000
-351.700	8.915	0.000	631.370	3477.580	0.000
-352.450	9.015	0.000	629.620	3517.280	0.000
-353.140	9.115	0.000	627.850	3556.980	0.000
-353.770	9.215	0.000	626.060	3596.680	0.000
-354.340	9.315	0.000	624.250	3636.380	0.000
-354.850	9.415	0.000	622.420	3676.080	0.000
-355.300	9.515	0.000	620.570	3715.780	0.000
-355.690	9.615	0.000	618.700	3755.480	0.000
-356.020	9.715	0.000	616.810	3795.180	0.000
-356.290	9.815	0.000	614.900	3834.880	0.000
-356.500	9.915	0.000	612.970	3874.580	0.000
-356.650	10.015	0.000	611.020	3914.280	0.000

TABLE 3.5: SELECTED TRAJECTORIES AND FORCES

x ft.	y ft.	z ft.	Fx	Fy	Fz
-209.137	10.843	0.000	640.612	135.109	0.000
-213.223	10.313	0.000	630.509	115.096	0.000
-217.122	9.767	0.000	620.500	126.589	0.000
-221.037	9.251	0.000	614.502	133.755	0.000
-224.962	8.772	0.000	612.502	143.134	0.000
-228.902	8.317	0.000	610.544	152.206	0.000
-232.855	7.887	0.000	608.555	161.233	0.000
-236.822	7.474	0.000	606.570	169.948	0.000
-240.800	7.077	0.000	604.597	178.447	0.000
-244.788	6.695	0.000	602.637	186.730	0.000
-248.782	6.329	0.000	600.689	194.821	0.000
-252.784	5.977	0.000	598.753	202.747	0.000
-256.792	5.637	0.000	596.827	210.549	0.000
-260.803	5.309	0.000	594.911	218.250	0.000
-264.817	4.993	0.000	593.002	225.775	0.000
-268.834	4.689	0.000	591.100	232.740	0.000
-272.854	4.397	0.000	589.206	239.730	0.000
-276.874	4.117	0.000	587.319	246.749	0.000
-280.894	3.849	0.000	585.437	252.776	0.000
-284.913	3.593	0.000	583.560	258.822	0.000
-288.930	3.349	0.000	581.687	264.872	0.000
-292.944	3.117	0.000	579.819	270.740	0.000
-296.954	2.897	0.000	577.954	276.759	0.000
-300.959	2.689	0.000	576.092	282.633	0.000
-304.959	2.493	0.000	574.232	288.764	0.000

TABLE 3.5: SELECTED TRAJECTORIES AND FORCES

x ft.	y ft.	z ft.	Fx	Fy	Fz
PULL RUDDER UNTIL 75 DEGREE TURN MADE					
0.000	3000.00	0.000	0.000	0.0	0.000
<del>-4.808</del>	3000.00	<del>-1.133</del>	<del>249.704</del>	0.0	<del>-4474.901</del>
-17.629	3000.00	-5.533	263.459	0.0	-4465.669
-26.454	3000.00	-1.196	260.789	0.0	-4401.878
-35.287	3000.00	-2.110	258.120	0.0	-4278.032
<del>-44.102</del>	3000.00	<del>-3.244</del>	<del>255.476</del>	0.0	<del>-4093.559</del>
-52.919	3000.00	-4.584	257.877	0.0	-3848.413
-61.713	3000.00	-6.301	250.343	0.0	-3543.123
-70.488	3000.00	-8.112	247.890	0.0	-3178.817
-79.244	3000.00	-10.095	245.530	0.0	-2757.237
-87.984	3000.00	-12.222	243.271	0.0	-2280.732
<del>-96.711</del>	3000.00	<del>-14.462</del>	<del>231.640</del>	0.0	<del>-1752.236</del>
-105.430	3000.00	-16.785	229.980	0.0	-1175.095
-114.150	3000.00	-19.150	228.435	0.0	-553.540
-122.480	3000.00	-21.533	226.990	0.0	108.054
<del>-131.629</del>	3000.00	<del>-23.942</del>	<del>225.644</del>	0.0	<del>804.982</del>
-140.407	3000.00	-26.161	224.339	0.0	1532.294
-149.225	3000.00	-28.326	223.053	0.0	2284.880
-158.040	3000.00	-30.313	221.770	0.0	3057.544
<del>-167.010</del>	3000.00	<del>-32.135</del>	<del>220.456</del>	0.0	<del>3845.067</del>
-175.988	3000.00	-33.688	218.935	0.0	4642.263
-185.025	3000.00	-34.942	217.244	0.0	5443.995
-194.117	3000.00	-35.948	215.430	0.0	6245.205
<del>-203.250</del>	3000.00	<del>-36.859</del>	<del>213.607</del>	0.0	<del>7040.907</del>
-212.421	3000.00	-36.827	211.572	0.0	7826.169
-221.546	3000.00	-36.807	209.522	0.0	8596.106
-230.750	3000.00	-35.953	207.269	0.0	9345.799
<del>-239.640</del>	3000.00	<del>-35.527</del>	<del>204.809</del>	0.0	<del>10070.270</del>
-248.846	3000.00	-31.322	202.069	0.0	10764.450
-257.890	3000.00	-28.920	199.100	0.0	11423.152

TABLE 3.5: SELECTED TRAJECTORIES AND FORCES

x ft.	y ft.	z ft.	Fx	Fy	Fz
-266.335	3000.00	-25.147	195.959	0.0	12041.088
<del>-274.707</del>	3000.00	<del>-21.074</del>	<del>192.864</del>	0.0	<del>12012.893</del>
-282.742	3000.00	-16.222	189.254	0.0	13133.168
-290.371	3000.00	-10.932	185.744	0.0	13596.545
-297.522	3000.00	-4.715	182.156	0.0	14001.777
<del>-304.126</del>	3000.00	<del>2.031</del>	<del>178.521</del>	0.0	<del>14343.273</del>
-310.116	3000.00	9.367	174.485	0.0	14610.762
-315.428	3000.00	17.242	171.277	0.0	14799.785
-320.008	3000.00	25.598	167.727	0.0	14906.410
<del>-323.610</del>	3000.00	<del>34.367</del>	<del>164.264</del>	0.0	<del>14927.368</del>
-326.799	3000.00	43.474	160.915	0.0	14860.142
-328.954	3000.00	52.841	157.705	0.0	14703.041
MANOEUVRE	COMPLETE				

TABLE 3.5: SELECTED TRAJECTORIES AND FORCES

x ft.	y ft.	z ft.	Fx	Fy	Fz
PULL RUDDER UNTIL BACK ON ORIGINAL HEADING					
-328.433	3000.00	52.041	157.705	0.0	14703.041
-324.809	3000.00	<del>62.467</del>	<del>154.674</del>	0.0	29955.413
-328.409	3000.00	72.278	137.420	0.0	30194.092
-326.105	3000.00	81.486	109.825	0.0	30495.760
-321.687	3000.00	91.278	81.462	0.0	30273.378
-315.576	3000.00	<del>99.470</del>	<del>52.634</del>	0.0	<del>29494.180</del>
-308.028	3000.00	107.540	24.416	0.0	27986.680
-299.290	3000.00	114.148	-1.966	0.0	25680.931
-299.634	3000.00	119.659	-22.811	0.0	22531.355
-279.324	3000.00	<del>124.141</del>	<del>40.645</del>	0.0	<del>18556.768</del>
-268.590	3000.00	127.759	-53.401	0.0	13847.942
-257.610	3000.00	130.759	-43.503	0.0	8557.655
-246.546	3000.00	133.413	-48.844	0.0	2873.691
-235.477	3000.00	<del>136.115</del>	<del>65.315</del>	0.0	<del>3021.144</del>
-224.505	3000.00	139.142	-64.857	0.0	-8977.000
-213.740	3000.00	142.454	-66.440	0.0	-14903.640
-203.339	3000.00	147.570	-69.627	0.0	-20902.085
-193.540	3000.00	<del>153.580</del>	<del>78.501</del>	0.0	<del>26898.453</del>
-184.675	3000.00	161.119	-95.138	0.0	-32904.618
-177.187	3000.00	170.282	-121.706	0.0	-39117.008
-171.633	3000.00	181.081	-160.951	0.0	-45737.338
-168.657	3000.00	<del>193.283</del>	<del>215.977</del>	0.0	<del>52988.886</del>
-168.940	3000.00	206.392	-290.571	0.0	-61126.167
-173.106	3000.00	219.580	-390.137	0.0	-70429.757
-181.586	3000.00	231.640	-521.318	0.0	-81137.864
-194.001	3000.00	<del>241.012</del>	<del>691.971</del>	0.0	<del>93287.692</del>
-210.951	3000.00	245.911	-910.953	0.0	-106522.392
-229.821	3000.00	244.627	-1187.702	0.0	-119727.914
MANOEUVRE	COMPLETE				

TABLE 3.5: SELECTED TRAJECTORIES AND FORCES

x ft.	y ft.	z ft.	F <sub>x</sub>	F <sub>y</sub>	F <sub>z</sub>
PULL DOWN	ELEVATOR UNTIL MAX DESCENT RATE ACHIEVED				
0.000	3000.000	0.000	0.000	0.000	0.000
-8.800	3000.100	0.000	259.769	5633.216	0.000
-17.631	3000.672	0.000	257.298	5648.498	0.000
-26.679	3001.512	0.000	253.359	5652.186	0.000
-35.324	3002.604	0.000	247.951	5643.679	0.000
-44.194	3004.202	0.000	241.086	5621.191	0.000
-53.007	3006.006	0.000	232.704	5582.283	0.000
-61.977	3008.275	0.000	223.099	5523.864	0.000
-70.890	3010.553	0.000	212.080	-459.794	0.000
-79.616	3012.852	0.000	210.995	-501.225	0.000
-88.754	3015.121	0.000	200.733	-542.178	0.000
-97.703	3017.355	0.000	200.115	-582.785	0.000
-106.664	3019.553	0.000	199.543	-623.105	0.000
-115.637	3021.713	0.000	199.010	-663.173	0.000
-124.621	3023.832	0.000	198.530	-703.025	0.000
-133.617	3025.908	0.000	198.082	-742.698	0.000
-142.624	3027.938	0.000	197.663	-782.231	0.000
-151.643	3029.920	0.000	197.264	-821.662	0.000
-160.672	3031.852	0.000	196.882	-861.033	0.000
-169.712	3033.731	0.000	196.546	-900.384	0.000
-178.764	3035.555	0.000	196.220	-939.757	0.000
-187.826	3037.321	0.000	195.910	-979.100	0.000
-196.898	3039.020	0.000	195.660	-1018.749	0.000
-205.981	3040.673	0.000	195.123	-1058.458	0.000
-215.074	3042.253	0.000	194.698	-1098.371	0.000
-224.171	3043.766	0.000	194.271	-1138.538	0.000
-233.291	3045.209	0.000	193.835	-1179.009	0.000
-242.414	3046.581	0.000	193.385	-1219.836	0.000
-251.540	3047.879	0.000	193.040	-1261.075	0.000
-260.668	3049.099	0.000	192.734	-1302.784	0.000
-269.839	3050.241	0.000	192.390	-1345.022	0.000



TABLE 3.5: SELECTED TRAJECTORIES AND FORCES

X ft.	Y ft.	Z ft.	Fx	Fy	Fz
-274.001	3051.354	0.000	192.009	547.612	0.000
-288.170	3052.500	0.000	187.394	286.574	0.000
-297.364	3053.644	0.000	186.978	.730	0.000
-306.563	3054.788	0.000	184.781	-301.786	0.000
-315.773	3055.932	0.000	182.900	-614.698	0.000
-324.942	3056.946	0.000	181.349	-950.944	0.000
-334.214	3057.964	0.000	180.109	-1289.617	0.000
-343.454	3058.475	0.000	179.115	-1622.607	0.000
-352.694	3058.678	0.000	178.370	-1962.930	0.000
-361.938	3058.353	0.000	177.822	-2309.024	0.000
-371.184	3058.890	0.000	177.349	-2659.454	0.000
-380.432	3058.734	0.000	176.862	-3013.071	0.000
-389.679	3058.145	0.000	176.296	-3369.053	0.000
-398.923	3058.341	0.000	175.522	-3726.947	0.000
-408.178	3058.894	0.000	174.181	-4093.825	0.000
-417.456	3059.552	0.000	168.446	-4491.685	0.000
-426.753	3059.741	0.000	167.207	-4897.468	0.000
-436.060	3059.626	0.000	155.415	-5312.013	0.000
-445.370	3057.142	0.000	140.031	-5734.977	0.000
-454.670	3055.343	0.000	120.016	-6166.015	0.000
-463.946	3053.205	0.000	131.331	-6604.756	0.000
-473.265	3051.779	0.000	121.937	-703.423	0.000
-482.456	3048.245	0.000	117.382	-1944.894	0.000
-491.698	3045.545	0.000	114.581	-1952.358	0.000
-500.929	3042.829	0.000	111.754	-1959.893	0.000
-510.148	3039.947	0.000	108.911	-1967.476	0.000
-519.352	3036.948	0.000	106.053	-1975.106	0.000
-528.541	3033.832	0.000	103.180	-1982.782	0.000
-537.712	3030.599	0.000	100.291	-1990.506	0.000
-546.866	3027.248	0.000	97.387	-1998.276	0.000
-556.000	3023.780	0.000	94.467	-2006.092	0.000
-565.112	3020.195	0.000	91.533	-2013.954	0.000

TABLE 3.5: SELECTED TRAJECTORIES AND FORCES

x ft.	y ft.	z ft.	Fx	Fy	Fz
-574.202	3016.491	0.000	88.583	-2021.842	0.000
-583.267	3012.676	0.000	85.619	-2027.819	0.000
-592.307	3004.730	0.000	82.640	-2037.814	0.000
<del>-601.314</del>	<del>3000.473</del>	<del>0.000</del>	<del>-79.647</del>	<del>-2045.857</del>	<del>0.000</del>
MANEUVER	COMPLETE				

TABLE 3.5: SELECTED TRAJECTORIES AND FORCES

x ft.	y ft.	z ft.	Fx	Fy	Fz
FULL UP ELEVATOR UNTIL DESCENT RATE = 0.					
-621.319	3044.673	0.000	79.647	-2045.857	0.000
-610.105	3044.155	0.000	76.639	-14205.435	0.000
-614.737	2974.924	0.000	92.985	-15113.865	0.000
-627.101	2944.954	0.002	76.554	-837.648	0.000
-635.493	2943.238	0.000	41.561	1414.589	0.000
-643.947	2977.595	0.000	39.424	-1315.510	0.000
-652.559	2972.061	0.000	42.746	6174.337	0.000
-661.343	2944.725	0.000	51.992	2550.349	0.000
-670.154	2951.400	0.000	60.828	-1829.933	0.000
-678.417	2955.478	0.000	59.790	-1909.272	0.000
-687.670	2951.515	0.000	52.686	500.991	0.000
-696.473	2945.999	0.000	47.211	-1633.102	0.000
-705.333	2939.741	0.000	46.954	943.117	0.000
-714.220	2934.471	0.000	47.427	6.563	0.000
-723.121	2929.058	0.000	45.764	-4.170	0.000
-732.043	2923.723	0.000	42.584	-548.643	0.000
-741.000	2918.417	0.000	39.892	842.642	0.000
-749.994	2913.140	0.000	38.271	706.181	0.000
-759.021	2907.902	0.000	36.868	519.378	0.000
-768.070	2902.674	0.000	34.972	-544.985	0.000
-777.164	2897.485	0.000	32.734	706.552	0.000
-786.287	2892.323	0.000	30.623	798.125	0.000
-795.448	2887.198	0.000	28.765	789.982	0.000
-804.644	2882.109	0.000	26.955	-773.576	0.000
-813.870	2877.056	0.000	25.030	809.420	0.000
-823.145	2872.042	0.000	23.031	873.190	0.000
-832.453	2867.070	0.000	21.061	917.578	0.000
-841.600	2862.142	0.000	19.157	-941.116	0.000
-851.184	2857.260	0.000	17.264	965.059	0.000
-860.613	2852.425	0.000	15.345	1000.266	0.000
-870.080	2847.640	0.000	13.417	1040.530	0.000
-879.588	2842.907	0.000	11.563	-1077.089	0.000

TABLE 3.5: SELECTED TRAJECTORIES AND FORCES

x ft.	y ft.	z ft.	F <sub>x</sub>	F <sub>y</sub>	F <sub>z</sub>
-859.138	2838.227	0.000	7.609	1109.112	0.000
-898.730	2833.603	0.000	7.725	1140.900	0.000
-938.365	2829.037	0.000	5.841	1174.971	0.000
-978.043	2824.531	0.000	3.961	1210.040	0.000
-927.764	2820.088	0.000	2.091	1244.360	0.000
-937.524	2815.708	0.000	.232	1277.615	0.000
-947.337	2811.395	0.000	-1.617	1310.690	0.000
-957.190	2807.150	0.000	-3.454	1344.130	0.000
-967.087	2802.977	0.000	-5.293	1377.733	0.000
-977.029	2798.876	0.000	-7.116	1411.067	0.000
-987.015	2794.849	0.000	-8.929	1444.061	0.000
-997.045	2790.891	0.000	-10.732	1476.897	0.000
-1007.120	2787.031	0.000	-12.524	1508.694	0.000
-1017.239	2783.243	0.000	-14.305	1542.404	0.000
-1027.402	2779.536	0.000	-16.075	1574.932	0.000
-1037.610	2775.929	0.000	-17.833	1607.254	0.000
-1047.861	2772.349	0.000	-19.579	1639.404	0.000
-1058.156	2768.949	0.000	-21.313	1671.405	0.000
-1068.493	2765.601	0.000	-23.034	1703.241	0.000
-1078.874	2762.340	0.000	-24.742	1734.887	0.000
-1089.297	2759.192	0.000	-26.430	1766.332	0.000
-1099.761	2756.134	0.000	-28.117	1797.578	0.000
-1110.267	2753.178	0.000	-29.783	1828.627	0.000
-1120.813	2750.325	0.000	-31.435	1859.469	0.000
-1131.398	2747.577	0.000	-33.072	1890.094	0.000
-1142.023	2744.937	0.000	-34.693	1920.495	0.000
-1152.680	2742.407	0.000	-36.298	1950.668	0.000
-1163.386	2739.989	0.000	-37.888	1980.607	0.000
-1174.123	2737.685	0.000	-39.461	2010.305	0.000
-1184.895	2735.497	0.000	-41.017	2039.756	0.000
-1195.701	2733.427	0.000	-42.555	2068.953	0.000
-1206.540	2731.477	0.000	-44.076	2097.890	0.000

TABLE 3.5: SELECTED TRAJECTORIES AND FORCES

x ft.	y ft.	z ft.	F <sub>x</sub>	F <sub>y</sub>	F <sub>z</sub>
-1217.411	2729.650	0.000	-45.574	2126.581	0.000
-1228.312	2727.447	0.000	-47.063	2154.959	0.000
-1239.243	2726.370	0.000	-48.528	2183.079	0.000
-1250.201	2725.422	0.000	-49.975	2210.914	0.000
-1261.186	2724.604	0.000	-51.401	2238.458	0.000
-1272.195	2723.414	0.000	-52.807	2265.705	0.000
-1283.220	2721.366	0.000	-54.193	2292.649	0.000
-1294.262	2720.450	0.000	-55.558	2319.283	0.000
-1305.356	2719.672	0.000	-56.902	2345.603	0.000
-1316.448	2719.033	0.000	-58.225	2371.601	0.000
-1327.556	2718.536	0.000	-59.525	2397.272	0.000
-1338.678	2719.142	0.000	-60.803	2422.611	0.000
-1349.813	2717.972	0.000	-62.058	2447.611	0.000
-1360.956	2717.909	0.000	-63.290	2472.268	0.000
-1372.111	2717.993	0.000	-64.499	2496.575	0.000
MANOEUVRE	COMPLETE				

TABLE 3.5: SELECTED TRAJECTORIES AND FORCES

x ft.	y ft.	z ft.	Fx	Fy	Fz
STEADY STATE TURN FROM 0-180 DEGREES					
0.000	3000.00	0.000	0.000	0.0	0.000
-8.797	3000.00	.416	254.769	0.0	3889.759
-17.585	3000.00	.833	254.343	0.0	3889.759
-26.371	3000.00	1.242	254.401	0.0	3889.759
-35.158	3000.00	1.652	254.458	0.0	3889.759
-43.945	3000.00	2.062	254.513	0.0	3889.759
-52.731	3000.00	2.467	254.566	0.0	3889.759
-61.515	3000.00	2.861	254.618	0.0	3889.759
-70.303	3000.00	3.257	254.669	0.0	3889.759
-79.090	3000.00	3.640	254.718	0.0	3889.759
-87.875	3000.00	4.018	254.765	0.0	3889.759
-96.661	3000.00	4.391	254.811	0.0	3889.759
-105.446	3000.00	4.753	254.856	0.0	3889.759
-114.231	3000.00	5.110	254.900	0.0	3889.759
-123.015	3000.00	5.468	254.943	0.0	3889.759
-131.800	3000.00	5.825	254.984	0.0	3889.759
-140.584	3000.00	6.180	255.025	0.0	3889.759
-149.369	3000.00	6.534	255.064	0.0	3889.759
-158.153	3000.00	6.887	255.103	0.0	3889.759
-166.938	3000.00	7.240	255.141	0.0	3889.759
-175.722	3000.00	7.592	255.177	0.0	3889.759
-184.507	3000.00	7.944	255.214	0.0	3889.759
-193.291	3000.00	8.295	255.249	0.0	3889.759
-202.076	3000.00	8.646	255.283	0.0	3889.759
-210.860	3000.00	8.996	255.317	0.0	3889.759
-219.645	3000.00	9.346	255.350	0.0	3889.759
-228.429	3000.00	9.695	255.383	0.0	3889.759
-237.214	3000.00	10.044	255.414	0.0	3889.759
-246.000	3000.00	10.392	255.446	0.0	3889.759
-254.785	3000.00	10.740	255.476	0.0	3889.759

TABLE 3.5: SELECTED TRAJECTORIES AND FORCES

x ft.	y ft.	z ft.	F <sub>x</sub>	F <sub>y</sub>	F <sub>z</sub>
-237.023	3000.00	94.901	255.507	0.0	3889.759
-243.112	3000.00	105.229	255.536	0.0	3889.759
-249.033	3000.00	111.704	255.566	0.0	3889.759
-254.780	3000.00	118.344	255.588	0.0	3889.759
-260.349	3000.00	125.129	255.623	0.0	3889.759
-265.737	3000.00	132.054	255.651	0.0	3889.759
-270.940	3000.00	139.127	255.678	0.0	3889.759
-275.954	3000.00	146.330	255.706	0.0	3889.759
-280.776	3000.00	153.663	255.733	0.0	3889.759
-285.402	3000.00	161.120	255.759	0.0	3889.759
-289.829	3000.00	168.696	255.786	0.0	3889.759
-294.055	3000.00	176.389	255.812	0.0	3889.759
-298.076	3000.00	184.184	255.838	0.0	3889.759
-301.889	3000.00	192.085	255.863	0.0	3889.759
-305.494	3000.00	200.084	255.889	0.0	3889.759
-308.882	3000.00	208.175	255.914	0.0	3889.759
-312.058	3000.00	216.352	255.939	0.0	3889.759
-315.015	3000.00	224.609	255.964	0.0	3889.759
-317.754	3000.00	232.941	255.989	0.0	3889.759
-320.271	3000.00	241.342	256.014	0.0	3889.759
-322.566	3000.00	249.807	256.036	0.0	3889.759
-324.635	3000.00	258.329	256.063	0.0	3889.759
-326.479	3000.00	266.901	256.087	0.0	3889.759
-328.295	3000.00	275.518	256.112	0.0	3889.759
-329.483	3000.00	284.175	256.136	0.0	3889.759
-330.642	3000.00	292.865	256.161	0.0	3889.759
-331.570	3000.00	301.583	256.185	0.0	3889.759
-332.268	3000.00	310.321	256.204	0.0	3889.759
-332.735	3000.00	319.074	256.233	0.0	3889.759
-332.970	3000.00	327.835	256.258	0.0	3889.759
-332.973	3000.00	336.609	256.282	0.0	3889.759
-332.744	3000.00	345.361	256.300	0.0	3889.759

TABLE 3.5: SELECTED TRAJECTORIES AND FORCES

x ft.	y ft.	z ft.	F <sub>x</sub>	F <sub>y</sub>	F <sub>z</sub>
-332.284	3000.00	354.112	256.331	0.0	3889.759
-331.543	3000.00	362.447	256.355	0.0	3889.759
-330.871	3000.00	371.561	256.379	0.0	3889.759
<del>-329.514</del>	3000.00	<del>380.247</del>	<del>256.404</del>	0.0	<del>3889.759</del>
-328.136	3000.00	388.898	256.429	0.0	3889.759
-326.528	3000.00	397.510	256.453	0.0	3889.759
-324.691	3000.00	406.075	256.478	0.0	3889.759
<del>-322.624</del>	3000.00	<del>414.589</del>	<del>256.503</del>	0.0	<del>3889.759</del>
-320.342	3000.00	423.044	256.527	0.0	3889.759
-317.433	3000.00	431.536	256.552	0.0	3889.759
-315.102	3000.00	439.157	256.577	0.0	3889.759
<del>-312.153</del>	3000.00	<del>448.003</del>	<del>256.603</del>	0.0	<del>3889.759</del>
-308.986	3000.00	456.168	256.628	0.0	3889.759
-305.685	3000.00	464.245	256.653	0.0	3889.759
-302.011	3000.00	472.230	256.679	0.0	3889.759
<del>-298.208</del>	3000.00	<del>480.116</del>	<del>256.704</del>	0.0	<del>3889.759</del>
-294.197	3000.00	487.899	256.730	0.0	3889.759
-289.983	3000.00	495.572	256.756	0.0	3889.759
-285.566	3000.00	503.130	256.782	0.0	3889.759
<del>-280.452</del>	3000.00	<del>510.568</del>	<del>256.808</del>	0.0	<del>3889.759</del>
-276.142	3000.00	517.042	256.834	0.0	3889.759
-271.141	3000.00	525.044	256.860	0.0	3889.759
-265.752	3000.00	532.112	256.887	0.0	3889.759
<del>-260.578</del>	3000.00	<del>539.018</del>	<del>256.914</del>	0.0	<del>3889.759</del>
-255.124	3000.00	545.781	256.940	0.0	3889.759
-249.243	3000.00	552.394	256.967	0.0	3889.759
-243.389	3000.00	558.851	256.994	0.0	3889.759
<del>-237.316</del>	3000.00	<del>565.150</del>	<del>257.022</del>	0.0	<del>3889.759</del>
-231.679	3000.00	571.286	257.049	0.0	3889.759
-224.683	3000.00	577.254	257.077	0.0	3889.759
-218.130	3000.00	583.049	257.104	0.0	3889.759
<del>-211.427</del>	3000.00	<del>588.669</del>	<del>257.132</del>	0.0	<del>3889.759</del>



TABLE 3.5: SELECTED TRAJECTORIES AND FORCES

x ft.	y ft.	z ft.	F <sub>x</sub>	F <sub>y</sub>	F <sub>z</sub>
-204.578	3000.00	594.110	257.160	0.0	3889.759
-197.588	3000.00	599.366	257.188	0.0	3889.759
-190.461	3000.00	604.435	257.217	0.0	3889.759
-183.203	3000.00	609.313	257.245	0.0	3889.759
-175.818	3000.00	613.997	257.274	0.0	3889.759
-168.312	3000.00	618.484	257.303	0.0	3889.759
-160.691	3000.00	622.769	257.332	0.0	3889.759
-152.954	3000.00	626.857	257.361	0.0	3889.759
-145.122	3000.00	630.726	257.390	0.0	3889.759
-137.186	3000.00	634.392	257.420	0.0	3889.759
-129.155	3000.00	637.846	257.449	0.0	3889.759
-121.031	3000.00	641.086	257.479	0.0	3889.759
-112.834	3000.00	644.110	257.509	0.0	3889.759
-104.554	3000.00	646.914	257.539	0.0	3889.759
-96.204	3000.00	649.498	257.569	0.0	3889.759
-87.795	3000.00	651.860	257.600	0.0	3889.759
-79.322	3000.00	653.998	257.630	0.0	3889.759
-70.795	3000.00	655.910	257.661	0.0	3889.759
-62.222	3000.00	657.595	257.692	0.0	3889.759
-53.607	3000.00	659.052	257.723	0.0	3889.759
MANOEUVRE	Cont. FTR				

## CHAPTER 4

### CAS-1 CABIN STRUCTURE DESIGN

#### 4.1 Introduction

In addition to the theoretical and programming work undertaken, this thesis, also provides the design and analysis of the cabin structure of airship CAS-1. The specifications as to cabin dimensions were provided by CASG (Canadian Airship Study Group, subsequently Canadian Airship Development Corporation). The loading requirements, which the structure was to meet, were partially specified by Ministry of Transport, Civil Aeronautics, Provisional Airworthiness Requirements, Airships<sup>[3]</sup>, sections SC. 2(a), SC.2(b), and SC.11

The design philosophy for the cabin are incorporated in the following considerations:

(1) The final configuration of the engine supports could not be determined at the time of the design.

(2) Considerable strength was to be built into the structure in order to permit subsequent modification for testing of various engine support configurations.

(3). An attempt was to be made to provide under floor strength and compressive strength in the verticals in order to provide reasonable protection inside the cabin in case of accidental impact.

(4) Due to airscrew clearance requirements, with respect to both the ground and the envelope, the cabin must be higher than needed for accommodation. This provided the basis for the decision to provide a deep floor structure providing good floor strength and generous space for other requirements such as ballast containment, handling cables, and fuel tanks.

The cabin structure can be separated into two distinct sections each of which must withstand certain loading conditions. Figure 4.1 illustrates the total cabin with both side and front views. The lower cabin structure (below the floor level), illustrated in Figure 4.2, is required to withstand the loading imposed by landing on the single main wheel at a specified sink rate. However, two other conditions should also be examined.

(1) the static condition occurring when the airship is at rest on its single landing wheel.

(2) the rigging condition occurring when the cabin is separated from the airship and is resting on four removeable castors.

The upper cabin structure, illustrated in Figure 4.3, can itself be divided into two distinct sections. The transverse sections are required to withstand the loading imposed by the internal catenary system. The longitudinal sections are required to withstand the loading due to the external suspension system and due to the force imparted by the engines.

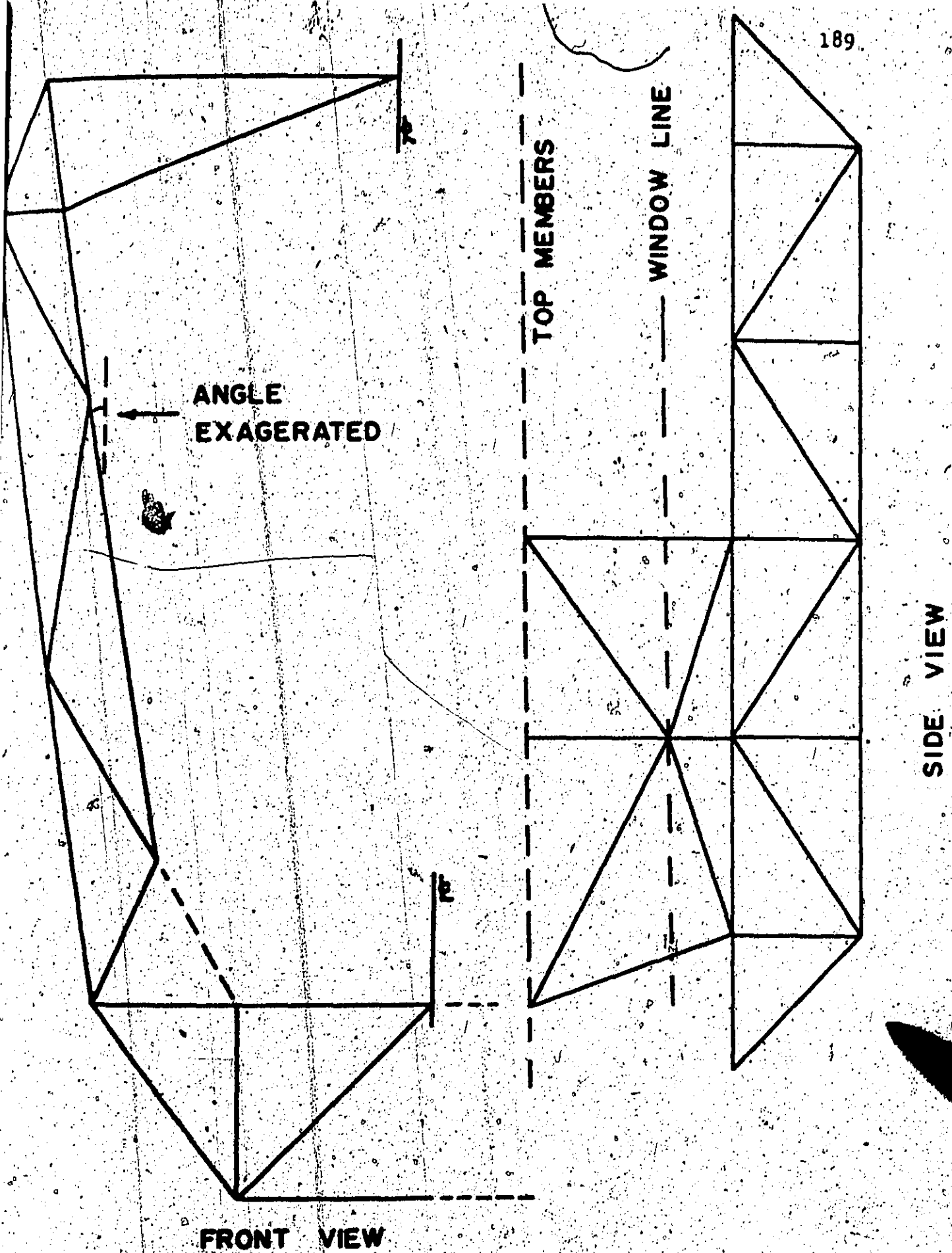


Figure 4.1: Cabin Structure Illustration Front and Side View

POSITION  
NUMBER

7

6

5

4

3

2

1

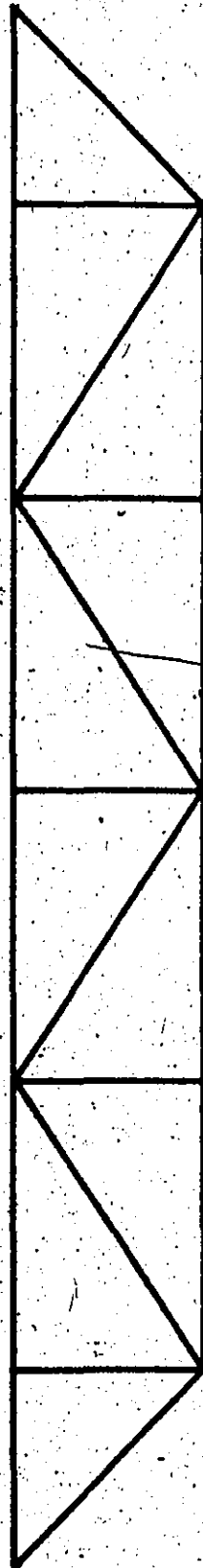


FIGURE 4.2: Lower Cabin Structure

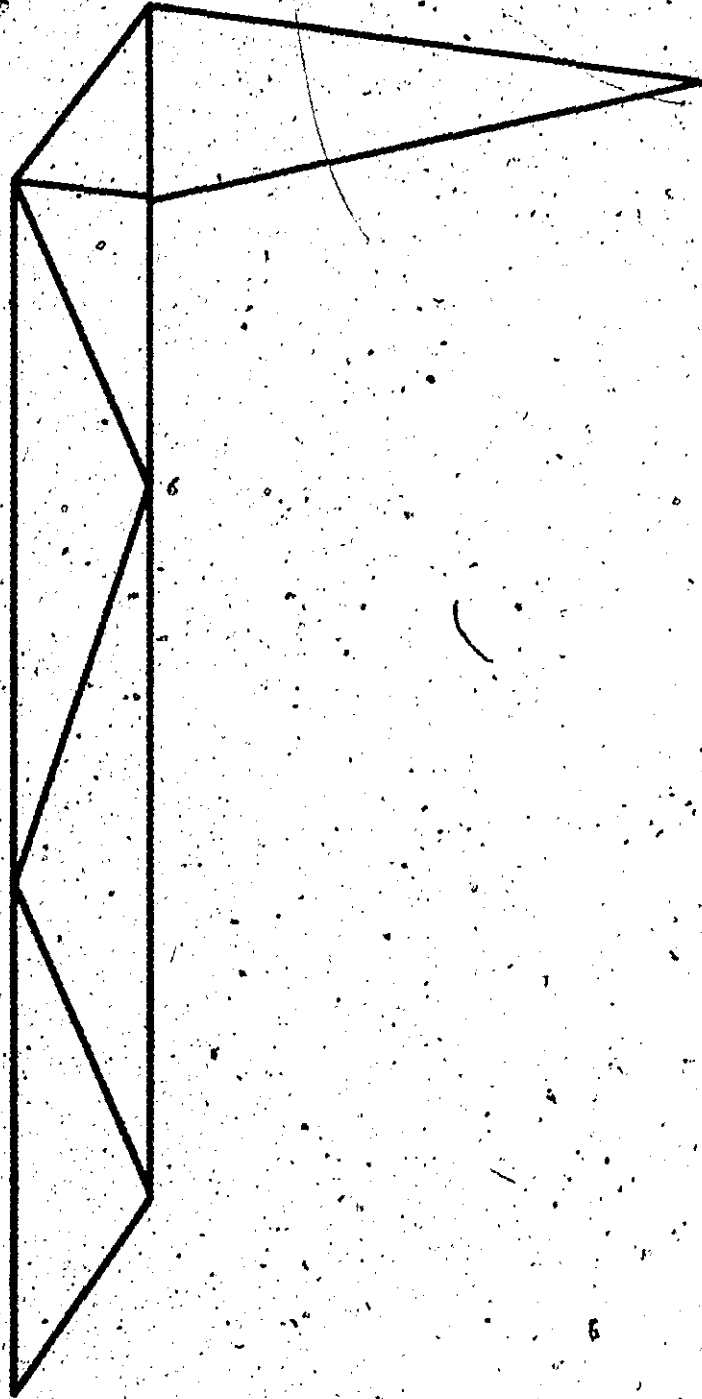


Figure 4.3: Upper Cabin Structure

#### 4.2 Upper Transverse Section Loading Analysis

The transverse upper cabin structure has three major transverse sections. Each section provides two attachment points for the internal suspension system. The cabin weight is usually taken 60% on the internal suspension system and 40% on the external suspension system. However, for the purposes of this analysis 100% of the cabin weight will be taken on the internal suspension system. This will tend to provide a conservative design. Another simplification involves the static engine weight input. The condition is illustrated by Figure 4.4. The struts shown in the illustration are in tension in both the static and the dynamic situation. Referring to Figure 4.5 it can be seen that the tension in the strut will reduce the load in the transverse structure.

The worst condition that occurs is the inflight dynamic loading. The assumption of a rigid body consisting of the engines, outriggers, and underfloor structure allows an analysis to be performed. The total torque of the engines is 382 foot-pounds. The resultant situation is illustrated by Figure 4.6. From static considerations

$$C_V = B_V$$

$$C_H = B_H$$

and from a moment analysis performed about point A

$$D_V = \frac{382}{5} = 76 \text{ pounds}$$

$$D_H = 1 \text{ pound}$$

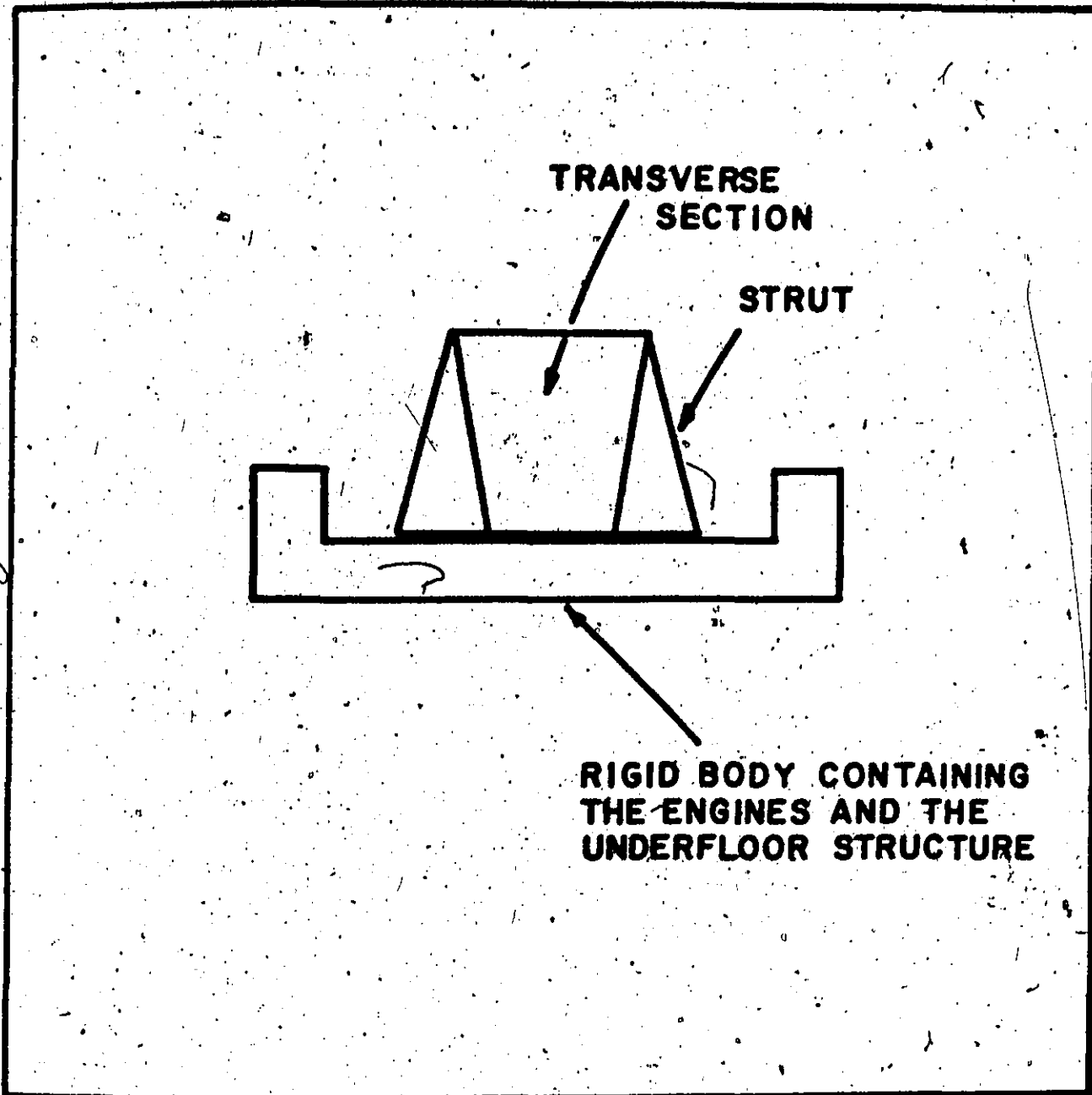


Figure 4.4: Engine Attachment Idealization



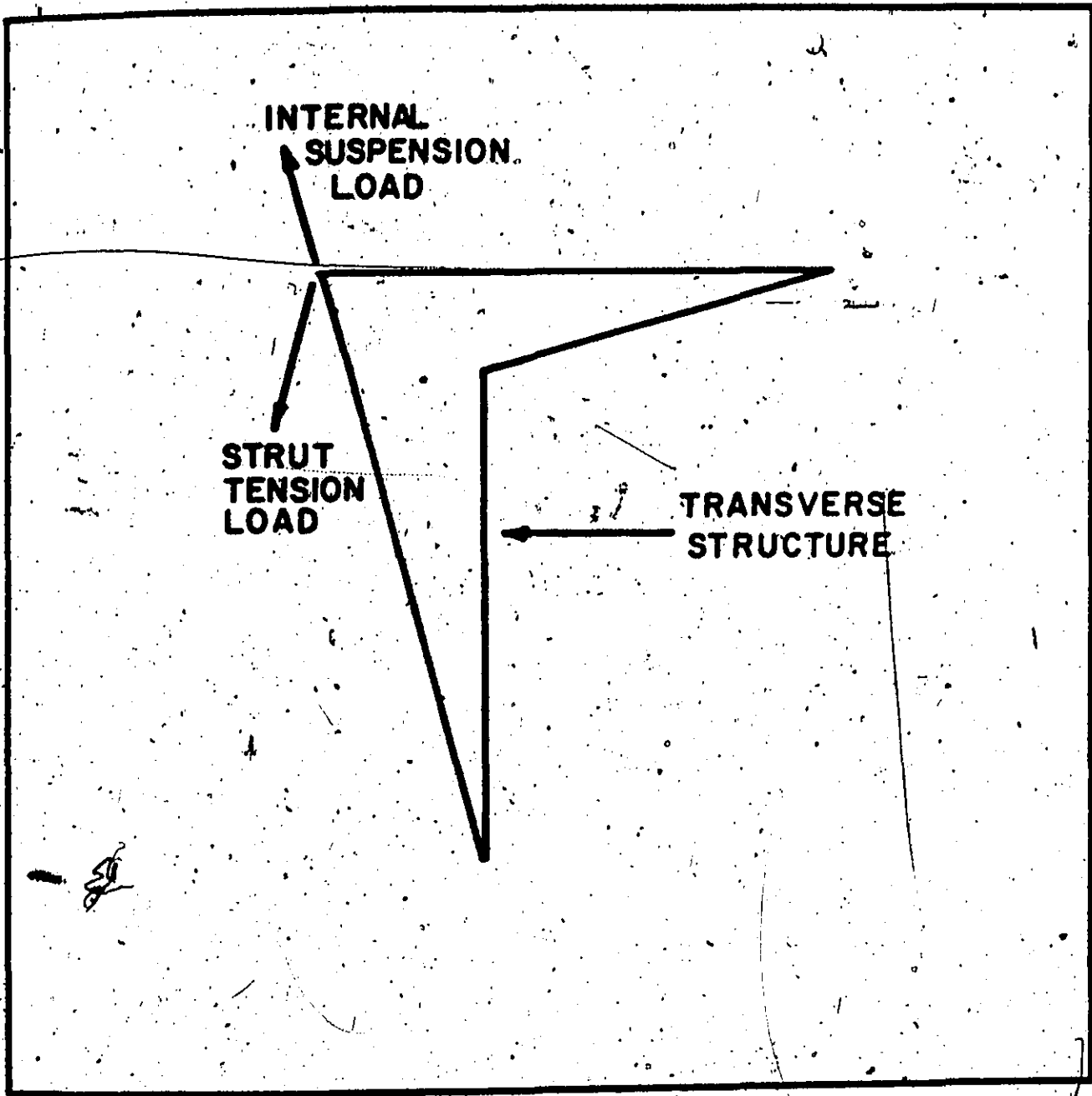


Figure 4.5: Engine Static Weight Input Arrangement

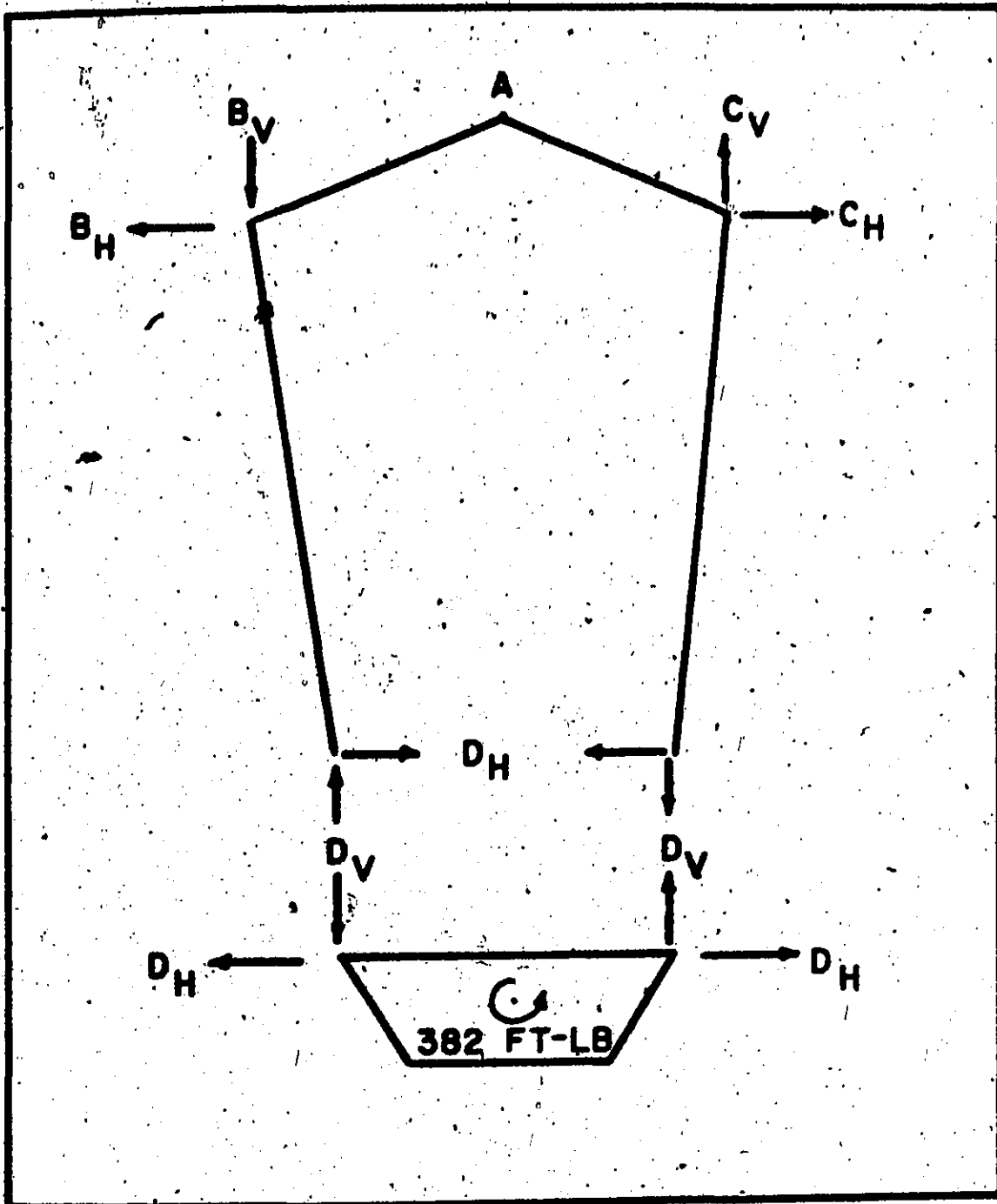


Figure 4.6: Engine Static Weight Input

These are the additional forces produced by the engine torque. These forces must be divided between the three transverse sections in the same proportion as the static cabin weight is proportioned to the internal suspension system.

The analysis of the internal suspension system loads is based on the assumption, as previously stated, that 100% of the static cabin weight is carried by the system. The system is symmetrical about the longitudinal center line of the cabin. The total cabin weight is taken as 3200 pounds. The free body diagram of the system is shown by Figure 4.7. The suspension cables will have load cells in order to allow the loads in the cables to be set at any desired quantity. Hence all combinations of tensions are possible if they obey the following conditions,

$$\sum F_V = 0 \quad (4.1)$$

$$\sum F_H = 0 \quad (4.2)$$

$$\sum M_{CG} = 0 \quad (4.3)$$

Some arbitrary choices must be made in order to solve the system shown by Figure 4.7. The following quantities were, therefore, arbitrarily chosen,

$$B_V = 750 \text{ pounds}$$

$$\theta = 75 \text{ degrees}$$

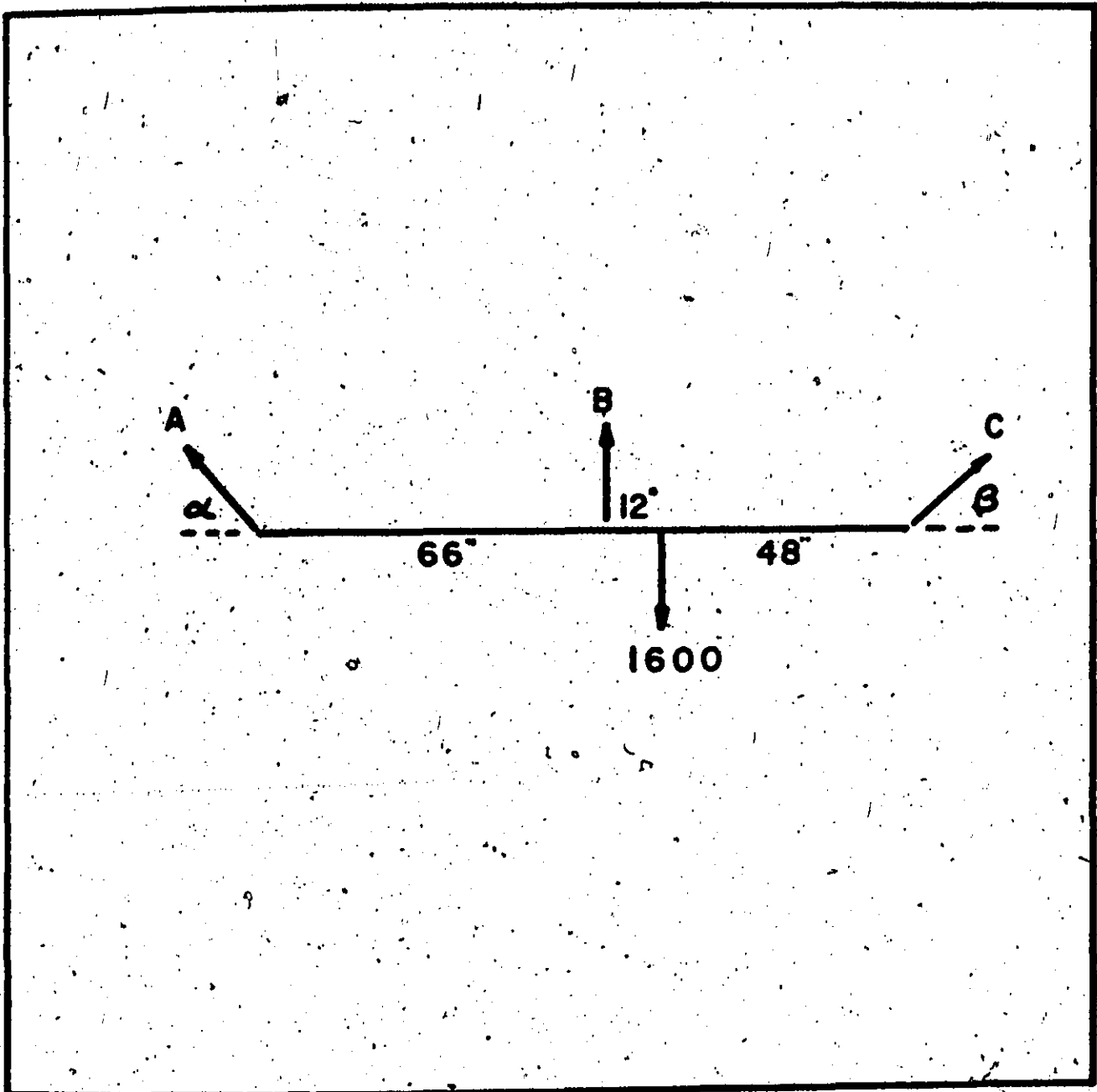


Figure 4.7: System Free Body Diagram

Referring to the free body diagram, the following equations can be formulated.

$$A \sin \alpha + 750 + C \sin 75 - 1600 = 0 \quad (4.1)$$

$$A \cos \alpha - C \cos 75 = 0 \quad (4.2)$$

$$A \sin \alpha \times 66 + 750 \times 12 - C \sin 75 \times 48 = 0 \quad (4.3)$$

From this system of equations, the following results can be obtained.

$$C = 590 \text{ pounds}$$

$$A = 318 \text{ pounds}$$

$$B = 750 \text{ pounds}$$

$$\alpha = 61.5 \text{ degrees}$$

$$\beta = 75 \text{ degrees}$$

However, for the purposes of this analysis, only the vertical components have significance.

$$A_v = 280 \text{ pounds}$$

$$B_v = 750 \text{ pounds}$$

$$C_v = 570 \text{ pounds}$$

The loads on the structure can be resolved into six components. These components, illustrated along with the basic structural design in Figure 4.8, are

- (1)  $F_{VI}$  the vertical load due to the static tension of the suspension cable plus or minus a force due to the engine torque
- (2)  $F_{HI}$  the horizontal load due to the static tension of the suspension cable plus a force due to the engine torque
- (3)  $F_{VII}$  the vertical balancing force
- (4)  $F_{HII}$  the horizontal balancing force

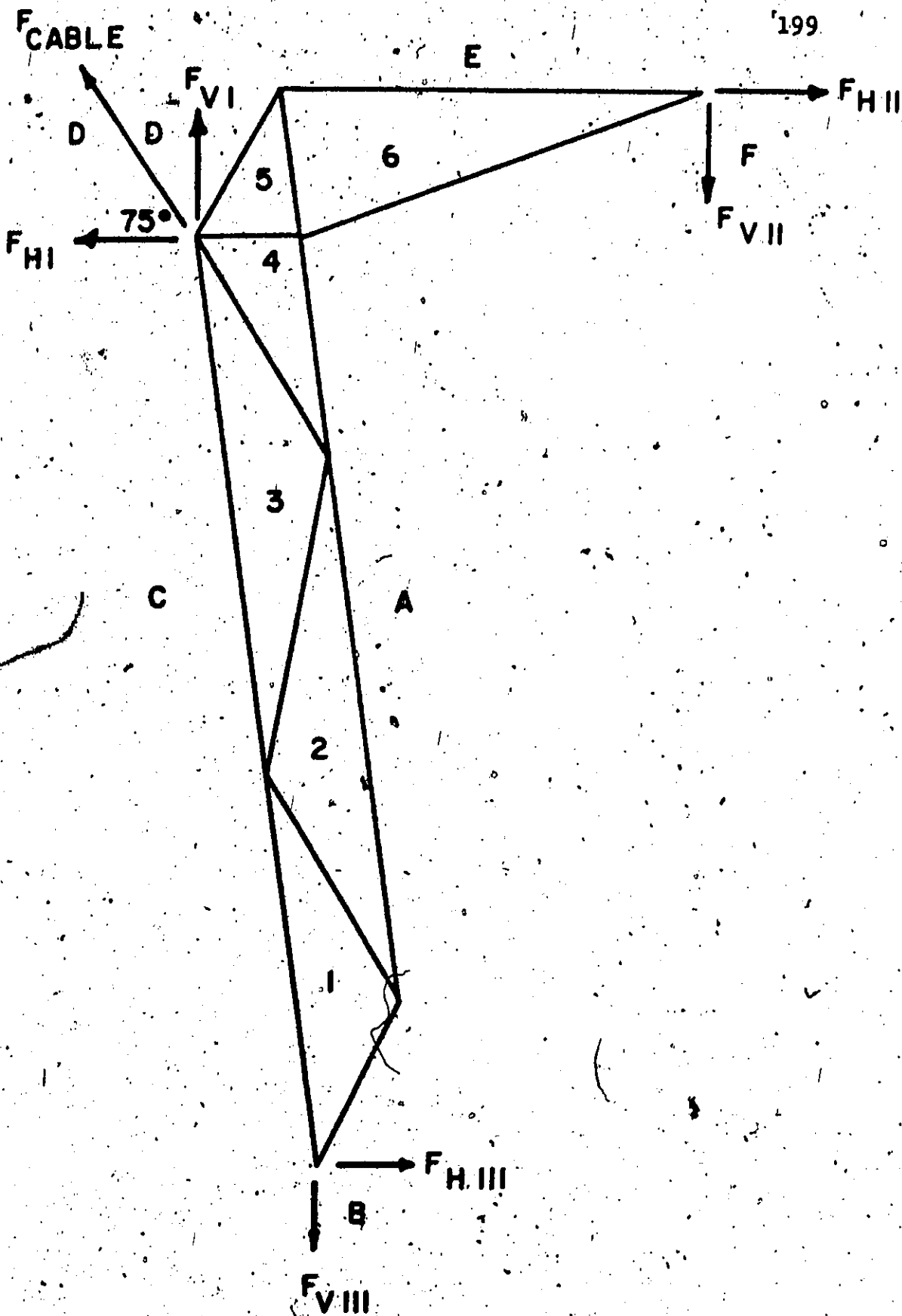


Figure 4.8: Transverse Structure Load Components

- (5)  $F_{VIII}$  the vertical load due to the static tension of the suspension cable plus or minus a force due to the engine torque
- (6)  $F_{HIII}$  the horizontal force due to the above and obtained by considering moments about the cabin center line.

These loads can be determined for each transverse section.

In order to simplify the design the decision was made to use a common size tubing in all the transverse structural sections. Hence, only the maximum loading, which occurs in section B, was considered and the total dynamic loading of the engines was also assumed to be taken in this one section. The suspension cables were assumed to have an inclination of 75 degrees to the horizontal, as shown in Figure 4.8, and the resulting loading is given by Table 4.1. The loading situations are shown in Figure 4.9 and Figure 4.10, while the graphical analysis used to solve the problem is presented in Figures 4.11 and 4.12. Table 4.2 presents the loads obtained from the analysis and also the ultimate design load. The ultimate design load was taken to be the larger of the left side or right side loads and a safety factor of two was applied.

One further situation must be considered. This is the situation which can occur due to wind gusts hitting the cabin side on. The result of such an occurrence is shown in Figure 4.13. If the quantity

$$W \sin \alpha = \text{maximum}$$

is arbitrarily chosen to be 750 pounds then  $\alpha$ , the gust swing angle, can be calculated to be 30 degrees.

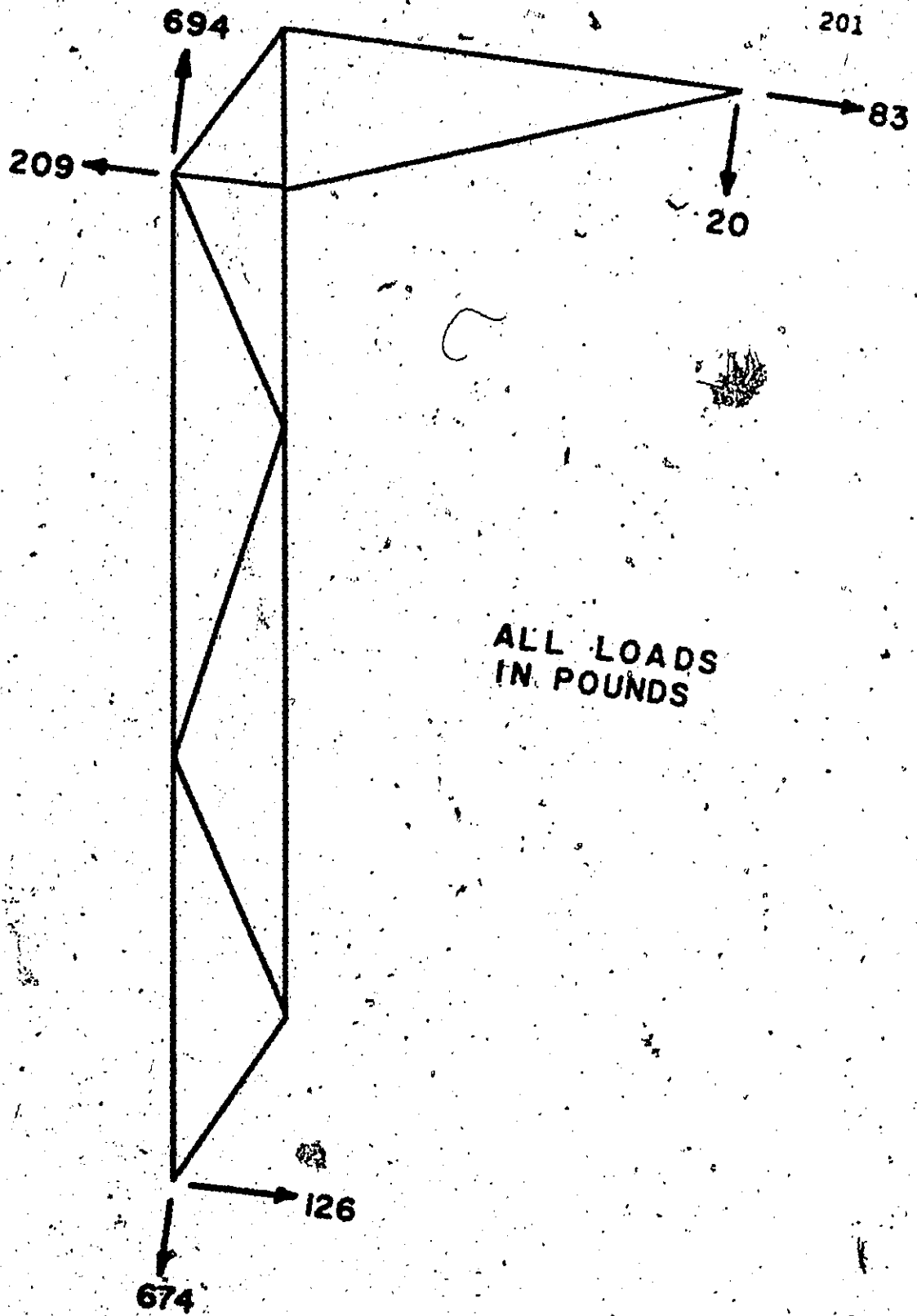


Figure 4.9: Transverse Structure Left Loading Diagram



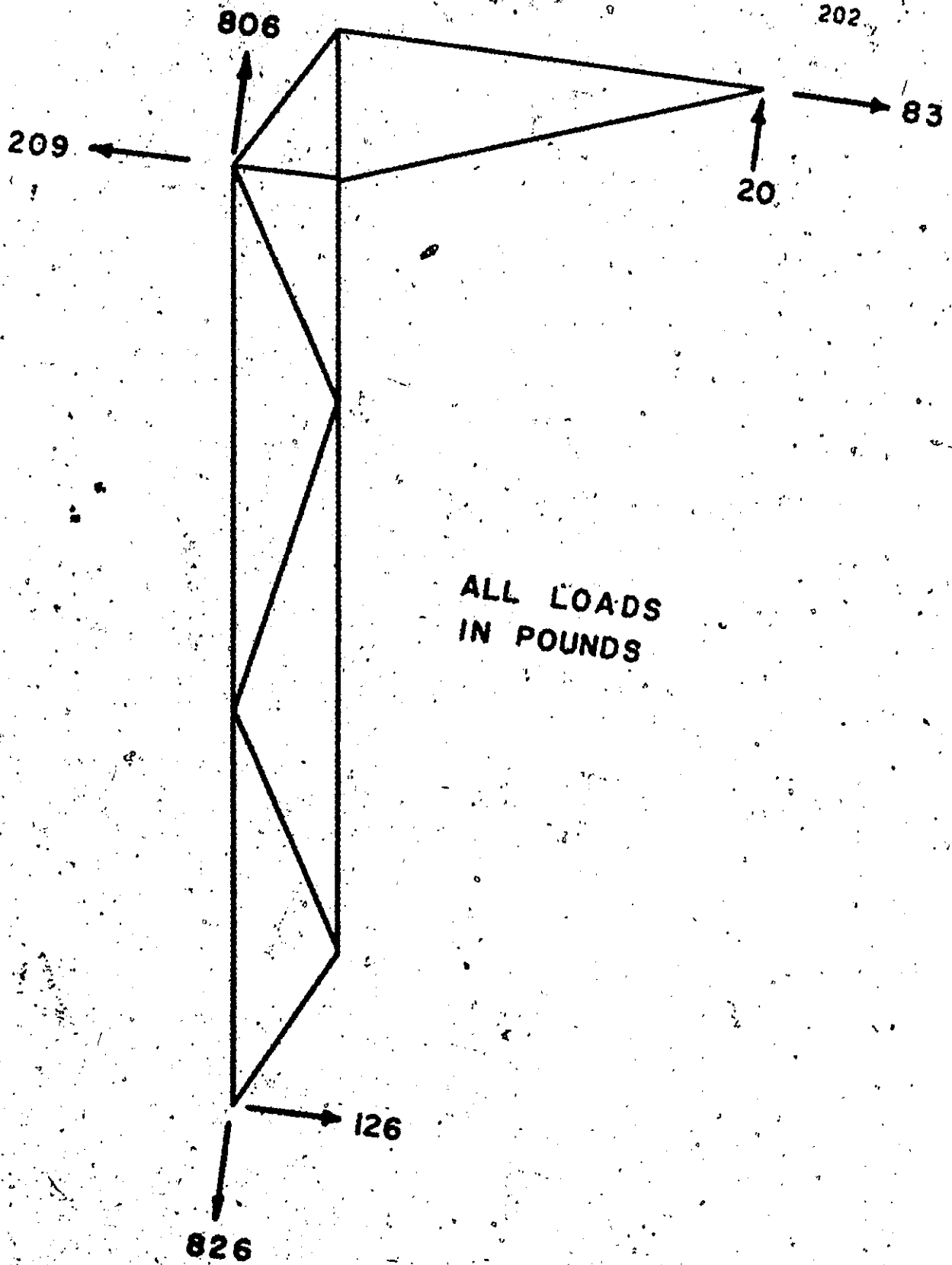


Figure 4.10: Transverse Structure Right Loading Diagram

SCALE  
 $\Gamma = 100^B$



Figure 4.11: Graphical Analysis Left Transverse Structure

SCALE  
1" = 100'

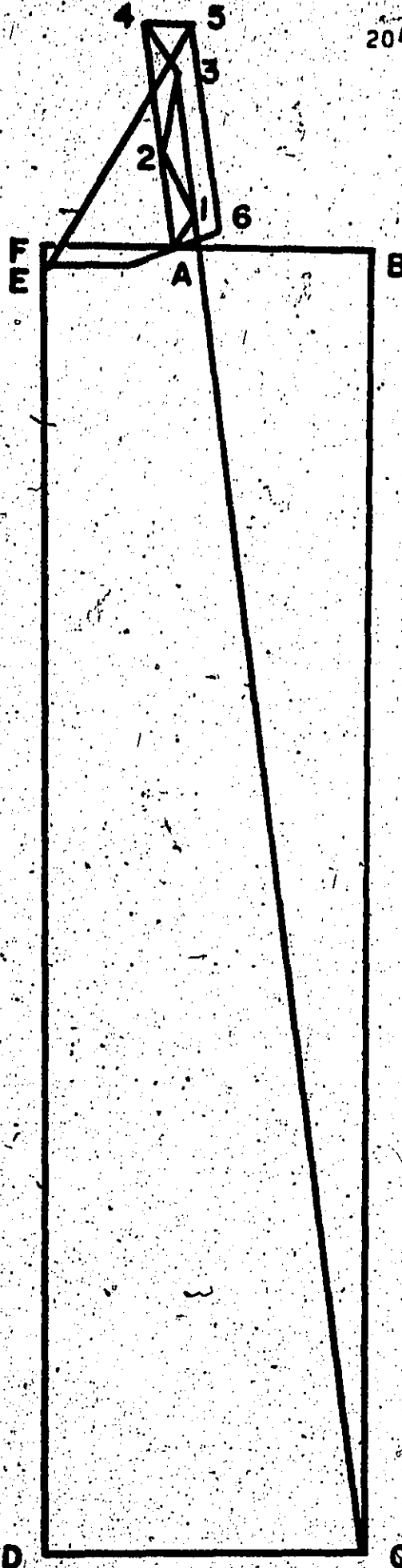


Figure 4.12: Graphical Analysis Right Transverse Structure

The division of this load into the various loads required for the structural analysis is given by Figure 4.14. The loading diagrams for these loads are presented in Figure 4.15 and Figure 4.16, and the graphical analysis, performed to obtain the loads in each member, is presented in Figure 4.17 and Figure 4.18.

The worst possible situation, and perhaps an unrealistic one, occurs when the above loading is combined with the previous loading using superposition. The results of such a combination, in terms of ultimate loads, is presented in Table 4.2(a). From the results presented in this table the structural members, required for the transverse sections, can be determined.

### 4.3 Upper Side Members Loading Analysis

The structure in this analysis must withstand various forces which can be combined into two basic situations, involving climb and dive maneuvers, constituting the extreme boundaries of the flight envelope. The structural configuration, shown in Figure 4.19, must withstand the following forces :

- (1) the weight of the cabin at the center of gravity location (3200 pounds),
- (2) the thrust force of the engines (480 pounds per engine)
- (3) the forces due to a 30 degree dive
- (4) the forces due to a 30 degree upwards inclination

Cases 1, 2 and 3 can be combined into one situation and Cases 1 and 4 can be combined into another situation.

TABLE 4.1: Section Loading

Force	LEFT			RIGHT		
	Static	Dynamic	Total	Static	Dynamic	Total
P <sub>VI</sub>	750	-56	694	750	56	806
P <sub>HI</sub>	202	7	209	202	7	209
P <sub>VII</sub>		20	20		20	20
P <sub>HII</sub>	77	6	83	77	6	83
P <sub>VIII</sub>	750	-76	674	750	76	826
P <sub>HIII</sub>	125	1	126	125	1	126

TABLE 4.2

Member Loads Level Condition

Member	Length	Left Side	T C	Right Side	T C	Ultimate Load	T C
A1	15	65	C	25	C	130	C
A2	42.5	140	C	60	C	280	C
A4	17	315	C	140	C	630	C
A6	33.5	120	C	30	T	240	C
C1	30.5	740	T	860	T	1720	T
C3	42.5	930	T	940	T	1880	T
E5	13.5	315	T	180	T	630	T
E6	33.5	195	T	50	T	390	T
12	20.5	90	T	40	T	180	T
23	25	110	C	50	C	220	C
34	20.5	80	T	40	T	160	T
45	8.5	115	C	30	C	230	C
56	11.5	280	C	130	C	560	C

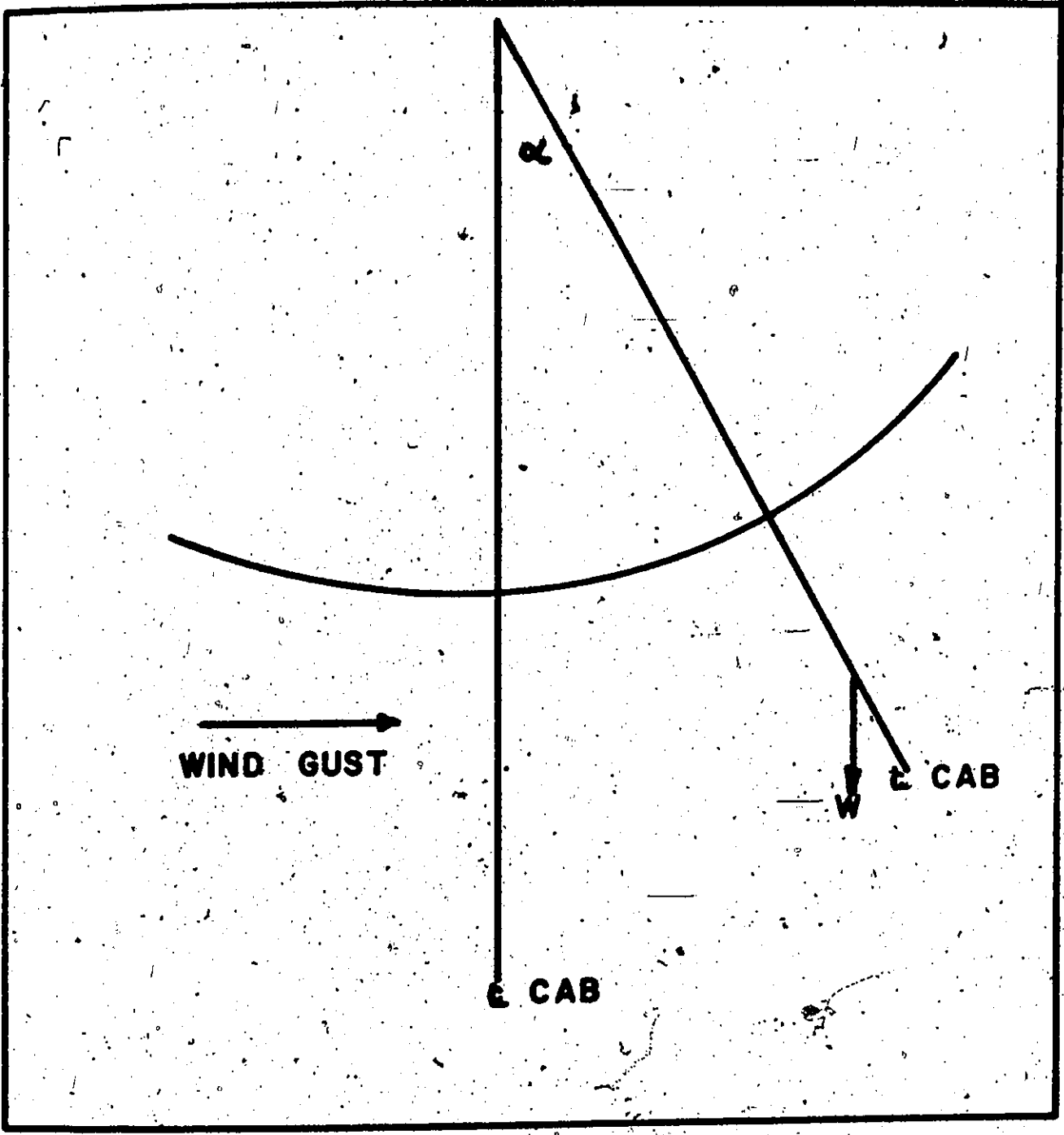


Figure 4.13: Wind Gust Situation

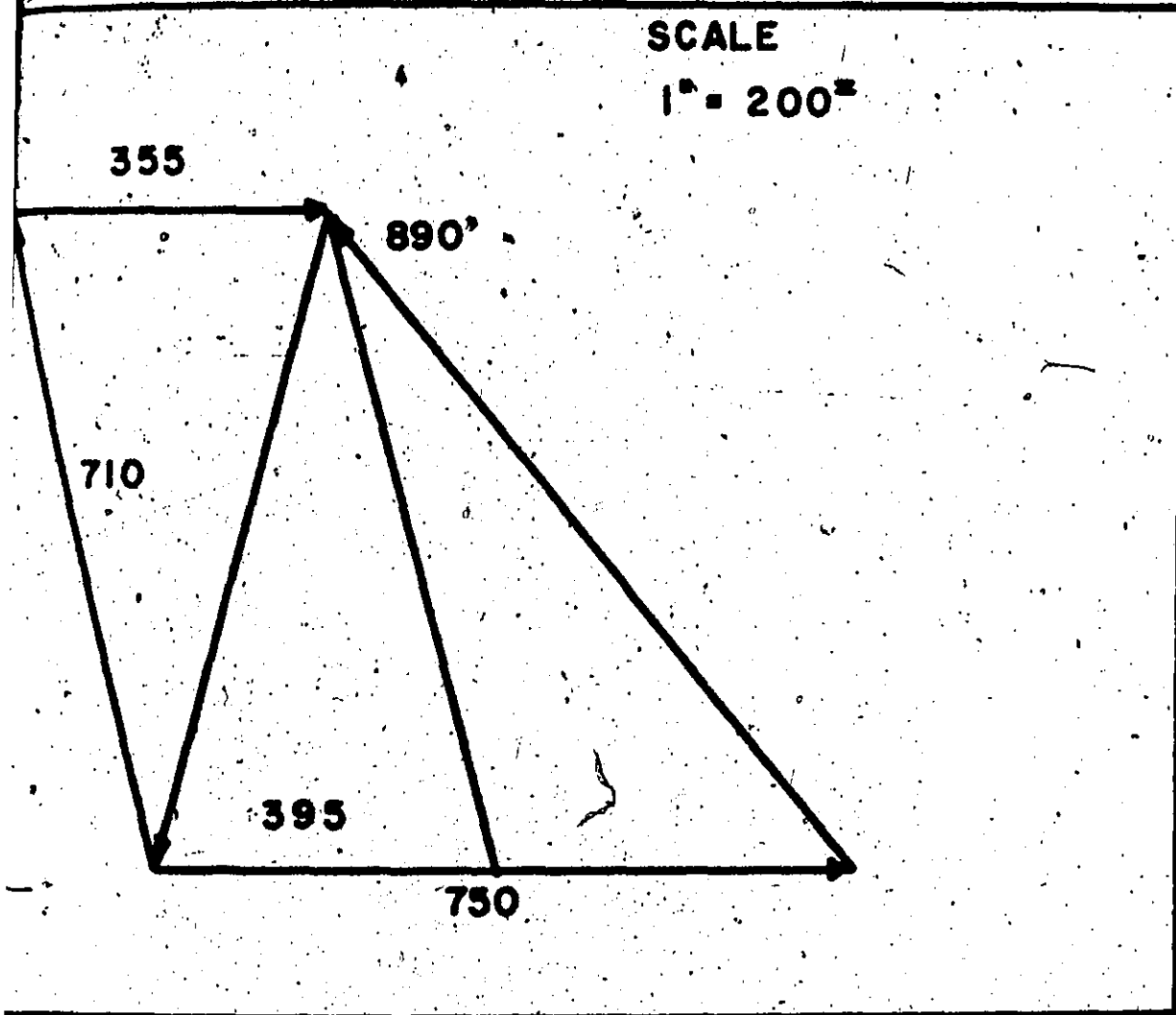


Figure 4.14: Load Analysis Gust Situation



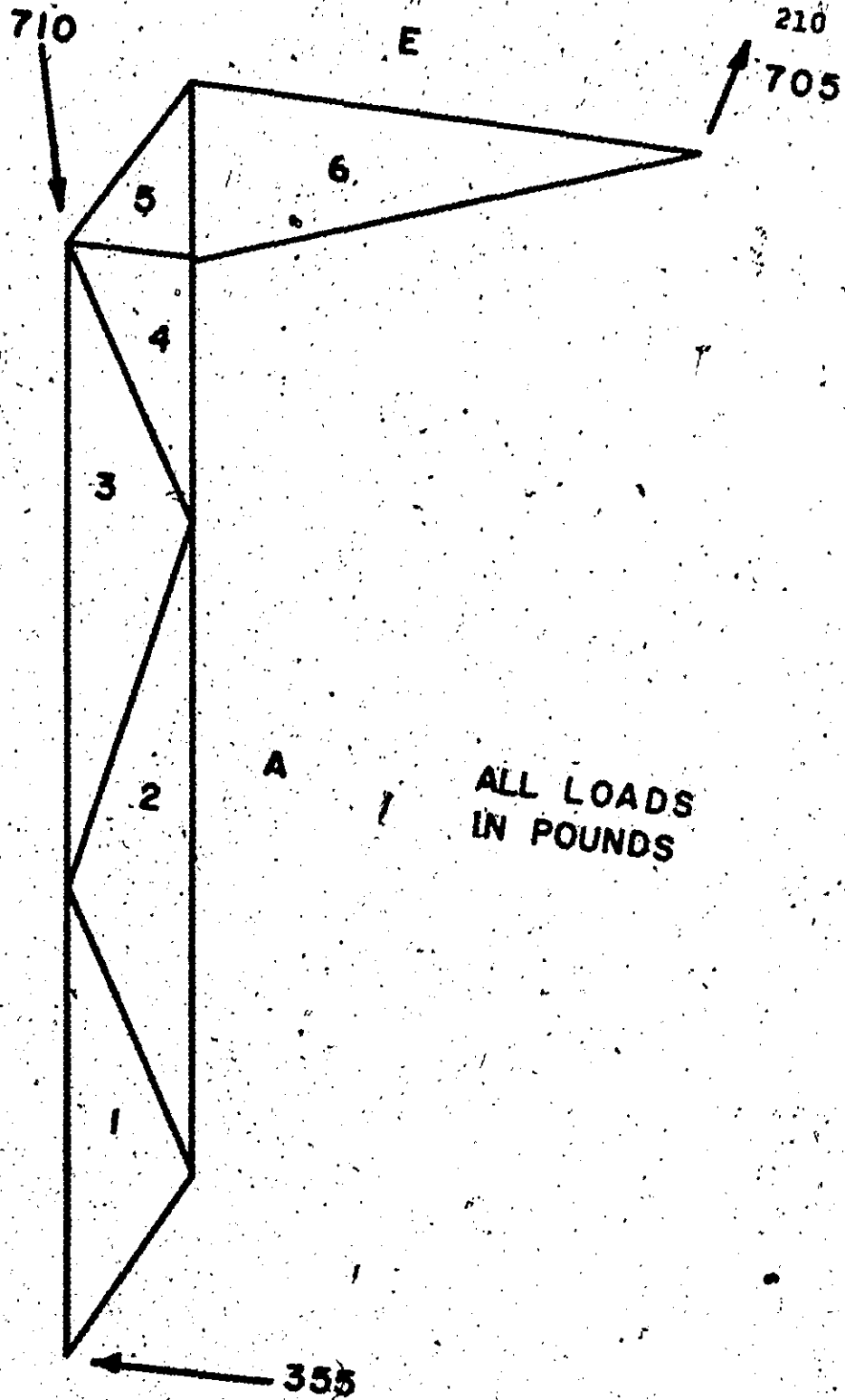


Figure 4.15: Gust Loading Left Transverse Structure

890

211

E

6

5

4

3

2

1

705

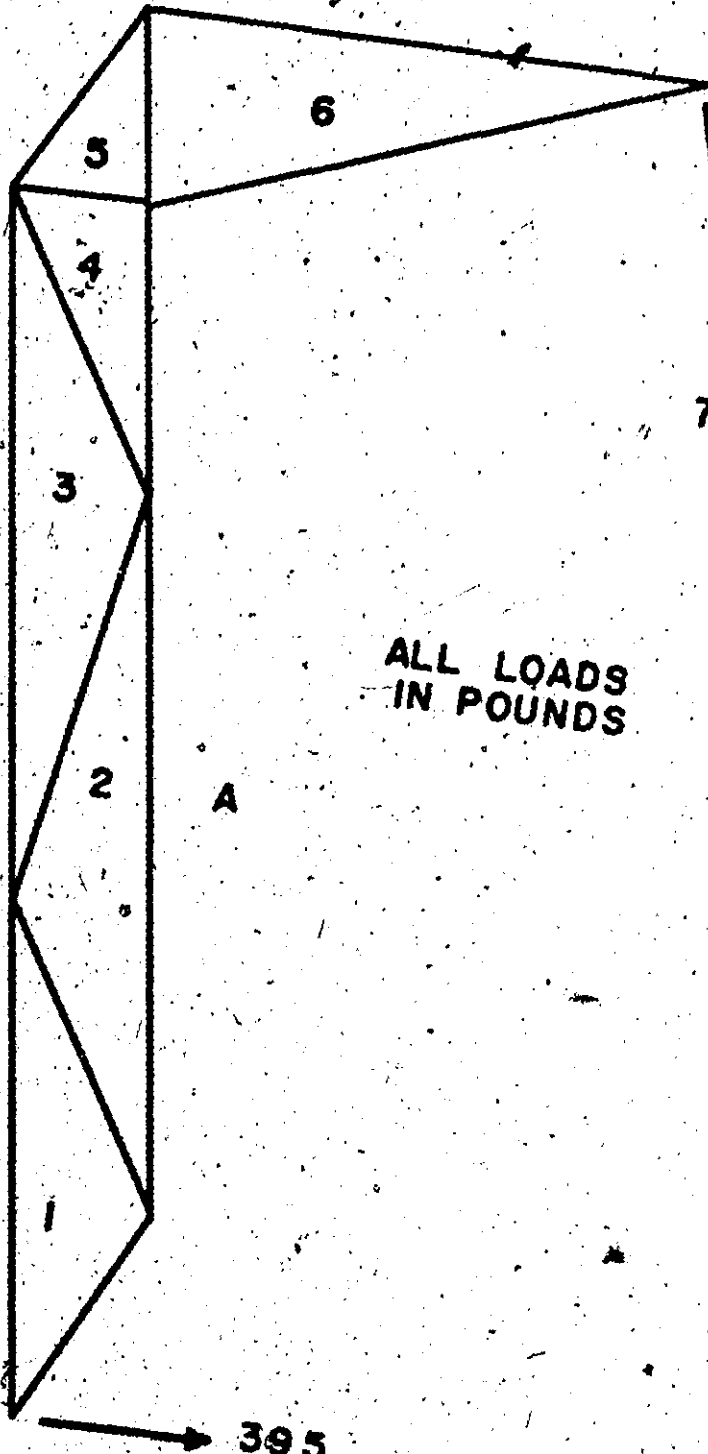
ALL LOADS  
IN POUNDS

C

A

395

Figure 4.16: Gust Loading Right Transverse Structure



SCALE  
1" = 400'

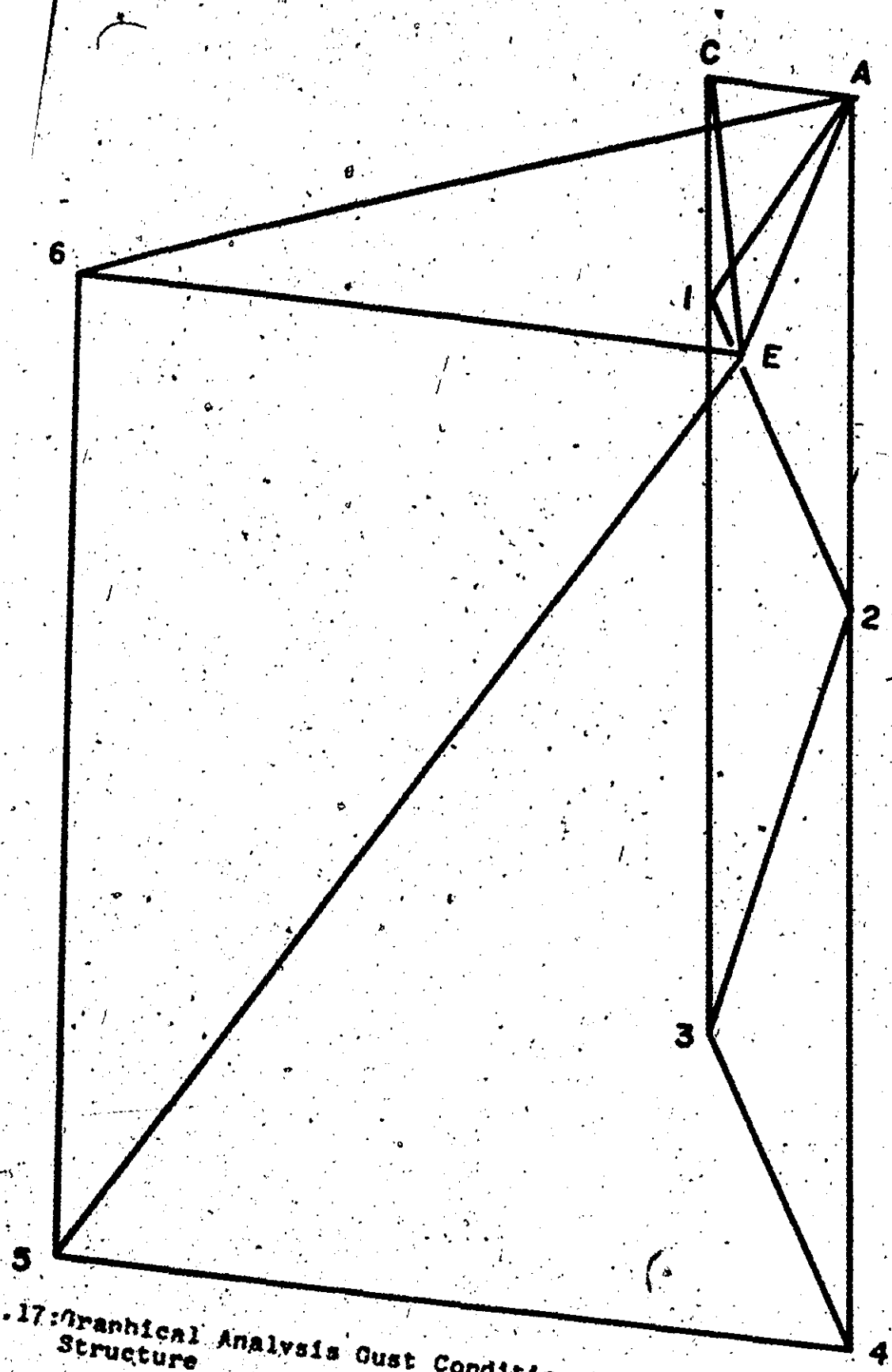


Figure 4.17: Graphical Analysis Gust Condition Left Transverse Structure

SCALE  
1" = 400'

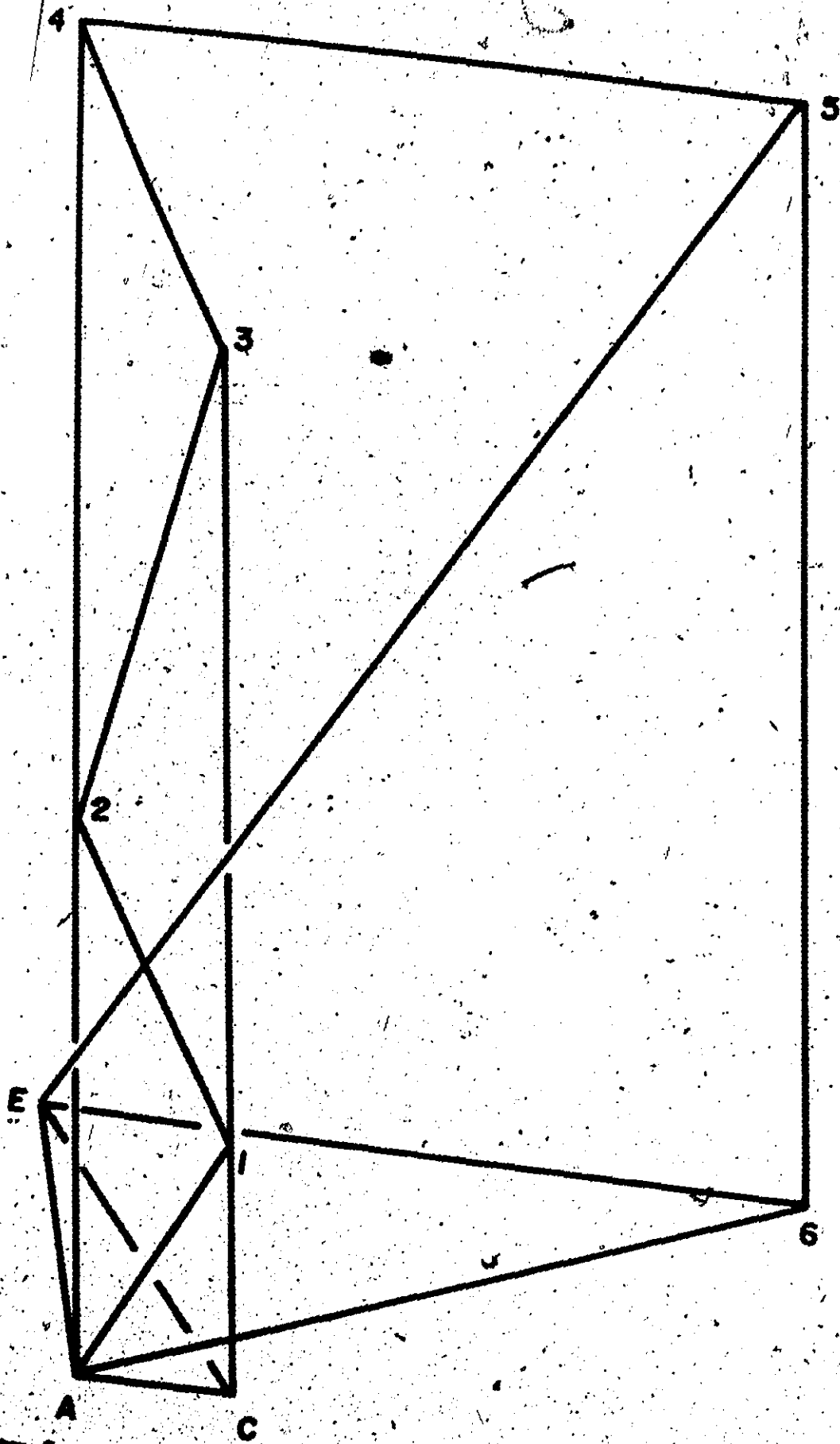


TABLE 4.2(a)

Combined Side Force and Level Condition Loads  
(Ultimate Loads)

Member	Length	Left				Right			
		Side	Dynamic	Total	T C	Side	Dynamic	Total	T C
A1	15	1280T	130C	1150	T	1440	130	1570	C
A2	42.5	2640T	280C	2360	T	2920	280	3200	C
A4	17	6480T	630C	5850	T	7000	630	7630	C
A6	33.5	4160T	240C	3920	T	3840	240	4080	C
C1	30.5	1120C	1720T	600	T	1280	1720	3000	T
C3	42.5	4920C	1880T	3040	C	5400	1880	7280	T
E5	13.5	5840C	630T	5210	C	6400	630	7030	T
E6	33.5	3600C	390T	3210	C	4000	390	4390	T
12	20.5	1760C	180T	1580	C	1920	180	2100	T
23	25	2280T	220C	2060	T	2440	220	2660	C
34	20.5	1760C	160T	1600	C	1920	160	2080	T
45	8.5	4120T	230C	3890	T	3760	230	3990	C
56	11.5	5040T	560C	5480	T	5680	560	6240	C

#### 4.3.1 Basic Case 1

This situation combines the full weight at the center of gravity with full engine thrust and a thirty degree dive. The free body diagram illustrating this situation is shown in Figure 4.20.

The value of  $R_V$  remains as determined in the previous analysis as it cannot resist any couples. An analysis of the vertical forces and the moments about the center of gravity implies that a negative cable force is produced at A. This is unrealistic. The most that can happen is that  $A_V = 0$  which implies that the cable is slack. Assuming  $A_V = 0$ , the following analysis can be performed.

$$\sum F_V = 0 \quad B_V + C_V = 1600$$

$$\sum M_{CG} = 0 \quad 1280 \times 72 = B_V \times 12 - C_V \times 66 = 0$$

The above equations give

$$C_V = 1351 \text{ pounds}$$

$$B_V = 249 \text{ pounds}$$

The loading situation thus produced is illustrated by Figure 4.21 and the idealized situation used to solve for the member loadings is shown by Figure 4.22. This situation is conservative as the real number will have smaller forces than the idealized member. The results for those members to be analysed in this section are presented in Table 4.3.

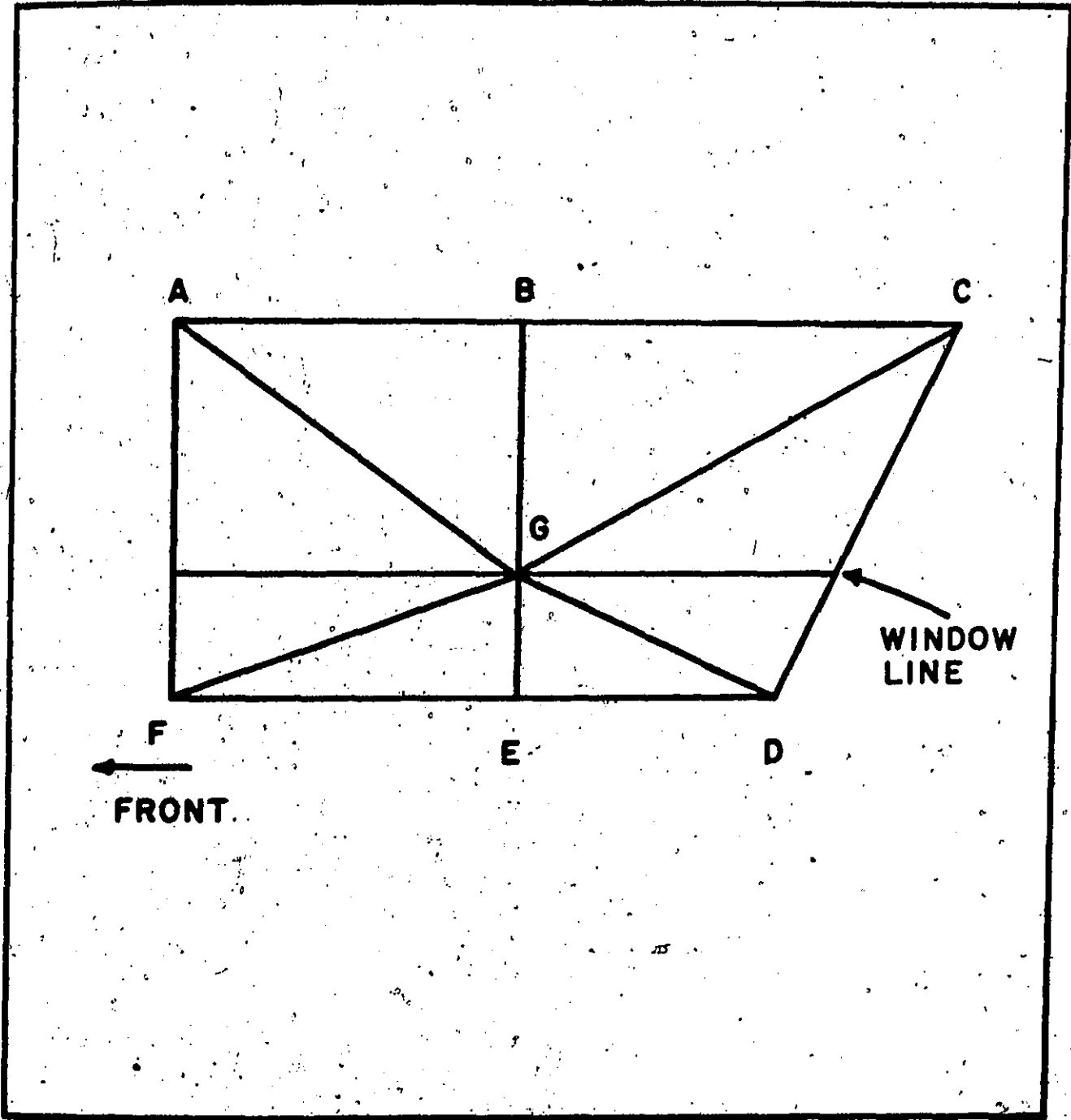


Figure A.19: Upper Side Structure

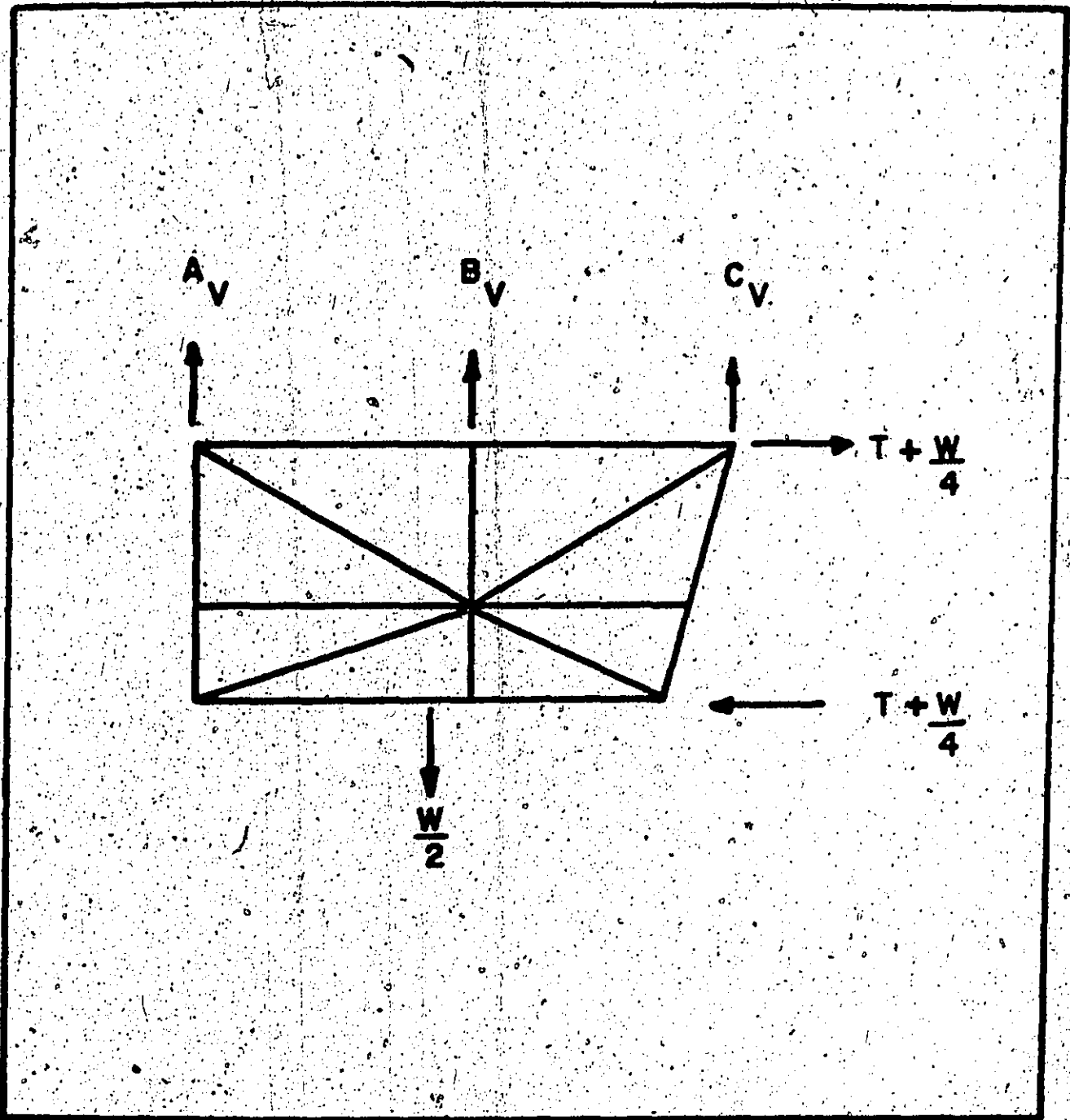


Figure 4.20: Upper Side Structure Loading Situation



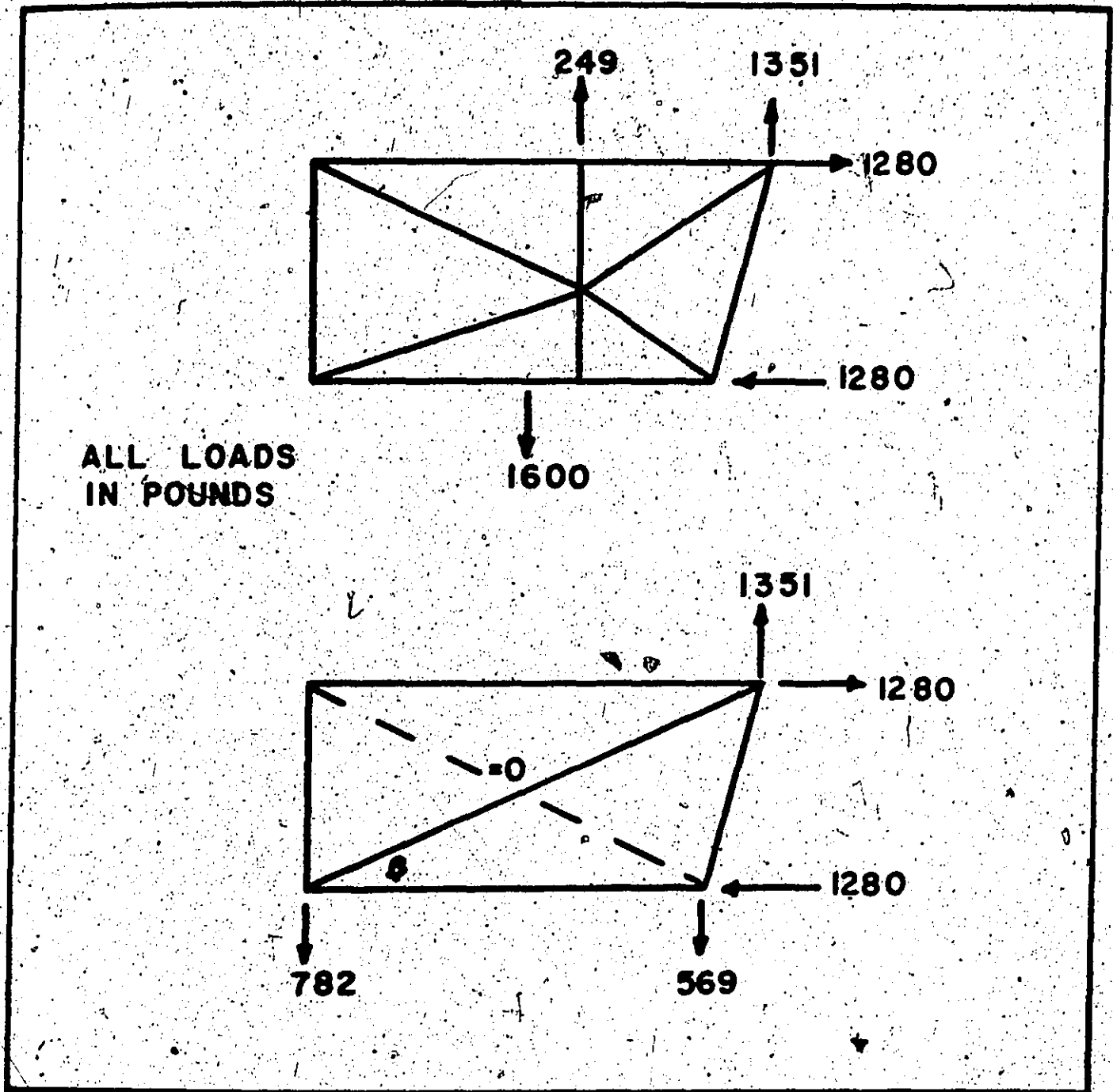


Figure 4.21: Upper Side Structure Actual Loading Basic Case 1

Figure 4.22: Upper Side Structure Idealized Loading Basic Case 1

TABLE 4.3

## Upper Side Structure Loading

Member	Load (lbs.) x 2	T C
AG	1710	T
GD	1710	T
FG	2910	T
GC	2910	T
AJ	1600	T
CK	2560	T

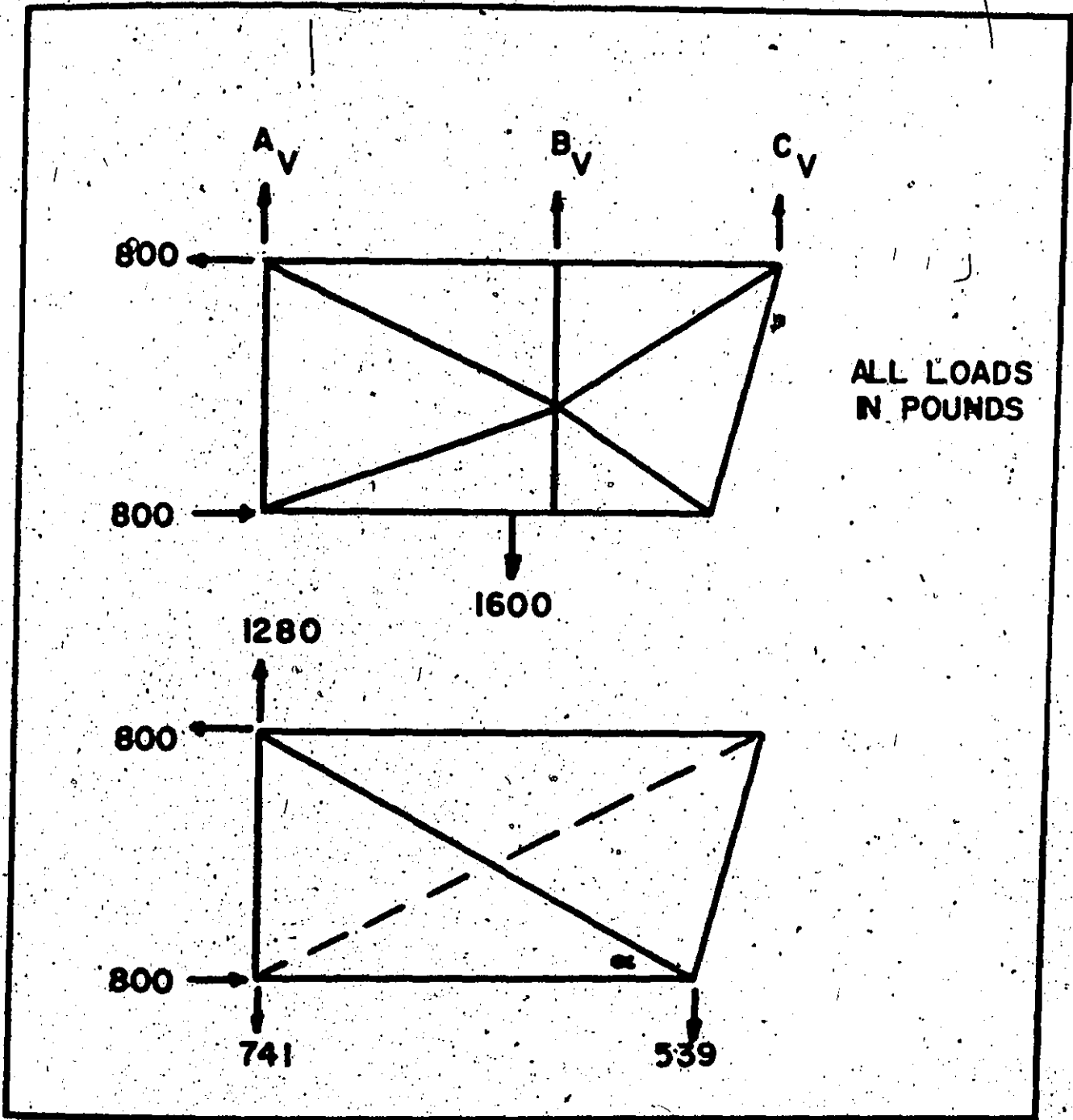


Figure 4.23: Upper Side Structure Actual Loading Basic Case 2

Figure 4.24: Upper Side Structure Idealized Loading Basic Case 2

#### 4.4.2 Basic Case #2

In this case the full weight at the center of gravity is combined with a thirty degree upwards inclination. The free body diagram is illustrated by Figure 4.23. Conditions similar to the previous situation prevail. Again an idealized situation is solved. The loading of this idealization is shown in Figure 4.24. Assuming  $C_V = 0$ , the force and moment analysis can once again be performed.

$$\sum F_V = 0 \quad A_V + B_V = 1600$$

$$\sum M_{CG} = 0 \quad 800 \times 72 + B_V \times 12 - A_V \times 48 = 0$$

The above equations yielded

$$A_V = 1280 \text{ pounds}$$

$$B_V = 320 \text{ pounds}$$

The results for those members to be analysed in this section, are also presented in Table 4.3. Several members shown in Figure 4.19 have no design structural function and are used only for truss integrity. In order to size these members the decision was made to use as much common sized material as possible. Boundary condition loading was used to estimate if the material size was satisfactory.

#### 4.4 Underfloor Structure Loading Analysis

The underfloor structure can be divided into two major segments. One segment consists of a longitudinal truss system as illustrated

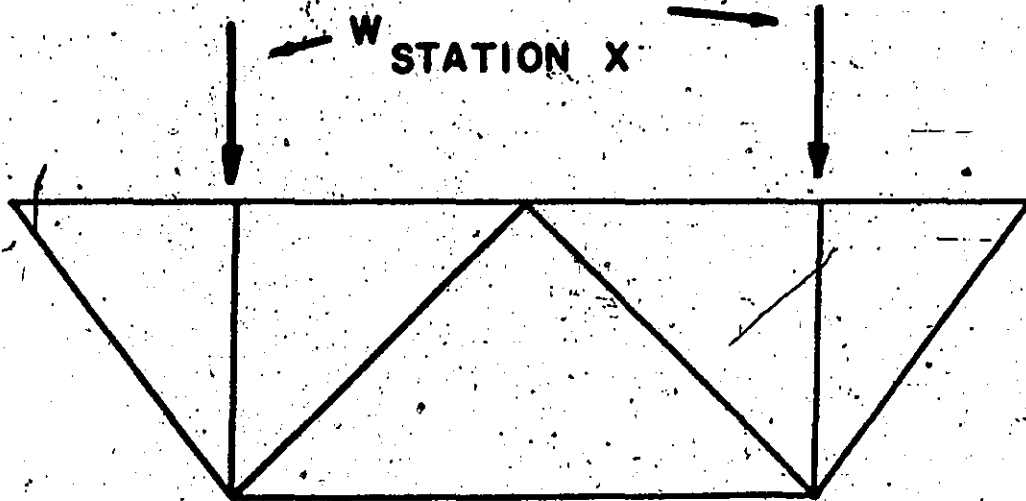


Figure 4.25: Transverse Truss Configuration

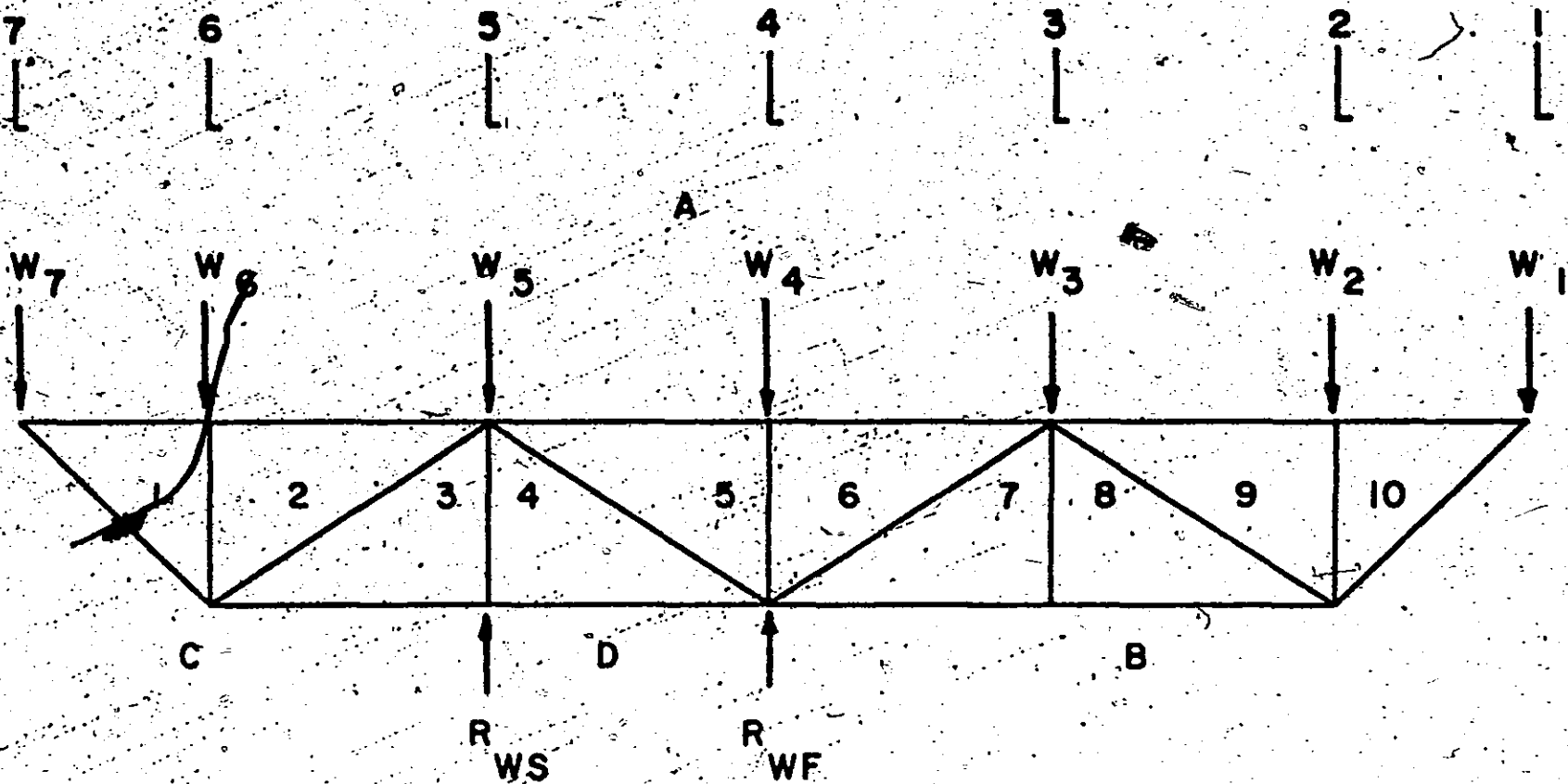


Figure 4.26: Longitudinal Truss Configuration

in Figure 4.25. The second segment is made up of the transverse truss systems that join the longitudinal truss in five positions. The transverse truss configuration is illustrated by Figure 4.25. As previously stated, the longitudinal structure must be examined for three support conditions. The transverse sections must be examined individually as the loading condition of each varies.

#### 4.4.1 Longitudinal Truss Structure Static Condition

Assume that the full weight of the cabin is resting on the landing gear. The design calls for the wheel to be located one foot forward of the horizontal center of gravity position of the cabin. This center of gravity position corresponds to station number five as shown in Figure 4.26. In this configuration, the cabin will maintain a horizontal attitude.

The weight of the cabin and its payload can be split into the weight categories listed in Table 4.4. These weights can now be distributed over the seven stations shown in Figure 4.26. The distribution of the weights is arbitrary as far as the structural and payload weights are concerned. Only the weight of the fuel must be specifically located in such a manner that the center of gravity position previously specified is attained. The location of these weights in relation to the transverse sections is shown by Figure 4.27. The location of the fuel is obtained by means of a moment balance. Table 4.5 gives the arbitrary distribution of the other weights. Using these values the following moment balance was performed.

ALL WEIGHTS IN POUNDS

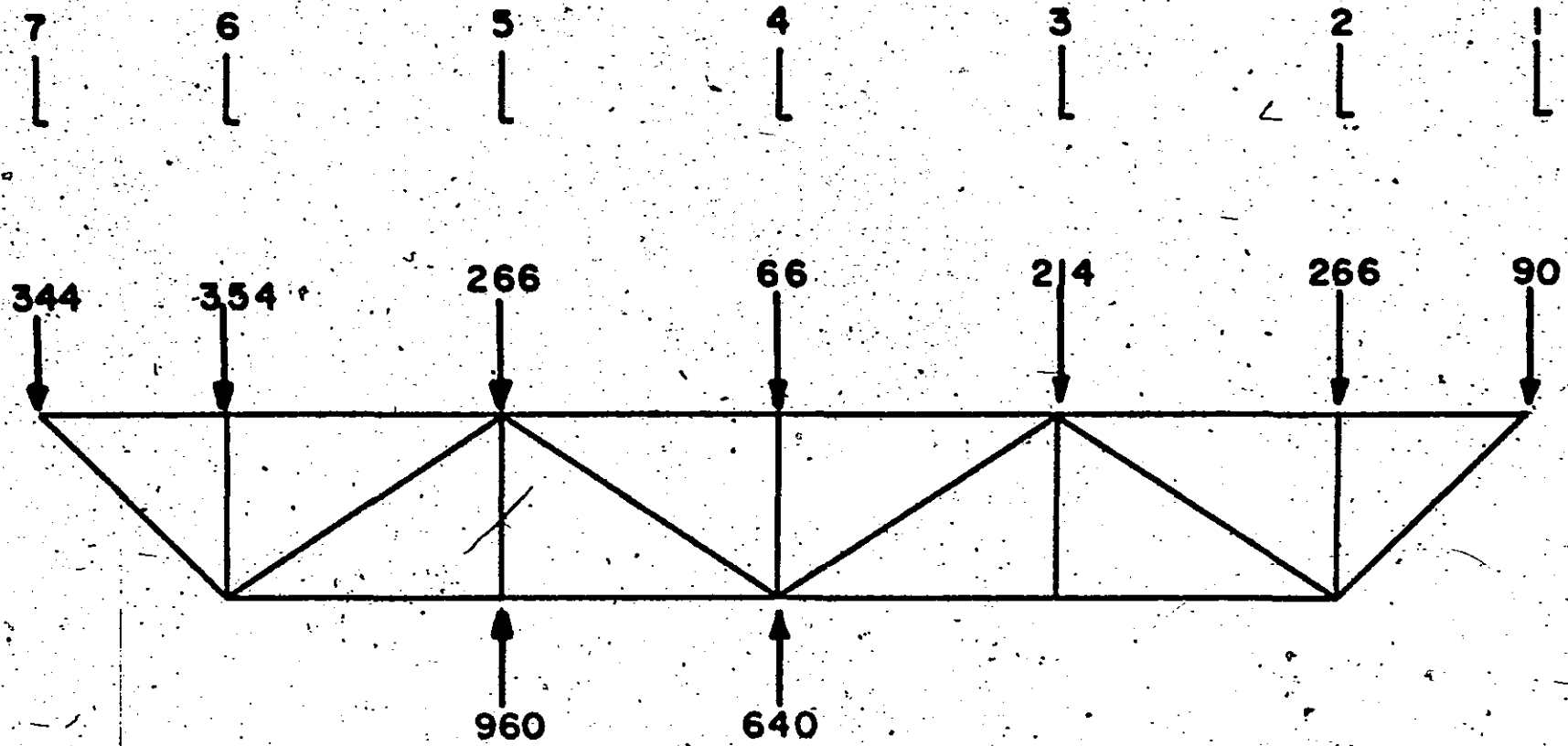


Figure 4.27: Longitudinal Truss Loading



Table 4.4

## Airship Load Distribution

engines	200 pounds per side
outriggers	50
pilots (2)	200
passengers (2)	200
above floor structure	240
below floor structure	160
floor and equipment on floor	300
fuel	<u>250</u>
	1600

TABLE 4.5

## Load Distribution on Underfloor Structure

Category	Weights on Station (lbs.)						
	1	2	3	4	5	6	7
Above floor structure	48		48		48	48	48
Below floor structure	22	23	23	23	23	23	23
Floor & equipment	20	43	43	43	43	65	43
Pilots (2)		200					
Passengers			100			100	
Engines					132	68	
Outriggers					20	30	
Sub Total	90	266	214	66	266	334	114
Fuel (used as Bal. Wt.)						20	230
Total	90	266	214	66	266	354	344

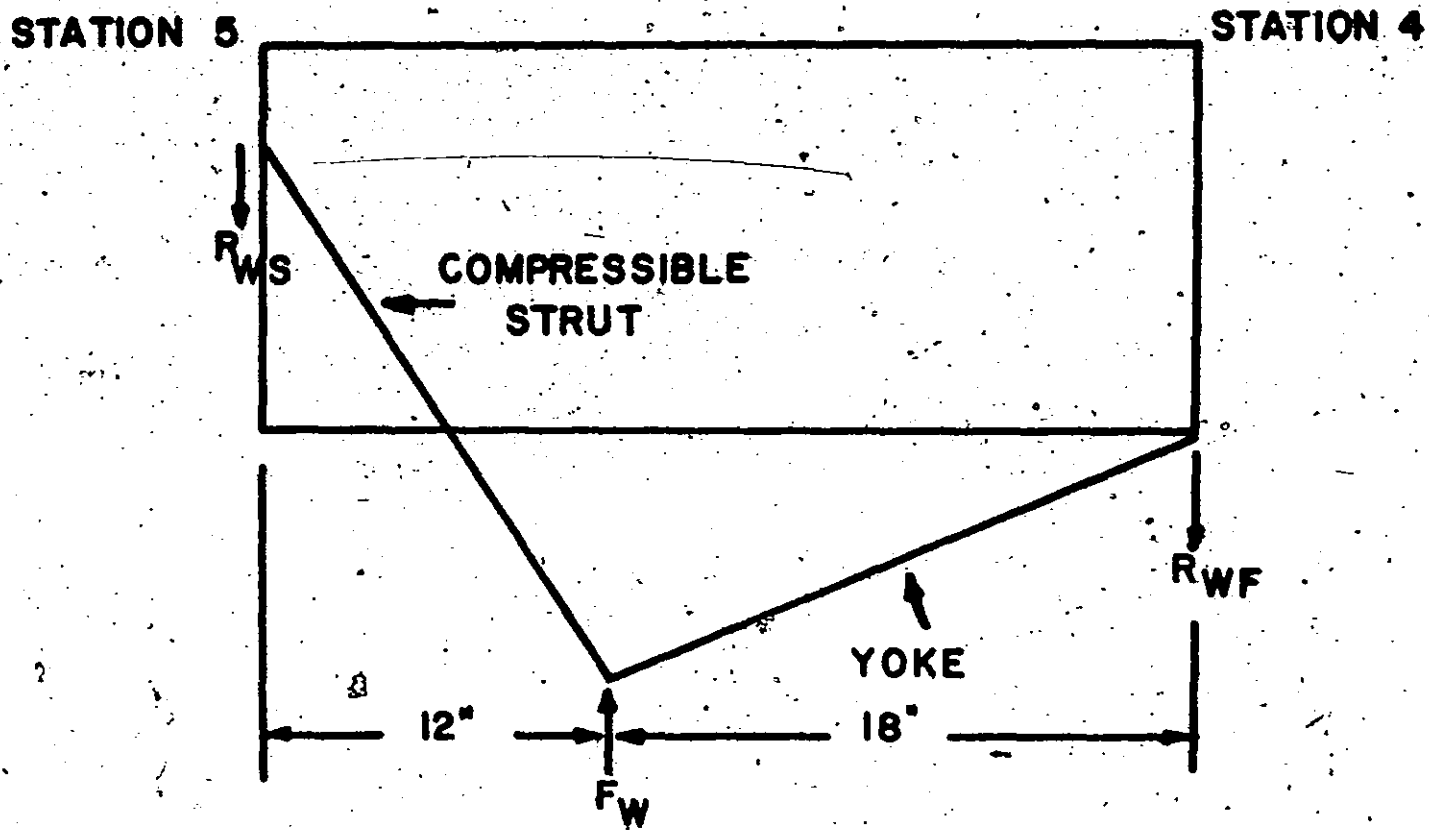


Figure 4.28: Landing Gear Arrangement

$$\therefore IM_{CG} = 0$$

CCW	
90 x 99 =	8910
266 x 78 =	20748
214 x 48 =	10272
66 x 18 =	<u>1188</u>
	41118

CW	
266 x 12 =	3192
344 x 42 =	14028
114 x 67 =	<u>7638</u>
	24858

$$\therefore \text{net moment} = 16260$$

$\therefore$  the fuel weight must be distributed between stations 6 and 7 so as to produce a clockwise moment of 16260.

$\therefore$ 230 x 67 =	15410
20 x 42 =	<u>840</u>
	16250

$\therefore$  at station 6 add 20 pounds  
at station 7 add 230 pounds

The total weight acting at each station after the fuel weight allocation is also given in Table 4.5. The landing gear arrangement is illustrated by Figure 4.28. It should be noted that not all the weights shown act in the vertical sense in reality and hence some of the stations have a horizontal component of force. These, however, are small and have thus been ignored. The reaction forces that the landing gear applies at stations 4 and 5, can now be obtained.

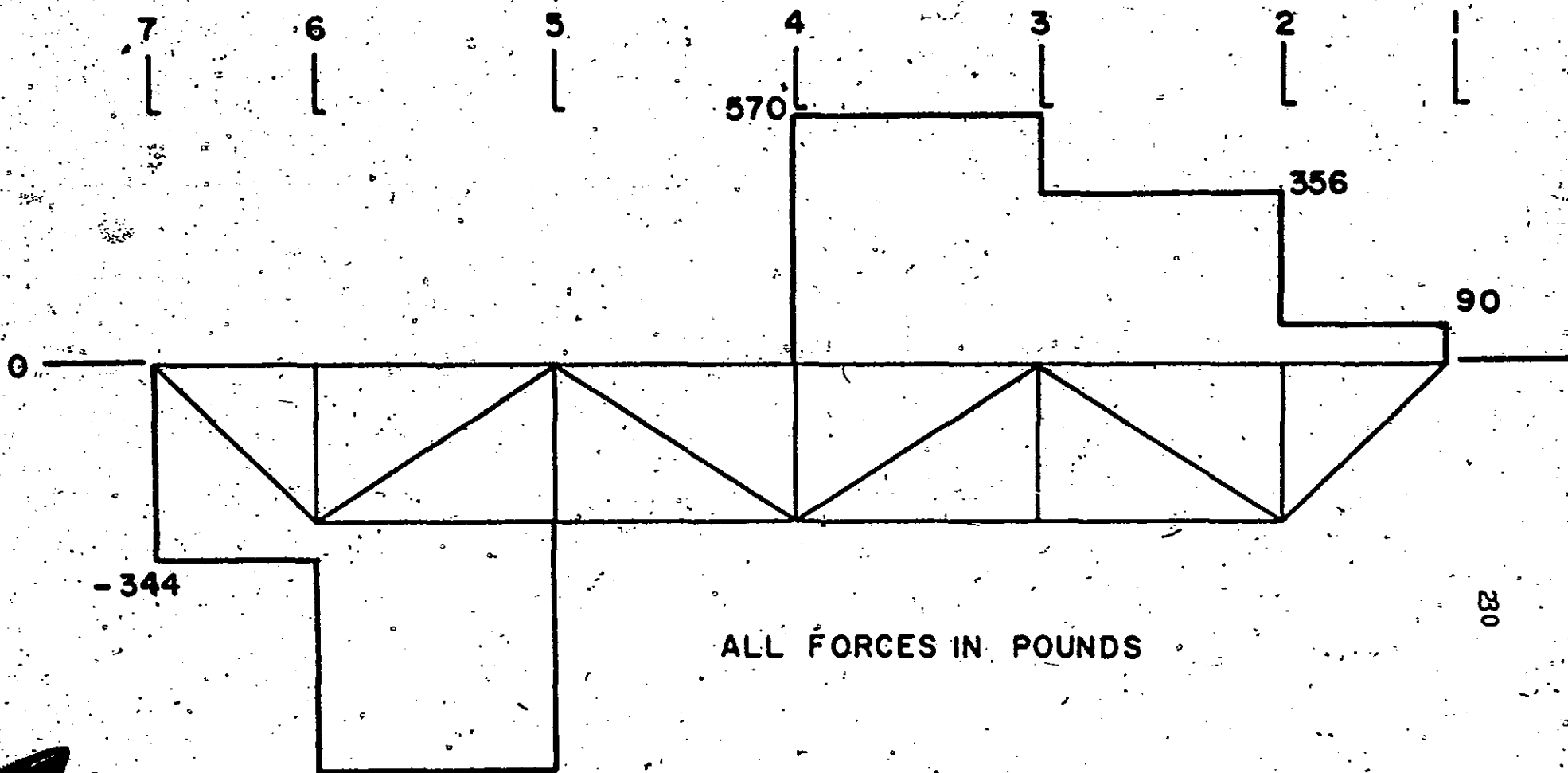
Referring to Figure 4.28 a force and moment balance must be obtained.

$$\sum F_y = 0$$

and  $\sum M_{PW} = 0$

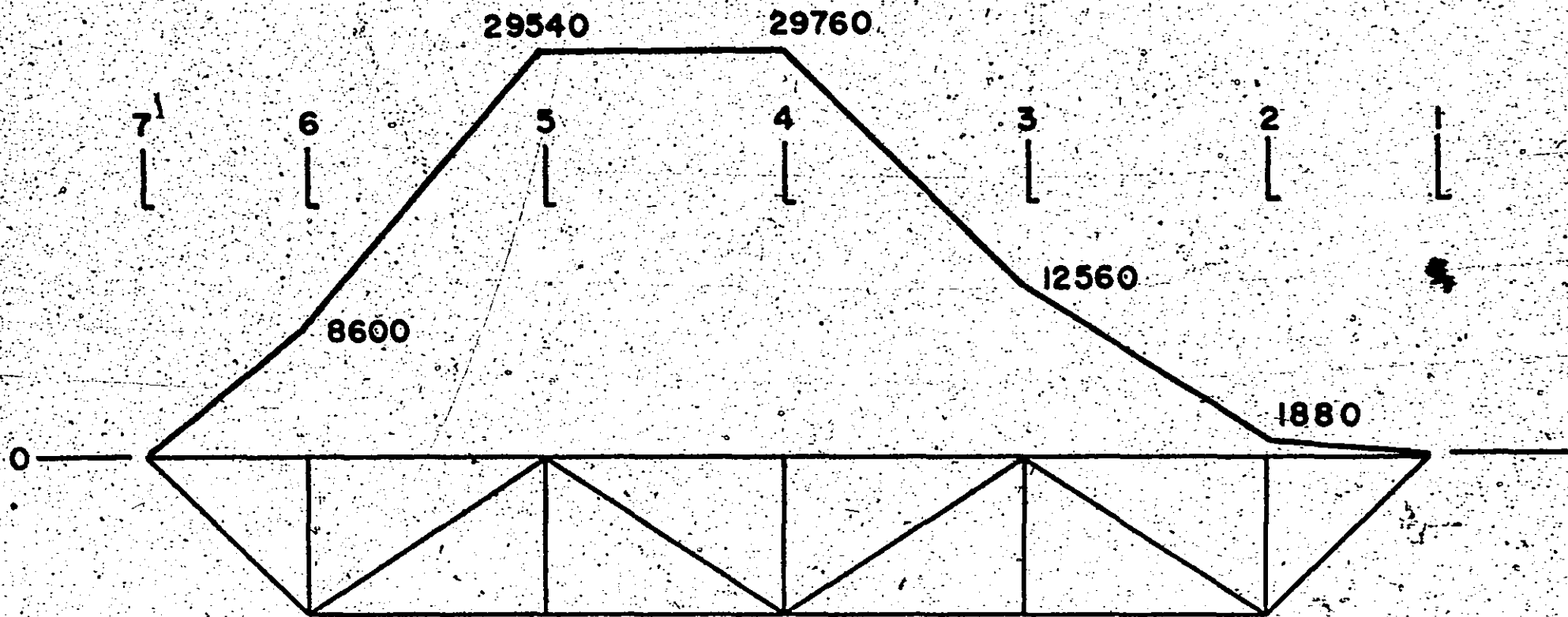
$$R_{WS} + R_{WP} = P_W$$

$$R_{WS} \times 12 - R_{WP} \times 18 = 0$$



ALL FORCES IN POUNDS

Figure 4.29: Shear Force Diagram (Normal)



ALL MOMENTS IN INCH POUNDS

Figure 4.30: Bending Moment Diagram (Normal)

Solution of these relationships gives values of:

$$R_{WS} = 0.6 P_W = 960 \text{ pounds}$$

$$R_{WP} = 0.4 P_W = 640 \text{ pounds}$$

Combining these values with the loads imposed on each station, a shear force diagram, as illustrated by Figure 4.29, may be attained. The bending moment, in inch pounds, at any point along the structure may be described by:

$$\begin{aligned} M = & 344x + 354(x-25) + 266(x-55) \\ & - 960(x-55) + 66(x-85) - 640(x-85) \\ & + 214(x-115) + 266(x-145) + 90(x-166) \end{aligned}$$

where  $x$  is the distance of the load from the longitudinal center of gravity position and if  $(x-y) < 0$  then  $(x-y) = 0$ .

The resulting bending moment diagram is described by Figure 4.30. Using the bending moment diagram and the shear force diagram the loads on the members may be determined. These loads are given in Table 4.6. Note that a safety factor of two has been incorporated when moving from the static load to the design load. This exceeds the safety factor of 1.5 that is specified in the airworthiness requirements [3].

#### 4.4.2 Longitudinal Truss Structure Static Castored Condition

For purposes of ground movement when not attached to the envelope, the cabin is fitted with removable castors at stations 2 and 6. Retaining the loadings as given in the previous analysis then the reactions at the castors can be calculated by means of a force and moment balance to be

## Longitudinal Underfloor Structure Static Loading

Member	Length (inches)	Static Load (lbs.)	Design Load (lbs.)	T C
A1	25	478	956	T
A2	30	478	956	T
A5	30	1640	3280	T
A6	30	1640	3280	T
A9	30	105	210	T
A10	21	105	210	T
B10	34	139	278	C
B8	30	698	1396	C
B7	30	698	1396	C
D4	30	1640	3280	C
C3	30	1640	3280	C
C1	35	590	1180	C
12	18	354	708	C
23	45	1745	3490	T
34	18	960	1920	C
45	45	0		
56	18	66	132	C
67	45	1425	2850	C
78	18	0		
89	45	890	1780	T
910	18	266	532	C



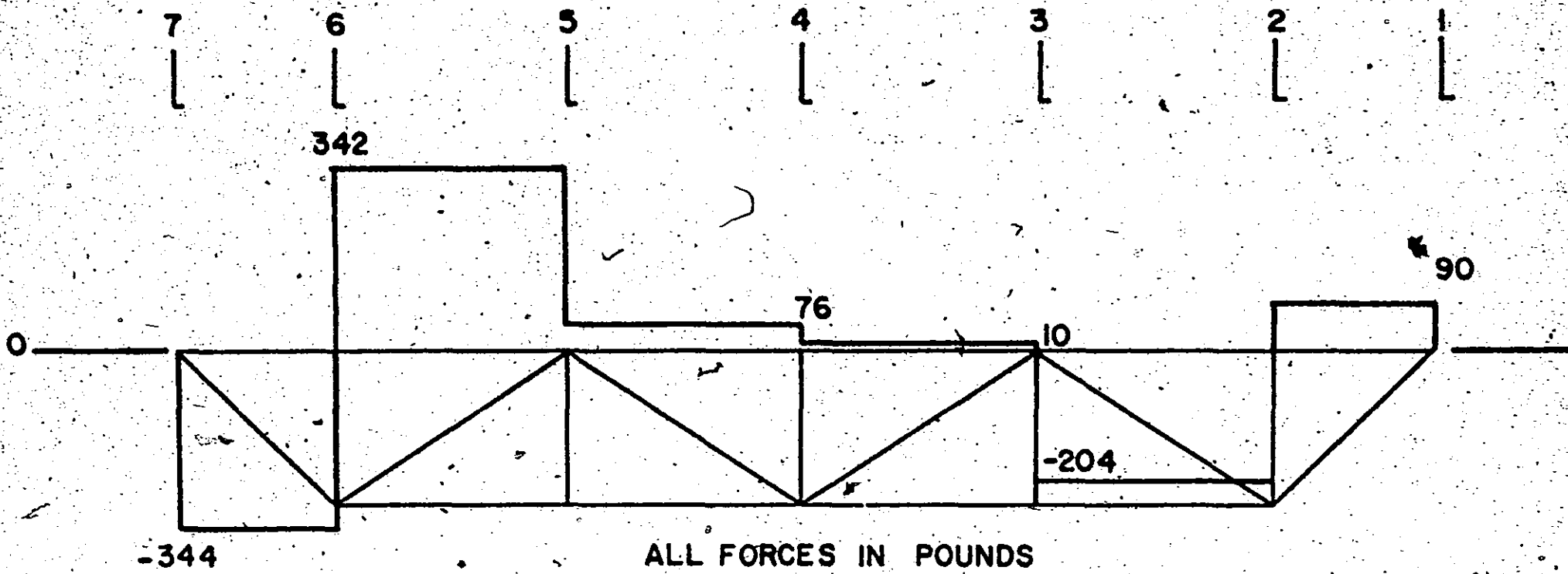
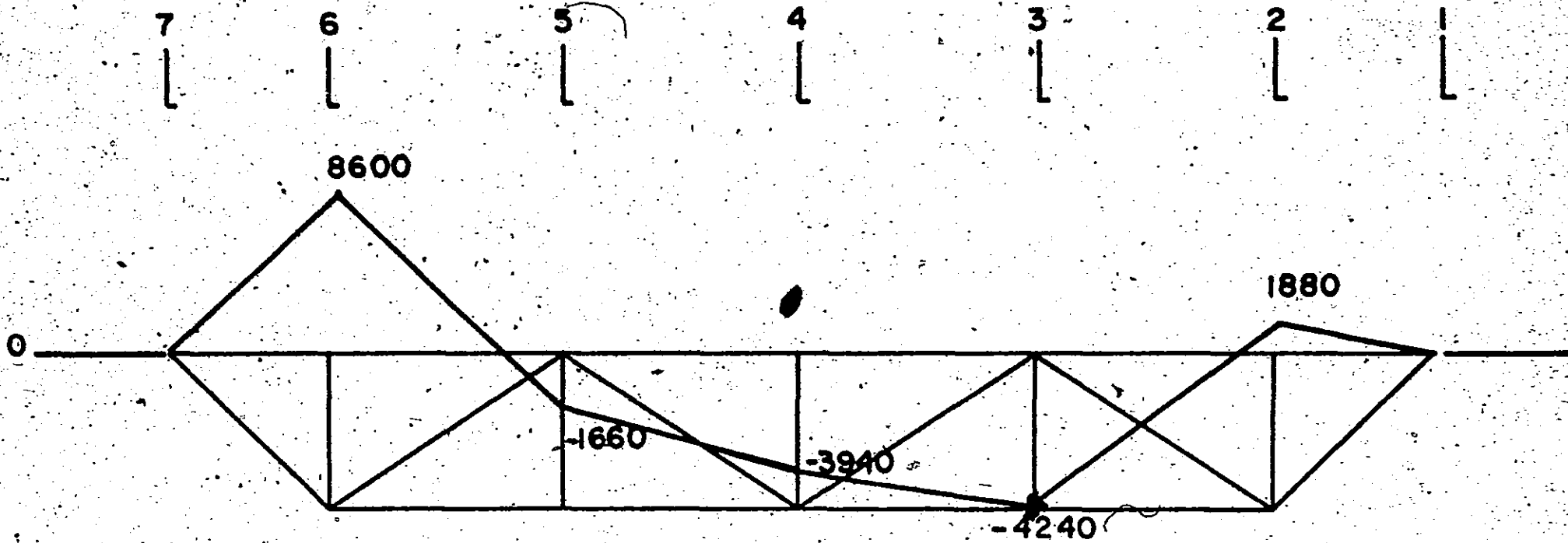


Figure 4.31: Shear Force Diagram (Castored)



ALL MOMENTS IN INCH POUNDS

Figure 4.32: Bending Moment Diagram (Castored)

$$R_2 = 560 \text{ pounds}$$

and  $R_6 = 1040 \text{ pounds}$

The shear force diagram for the loading condition is shown by Figure 4.31. Once again the bending moment at any point along the length is given by

$$\begin{aligned} M = & 344x + 354(x-25) - 1040(x-25) + 266(x-55) \\ & + 66(x-85) + 214(x-115) + 266(x-145) - 560(x-145) \\ & + 90(x-166) \end{aligned}$$

where the same conditions apply as in the previous moment expression. The result of this expression is given by Figure 4.32.

The loading of the members, as calculated from the shear force and moment values, is given in Table 4.7.

#### 4.4.3. Longitudinal Truss Structure Dynamic Condition

The case of the dynamic loading due to landing at some sink rate can be considered by assuming that the wheel force at this sink rate would be some multiple of the static wheel force. If a multiple of two is chosen, then the wheel force,  $F_w$ , would be equal to 6400 pounds. The sink rate necessary to achieve this loading can be calculated using the following expressions.

$$\delta_{\max} = \delta_w + \delta_s \quad (4.4)$$

$$F_w = k \delta_{\max} \quad (4.5)$$

$$\text{K.E.} = 1/2(w/r)v^2 \quad (4.6)$$

and  $E.A. = 1/2k \delta_{\max}^2 \quad (4.7)$

TABLE 4.7  
 Longitudinal Underfloor Structure Static Loading  
 (on castors)

Member	Load	Design Load	T C	Section A Design Load	T C
A1	478	956	F	956	T
A2	478	956	C	956	T
A5	219	438	F	3280	T
A6	219	438	C	3280	T
A9	105	210	F	210	T
A10	105	210	T	210	T
B10	139	278	C	278	C
B8	235	470	F	1396	C
B7	235	470	F	1396	C
D4	92	184	T	3280	C
C3	92	184	C	3280	C
C1	590	1180	C	1180	C
12	354	708	C	708	C
23	855	1710	C	3490	F
34	0		C	1920	C
45	190	380	F		C
56	66	132	C	132	C
67	25	50	C	2850	C
78	0				
89	510	1020	C	1780	F
910	266	532	C	532	C

where

$\delta_w$  = the deflection possible in the landing gear wheel  
in inches

$\delta_s$  = the deflection possible in the strut in inches

K.E. = the kinetic energy of the system

E.A. = the energy that the system can absorb

Substituting from (4.4) for  $k$  in (4.7) and equating  
(4.6) and (4.7) gives

$$v = \frac{P_w \times g \times \delta_{max}}{W} \quad (4.8)$$

where

$g$  = the gravitational constant

$W$  = the weight of the cabin

For our design

$W = 3200$  pounds

$g = 32$

$\delta_w = 1$  inch

$\delta_s = 9$  inches

and  $P_w = 6400$  pounds

This gives a value of the sink rate upon substitution  
in (4.8) for a multiple of two, of 7.3 ft/sec. The government  
airworthiness requirements [3] specify a design sink rate of  
"not less than 3 ft/sec". Clearly a multiple of two times  
the static main wheel condition is satisfactory for this  
design purpose. Table 4.8 gives the dynamic loading and the  
dynamic design load of each member. The dynamic design load  
incorporates the previously stated safety factor of two.

Longitudinal Underfloor Structure Dynamic Loading

Member	Design Load A	T C	Design Load B	T C	Dynamic Load Design	T C
A1	956	T	956	T	1912	T
A2	956	T	956	T	1912	T
A5	3280	T	438	C	6560	T
A6	3280	T	438	C	6560	T
A9	210	T	210	T	420	T
A10	210	T	210	T	420	T
B10	278	C	278	C	556	C
B8	1396	C	470	T	2792	C
B7	1396	C	470	T	2792	C
D4	3280	C	184	T	6560	C
C3	3280	C	184	C	6560	C
C1	1180	C	1180	C	2360	C
12	708	C	708	C	1416	C
23	3490	T	1710	C	6980	T
34	1920	C	0	C	3840	C
45	0	C	380	T	0	C
56	132	C	132	C	264	C
67	2850	C	50	C	5700	C
78	0	C	0	C	0	C
89	1780	T	1020	C	3560	T
910	532	C	532	C	1064	C

A comparison of the values for the design loads of the members as given by Table 4.6, Table 4.7 and Table 4.8 respectively shows that the design loads to be used for the side truss members are those of Table 4.8

#### 4.4.4 Underfloor Structure Transverse Sections

The underfloor structure consists of two longitudinal truss systems joined by transverse sections at stations 2, 3, 4, 5, and 6. These five sections can be separated into three distinct groups having different design loading conditions.

##### (i) Sections at stations 5 and 6

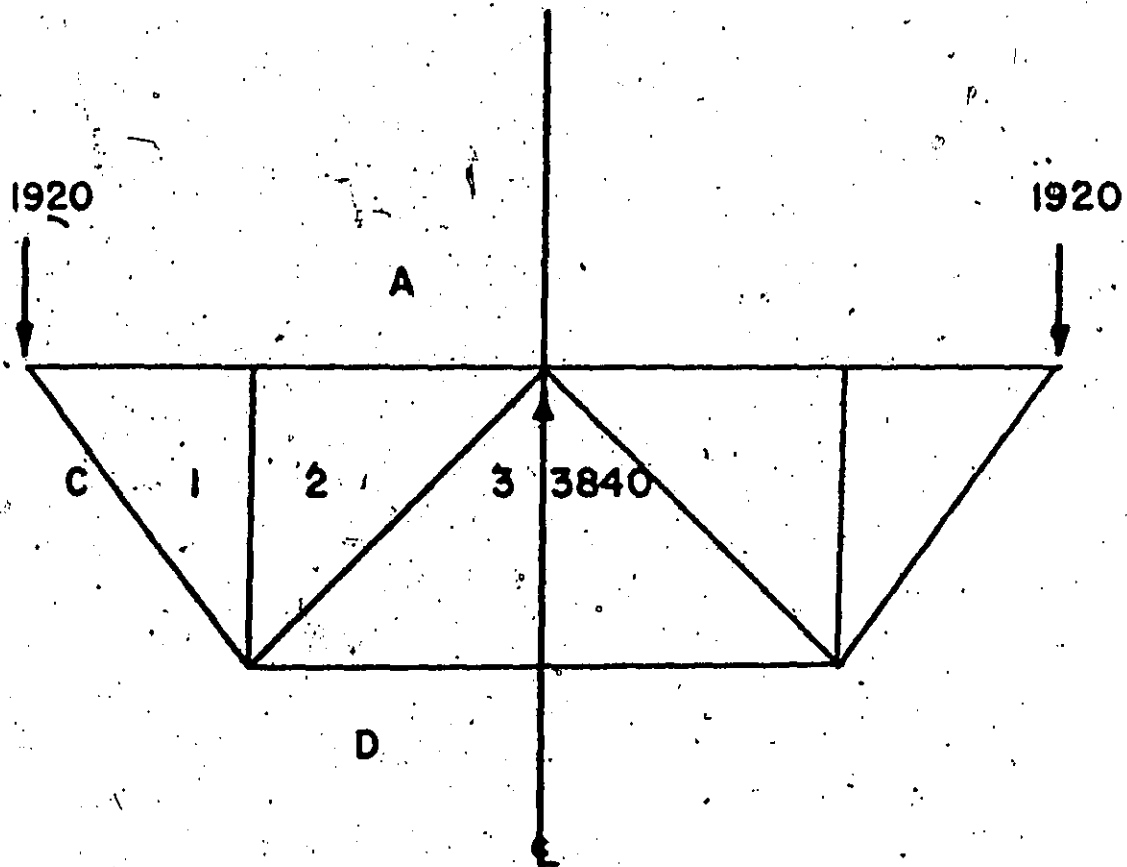
Station 5 contains the rear landing gear attachment and hence must withstand the dynamic landing situation. Station 6 must also withstand heavy loads carried over from station 5. Therefore, the same loading will be assumed in both sections. If  $P_W = 6400$  then the loading of these stations is

$$R_{WS} = 0.6 P_W = 3840 \text{ pounds}$$

distributed as illustrated in Figure 4.33. The graphical analysis used to solve for the member loads, given in Table 4.9, is illustrated by Figure 4.34.

##### (ii) Sections at stations 4 and 3

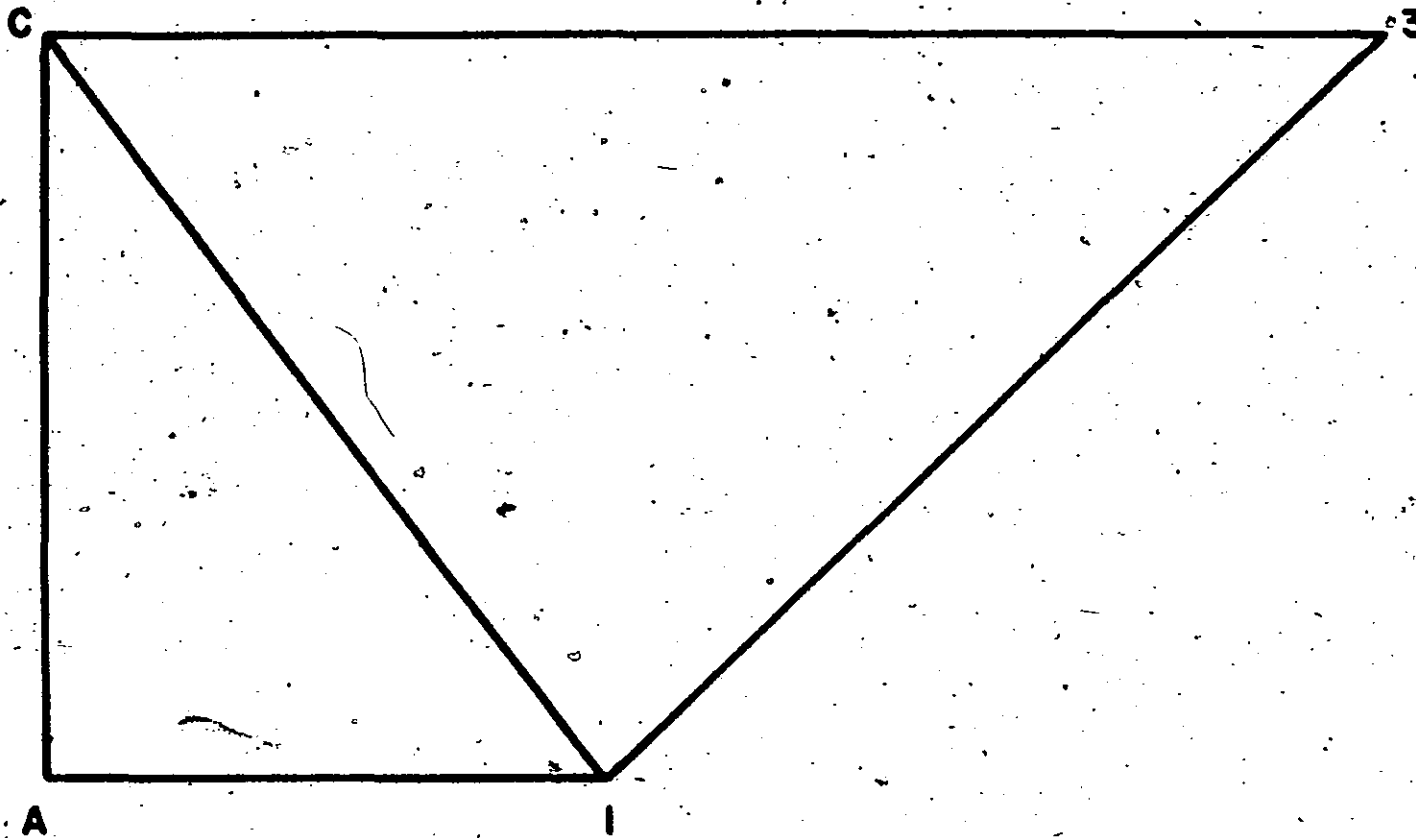
Station 4 contains the forward landing gear attachment and thus the loading of this section, and also section 3, for the reasons expressed previously, is dictated by the dynamic landing condition.



ALL FORCES IN POUNDS

Figure 4,33: Transverse Section Loading.





SCALE 1" = 500'

Figure 4.34: Graphical Analysis of Transverse Section

TABLE 4.9

## Transverse Section Loads

Member	Length	Load	Design Load	T C
A1	13.5	1425	2850	T
A2	18	1425	2850	T
A4	18	1425	2850	T
A5	13.5	1425	2850	T
B5	22.5	2405	4810	C
C1	22.5	2405	4810	C
D3	36	3345	6690	C
12	18			
23	25	2700	5400	T
34	25	2700	5400	T
45	18			
A1	13.5	425	850	T
A2	18	425	850	T
A4	18	425	850	T
A5	13.5	425	850	T
B5	22.5	715	1430	C
C3	36.0	425	850	C
D1	22.5	715	1430	C
12	18			
23	25	0		
34	25	0		
45	18			
A1	13.5	970	1940	T
A2	18.0	970	1940	T
A4	18.0	970	1940	T
A5	13.5	970	1940	T
B5	22.5	1630	3260	C
C3	36.0	970	1940	C
D1	22.5	1630	3260	C
12	18			
23	25	0		
34	25	0		
45	18			

$$R_{WP} = 0.4 P_W = 2560 \text{ pounds}$$

As the configuration is the same in all the transverse sections, the member loads are just a multiple of those attained in (1). These member loads are also given in Table 4.9.

(iii) Section at station 2

The maximum loading situation at station 2 is dictated by the condition of the cabin resting on castors. This loading has previously been determined as

$$R_2 = 560 \text{ pounds}$$

Hence the member loads are again a multiple of (1) and are also given in Table 4.9.

#### 4.5 Summary

The loading which each member of the structure is subjected to, has been determined and tabulated in Tables 4.2, 4.3, 4.8, and 4.9. These loads are for the most part determined in an extremely conservative manner and use a safety factor higher than specified. Hence any inaccuracies due to assumptions made in the analysis should not prove serious. The loading as tabulated, was used to determine structural member sizes for the construction of the cabin. This construction has been completed and the structure as built is illustrated by Figures 4.35 through 4.36. The calculated structural weight for the members, as per the loading requirements, was 280 pounds and the actual final weight as constructed was 316

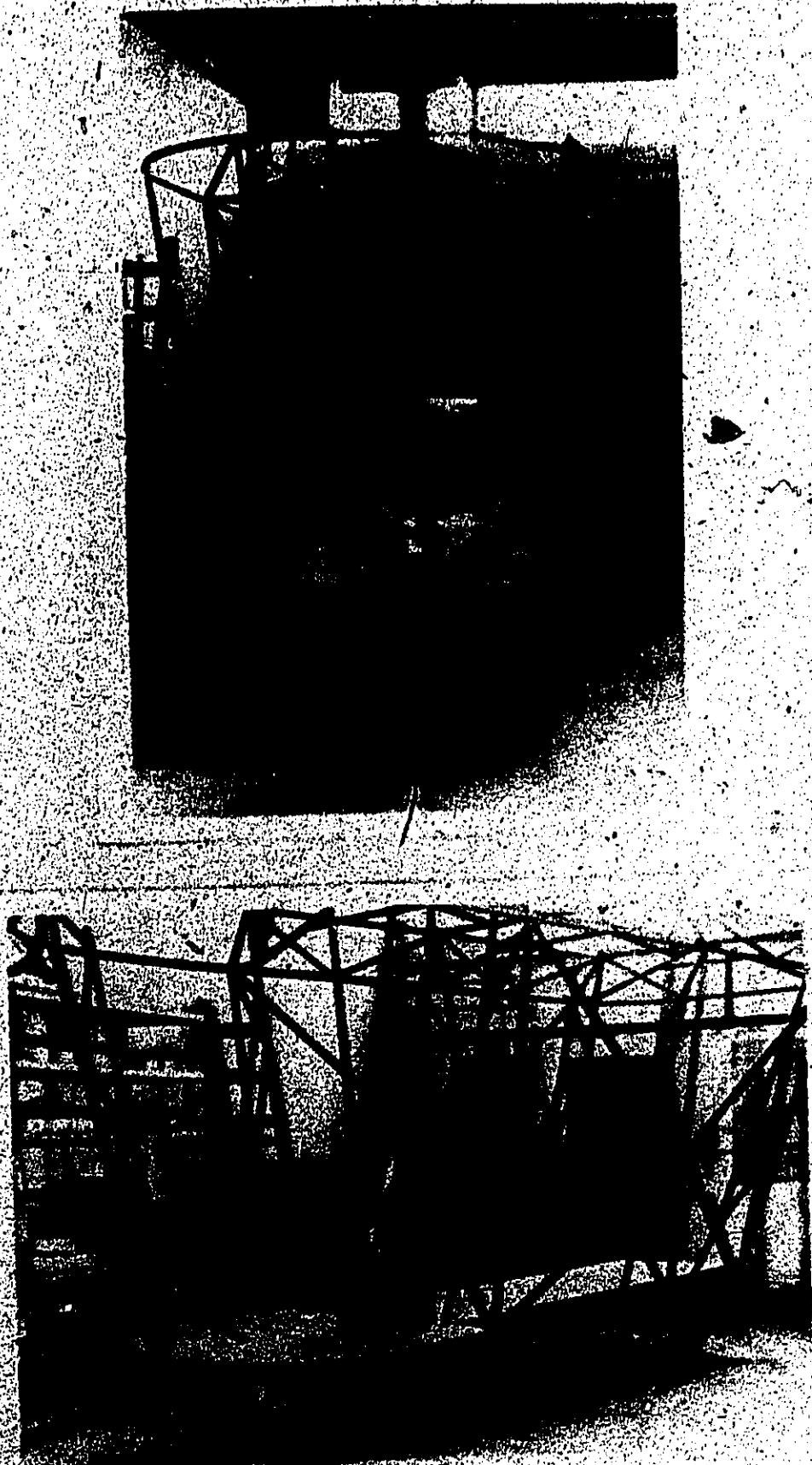


Figure 4.35: Cabin Structure as Completed

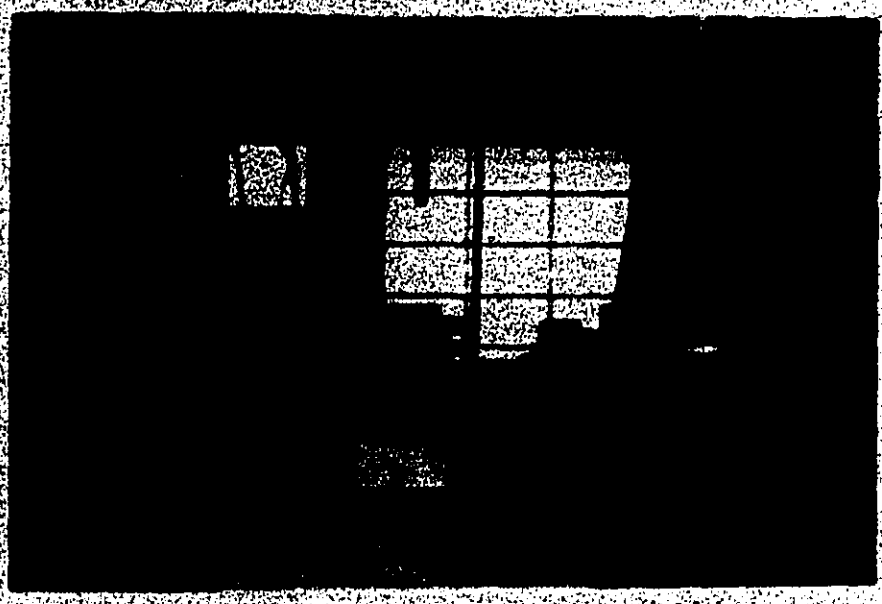
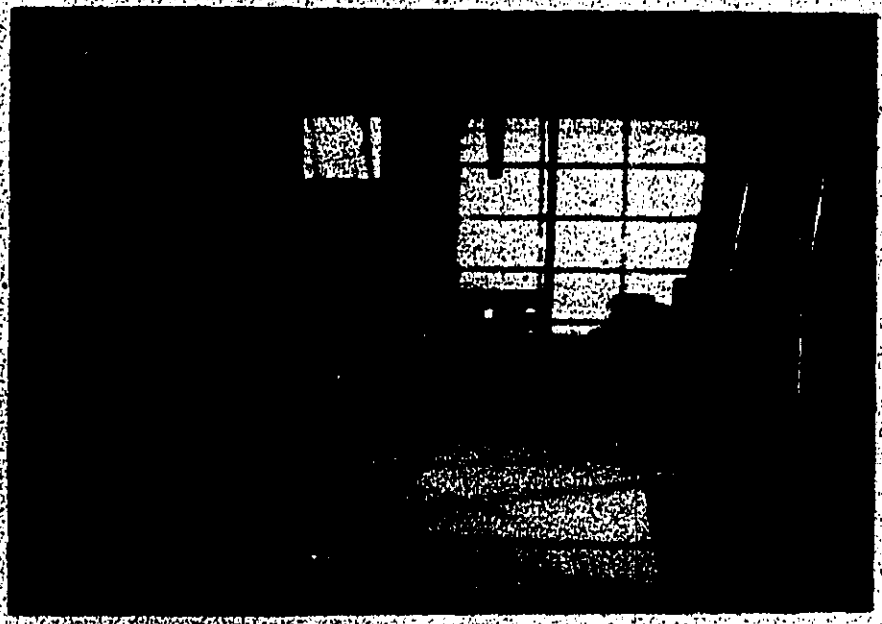
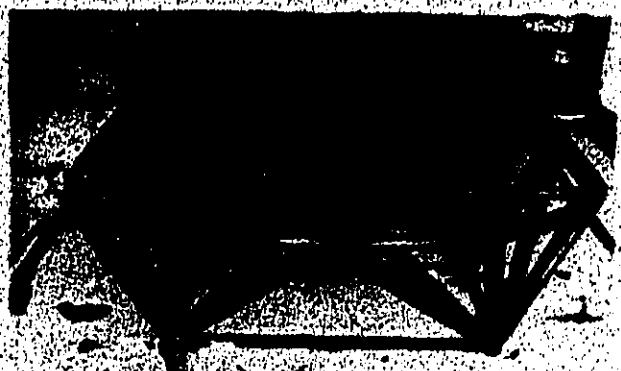


Figure 4.36: Cabin Structure During Construction

pounds. This weight increase is mainly due to inclusion of several members for non-structural (i.e. shaping of exterior) purposes.

It is anticipated that operating experience will lead to some simplification of the cabin structure.

## CHAPTER 5

## Conclusions

This work has examined several aspects of airship design. The areas covered include:

## (A) Preliminary Design Evaluation

- (i) shape
- (ii) aerodynamics
- (iii) structural considerations
- (iv) pressure distribution

## (B) Trajectory and Inflight Load Determination

## (C) Gondola Structural Design.

The first two categories involved computer aided design and user oriented design packages have been developed.

The results achieved in the gondola structural design have been used to construct the actual gondola for CAS-1, an airship under construction by the Canadian Airship Development Corporation. Output from the computer design packages has been used to establish the design parameters for CAS-1 and the trajectory results can be used in the compliance report required by the Ministry of Transport. The output from the trajectory program will also be used to check the results of a highly theoretical mathematical model now being developed by the University of Toronto to analyse various aerodynamic effects.

Much work remains to be done in the airship field before it as a transportation system reaches a technological level equal to that having been obtained by other transportation systems.

Areas of immediate importance include:

- (1) aerodynamics. Any improvement in the manouverability of the airship would be greatly welcomed.
- (2) trim and ballast systems. Improvements are necessary in this area in order to achieve an efficient transportation system.
- (3) propulsion systems.
- (4) cargo handling systems.
- (5) avionics systems.

It is hoped that this work will be the first of many in this field and that the airship revival effort will continue and grow.



APPENDIX A  
PROGRAMME FOR ENVELOPE SHAPES























PROGRAM T (INPUT, OUTPUT, PLOT, TAPE, INPUT, TAPE, OUTPUT, TAPE, PLOT)  
A 2551  
A 2552  
A 2553  
A 2556

71

CALL PAPA0  
CONTINUE  
CONTINUE  
STOP  
PAP0

50

APPENDIX B

PROGRAMME FOR BODY DEPENDENT PARAMETERS





115

CALCULATION OF THE CENTER OF BUOYANCY

120

$$CBX = (2.0 * XN(II) + 1.0) / (2.0 * XN(II) + 2.0 * XM(III) + 2.0) * XL$$

125

CALCULATION OF THE ENVELOPE SURFACE AREA

$$\begin{aligned} YX &= XN(II) + 1.0 \\ YX &= XM(III) + 1.0 \\ ZX &= XN(II) + XM(III) * 2.0 \end{aligned}$$

130

CALL GAMMA (XY, XG, IER)  
CALL GAMMA (YA, XT, IER)  
CALL GAMMA (ZA, XS, IER)

$$ZY = (XG * XT) / XS$$

135

$$ESA = (3.14 * (XN(II) * XN(III)) * (XN(II) * XM(III))) / (F(II) * XN(II) * XN(III) * XM(III) * ZY * XL ** 2)$$

140

CALCULATION OF THE ENVELOPE CENTER OF GRAVITY

$$CGEX = (XN(II) + 1.0) / (XN(II) + XM(III) * 2.0) * XL$$

145

CALCULATION OF THE HOGGING BENDING MOMENT

$$\begin{aligned} R &= XL / (2.0 * F(II)) \\ H &= 2.0 * R \\ BMH &= 0.063 * 3.14 * R ** 3 * H / 4.0 \end{aligned}$$

150

CALCULATION OF THE AERODYNAMIC BENDING MOMENT

$$BMA = 0.01 * RGE * VEL ** 2 * VOL * 0.67 * XL$$

160

CALCULATION OF THE INTERNAL PRESSURE REQUIRED

$$PINT = BMA * 2.0 / (3.14 * R ** 3)$$

165

CALCULATION OF THE CONTROL SURFACES

FIXED HORIZONTAL SURFACE AREA

170





230

A  
S  
C

```

FORMAT (1H1.1X.0 N HMA M PINT XL DPAG E. AREA
1E. CG CB RMM HMA M PINT MFSA VFSA EA
2 RA CSCA)
FORMAT (1H0.1X.16( F7.1.1X ))
FORMAT (1H0.1X. VELOCITY IN FEET PER SECOND = .F10.0.5X. VOLUME I
1N. CUBIC FEET = .F10.27.1X. AREAS ARE IN SQUARE FEET AND DISTANCES
2 ARE IN FEET)

```

235

STOP  
END

```
FUNCTION FTABLE ( VAR , FUNC , XX , M )
VAR=DISCRETE TABULAR VALUES OF THE VARIABLE
FUNC=DISCRETE TABULAR VALUES OF THE FUNCTION
XX=GIVEN VALUE OF THE VARIABLE
M=NUMBER OF STATIONS OR TABLE VALUES
FTABLE=INTERPOLATED VALUE OF FUNCTION CORRESPONDING TO XX

DIMENSION VAR(1),FUNC(1)
NEND=M-1
DO 10,I=1,NEND
  INT=I
  IF (XX.GT.VAR(I).AND.XX.LE.VAR(I+1)) GO TO 11
CONTINUE
FTABLE=FUNC(INT)+(XX-VAR(INT))*(FUNC(INT+1)-FUNC(INT))/(VAR(INT+1)
1-VAR(INT))
RETURN
END
```

5

10

15

20

25

APPENDIX C  
PROGRAMME FOR PRESSURE DISTRIBUTION





0000  
0000  
0000

I=J  
CALCULATION OF RADIUS

IF (I.NE.J) GO TO 1  
ROEP(I,J)=SQRT(R(J)\*\*2.0\*(A/2.0)\*\*2.0)  
ROEP(I,J)=ROEP(I,J)

CALCULATION OF THE ANGLES

SINIP(I,J)=R(J)/ROEP(I,J)  
SINOP(I,J)=SINIP(I,J)  
COSIP(I,J)=(A/2.0)/ROEP(I,J)  
COSOP(I,J)=-COSIP(I,J)

CALCULATION OF THE UNSYMMETRICAL FLOW PARAMETERS

A  
101  
A  
102  
A  
103  
A  
104  
A  
105  
A  
106  
A  
107  
A  
108  
A  
109  
A  
110  
A  
111  
A  
112  
A  
113  
A  
114  
A  
115  
A  
116  
A  
117  
A  
118  
A  
119













0110Y

PROGRAM IST (INPUT, OUTPUT, TAPE5=INPUT, TAPE4=OUTPUT)

26 FORMAT (1H0,1X1,4VELDCTY =,F7.2,2X,4HFT/SEC//1X,17MANGLE OF ATTA A 351  
1CK =,F5.2,2X,17M) CP (FS) A 352  
END A 353-

PAGE 16

APPENDIX D

PROGRAMME FOR STATIC SHEAR FORCE  
AND BENDING MOMENT













7	FORMAT (10X,4HLEN=,15)	A	251
8	FORMAT (1H1)	A	252
9	FORMAT (10X,14HTOTAL VOLUME =,F20.10)	A	253
10	FORMAT (5X,13HRADIUS (FT) =,F10.5,5X,12HSTATION NO. ,5X,16)	A	254
11	FORMAT (5X,11HSTATION NO.,4X,14.10X,7HVOLUME=,F20.10,4X,5HFT**3)	A	255
12	FORMAT (5X,14HTOTAL VOLUME =,F20.10)	A	256
13	FORMAT (5X,10HLIFT (LBS)=,F10.2,5X,23HENVELOPE WEIGHT (LBS) =,F10.2	A	257
14	1.5X,22HSURFACE AREA (FT**2) =,F10.2,5X,14)	A	258
14	FORMAT (5X,11HTOTAL LIFT=,F10.2,5X,19HTOTAL SURFACE AREA=,F10.2,5X	A	259
15	1.16HENVELOPE WEIGHT=,F10.2)	A	260
15	FORMAT (5X,26HWEIGHT OF HALLONET (LBS) =,F10.5)	A	261
16	FORMAT (5X,25HCENTER OF BOUYANCY (FT) =,F10.5,5X,18HENVELOPE CG (F	A	262
17	IT) =,F10.5,5X,17HAIKSHIP CG (FT) =,F10.5)	A	263
17	FORMAT (5X,11HSTATION NO.,4X,14.10X,16HNET LIFT (LBS) =,4X,F20.10)	A	264
18	FORMAT (5X,22HTOTAL NET LIFT (LBS) =,F10.4)	A	265
	END	A	266

SUBROUTINE VOLAPHX (AN,AM,AA,N,XL,F,VOL,Y)

THIS SUBROUTINE APPROXIMATES THE VOLUME OF AN AIRSHIP SHAPE BY  
USING  
CIRCULAR CONE SEGMENTS.

DIMENSION Y(1), VOL(1)

CALCULATING THE RADIUS AT THE FRONT AND THE BACK OF THE SEGMENT

X=0.0

DO 1 I=1,N

$$Y(I) = ((XN \cdot XM) \cdot (XN \cdot XM) \cdot A \cdot XN \cdot (XL - X) \cdot XM) / (2.0 \cdot F \cdot XN \cdot XN \cdot XM \cdot XM \cdot XL \cdot (XN \cdot XM - 1.0))$$

X=X+XX

CONTINUE

CALCULATION OF THE VOLUME.

DO 2 I=2,N

J=I-1

$$VOL(J) = 0.33 \cdot 3.14 \cdot XX \cdot (Y(I) \cdot 2.0 + Y(I) \cdot Y(J) + Y(J) \cdot 2.0)$$

CONTINUE

RETURN

END





Y SUBROUTINE LAYERS (Y.VOC.M.N.SLIFT.WSURF.SURM.A.S.SA.W.SW.AX)

00000000  
1234567  
8901234  
5678901

MSURF (1)  
CONTINUE  
RETURN  
END

C  
C  
C





















APPENDIX E  
PROGRAMME FOR AIRSHIP TRAJECTORIES

















X-AXIS

XXI=((3.14\*W\*(XN\*XM)\*\*(3.0\*(XN\*XM)))/(4.0\*F\*\*3.0\*AN\*\*((3.0\*XN)\*XM\*\*1(3.0\*XM)))+(AB\*BA/CA)\*XL\*\*4.0

XXIG=3.14\*WG\*(XN\*XM)\*\*(4.0\*(XN\*XM))/(32.0\*F\*\*4.0\*AN\*\*((4.0\*XN)\*XM\*\*14.0\*XM))+(GA\*HA/DA)\*XL\*\*5

Y-AXIS

YYI=XXI/2.0\*((3.14\*W\*(XN\*XM)\*\*(XN\*XM))/(F\*XN\*\*XN\*XM\*\*XM))\*(DA\*EA/FA)\*XL\*\*4.0

YYIG=XXIG+3.14\*WG\*(XN\*XM)\*\*(2.0\*(XN\*XM))/(4.0\*F\*\*2.0\*AN\*\*((2.0\*XN)\*XM\*\*14.0\*(2.0\*XM))+(PA\*QA/RA)\*XL\*\*5

Z-AXIS

ZZI=YYI

ZZIG=YYIG

CALCULATION OF THE BOUYANCY FORCE

BFX=0.0
BFY=0.063\*VOL
BFZ=0.0

CALCULATION OF CG

TAKING MOMENTS ABOUT CENTER OF BOUYANCY

X DIRECTION

XX=(XF-XCB)\*WN+(XCAB-XCB)\*WCAB+(XT-XCB)\*WT+(XE-XCB)\*EW+(XCGE-XCB)\*WE

1WE

Vertical column of characters on the right side of the page, possibly a page number or index, ranging from 370 to 400.

PROGRAM TEST (INPUT, OUTPUT, TAPES=INPUT, TAPES=OUTPUT)

XXX=WN+W CAB\*WT+WE\*EW

XCG=XX/XXX\*XCG

Y DIRECTION

YY=(YN-YCB)\*WN+(Y CAB-YCB)\*W CAB+(YT-YCB)\*WT+(YE-YCB)\*EW+(YCGE-YCB)\*WE

YYY=WN+W CAB\*WT+EW\*WE

YCG=YY/YYY

Z DIRECTION

ZZ=(ZN-ZCB)\*WN+(Z CAB-ZCB)\*W CAB+(ZT(1)-ZCB)\*WT/2.0+(ZT(2)-ZCB)\*WT/2.0+(ZE(1)-ZCB)\*EW/2.0+(ZE(2)-ZCB)\*EW/2.0+(ZCGE-ZCB)\*WE

ZZZ=YYY

ZCG=ZZ/ZZZ

CALCULATION OF THE TOTAL MASS MOMENT OF INERTIA ABOUT THE CG

NOSE COMPONENT

XXIPN=XXIN\*WN/G\*((YN-YCB)\*\*2+(ZN-ZCB)\*\*2)

YYIPN=YYIN\*WN/G\*((ZN-ZCB)\*\*2+(XF-XCB)\*\*2)

ZZIPN=ZZIN\*WN/G\*((YN-YCB)\*\*2+(XF-XCB)\*\*2)

CABIN COMPONENT

XXIPC=XXIC\*W CAB/G\*((Y CAB-YCB)\*\*2+(Z CAB-ZCB)\*\*2)

YYIPC=YYIC\*((Z CAB-ZCB)\*\*2+(X CAB-XCB)\*\*2)\*W CAB/G

ZZIPC=ZZIC\*((X CAB-XCB)\*\*2+(Y CAB-YCB)\*\*2)\*W CAB/G

TAIL ASSEMBLY COMPONENT

XXIPT=XXITA\*((YT-YCB)\*\*2+(ZT(1)-ZCB)\*\*2)\*WT/G

Vertical column of characters on the right side of the page, possibly a page number or index, ranging from 401 to 450.

Vertical column of characters on the left side of the page, possibly a page number or index, ranging from 401 to 450.

YYIPT=YYITA\*WT/G\*((ZI(1)-ZCB)\*\*2+(XT-XCH)\*\*2)  
ZZIPT=ZZITA\*WT/G\*((XT-XCB)\*\*2+(YT-YCB)\*\*2)

ENGINE COMPONENT

XXIPE=XXIE\*EW/(G)\*((YE-YCB)\*\*2+(ZE(1)-ZCH)\*\*2)  
YYIPE=YYIE\*EW/(G)\*((ZE(1)-ZCB)\*\*2+(XE-XCH)\*\*2)  
ZZIPE=ZZIE\*EW/(G)\*((XE-XCB)\*\*2+(YE-YCB)\*\*2)

XXIT=XXIPN\*XXIPT+XXIPC+XXIPE\*XXI\*WE/G\*(YCB\*\*2+ZCB\*\*2)+XXIG\*GM/G\*(  
YCB\*\*2+ZCB\*\*2)  
YYIT=YYIPN\*YYIPT+YYIPC+YYIPE\*YYI\*WE/G\*(XCB\*\*2+ZCB\*\*2)+YYIG\*GM/G\*(  
XCB\*\*2+ZCB\*\*2)  
ZZIT=ZZIPN\*ZZIPT+ZZIPC+ZZIPE\*ZZI\*WE/G\*(XCB\*\*2+YCB\*\*2)+ZZIG\*GM/G\*(  
YCB\*\*2+XCB\*\*2)

DETERMINATION OF TAKE-OFF MASS

TM=TOW/G

IF (K.GT.0) GO TO 2

SMOOTH APPLICATION OF POWER FOR TAKE OFF

J=20

IF (I.EQ.1) POX=POW/20

ACCELERATION IN THE F DIRECTION DUE TO THE SUDDEN APPLICATION OF POWER

ACCF=-POX/TM

SIMILARLY IN THE Y DIRECTION

ACCY=-((TOW-BFY)/TM

CALCULATION OF THE FIRST POINT OF THE TRAJECTORY

A 451  
A 452  
A 453  
A 454  
A 455  
A 456  
A 457  
A 458  
A 459  
A 460  
A 461  
A 462  
A 463  
A 464  
A 465  
A 466  
A 467  
A 468  
A 469  
A 470  
A 471  
A 472  
A 473  
A 474  
A 475  
A 476  
A 477  
A 478  
A 479  
A 480  
A 481  
A 482  
A 483  
A 484  
A 485  
A 486  
A 487  
A 488  
A 489  
A 490  
A 491  
A 492  
A 493  
A 494  
A 495  
A 496  
A 497  
A 498  
A 499  
A 500

















6  
7  
8  
9  
30

RUDDER NOT IN USE

CONTINUE

AFR=0.0  
XIMB=0.0

GO TO 3A

LEFT AND RIGHT RUDDER

CONTINUE

TYAW=2.0\*YAW  
CLR=FTABLE(ALD,CLD,TYAW,13)  
AFR=-CLR\*ROE\*VD\*\*2\*AHCL

GO TO 29

CONTINUE

TYAW=2.0\*YAW  
CLR=FTABLE(ALD,CLD,TYAW,13)  
AFR=CLR\*ROE\*VD\*\*2\*AHCL

GO TO 29

CONTINUE

CALCULATING FIN AND AERODYNAMIC FORCES

AERODYNAMIC FORCE

XA=0.0  
XIM9=0.0  
XIMB=0.0

CALCULATION OF THE TURNING RADIUS AT EACH TIME INTERVAL

IF (YAWR.EQ.0.0) GO TO 31  
CONTINUE  
R1=2.0\*(XT-XCB)/(DYK\*SIN(2.0\*YAWR))

A 851  
A 852  
A 853  
A 854  
A 855  
A 856  
A 857  
A 858  
A 859  
A 860  
A 861  
A 862  
A 863  
A 864  
A 865  
A 866  
A 867  
A 868  
A 869  
A 870  
A 871  
A 872  
A 873  
A 874  
A 875  
A 876  
A 877  
A 878  
A 879  
A 880  
A 881  
A 882  
A 883  
A 884  
A 885  
A 886  
A 887  
A 888  
A 889  
A 890  
A 891  
A 892  
A 893  
A 894  
A 895  
A 896  
A 897  
A 898  
A 899  
A 900







```

C 41 CONTINUE
C 41 ACCF=0.0
C GO TO 43
C 42 CONTINUE
C 42 ACCF=FACH/TM
C 43 CONTINUE
C 43 ACCY=FACV/TM
C ACCX=ACCF * COS(PHIR * YAWR) * (FACZ/TM) * SIN(PHIR * YAWR)
C ACCZ=ACCF * SIN(PHIR * YAWR) * (FACZ/TM) * COS(PHIR * YAWR)

```

CCCC

TRAJECTORY CALCULATIONS

```

C X=X+ACCX*DELT**2/2.0+VX*DELT
C Y=Y+ACCY*DELT**2/2.0+VY*DELT
C Z=Z+ACCZ*DELT**2/2.0+VZ*DELT
C IF ((ACCY.LE.0.0).AND.(Y.LE.0.0)) Y=0.0
C IF (IST.EQ.0) DX=X1-X
C IF (IST.EQ.1) DX=X-X1
C DY=ABS(Y-Y1)
C DZ=ABS(Z1-Z)
C DELTAY=Y-Y1
C DELTAZ=Z-Z1
C DX1=SQRT(ABS(X1-X)**2+ABS(Z1-Z)**2)
C X1=X
C Y1=Y
C Z1=Z

```

CCCC

VELOCITY CALCULATIONS

```

VX=VX+ACGX*DELT
VZ=VZ+ACGZ*DELT
VY=VY+ACGY*DELT

```

A1051  
A1052  
A1053  
A1054  
A1055  
A1056  
A1057  
A1058  
A1059  
A1060  
A1061  
A1062  
A1063  
A1064  
A1065  
A1066  
A1067  
A1068  
A1069  
A1070  
A1071  
A1072  
A1073  
A1074  
A1075  
A1076  
A1077  
A1078  
A1079  
A1080  
A1081  
A1082  
A1083  
A1084  
A1085  
A1086  
A1087  
A1088  
A1089  
A1090  
A1091  
A1092  
A1093  
A1094  
A1095  
A1096  
A1097  
A1098  
A1099  
A1100











```

Z=0.0
T=0.0
THETAR=0.0673
ALPHAR=0.0
PHIR=0.0
YAWR=0.0
BTR=THETAR
POX=POX
VD=-RR.0
ANGV=0.0
ANGVZ=0.0
ANGACZ=0.0
VX=V1
VY=0.0
VZ=0.0
ACCLX=0.0
ACCLY=0.0
ACCLZ=0.0
YAW=0.0
ALPHA=0.0
PHI=0.0
BETAR=0.0
YAWD=1.0E04
XIMR=0.0
SUMFX=0.0
SUMFY=0.0
SUMFZ=0.0

```

C  
C  
C

CALCULATION TO DETERMINE THETA SUCH THAT THE VERTICAL FORCE IS ZERO

65

```

FS=BFY-TOW
PV=POX*SIN(THETAR)
CLA=1.25*THETAR
DLP=CLA*ROE*VD**2*VOLT**0.67/2.0
CDT1=0.0

```

C

THETA=180.0\*THETAR/3.14

C

```

ABSTA=ABS(THETA)
CDT=FTABLE(AD,CD,ABSTA,9)
CLT=FTABLE(AL,CL,ABSTA,10)

```

C

IF (THETA.LT.0.0) CLT=-CLT

C

```

FLTY=CLT*ROE*VD**2*AVCL
DRTY=CDT*ROE*VD**2*ADR*CDT1*ROE*VD**2*ADRH

```

C

```

CALL UMBZ (TOW,POX,ROE,VD,THETAR,BTR,VOLT,DYK,YCB,YE,YCG,FLTY,DRTY
1,XT,XCB,UBM)

```

```

A1301
A1302
A1303
A1304
A1305
A1306
A1307
A1308
A1309
A1310
A1311
A1312
A1313
A1314
A1315
A1316
A1317
A1318
A1319
A1320
A1321
A1322
A1323
A1324
A1325
A1326
A1327
A1328
A1329
A1330
A1331
A1332
A1333
A1334
A1335
A1336
A1337
A1338
A1339
A1340
A1341
A1342
A1343
A1344
A1345
A1346
A1347
A1348
A1349
A1350

```

C  
C  
66  
C  
C  
C  
67  
C  
C  
C  
C  
C  
68  
69  
70

```

AFE=UBM/(XT-XCB)
AFC=DLF*FLTY*AFE
FAV=AFC*FS*PV
IF (ABS(FAV)/LT*.1.) GO TO 66
IF (FAV.GT.0.0) THETAR=THETAR-0.001
IF (FAV.LT.0.0) THETAR=THETAR+0.00001
GO TO 65

```

CONTINUE

ANGACC=UBM/ZZIT

THETA=THETAR\*180.0/3.14

```

DELTAY=0.0
X1=X
Y1=Y
Z1=Z
I=I+1
KK=K+1

```

CONTINUE

IF ((K.EQ.11).OR.(K.EQ.13)) ANGV=0.0

```

IST=0
IKY=0
ILY=0

```

THETA=THETAR

WRITE APPROPRIATE HEADINGS

GO TO (68,69,70,71,72,73,74,75,76,77,78,79,80,81,82), KK

CONTINUE

GO TO 83

CONTINUE

```

WRITE (6,134)
WRITE (6,115)
WRITE (6,116)
WRITE (6,120)

```

GO TO 83

CONTINUE

```

WRITE (6,134)
WRITE (6,115)
WRITE (6,116)

```

```

A1 351
A1 352
A1 353
A1 354
A1 355
A1 356
A1 357
A1 358
A1 359
A1 360
A1 361
A1 362
A1 363
A1 364
A1 365
A1 366
A1 367
A1 368
A1 369
A1 370
A1 371
A1 372
A1 373
A1 374
A1 375
A1 376
A1 377
A1 378
A1 379
A1 380
A1 381
A1 382
A1 383
A1 384
A1 385
A1 386
A1 387
A1 388
A1 389
A1 390
A1 391
A1 392
A1 393
A1 394
A1 395
A1 396
A1 397
A1 398
A1 399
A1 400

```

```

WRITE (6,121)
CONTINUE (6,134)
WRITE (6,115)
WRITE (6,122)
CONTINUE (6,134)
WRITE (6,115)
WRITE (6,123)
CONTINUE (6,134)
WRITE (6,115)
WRITE (6,124)
CONTINUE (6,134)
WRITE (6,115)
WRITE (6,125)
CONTINUE (6,134)
WRITE (6,115)
WRITE (6,126)
CONTINUE (6,134)
WRITE (6,115)
WRITE (6,127)
CONTINUE (6,134)
WRITE (6,115)
WRITE (6,128)
CONTINUE (6,134)
WRITE (6,115)
WRITE (6,129)
CONTINUE (6,134)

```

```

1101
1102
1103
1104
1105
1106
1107
1108
1109
1110
1111
1112
1113
1114
1115
1116
1117
1118
1119
1120
1121
1122
1123
1124
1125
1126
1127
1128
1129
1130
1131
1132
1133
1134
1135
1136
1137
1138
1139
1140
1141
1142
1143
1144
1145
1146
1147
1148
1149
1150

```

79

CONTINUE

WRITE (6,134)

WRITE (6,135)

WRITE (6,136)

WRITE (6,130)

GO TO 83

80

CONTINUE

WRITE (6,134)

WRITE (6,135)

WRITE (6,136)

WRITE (6,131)

GO TO 83

81

CONTINUE

WRITE (6,134)

WRITE (6,135)

WRITE (6,136)

WRITE (6,132)

GO TO 83

82

CONTINUE

WRITE (6,133)

WRITE (6,133)

C

GO TO 84

C

C

CONTINUE

C

THETA=THETA

C

KOUNT=KOUNT+1

C

IF (MOD(KOUNT,12).EQ.0) WRITE (6,117)

C

WRITE (6,118) VX,VY,VZ,ACCX,ACCY,ACCZ,PHI,YAW,ALPHA,THETA,X,Y,Z

C

WRITE (6,135) SUMFX,SUMFY,SUMFZ

C

IF (ILY.EQ.1) GO TO 63

C

IF (K.EQ.14) GO TO 84

C

GO TO 4

C

C

CONTINUE

C

C

DATA OUTRUT

C

C

WRITE (6,85)

WRITE (6,86) XCB

WRITE (6,92) YCB

C

C

C

A1451  
A1452  
A1453  
A1454  
A1455  
A1456  
A1457  
A1458  
A1459  
A1460  
A1461  
A1462  
A1463  
A1464  
A1465  
A1466  
A1467  
A1468  
A1469  
A1470  
A1471  
A1472  
A1473  
A1474  
A1475  
A1476  
A1477  
A1478  
A1479  
A1480  
A1481  
A1482  
A1483  
A1484  
A1485  
A1486  
A1487  
A1488  
A1489  
A1490  
A1491  
A1492  
A1493  
A1494  
A1495  
A1496  
A1497  
A1498  
A1499  
A1500





101	1T	Y1	FORMAT (1H0,1X,34HPOINT OF APPLICATION OF GAS MASS =,F20.10,6X,6HF	A1551
	1T	Z1	FORMAT (1H0,1X,34HPOINT OF APPLICATION OF GAS MASS =,F20.10,6X,6HF	A1552
102	1T	Y1	FORMAT (1H0,1X,16HBOUANCY FORCE =,F20.10,6X,7HMBF	A1553
103	1T	Z1	FORMAT (1H0,1X,16HBOUANCY FORCE =,F20.10,6X,7HMBF	A1554
104	1T	Y1	FORMAT (1H0,1X,16HBOUANCY FORCE =,F20.10,6X,7HMBF	A1555
105	1T	Z1	FORMAT (1H0,1X,16HBOUANCY FORCE =,F20.10,6X,7HMBF	A1556
106	1T	Y1	FORMAT (1H0,1X,29HMASS OF THE LIFTING GAS =,F20.10,6X,3HMBM)	A1557
107	1T	Z1	FORMAT (1H0,1X,29HMASS OF THE LIFTING GAS =,F20.10,6X,3HMBM)	A1558
108	1T	Y1	FORMAT (1H0,1X,38HTOTAL AIRSHIP MASS MOMENT OF INERTIA =,F20.10,6X	A1559
109	1T	Z1	FORMAT (1H0,1X,38HTOTAL AIRSHIP MASS MOMENT OF INERTIA =,F20.10,6X	A1560
110	1T	Y1	FORMAT (1H0,1X,38HTOTAL AIRSHIP MASS MOMENT OF INERTIA =,F20.10,6X	A1561
111	1T	Z1	FORMAT (1H0,1X,38HTOTAL AIRSHIP MASS MOMENT OF INERTIA =,F20.10,6X	A1562
112	1T	Y1	FORMAT (1H0,1X,39HMASS MOMENT OF INERTIA OF THE GAS (X) =,F20.10)	A1563
113	1T	Z1	FORMAT (1H0,1X,39HMASS MOMENT OF INERTIA OF THE GAS (Y) =,F20.10)	A1564
114	1T	Y1	FORMAT (1H0,1X,39HMASS MOMENT OF INERTIA OF THE GAS (Z) =,F20.10)	A1565
115	1T	Z1	FORMAT (1H0,1X,39HMASS MOMENT OF INERTIA OF THE GAS (Z) =,F20.10)	A1566
116	1T	Y1	FORMAT (1H0,1X,44HLOCATION OF AIRSHIP CENTER OF PRESSURE (X) =,F20	A1567
117	1T	Z1	FORMAT (1H0,1X,44HLOCATION OF AIRSHIP CENTER OF PRESSURE (Y) =,F20	A1568
118	1T	Y1	FORMAT (1H0,1X,44HLOCATION OF AIRSHIP CENTER OF PRESSURE (Z) =,F20	A1569
119	1T	Z1	FORMAT (1H0,1X,44HLOCATION OF AIRSHIP CENTER OF PRESSURE (Z) =,F20	A1570
120	1T	Y1	FORMAT (1H0,1X,44HLOCATION OF AIRSHIP CENTER OF PRESSURE (Z) =,F20	A1571
121	1T	Z1	FORMAT (1H0,1X,44HLOCATION OF AIRSHIP CENTER OF PRESSURE (Z) =,F20	A1572
122	1T	Y1	FORMAT (1H0,1X,44HLOCATION OF AIRSHIP CENTER OF PRESSURE (Z) =,F20	A1573
123	1T	Z1	FORMAT (1H0,1X,44HLOCATION OF AIRSHIP CENTER OF PRESSURE (Z) =,F20	A1574
124	1T	Y1	FORMAT (1H0,1X,44HLOCATION OF AIRSHIP CENTER OF PRESSURE (Z) =,F20	A1575
125	1T	Z1	FORMAT (1H0,1X,44HLOCATION OF AIRSHIP CENTER OF PRESSURE (Z) =,F20	A1576
126	1T	Y1	FORMAT (1H0,1X,44HLOCATION OF AIRSHIP CENTER OF PRESSURE (Z) =,F20	A1577
127	1T	Z1	FORMAT (1H0,1X,44HLOCATION OF AIRSHIP CENTER OF PRESSURE (Z) =,F20	A1578
128	1T	Y1	FORMAT (1H0,1X,44HLOCATION OF AIRSHIP CENTER OF PRESSURE (Z) =,F20	A1579
129	1T	Z1	FORMAT (1H0,1X,44HLOCATION OF AIRSHIP CENTER OF PRESSURE (Z) =,F20	A1580
130	1T	Y1	FORMAT (1H0,1X,44HLOCATION OF AIRSHIP CENTER OF PRESSURE (Z) =,F20	A1581
131	1T	Z1	FORMAT (1H0,1X,44HLOCATION OF AIRSHIP CENTER OF PRESSURE (Z) =,F20	A1582
132	1T	Y1	FORMAT (1H0,1X,44HLOCATION OF AIRSHIP CENTER OF PRESSURE (Z) =,F20	A1583
133	1T	Z1	FORMAT (1H0,1X,44HLOCATION OF AIRSHIP CENTER OF PRESSURE (Z) =,F20	A1584
134	1T	Y1	FORMAT (1H0,1X,44HLOCATION OF AIRSHIP CENTER OF PRESSURE (Z) =,F20	A1585
135	1T	Z1	FORMAT (1H0,1X,44HLOCATION OF AIRSHIP CENTER OF PRESSURE (Z) =,F20	A1586
136	1T	Y1	FORMAT (1H0,1X,44HLOCATION OF AIRSHIP CENTER OF PRESSURE (Z) =,F20	A1587
137	1T	Z1	FORMAT (1H0,1X,44HLOCATION OF AIRSHIP CENTER OF PRESSURE (Z) =,F20	A1588
138	1T	Y1	FORMAT (1H0,1X,44HLOCATION OF AIRSHIP CENTER OF PRESSURE (Z) =,F20	A1589
139	1T	Z1	FORMAT (1H0,1X,44HLOCATION OF AIRSHIP CENTER OF PRESSURE (Z) =,F20	A1590
140	1T	Y1	FORMAT (1H0,1X,44HLOCATION OF AIRSHIP CENTER OF PRESSURE (Z) =,F20	A1591
141	1T	Z1	FORMAT (1H0,1X,44HLOCATION OF AIRSHIP CENTER OF PRESSURE (Z) =,F20	A1592
142	1T	Y1	FORMAT (1H0,1X,44HLOCATION OF AIRSHIP CENTER OF PRESSURE (Z) =,F20	A1593
143	1T	Z1	FORMAT (1H0,1X,44HLOCATION OF AIRSHIP CENTER OF PRESSURE (Z) =,F20	A1594
144	1T	Y1	FORMAT (1H0,1X,44HLOCATION OF AIRSHIP CENTER OF PRESSURE (Z) =,F20	A1595
145	1T	Z1	FORMAT (1H0,1X,44HLOCATION OF AIRSHIP CENTER OF PRESSURE (Z) =,F20	A1596
146	1T	Y1	FORMAT (1H0,1X,44HLOCATION OF AIRSHIP CENTER OF PRESSURE (Z) =,F20	A1597
147	1T	Z1	FORMAT (1H0,1X,44HLOCATION OF AIRSHIP CENTER OF PRESSURE (Z) =,F20	A1598
148	1T	Y1	FORMAT (1H0,1X,44HLOCATION OF AIRSHIP CENTER OF PRESSURE (Z) =,F20	A1599
149	1T	Z1	FORMAT (1H0,1X,44HLOCATION OF AIRSHIP CENTER OF PRESSURE (Z) =,F20	A1600

132

1. ACHIEVED)  
FORMAT (1H0.1X.6) INSTEADY STATE TURN AND FULL DOWN ELEVATOR UNTIL C

A1601  
A1602  
A1603  
A1604  
A1605  
A1606  
A1607  
A1608-

133

1. LIM RATE = 0)  
FORMAT (1H0.1X.7) LANDING)

134

FORMAT (1H0.1X.9) MANOEUVER COMPLETE \*)

135

FORMAT (1H0.9) SUM FX = \*.F20.6.\* SUM FY = \*.F20.6.\* SUM FZ = \*.F20

1.6)  
END







## REFERENCES

1. Von Karman, T., "Calculation of Pressure Distribution on Airship Hulls", NACA Technical Memorandum No. 574, 1927.
2. Klinkoff, W. A., "Pressure in Airships", A.S.M.E. Transactions, 1931.
3. Ministry of Transport, Civil Aeronautics, Provisional Airworthiness Requirements, Airships.
4. Kleiner, H. J., "The Response to the McMaster University Airship Proposal", Private Report, McMaster University, 1973.
5. Gordon, S. A., "The Possible Role of Lighter-than-Air Vehicles in Canadian Transportation, Report prepared for the Transportation Development Agency, March 1973.
6. Sonstegaard, M. H., "Transporting Gas by Airship, Mechanical Engineering, June 1973, pp. 19-25.
7. Howe, D., "The Feasibility of the Large Freight Airship", Cranfield Institute of Technology Report Aero No. 5, March 1971.
8. Stinton, D., "A New Look at Airships", Flight International, November 19, 1970.
9. Iurich, L., "The Nuclear Powered Airship", SAE paper No. 169 A/60, April 1960.
10. Morse, P., et. al., "Dirigibles: Aerospace Opportunities for the '70s and '80s, Astronautics and aeronautics, November 1972, pp. 32-40.
11. Hecks, K., "Pressure Airships: a review" Aeronautical Journal, November 1972, pp. 647-656.
12. Blakemore, T. L., and Pagon, W. W., "Pressure Airships," Ronald Press, New York, 1927.

13. Burgess, C. P., "Airship Design", Ronald Press, New York, 1927.
14. Mowforth, E., "A Design Study for a Freight-Carrying Airship, Aeronautical Journal, March 1971, pp. 166-174.
15. Hval, B., "Lighter-than-Air in Canada," Canadian Aeronautics and Space Journal, January 1971, pp. 15-23.
16. Rynish, M. J., "Cargo Airships - a plan for the future", Engineering, June 1971, pp. 290-296.
17. Goodyear Aerospace, Memorandum ARD 13,551, September 1970.
18. Goodyear Aerospace, Memorandum ARD 13,078, February 1970.
19. Goodyear Aerospace, Memorandum ARD 13,516, August 1970.
20. Goodyear Aerospace, Memorandum ARD 13,135, March 1970.
21. Goodyear Aerospace, Memorandum ARD 13,458, July 1970.
22. Goodyear Aerospace, Memorandum ARD 13,579, September 1970.
23. Goodyear Aerospace, Report GER 13564, pp. VIII-47, 242-293.
24. Airship Aerodynamics, U.S. War Department Technical Manual, T.M. 1-320, 11 February, 1941.
25. Navtz, H., "Bending Stresses on an Airship in Flight", NACA Technical Memorandum No. 276, 1924.
26. Navtz, H., "Forces of Flow on a Moving Airship and the Effect of the Control Surfaces," NACA Technical Memorandum No. 275, 1924.

27. Kuethe, A. M., and Schetzer, J. D., "Foundations of Aerodynamics", John Wiley and Sons, Inc., New York, 1950, pp. 70-87.
28. Anderson, A. A., Erickson, M. L., Frochlich, H. E., Henjum, H. E., Schwoebel, R. L., Stone, V. H., Torgeson, W. L., "Lighter-than-Air Concepts Study", Final Report Nonr1589(07), General Mills, Inc., Minneapolis, Minnesota, 1960.
29. Hoerner, S. P., "Fluid Dynamic Drag", Published by Author, Midland Park, New Jersey, 1958.
30. Goodyear Aerospace, Executive Summary GER 16033 Volume I, "Airships For Use In Law Enforcement", January 1974.
31. Vaeth, G. J., "The Airship Can Meet the Energy Challenge", Astronautics and Aeronautics, February 1974, pp. 25-27.
32. Seemann, G. R., Harris, G. L., Brown, G. J., Cullian, C. A., "Remotely Piloted Mini-Blimps for Urban Applications", Astronautics and Aeronautics, February 1974, pp. 31-35.
33. Munk, M. M., "Aerodynamics of Airships", Div. Q: Vol. VI, Aerodynamic Theory, edited by W. R. Durand, Dover Publications, New York, 1963.
34. Arnstein, K. and Klemperer, W., "Performance of Airships", Div. R., Vol. VI, Aerodynamic Theory, edited by W. P. Durand, Dover Publications, New York, 1963.